Improved Understanding of Fenton-like Reactions for the In Situ Remediation of Contaminated Groundwater Including Treatment of Sorbed Contaminants and Destruction of DNAPLs

SERDP Project No. CU-1288

Washington State University

Richard J. Watts, lead principal investigator

April 29, 2006

REPORT DOCUMENTATION PAGE		Form Approved OMB No. 0704-0188

The public reporting burden for this collection of information is estimated to average 1 hour per response, including the time for reviewing instructions, searching existing data sources, gathering and maintaining the data needed, and completing and reviewing the collection of information. Send comments regarding this burden estimate or any other aspect of this collection of information, including suggestions for reducing the burden, to the Department of Defense, Executive Services and Communications Directorate (0704-0188). Respondents should be aware that notwithstanding any other provision of law, no person shall be subject to any penalty for failing to comply with a collection of information if it does not display a currently valid OMB control number.
PLEASE DO NOT RETURN YOUR FORM TO THE ABOVE ORGANIZATION.

1. REPORT DATE (DD-MM-YYYY) 30-04-2006	2. REPORT TYPE Final	3. DATES COVERED (From - To) Oct 2002-Apr 2006

4. TITLE AND SUBTITLE

Improved Understanding of Fenton-like Reactions for the In Situ Remediation of Contaminated Groundwater Including Treatment of Sorbed Contaminants and Destruction of DNAPLs

5a. CONTRACT NUMBER

5b. GRANT NUMBER

5c. PROGRAM ELEMENT NUMBER

6. AUTHOR(S)

Richard J. Watts, Frank J. Loge, and Amy L. Teel

5d. PROJECT NUMBER
CU-1288

5e. TASK NUMBER

5f. WORK UNIT NUMBER

7. PERFORMING ORGANIZATION NAME(S) AND ADDRESS(ES)

Washington State University
Pullman, WA 99164

8. PERFORMING ORGANIZATION REPORT NUMBER

9. SPONSORING/MONITORING AGENCY NAME(S) AND ADDRESS(ES)

Strategic Environmental Research and Development Program
901 N. Stuart St., Ste. 303
Arlington, VA 22203

10. SPONSOR/MONITOR'S ACRONYM(S)
SERDP

11. SPONSOR/MONITOR'S REPORT NUMBER(S)

12. DISTRIBUTION/AVAILABILITY STATEMENT

Unlimited distribution

13. SUPPLEMENTARY NOTES

14. ABSTRACT

The study of CHP ISCO (catalyzed H_2O_2 propagations in situ chemical oxidation) demonstrates that it is characterized by more complex chemistry than previously conceived. In particular, superoxide has a major role in the degradation of highly oxidized contaminants, the destruction of DNAPLs, and the enhanced desorption of hydrophobic contaminants from soils and subsurface solids. The suite of reactive oxygen species generated in CHP reactions, including hydroxyl radical, superoxide, and the strong nucleophile hydroperoxide, provide a near-universal treatment matrix. However, the rapid decomposition of hydrogen peroxide, promoted by natural iron and manganese oxides in the subsurface, has previously limited the utility of CHP for the remediation of contaminated sites. Advances attained through the completed research in the stabilization of hydrogen peroxide by citrate, malonate, and phytate will increase the utility and economic viability of CHP treatment. The results of this research will enable field personnel to better design CHP ISCO systems and apply the process more effectively and economically.

15. SUBJECT TERMS

In situ chemical oxidation (ISCO), catalyzed H_2O_2 propagations (CHP), Fenton's reagent, superoxide, dense nonaqueous phase liquids (DNAPLs)

16. SECURITY CLASSIFICATION OF:			17. LIMITATION OF ABSTRACT	18. NUMBER OF PAGES	19a. NAME OF RESPONSIBLE PERSON
a. REPORT	b. ABSTRACT	c. THIS PAGE	UU	274	Richard J. Watts, Ph.D.
Unclassified	Unclassified	Unclassified			19b. TELEPHONE NUMBER (Include area code) 509-335-3761

Reset

Standard Form 298 (Rev. 8/98)
Prescribed by ANSI Std. Z39.18

FRONT MATTER

Table of Contents

List of Acronyms

BaP   Benzo[*a*]pyrene

CHP   Catalyzed H_2O_2 Propagations

CT   Carbon tetrachloride

DCA   Dichloroethane

DNAPL   Dense nonaqueous phase liquid

DTPA   Diethylenetriamine-pentaacetic acid

DTPA   Diethylenetriamine-pentaacetic acid

EDTA   Ethylenediaminetetraacetic acid

GC-MS   Gas chromatography/mass spectroscopy

HCA   Hexachloroethane

HCB   Hexachlorobenzene

HKCH   Hexaketocyclohexane

HO_2^- Hydroperoxide anion

ICS   Iron coated sand

ISCO   In situ chemical oxidation

KO_2 Potassium superoxide

MCS   Manganese coated sand

NAPL   Nonaqueous phase liquid

NOM   Natural organic matter

NPOM   Nonparticulate organic matter

NTA   Nitrilotriacetic acid

$O_2 \bullet^-$ Superoxide radical anion

$OH \bullet$ Hydroxyl radical

PCE   Perchloroethylene

POM   Particulate organic matter

SOM   Soil organic matter

TCA   Trichloroethane

TCE   Trichloroethylene

List of Figures

xiii

List of Tables

3. ACKNOWLEDGEMENTS

4. EXECUTIVE SUMMARY

A comprehensive study was conducted to investigate processes and mechanisms associated with the use of catalyzed H_2O_2 propagations (CHP; modified Fenton's reagent) for in situ chemical oxidation (ISCO). CHP ISCO has been used in the field for over 10 years, but little is known about the mechanisms and pathways of treatment, and practitioners often apply the technology with minimal knowledge of fundamental process dynamics. The tasks investigated through SERDP Project CU-1288 focused on 1) rates of hydrogen peroxide decomposition mediated by naturally occurring minerals and native soils and subsurface solids, 2) rates of production of reactive oxygen species in CHP systems, 3) degradation products formed during the treatment of reduced and oxidized contaminants, 4) mechanisms of destruction of dense nonaqueous phase liquids (DNAPLs) by CHP, 5) the reactive oxygen species responsible for the enhanced desorption and treatment of sorbed contaminants, and 6) mechanisms of improved delivery of hydrogen peroxide to the subsurface.

Rates of mineral- and soil-mediated hydrogen peroxide decomposition and accompanying generation of reactive oxygen species were evaluated. Eleven minerals were evaluated for their potential to decompose hydrogen peroxide. When the minerals were studied individually, the manganese oxide minerals pyrolusite and manganite were the most active catalysts for the decomposition of hydrogen peroxide on a per mass basis. The iron minerals goethite and hematite were also active in promoting hydrogen peroxide decomposition, but decomposed hydrogen peroxide at approximately an order of magnitude slower than the manganese oxides. Trace minerals, such as anatase and bauxite, showed minimal activity in decomposing hydrogen peroxide. Hydrogen peroxide decomposition rates were then quantified in eleven soils and subsurface solid samples, and the decomposition rates were correlated with soil physical and chemical properties. Hydrogen peroxide decomposition rates at neutral pH were found to correlate most with the crystalline iron oxide content and the crystalline manganese oxide content of the soils. In addition, pH had a significant effect on hydrogen peroxide decomposition rates; rates were approximately an order of magnitude lower at acidic pH compared to neutral pH. Hydrogen peroxide decomposition rates at acidic pH regimes correlated with the amorphous iron oxide content and the amorphous manganese oxide content, likely because many of the crystalline iron and manganese oxides were altered at acidic pH. These results demonstrate that crystalline iron and manganese oxides will require deactivation or sequestration in order to stabilize hydrogen peroxide in the subsurface at neutral pH regimes.

Different forms of iron, including chelated iron at neutral pH, generate both hydroxyl radical and superoxide. Hydrogen peroxide decomposition by soluble iron generates an increasing flux of superoxide anion as the hydrogen peroxide concentration is increased. Manganese-mediated decomposition of hydrogen peroxide provides more specific generation of reactive oxygen species. Soluble manganese (II) mediates the decomposition of hydrogen peroxide with the generation of hydroxyl radical at a relatively slow rate, but with efficient stoichiometry. Solid manganese dioxides decompose hydrogen peroxide rapidly to superoxide anion.

Degradation products for carbon tetrachloride, perchloroethylene, 1,1,1-trichloroethane, benzo[*a*]pyrene, and hexadecane were evaluated under a range of CHP process conditions.

Carbon tetrachloride is not degraded by oxidative CHP reactions. However, its reactivity with superoxide was demonstrated, which is not in agreement with the conventional concept of superoxide reactivity in water. Superoxide has been considered unreactive with carbon tetrachloride and other chlorinated aliphatic compounds in water, although it is highly reactive with these compounds when dissolved in aprotic solvents. The minimal reactivity of carbon tetrachloride with superoxide in deionized water was confirmed in this study; however, the addition of hydrogen peroxide in concentrations characteristic of typical CHP conditions significantly increased the reactivity of superoxide with carbon tetrachloride, likely due to the effect of hydrogen peroxide on lowering the net polarity of the water. Carbon tetrachloride degradation products included phosgene, which was short lived, as well as carbonate and chloride. Perchloroethylene degradation products found under oxidizing conditions included dichloroacetic acid and dichloroacetyl chloride. Reduced products from destruction of a 1,1,1-trichloroethane DNAPL included trichloroethylene, dichloroethylenes, and vinyl chloride. Benzo[a]pyrene and hexadecane were not degraded under reducing conditions; they were degraded under oxidizing conditions, but oxidation products were not observed under the aggressive conditions typical of CHP reactions, with the exception of a C_{14} carboxylic acid found in the systems containing hexadecane. The relative lack of degradation products was due to mineralization of both benzo[a]pyrene and hexadecane, which was observed through the use of ^{14}C-labeled parent compounds. Mineralization of benzo[a]pyrene was 85% in a Palouse loess soils and mineralization of hexadecane was 73% in a silica sand system. The contaminant carbon not converted to carbon dioxide was found primarily in the form of unreacted parent compound that remained sorbed.

The dynamics of DNAPL destruction were investigated in CHP systems by comparing rates of DNAPL destruction to rates of gas-purge dissolution. In addition, the reactive oxygen species responsible for the destruction of six different DNAPL contaminants was elucidated by conducting parallel reactions in systems containing only one reactive oxygen species. DNAPLs containing contaminants characterized by low rates of dissolution were degraded faster than the rate at which they dissolved into the aqueous phase, suggesting that one of the reactive oxygen species is capable of increasing contaminant mass transfer and corresponding destruction. The reactive oxygen species responsible for DNAPL destruction varied with each contaminant, and was a function of its relative rate of reaction with hydroxyl radical and superoxide as well as its rate of dissolution. For example, carbon tetrachloride DNAPLs were destroyed only by superoxide and were destroyed at rates significantly greater than the rate of dissolution; in contrast, trichloroethylene DNAPLs were degraded by both hydroxyl radical and superoxide at rates near the rate of the DNAPL dissolution.

Similar to the enhanced destruction of DNAPLs, CHP is capable of treating hydrophobic contaminants significantly more rapidly than their rates of desorption. The hydrogen peroxide dosage required for enhanced treatment of sorbed contaminants was found to be directly proportional to the contaminant octanol-water partition coefficient; i.e., sorbed contaminants of higher hydrophobicity required higher dosages of hydrogen peroxide. The reactive oxygen species responsible for the enhanced contaminant desorption observed in CHP reactions was investigated using dodecane as a probe molecule. Dodecane was sorbed onto silica sand, and its rate of desorption was measured by gas purge methodology from the sand in deionized water. Using the same gas-purge system, but with solutions containing one reactive oxygen species, superoxide was found to be the reactive oxygen species responsible for enhanced contaminant

desorption. The conceptual model for the enhanced treatment of sorbed contaminants is that desorption of the contaminant is promoted by superoxide, followed by contaminant destruction via hydroxyl radical or superoxide in the bulk solution.

Delivery of hydrogen peroxide and its interaction with subsurface chemistry was the final aspect of the project. Soil organic matter does not significantly affect contaminant destruction when CHP is conducted at acidic pH regimes. At neutral pH regimes, soil organic matter enhances the effectiveness of CHP treatment. Release of metals during CHP remediation is metal- and sorbent-specific. Superoxide generated at neutral pH can promote the release of some metals sorbed on kaolinite. However, cadmium and lead sorbed on the natural soils studied were not released by CHP reactions conducted at neutral pH, but were released in reactions at pH 3, due primarily to the destruction of organic matter. Screening of 14 salts of low-molecular weight organic acids showed that three have potential for stabilizing hydrogen peroxide: citrate, malonate, and phytate slowed hydrogen peroxide decomposition by up to three orders of magnitude in some mineral slurries and soils. Furthermore, the generation of hydroxyl radical and superoxide was not affected significantly in the presence of the stabilizers. The effectiveness of the stabilizers was confirmed in column flow-through studies; minimal hydrogen peroxide decomposition or plugging of the column occurred in columns of iron oxide- and manganese oxide-coated sand in the presence of stabilizers. Dosing the one-dimensional columns with a combined stabilizer-hydrogen peroxide solution resulted in equally effective hydrogen peroxide stabilization compared to preconditioning the columns with the stabilizer followed by dosing with hydrogen peroxide. Furthermore, the stabilizers were not destroyed in the columns and were transported through the columns at the same rate as the hydrogen peroxide.

The results of this research demonstrate that CHP is characterized by more complex chemistry than previously conceived. In particular, superoxide has a major role in the degradation of highly oxidized contaminants, the destruction of DNAPLs, and the enhanced desorption of hydrophobic contaminants from soils and subsurface solids. The suite of reactive oxygen species generated in CHP reactions, including hydroxyl radical, superoxide, and the strong nucleophile hydroperoxide, provide a near-universal treatment matrix. However, the rapid decomposition of hydrogen peroxide, promoted by natural iron and manganese oxides in the subsurface, has previously limited the utility of CHP for the remediation of contaminated sites. Advances attained through the completed research in the stabilization of hydrogen peroxide by citrate, malonate, and phytate will increase the utility and economic viability of CHP treatment. The results of this research will enable field personnel to better design CHP ISCO systems and apply the process more effectively and economically.

5. OBJECTIVES

SERDP Relevance

Contamination of aquifers with synthetic organic chemicals is a significant concern. In particular, chlorinated solvents, such as 1,1,1-trichloroethane (TCA) and trichloroethylene (TCE), are commonly found in the sorbed phase or as dense nonaqueous phase liquids (DNAPLs) in groundwaters underlying Department of Defense (DoD) facilities. In recent years, various methods of *in situ* chemical oxidation (ISCO) have been used at DoD sites; however, results have been mixed and there is a need for basic research that can be applied to the full-scale use and optimization of ISCO.

Catalyzed H_2O_2 propagations (CHP; modified Fenton's reagent) is an increasingly popular ISCO process. It is based on the standard Fenton's reaction, in which the decomposition of a solution of dilute hydrogen peroxide is catalyzed by excess iron (II), resulting in near-stoichiometric generation of hydroxyl radicals (OH):

$$H_2O_2 + Fe^{2+} \rightarrow OH\bullet + OH^- + Fe^{3+} \quad [1]$$

Hydroxyl radical, a relatively non-specific oxidant that reacts with most organic compounds at near diffusion-controlled rates, readily attacks even highly chlorinated compounds, such as TCA, TCE, perchloroethylene (PCE), and polychlorinated biphenyls (Haag and Yao, 1992). Fenton's reagent is usually modified for ISCO by using higher concentrations of hydrogen peroxide and varying the type of catalyst (i.e., iron (III), iron chelates, or iron oxyhydroxide minerals).

CHP has been applied at hundreds of sites over the past few years (ESTCP, 1999). Practitioners have used a range of catalysts with and without acid addition (acidic conditions maintain the solubility of the iron catalyst). Results from CHP ISCO have been mixed: soluble, sorbed, and DNAPL forms of contamination have been destroyed at some sites, while minimal treatment has been found at other sites. The common practice in the field has been to increase the concentration of hydrogen peroxide when treatment has been unsuccessful. This practice often enhances treatment effectiveness, which is likely related to driving propagation reactions that form reactive transient oxygen species other than hydroxyl radicals.

Hydroxyl radical reactions in CHP reactions are important because they provide the potential for oxidizing many biorefractory compounds, such as TCE and PCE. However, hydroxyl radicals react at diffusion-controlled rates; i.e., they are extremely short-lived and react as soon as they are formed at that very location. Therefore, hydroxyl radicals are incapable of reacting with sorbed or DNAPL contaminants (Sedlak and Andren, 1994). However, other species formed in CHP reactions, such as superoxide anion, are relatively long-lived in water, and also long-lived in DNAPLs and soil organic matter (Afanas'ev, 1989), allowing for their transport into these regions to displace and degrade sorbed contaminants and to disrupt and destroy DNAPLs. The proposed research is based on the tenet that, in order for CHP ISCO to be successful, the generation of an optimum mixture of hydroxyl radicals and other transient oxygen species is necessary. This goal may be achieved by practitioners if the fundamental reactions that promote the generation of the different oxygen transients are further elucidated.

Technical Objectives

Based on the recent developments in the application of Fenton's chemistry to subsurface remediation, the research focused on the following objectives:

1.   To determine the potential for natural subsurface materials to catalyze the decomposition of hydrogen peroxide to transient oxygen species.

2.   To investigate the generation of hydroxyl radicals, superoxide, and hydroperoxide anions produced in CHP reactions as a function of soluble iron and hydrogen peroxide concentrations.

3.   To determine the degradation pathways of one reduced contaminants and oxidized contaminants under the influence of varying concentrations of hydroxyl radicals, superoxide, and hydroperoxide anions.

4.   To determine the reactive oxygen species responsible for DNAPL destruction by CHP reactions and to determine the optimal reaction conditions for DNAPL destruction.

5.   To determine the reactive oxygen species responsible for the enhanced desorption of sorbed.

6.   To investigate CHP process conditions that promote the effective delivery of hydrogen peroxide to the subsurface, effective transport downgradient, and effective treatment stoichiometry.

6. BACKGROUND

The improper disposal of hazardous wastes has resulted in tens of thousands of contaminated sites in the United States and throughout the world. Methods for the cleanup of these sites have evolved over the past 25 years; the first approaches focused on excavation of source areas and the pump-and-treat cleanup of groundwater. Subsequently, bioremediation was the primary remediation process used throughout the 1980s and much of the 1990s. Tens of millions of dollars were spent on bioremediation research and many new advances were established in the areas of electron acceptor systems, reductive dehalogenation of chlorinated and fluorinated solvents, and the use of methanothrophs (Rittman et al., 2002). However, when controlled field experiments were performed at many bioremediation sites in the early 1990s, contaminants at the active bioremediation plots often degraded no faster than control plots (Wiedemeier et al., 1999). As a result, natural attenuation, or allowing the contaminants to degrade without addition of nutrients, terminal electron acceptors, or other active remedial process additions, often became the treatment method of choice. However, monitored natural attenuation (MNA) has numerous limitations. Years or decades may be required before site closure can be established, and responsible parties are liable until the contaminants are transformed to acceptable levels (Small, 1998). Numerous other site remediation processes have been used for the saturated and unsaturated zones. Saturated zone technologies include air sparging and permeable reactive barriers, and common technologies for the unsaturated zone include soil vapor extraction and bioventing. Like most remediation technologies, each of these has limitations, which generally fall into two categories: 1) reactivity with contaminants of concern and 2) mass transfer of contaminants from the sorbed phase and DNAPLs to the medium in which the reactive species exists, usually water (Watts, 1998).

In the 1990s, the first reports were published on *in situ* chemical oxidation (ISCO) (Watts et al., 1990; Schnarr and Farquhar, 1992), and by the mid-1990s, specialty companies had been established that offered ISCO services almost exclusively. *In situ* chemical oxidation is the delivery of strong chemical oxidants to the subsurface for the purpose of treating organic contaminants. The first ISCO process that was investigated in laboratory research and developed at full scale was catalyzed H_2O_2 propagations (CHP), commonly known as modified Fenton's reagent (Watts et al., 1990; Tyre et al., 1991). Shortly following the initial use of Fenton's reagent, ozone sparging and permanganate treatment came into widespread use (Siegrist et al., 2001). In just the past few years, interest in another oxidant, persulfate, has provided yet another option for ISCO remediation.

Three limitations are commonly found in soil and groundwater remediation processes: contaminant sorption, the low reactivity of some contaminants and their degradation products with the transforming species, and the presence of NAPLs. Enhanced degradation of sorbed contaminants has recently been documented using CHP (Watts et al., 1994; Spencer et al., 1996). Watts et al. (1994) found that, at successively high hydrogen peroxide concentrations, sorbed hexachlorobenzene was degraded more rapidly than it was desorbed. Similar enhanced desorption was reported by Gates and Siegrist (1995) and Watts et al. (1997). In addition, destruction of DNAPLs under field conditions has been observed by Denham et al. (2000). Because hydroxyl radicals are so short lived, the key to the destruction of sorbed and nonaqueous phase contaminants appears to be in non-hydroxyl radical mechanisms.

CHP Chemistry. The use of modified Fenton's reagent, or catalyzed H_2O_2 propagations (CHP), has become increasingly popular for the *in situ* and *ex situ* treatment of surface soils and the *in situ* remediation of the subsurface. The process is based on the catalyzed decomposition of hydrogen peroxide by soluble iron, iron chelates, or iron minerals to generate the strong oxidant hydroxyl radical (OH•), as well as other reactive oxygen species. CHP is very different from Fenton's reagent, which is a laboratory procedure in which dilute hydrogen peroxide is slowly added to a solution of excess iron (II) to generate hydroxyl radical (Walling, 1975):

$$H_2O_2 + Fe^{2+} \rightarrow OH• + OH^- + Fe^{3+} \qquad k = 76 \text{ M}^{-1} \text{ s}^{-1} \qquad (1)$$
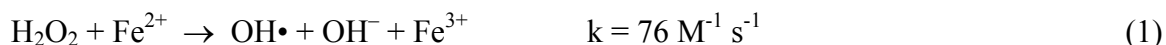
Hydroxyl Radical Reactions. The oxidant of interest in CHP has traditionally been hydroxyl radical, one of the strongest oxidants found in nature. The most common reactions of hydroxyl radical are electrophilic substitution to aromatic compounds and addition to alkenes. Another class of hydroxyl radical reactions is hydrogen abstraction from saturated compounds such as alkanes, a pathway that proceeds at a slower rate relative to electrophilic substitution and addition.

The rate of reaction of hydroxyl radical with an organic compound (C) is described by the second-order rate expression:

$$-\frac{dC}{dt} = k[C][OH•] \qquad (2)$$

Chemicals that react very rapidly with hydroxyl radical are limited by the rate of diffusion of hydroxyl radical in water, which is $\approx 10^{10}$ M^{-1} s^{-1}, rather than the rate at which it attacks the chemical. Therefore, the rate at which hydroxyl radical attacks highly reactive contaminants in aqueous systems is referred to as diffusion-controlled. Some general rules have been established for the reactivity of hydroxyl radical with organic contaminants. Rate constants $>10^9$ M^{-1} s^{-1} are considered high enough to be effective for ISCO treatments, while rate constants $<10^8$ M^{-1} s^{-1} are considered too low to be effective (Watts, 1998). The data of Table 2 show that almost all aromatic compounds, even those with a high degree of halogenation, react rapidly with hydroxyl radical. Chlorinated alkenes, such as trichloroethylene (TCE) and perchloroethylene (PCE), also react rapidly. In contrast, alkanes exhibit relatively low reactivity with hydroxyl radical; in particular, chlorinated and fluorinated alkanes such as carbon tetrachloride, chloroform, hexachloroethane, and freons (e.g., 1,1,2-trichloro-2,2,1-trifluoroethane), are effectively non-reactive.

Non-Hydroxyl Radical Species. With the high concentrations of hydrogen peroxide used for CHP ISCO (i.e. 2–20% [0.6–3.6 M]), hydroxyl radical generated in the Fenton's initiation reaction (equation 1) reacts with hydrogen peroxide to promote a series of propagation reactions (Walling, 1975; Buxton et al., 1988):

$$OH• + H_2O_2 \rightarrow HO_2• + H_2O \qquad k = 2.7 \text{ x} 10^7 \text{ M}^{-1}\text{s}^{-1} \qquad (3)$$

$$HO_2• \leftrightarrow O_2•^- + H^+ \qquad pK_a = 4.8 \qquad (4)$$

$$R• + H_2O_2 \rightarrow ROH + OH• \qquad k = 10^6\text{-}10^8 \text{ M}^{-1}\text{s}^{-1} \qquad (5)$$

$$HO_2\bullet + Fe^{2+} \rightarrow HO_2^- + Fe^{3+} \qquad\qquad k = 1.2 \text{ x } 10^6 \text{ M}^{-1}\text{s}^{-1} \qquad\qquad (6)$$
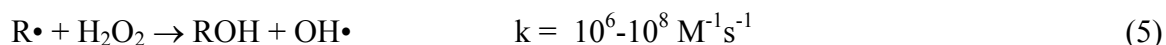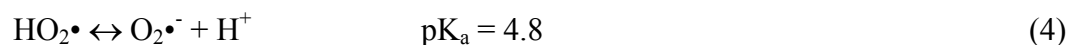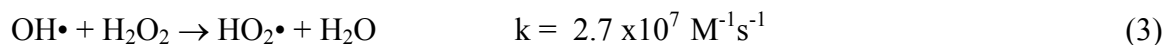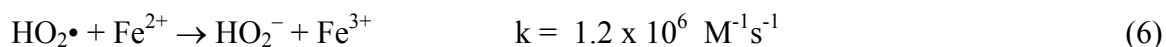
Although the rate constant for reaction (3) is relatively low, these reactions become important when the concentration of hydrogen peroxide is high (e.g., > 1%). Therefore, the rates of generation of perhydroxyl radical ($HO_2\bullet$), superoxide radical anion ($O_2\bullet^-$), and hydroperoxide anion (HO_2^-) become significantly greater at higher hydrogen peroxide concentrations. Perhydroxyl radical is a relatively weak oxidant; superoxide is a weak reductant and nucleophile in aqueous systems, and hydroperoxide anion is a strong nucleophile. Although some of these species (e.g., superoxide) are not very reactive in deionized water, their reactivity is significantly increased in systems that have solutes such as hydrogen peroxide, which provides a solvent effect, increasing the reactivity of superoxide (Smith et al., 2004). CHP reactions that generate hydroxyl radicals, superoxide, and hydroperoxide provide a mixture of oxidants, reductants, and nucleophiles that can degrade almost all organic contaminants. For example, carbon tetrachloride and hexachloroethane, which are unreactive with hydroxyl radical, are rapidly degraded in CHP systems through reactions with superoxide in the presence of sufficient hydrogen peroxide to provide a solvent effect (Watts et al., 1999; Teel and Watts et al., 2001; Smith et al., 2004). Therefore, these reactive oxygen species increase the range of CHP reactivity, making CHP a near-universal treatment system.

CHP ISCO. Some of the important process parameters for CHP ISCO include the nature of the catalyst, the pH, and the hydrogen peroxide concentration. Soluble iron and iron chelates have been added as CHP catalysts (Sun and Pignatello, 1992; Pignatello and Baehr, 1994). In addition, the iron oxide minerals naturally present in the subsurface serve as effective CHP catalysts (Tyre et al., 1991; Watts et al., 1993). Soluble iron and iron minerals are most effective at acidic pH, and iron chelates are also effective at neutral pH regimes. The pH of CHP systems is a very important process parameter. If iron minerals are used as the CHP catalyst, the pH must be maintained at less than pH 4. Reactions 1–5 are sensitive oxidation-reduction conditions, and the acidic pH regime provides suitable redox conditions; in addition, the acidic conditions aid in maintaining soluble iron in solution. If iron chelates are used, the reactions can be conducted at neutral pH regimes. Hydrogen peroxide concentrations in the 2–12% (0.6–3.6 M) range are typically used for ISCO applications, and the common practice in the field has been to increase the concentration of hydrogen peroxide when treatment has been unsuccessful. This practice often enhances treatment effectiveness, in part because the high hydrogen peroxide concentration provides a pool of the oxidant source. More importantly, however, high hydrogen peroxide concentrations (> 1% [0.3 M]) also promote propagation reactions that form reactive oxygen species other than hydroxyl radicals, such as perhydroxyl radicals, superoxide radical anions, and hydroperoxide anions, which have a significant role in CHP remediation (Watts and Teel, 2005).

Enhanced Treatment of Sorbed Contaminants and DNAPLs. A distinct advantage of CHP over other ISCO processes is the documented enhanced treatment of sorbed contaminants and DNAPLs. These contaminants are problematic because almost all reactants used in soil and groundwater remediation (e.g., bacteria, hydroxyl radical, reductants) exist in the aqueous phase. Therefore, sorbed contaminants must desorb or dissolve into the aqueous phase before transformation can occur. As the contaminants are degraded in the aqueous phase, a concentration gradient increases between the sorbed phase and the aqueous phase, driving subsequent desorption or dissolution (Watts et al., 1994; Yeh et al., 2003; Watts et al., 2004). Such treatment is referred to as desorption- or dissolution-limited, and can require years or even

9

decades for site cleanup (Watts, 1998). However, CHP has the potential to treat sorbed contaminants and DNAPLs significantly more rapidly than the rate of desorption or dissolution. In some cases, the rate of sorbed contaminant or DNAPL destruction can be up to 100 times faster than the rate of desorption- or dissolution-limited treatment. These results have also been seen in the field; rapid treatment of sorbed contaminants and DNAPLs has been demonstrated in numerous field studies (U.S. DOE, 1999).

Hydrogen Peroxide Stability. Although CHP is a universal treatment system that degrades any organic contaminant studied to date, it is characterized by a significant shortcoming: high rates of hydrogen peroxide decomposition in surface soils and the subsurface. The half life of hydrogen peroxide varies substantially in ISCO applications, ranging from a few hours to 10 days at its uppermost limit (ESTCP, 1999). Soil organic matter (SOM) may affect hydrogen peroxide stability; however, the reactions between SOM and hydrogen peroxide are complex and not well studied. Soil organic matter is destroyed by hydrogen peroxide; however, SOM does not appear to have a significant effect on hydroxyl radical activity (Tyre et al., 1991). Therefore, hydrogen peroxide stability is the primary factor that determines well spacing at CHP treatment sites. The rate of hydrogen peroxide decomposition should be used in conjunction with the pore water velocity to determine the radius of influence for injection wells. If the hydrogen peroxide decomposition rate is slow, well centers are typically 25–30 feet (7.6–9.1 m); rapid hydrogen peroxide decomposition dictates injection wells on 5–10 foot (1.5–3.0 m) centers.

In summary, the combination of hydroxyl radicals, superoxide, and hydroperoxide anions likely have important roles in CHP ISCO;, they can potentially oxidize reduced compounds and reduce oxidized compounds, increasing the likelihood of mineralization of recalcitrant contaminants. Some trace minerals may provide the key to mediating the generation of these reactive oxygen species, which may explain why modified CHP ISCO has been successful at some sites, but not others. The research conducted through Project CU-1288 was initiated to better understand the mechanisms and pathways of CHP ISCO with the ultimate goal of providing more effective clean up of contaminated sites.

7. MATERIALS AND METHODS

Common materials and analytical procedures used throughout the project.

Material.s

Sodium thiosulfate, sulfuric acid, sodium hydroxide, potassium iodide, ammonium molybdate, toluene (>99%), isopropanol (2-propanol) (>99%), ethanol (>99%), acetone (propanone) (99.6%) Scintilene, ethyl acetate, Ethylenediaminetetraacetic acid (EDTA), mixed hexanes, iron (III) sulfate, and Millipore Millex-GP 0.22 μm filters were obtained from Fisher Scientific (Fair Lawn, NJ). Carbosorb and Scint-A-XF, iron (II) sulfate, ethyl acetate, pentane, sulfuric acid, Scintallene counting cocktail, and phosphoric acid were also purchased from Fisher Scientific.

Carbon tetrachloride (99.9%), pentane, purified silica sand, potassium hydroxide (99.9%), and magnesium chloride (99.9%), chloroform (99.9%), and tert-butyl alcohol (99.8%), manganese (II) sulfate (99%), 1-hexanol, sodium nitrilotriacetate (NTA), zinc (II) sulfate, and copper (II) chloride were purchased from JT Baker (Phillipsburg, NJ).

Potassium superoxide (KO_2), diethylenetriamine-pentaacetic acid (DTPA), decane (>99%), and hexaketocyclohexane (HKCH) (97%), 1,1,1-trichloroethane (TCA), 1,2-dichloroethane (DCA),), sodium citrate, and decane (>99%), trichloroethylene (trichloroethene) (99.9%), perchloroethylene, (tetrachloroethene) (99.9%), decane (>99%), 1-heptanol (99%), 1-octanol (99%), 1-nonanol (98%), 1-decanol, iron (II) perchlorate (99%), *n*-dodecane (99%), dodecyl aldehyde (92%), sodium perborate, perchloroethylene (PCE) nitrilotriacetic acid (NTA), potassium nitrate, ethylene glycol (ethane diol) (>99%), 2-(hydroxymethyl)piperidine (2-HMP, 97%), and N,N-dimethylformamide (DMF; 99.8%), ethylene diaminetetraacetic acid disodium salt (EDTA), nickel (II) sulfate, cadmium (II) sulfate, lead (II) nitrate, sodium gallate, sodium malate, sodium malonate, sodium oxalacetate, sodium oxalate, sodium phytate, sodium pyruvate, and sodium succinate , hexachlorobenzene (99%) were purchased from Sigma-Aldrich (Milwaukee, WI).

ORBO[fi] 24, ORBO[fi] 32s, and Carbotrap 200 gas adsorbent tubes were purchased from Supelco (St. Louis, MO). Magnesium hydroxide (>99%), methanol (>99%), sodium hexametaphosphate were purchased from VWR (West Chester, PA). Hydrogen peroxide was provided *gratis* by Solvay Interox (Deer Park, TX). A Barnstead NANOpure II system was used to purify water used in all reactions to >18 MΩ-cm. Borosilicate vials with PFTE septum closures (VWR) were used as laboratory-scale batch reactors.

For potassium superoxide systems, sodium hydroxide was purified by adding 0.2 g magnesium chloride to 1 L of a 0.1 M NaOH solution, which was then stirred for 12 h and passed through a 0.45 μm membrane filter (Monig et al., 1983).

Common analytical procedures.

The probe compounds *n*-hexanol and carbon tetrachloride were analyzed using a HP 5890A gas chromatograph fitted with a 30 m x 0.53 mm DB-5 capillary column (J & W Scientific). *n*-Hexanol and CT were analyzed by a flame ionization detector (FID) and electron capture detector (ECD) respectively. For FID analysis, the injection temperature was set at 275˚C with the detector temperature at 350˚C. The injection and detector temperatures were set 260˚C and 400˚C respectively for the ECD. For analysis of both probes, the initial temperature was set at 40˚C with an initial time of 3 minutes while the intermediate program rate was 5˚C. When the temperature reached 45˚C, the final program rate was set at 45˚C min^{-1} with a final temperature of 280˚C.

Aliquots collected for metals analysis were acidified with 0.01 mL concentrated HNO_3 and then analyzed for the metals using a Perkin-Elmer 3100 atomic absorption spectrophotometer with an acetylene flame. Cadmium was measured at 326.1 nm, copper at 222.6 nm, lead at 368.3 nm, nickel at 323.3 nm and zinc at 213.9 nm.

Chloride ions released in CT experiments were measured by a Fisher ion electrode and a double junction reference electrode, and the pH of the samples was measured with a Fisher Accumet pH meter 9100.

Hydrogen peroxide concentrations > 100 mg/L were determined by iodometric titration with 0.1 N sodium thiosulfate (Schumb et al., 1955). Hydrogen peroxide concentrations < 100 mg/L were determined by complexation with $TiSO_4$ followed by spectrophotometric quantitation of the complex using a Genesys Spectronic 20 (Masschelein, 1977).

7.1 Factors That Control Hydrogen Peroxide Decomposition

7.1.1 Rates of Hydrogen Peroxide Decomposition Mediated by Iron Oxides, Manganese Oxides, and Trace Minerals

Minerals

Samples of four naturally occurring iron and manganese minerals (goethite [FeO(OH)], hematite [Fe_2O_3], manganite [MnO(OH)], and pyrolusite [MnO_2]) and seven naturally occurring trace minerals (anatase [TiO_2], bauxite [Al(OH)$_3$], cuprite [Cu_2O], ilmenite [$FeTiO_3$], magnesite [$MgCO_3$], siderite [$FeCO_3$], and willemite [Zn_2SiO_4]), collected from sites through North America were purchased from DJ Minerals (Butte, MT). The minerals, which were received as cubes approximately 1 cm x 1 cm 1 cm, were crushed to a fine powder using a 150 mL capacity Spex shatter box with hardened steel as a grinder. Surface areas were determined by BET analysis under liquid nitrogen on a Coulter SA 3100 (Carter et al., 1986).

Procedures

The catalyzed decomposition of H_2O_2 was investigated by adding 10 mL of varying concentrations (0.5% and 2%) of H_2O_2 to 1 g of each of the minerals at pH 3 or pH 7 regimes (i.e., a 2 x 2 matrix of two H_2O_2 concentrations and two pH regimes). Aliquots of 0.2 mL were collected at a minimum of ten time points and analyzed for residual H_2O_2 by iodometric titration (Schumb et al., 1955). All reactions were conducted in triplicate in a water bath at 25 ± 2 ˚C. Control systems consisted of the same reactors with H_2O_2 without the addition of minerals. Hydrogen peroxide residuals as a function of time were plotted and fit to first order kinetics. First order rate constants were then normalized to the surface area of the mineral.

7.1.2 Correlation of Hydrogen Peroxide Decomposition Rates with Soil Properties

Samples of 11 naturally occurring soils or subsurface solids collected from sites through North America were investigated for their potential to decompose hydrogen peroxide. The soil samples and subsurface solids were analyzed for surface area, organic carbon content, and amorphous and crystalline iron and manganese oxides.

Catalyzed decomposition of hydrogen peroxide was investigated by adding 10 mL of 2% hydrogen peroxide to 1 g of the soils or subsurface solids at pH 3 or pH 7 regimes. Hydrogen peroxide concentrations were then analyzed at specified time points by iodometric titration with 0.1N sodium thiosulfate.

7.2 Reactive Oxygen Species Generation in Different CHP Systems

7.2.1 Oxidative and Reductive Pathways in Manganese-Catalyzed CHP Reactions

Manganese oxide

The manganese oxide mineral pyrolusite (ß-MnO_2) was purchased from D. J. Minerals (Butte, Montana) and was crushed to a fine powder using a 150 mL capacity Spex shatter box with hardened steel as a grinder. The pyrolusite surface area was 5.2 m^2/g, as determined by BET analysis under liquid nitrogen on a Coulter SA 3100 (Carter et al., 1986). Its mineralogical content was verified by x-ray diffraction. Amorphous manganese oxides were prepared by raising the pH of 400 ml of 1 M manganese (II) sulfate (pH 3.0) to pH 7.8 using 1 M NaOH followed by the addition of 50 ml of 1200 mM hydrogen peroxide (Stone and Morgan, 1984). The manganese oxide was removed, rinsed twice in double deionized water, and air-dried. X-ray diffraction of the solid showed a mineralogical content of 52 amorphous and crystalline manganese oxides. The predominant amorphous manganese oxides included MnO, Mn_2O_3, Mn_2O_7, and the major crystalline manganese oxide was hausmannite.

Probe compounds

The probe compounds were selected based on their ability to react solely through either oxidation or reduction. Carbon tetrachloride (CT) was used as a reductant probe (Peyton et al., 1995) because it is readily reduced (k_{e-} = 1.6 x 10^{10} $M^{-1}s^{-1}$) (Buxton et al., 1988) but is not oxidized by hydroxyl radicals ($k_{OH\bullet}$ < 6 x 10^6 $M^{-1}s^{-1}$) (Buxton et al., 1988). In contrast, 1-hexanol was used as an oxidant probe because it is readily oxidized by hydroxyl radicals ($k_{OH\bullet}$ = 3 x 10^9 $M^{-1}s^{-1}$) but is not readily reduced (k_{e-} = 2 x 10^7 $M^{-1}s^{-1}$) (Buxton et al., 1988). Based on the linear range of analysis, initial concentrations of CT and 1-hexanol were 10 µM and 2 mM, respectively. Stock solutions of the individual probe compounds were prepared within 24 h of each reaction.

CHP reactions

Two variables were investigated in manganese-catalyzed CHP reactions: the nature of the manganese catalyst and the pH of the reaction. CHP reactions with 10 ml total volume were conducted in 40 ml borosilicate glass reactors fitted with PFTE caps; triplicate reactors were prepared for each time point. When soluble manganese was used as the catalyst, manganese (II) sulfate was combined with the probe compound stock solution and then hydrogen peroxide was added for a final concentration of 200 mM manganese (II) and 600 mM hydrogen peroxide. The pH was then adjusted by adding 0.1 M H_2SO_4 or 0.1 M NaOH; specific pH regimes investigated included pH 3, 4, 5, 6, 6.4, and 6.8. Reactions using solid forms of manganese oxides received 25 mg of the manganese oxide and 10 ml of hydrogen peroxide followed by adjustment to pH 6.8. As the reactions proceeded, total reactor contents were extracted with hexane at selected times, which varied depending on the rate of the reaction. The extracts were then analyzed by gas chromatography. Control reactions were conducted in parallel using the manganese catalysts but with double deionized water in place of hydrogen peroxide.

Verification of CT degradation

Carbon tetrachloride degradation was confirmed by monitoring chloride release in parallel reactions, which contained 1 mM CT in order to generate sufficient chloride for detection. Aliquots were collected and chloride was measured using a Fisher Accumet chloride ion-specific electrode paired with a double-junction reference electrode.

7.2.2 Mechanisms of Oxidation and Reduction in CHP Reactions Catalyzed by Soluble Iron at Different pH Regimes

Catalyst.

Iron (III) perchlorate was reported to be the most effective catalyst in CHP reactions (Watts and Dilly, 1997); therefore, it was used as the catalyst for most reactions. However, to eliminate interferences caused by chlorate ions from iron (III) perchlorate, iron (III) sulfate was used for reactions in which chloride release was measured.

Probe compounds.

n-Hexanol and carbon tetrachloride (CT) were used as an oxidant probe and a reductant probe, respectively. *n*-Hexanol exhibits high reactivity with hydroxyl radicals (k_{OH} = 7.0 x 10^9 M^{-1} S^{-1}, Buxton et al., 1988), but is almost unreactive with reductants (k_{e^-} = < 10^6 M^{-1} S^{-1}). Conversely, CT is reactive with superoxide in water in the presence of a cosolvent (Smith et al., 2004).

Sample preparation.

Stock aqueous solutions containing either carbon tetrachloride (CT) or *n*-hexanol were prepared in 1 L flat bottom flasks using deionized water and stirred until dissolution was complete. Nitrilotriacetic acid (NTA) was prepared fresh in 1 L round bottom flasks at 80 ˚C. Iron (III) perchlorate was then added to the flask to form iron-NTA complex. The mixture was allowed to cool to room temperature and the pH was then slowly adjusted to pH 3, 5, 7, or 9 by adding 1N sodium hydroxide. Hydrogen peroxide stock solutions were diluted using double deionized water.

Experimental procedures.

All reactions were run in triplicate, 10 mL in volume, and conducted in 40 mL borosilicate glass vials with Teflon septa caps at room temperature (20 ± 3˚C). The initial concentration of the probe compounds was 1.0 ± 0.05 mM and the range of hydrogen peroxide concentrations varied from 14.7 to 1470 mM. Hydrogen peroxide concentrations higher than 1470 mM were avoided to minimize oxygen evolution that could enhance volatilization of the probe compounds. The reactions were conducted at pH 3, 5, 7 and 9. The concentration of the iron-NTA complex (1:1 molar ratio) was maintained at 1 mM in all experiments. The reactions that used iron catalysts without NTA chelation were carried out to assess any possible effect of NTA on the degradation of the probe compounds. Over several time points, 0.5 mL of sulfuric acid was added to quench the reactions (Watts et al., 1990) before the probe compounds were extracted with 10 mL of hexane. Due to the high sensitivity of the electron capture detector

toward chlorinated compounds, CT extractions were further diluted 1000 fold before analysis. Control experiments were conducted in parallel using systems in which either the iron complex catalyst or hydrogen peroxide was replaced by deionized water.

Scavenging analyses.

  To confirm reaction mechanisms, a variety of oxidant and reductant scavengers were added in excess to the probe compounds; isopropanol and *tert*-butyl alcohol were used to scavenge oxidizing species; Rush and Koppenol (1986) used isopropanol as a ferryl (FeO^{2+}) - chelate complex quencher and tert-butyl alcohol as hydroxyl radical scavenger. Teel and Watts (2002) proposed the use of excess nitrate for quenching aqueous electrons and excess chloroform for scavenging reductants.

7.2.3 Evaluation of Oxidation and Reduction Processes in CHP Reactions Catalyzed by Soluble Iron at Different pH Regimes

Probe compounds and experimental procedures.

  The same probe compounds and experimental procedures were used as in the procedures outlined in Section 7.2.2.

Experimental design.

  A central composite rotatable experimental design was used to investigate the effect of iron complex catalyst and hydrogen peroxide concentrations on relative rates of hydroxyl radical and superoxide generation measured by the degradation of the probe compounds. The rotatable design included 8 corner points, 6 star points and 5 center points. The contour plots were generated from those points and the interactive effects of variables were represented by a three-dimensional regression equation (Box et al., 1987). Three-dimensional plots were developed from the regression equations using SYSTAT software. The relative amount of destruction of the probe compounds were represented by the contour plots. Iron catalyst and hydrogen peroxide concentrations ranged from 0.05 mM to 5 mM. Central composites were developed for *n*-hexanol at pH 3 and 5, CT at pH 3, 5, 7, 9, and one experiment with the iron catalyst. All CT central composite experiments were conducted within a 3-hour time period. Response surfaces for *n*-hexanol destruction at pH 7 and 9, and for one experiment in the absence of NTA, were not conducted due to the relative high reaction rates of *n*-hexanol in these CHP systems.

7.3 Degradation Products

7.3.1 Identification of the Reactive Oxygen Species Responsible for Carbon Tetrachloride Degradation in CHP Systems

Materials

Stock solutions of CT (5 mM) and iron (III) sulfate (75 mM) were prepared prior to conducting reactions and were used within one day. Sodium hydroxide solutions were purified to remove transition metals by the addition of magnesium hydroxide (Monig et al., 1983). The magnesium hydroxide–NaOH solution was stirred for 8 h, allowing a floc to form; the solution was then passed through a 0.45 μm filter to remove the floc containing the metal impurities.

CHP reactions

CHP reactions were conducted under minimal light in 20 mL borosilicate vials capped with PTFE-lined septa. All reactions were performed in triplicate, and the data were analyzed by averaging the results from the three replicates. Reactions consisted of 15 mL of 1 mM CT, 0.5 mM iron (III), and 0.1 M, 0.5 M, or 1 M H_2O_2 to provide a $HO_2\bullet/O_2\bullet^-$-driven reaction (Eq. 5). The pH (initially 2.2–2.4) was adjusted to 3.0 using 60 mM NaOH. The reactions were conducted at $20 \pm 1°C$ in a water bath, and steady-state conditions were maintained by adding 60 mM NaOH and 13.8 M H_2O_2 when the pH dropped below 2.7 and $[H_2O_2]$ dropped more than 7% below the initial concentration. Triplicate control reactions were conducted in parallel with double-deionized water used in place of H_2O_2. Carbon tetrachloride concentrations were quantified at selected time points by extracting the entire reactor with decane and analyzing the extracts by gas chromatography. Carbonate concentrations were evaluated by trapping the off gas in 0.1 M NaOH and analyzing with ion chromatography. For $OH\bullet$ scavenging experiments, reactions consisted of 1 mM CT, 1 M H_2O_2, and 0.5 mM iron (III) and were amended with 1 M isopropanol to scavenge $OH\bullet$ generated in the system, resulting in a perhydroxyl-driven reaction:

$$H_2O_2 + Fe^{3+} \rightarrow HO_2\bullet + Fe^{2+} + H^+ \tag{1}$$

Reaction of CT with $O_2\bullet^-$

Potassium superoxide in deionized water was used to generate $O_2\bullet^-$ as the sole reactive species, based on the methodology of Marklund (1976). Reactions were conducted in triplicate borosilicate reactors and consisted of a 15 mL volume of 1 mM CT, 2 M KO_2, 33 mM purified NaOH, and 1 mM DTPA (to bind and inactivate transition metals) at pH 14 to minimize the dismutation of $O_2\bullet^-$ (Csanyi et al., 1983). Solid KO_2 was mixed into a 4°C NaOH-DTPA solution; under these conditions, the half-life of $O_2\bullet^-$ was 110 min, which was quantified by measuring the rate of oxygen evolution using a manometer attached to a reaction vessel. Triplicate control reactions were conducted in parallel using deionized water in place of KO_2.

Monitoring of volatile compounds

Volatilized CT and its degradation products were trapped using gas adsorbent tubes connected to a Teflon gas sampling port inserted into a silicone-sealed hole placed in the septum. ORBO® 24 tubes were used to trap phosgene in the off gas using OSHA Method 61 (OSHA, 1986). ORBO® 32s tubes were used to trap CT, which was extracted with decane over 30 min followed by analysis of the extract using gas chromatography. Carbotrap 200 tubes were used to trap all possible degradation products in the off gas for GC-MS analysis.

Reactivity of $O_2\bullet^-$ with CT in the presence of solvents

Hydrogen peroxide, ethylene glycol, methanol, ethanol, isopropanol, and acetone were added to KO_2–CT reactions to evaluate their effect on the reactivity of $O_2\bullet^-$. The KO_2-based reactions at pH 14 were repeated with the addition of 1 M of each of the solvents. Triplicate control reactions were conducted in parallel with deionized water used in place of KO_2.

Analysis

Decane extracts were analyzed using a Hewlett-Packard 5890A gas chromatograph with a 0.53 mm (i.d.) x 60 m Equity® 1 capillary column and flame ionization detector (FID). The injector temperature was 240˚C and the detector temperature was 300˚C; the initial temperature was 80˚C, the program rate was 20˚C min^{-1}, and the final temperature was 240˚C. Toluene extracts from OSHA Method 61 were analyzed on the same GC-FID with an initial temperature of 180˚C, program rate of 10˚C min^{-1}, and final temperature of 240˚C.

An Agilent 6890 gas chromatograph coupled with an Agilent 5973N mass selective detector fitted with a 30 m x 0.32 mm i.d. DB-5MS column was used to analyze off gas collected in Carbotrap 200 gas adsorbent tubes. Thermal desorption was used to release degradation products; prior to injection they were held in a liquid oxygen cooled cryogenic loop attached to the injection valve. Following injection, the initial oven temperature was -20˚C with a program rate of 10˚C min^{-1} to a final temperature of 180˚C.

Carbonate and chloride were analyzed using a Dionex-500 ion chromatograph with a 4 x 250 mm IonPac AS11-HC column and a Dionex CD 20 conductivity detector. The eluent was held at 10 mM NaOH for 8 min and then increased to 50 mM NaOH at a rate of 1.8 mM min^{-1} to a final time of 30 min.

7.3.2 Degradation of Perchloroethylene in CHP Systems

Sorbent

Silica sand (40–100 mesh) was purchased from Fisher Scientific.

Experimental methods

The reactions were conducted with 3.5 g of silica sand in 40 mL borosilicate glass vials using a PCE concentration of 100 mg PCE/kg sand. Since PCE has a relatively low boiling point (121˚C; melting point –22˚C), sand samples were kept at –5˚C for 2 h before and after spiking with PCE to prevent evaporation loss. The PCE recovered by this procedure without CHP treatment was > 90%. PCE was spiked on the sand by first dissolving it in pentane; the pentane was allowed to evaporate, leaving the PCE sorbed on the sand. To each vial, 17.5 mL of hydrogen peroxide was added, followed by 1.4 mL of $FeSO_4$ after pH adjustment with dilute H_2SO_4. The concentration of hydrogen peroxide was 2 M and the $FeSO_4$ concentration was 5 mM. The reaction was adjusted to pH 3 initially by an addition of dilute NaOH. The vials were closed with Teflon-coated septa caps and kept at 20±1˚C on a constant speed orbital shaker. The maximum reaction time for all samples was no more than 5 h. At each measurement period, CHP

reactions were terminated by an addition of 10 drops of concentrated H_2SO_4 before all the analytical measurements were made; the resulting pH for the sample was approximately 1.5. Perchloroethylene and other hydrophobic organic products were extracted with 3 mL of ethyl acetate.

Analysis

Perchloroethylene and the organic products were analyzed using a Hewlett-Packard 5890 gas chromatograph with flame ionization detector and a 0.32 mm (i.d.) x 30 m Supelco Nukol capillary column, or a 90 cm by 0.32 cm 60/80 Carbopack B/1% SP-1000 glass column; nitrogen was the carrier gas. Carbon dioxide evolved from mineralization of PCE with CHP was measured by the sealed ampule method with an OI Corporation Model 700 Total Organic Carbon (TOC) analyzer equipped with a purging and sealing unit; high purity nitrogen (>99.9%0 was used as the purging gas. Intermediate species were identified by comparing GC retention times with retention times of authentic standard of probable degradation products. In addtion, a Finnigan 4023 gas chromatograph-mass spectrometer with electron impact and chemical ionization capability and an INCOS data system was used to confirm product identification. Chloride measurements were conducted using a solid state Fisher chloride ion electrode paired with a double junction reference electrode.

7.3.3 Mineralization of a Sorbed Polycyclic Aromatic Hydrocarbon, Benzo[*a*]pyrene, in Two Soils Using Catalyzed Hydrogen Peroxide.

Materials.

[2,4-^{14}C]-Benzo[*a*]pyrene (^{14}C-BaP; 99% purity) with a specific activity of 10.7 mCi/mmol was purchased from Aldrich. Washed silica sand (80-100 mesh; 0.15-0.18 μm) was obtained from JT Baker. Sand characteristics were reported previously by Watts et al. *(*1999).

Soil characterization.

A Palouse loess soil was sampled from a wheat field near Pullman, WA. Particle size distribution was determined by the pipette method (Gee and Bauder, 1986). Organic carbon content was determined by combustion at 900 °C with evolved CO_2 trapped in KOH and measured by back titration of unreacted OH⁻ (Nelson and Summers, 1982). Amorphous and crystalline iron and manganese oxyhydroxides were assayed by citrate-bicarbonate-dithionite extractions (Jackson et al., 1986). Cation exchange capacity was established by saturation with sodium acetate at pH 8.2 (U.S. Soil Conservation Service, 1972). The soil characteristics are listed in Table 7.3.3-1. Based on the particle size distribution, the soil is classified as a silt loam.

Experimental design.

The experimental matrix for investigating BaP degradation conditions was a central composite rotatable experimental design using the concept of response surfaces (Cochran and Cox, 1992). Central composite rotatable designs are multivariable, multilevel experimental procedures that analyze the interactions between variables and produce response equations. These procedures have the potential to show statistically significant interactions between

variables, unlike a one-variable-at-a-time strategy, and can also lower the ultimate number of experiments conducted while maintaining a high degree of statistical significance in the results. In central composite designs, experimental parameters are chosen to achieve complete rotatability around the central point of a two-level matrix. Using such matrix designs, all of the vertices within the experimental boundaries are tested, and interpolation anywhere within the three-dimensional space is valid (Diamond, 1989).

The three variables investigated for oxidation of BaP in silica sand were H_2O_2 concentration (2,400 mM–12,300 mM), slurry volume (0.3–3.7 × 0.31 g/ml, field capacity of the silica sand), and iron (II) amendment (6.6 mM–23.4 mM). The levels for each variable were chosen to produce a completely rotatable design. The three variables investigated for oxidation of BaP in the Palouse loess soil were H_2O_2 concentration (1,500 mM–14,000 mM), slurry volume (1.0–20.0 × 0.42 g/l, field capacity of the Palouse loess), and pH (2.0–8.0) with CHP reactions catalyzed by naturally-occurring iron oxyhydroxides (Watts et al., 1993; Ravikumar and Gurol, 1994). The specific conditions and concentrations used for each variable based on the algorithm used for central composite rotatable experimental designs (Diamond, 1989) are listed in Table 7.3.3-2. The experimental data were analyzed by linear regression through least squares analysis to develop regression equations to describe the systems and to provide graphical representations of the data in the form of response surfaces (Box and Draper, 1987). Each term of the regression equation was validated by quantifying its standard error to ensure that it was within the 90% interval of a single sided t-distribution. In addition, the entire regression equation was evaluated based on the R^2 fit. The corresponding response surfaces were created using a SYSTAT® software package.

Oxidation procedures.
Soil and sand were dried at 105 °C for 24 hr followed by cooling in a dessicator for 2 hr. CHP reactions were conducted in 40-ml borosilicate glass vials containing 5 g of silica sand or Palouse loess spiked with 0.1 mmol/kg ^{14}C-BaP. The soils were prepared by adding 100 μl of a 1000 mM solution of BaP in ethyl acetate to produce a final concentration of 0.1 mmol/kg BaP with an activity of 548 μCi. The ethyl acetate was allowed to evaporate with the BaP remaining on the soil. It is likely that a portion of the BaP was not sorbed but remained as nonaqueous phase liquid (NAPL). In a similar study using hexadecane, 43% of the hexadecane remained in NAPL form in the soil and was destroyed along with sorbed hexadecane by CHP reactions (Watts and Stanton, 1999).

CHP reactions were conducted in the silica sand systems by adding freshly-prepared iron (II) sulfate and H_2O_2 followed by adjustment to pH 3 with 4.5 M H_2SO_4. The H_2O_2 was diluted to the concentrations listed in Table 7.3.3-2 before addition to the soils. Because the CHP reactions in the Palouse loess were catalyzed by naturally-occurring iron minerals, only H_2O_2 was added to the soil followed by pH adjustment of 4.5 M H_2SO_4 or 4.5 M NaOH. The systems were purged with a stream of nitrogen and the off gas was trapped for scintillation counting. Gas transfer was accomplished using 0.18 mm (i.d.) fused silica tubing and the evolved ^{14}C-CO_2 was trapped in 10 ml of a 20% (v/v) solution of Carbosorb in Scint-A XF scintillation cocktail (Watts and Stanton, 1999). A mass balance was established by extracting the remaining ^{14}C-BaP from the vials through shake extractions with 10 ml of ethyl acetate for 24 hr; 5 ml of the extract were then added to a scintillation vial containing 5 ml of Scintilene counting cocktail. All experiments were conducted in triplicate, and control experiments were carried out in parallel using deionized

water in place of H_2O_2. No significant loss of BaP was found in any of the control reactions. All experiments were conducted at $20° \pm 2°$ C.

Desorption.

Benzo[*a*]pyrene desorption from the soils was determined by gas-purge (GP) methodology (Brusseau et al., 1992). Because the system is purged vigorously, contaminants volatilize rapidly after they are desorbed, and their rate of removal from the aqueous phase is equal to the rate of desorption. Vials containing 5 g of sand spiked with 0.1 mmol/kg ^{14}C-BaP were filled with 10 ml of deionized water and purged with nitrogen gas as a flow rate of 120 ml/min. The purge vial was connected to a trap vial containing Carbosorb in Scint-A XF scintillation cocktail by 0.18 mm diameter fused silica tubing. Originally, BaP concentrations were measured on the soil, in the aqueous phase, and in the off gas (trapped in gas adsorbent tubes packed with Tenax). No BaP was detected in the aqueous phase, and the residual on the soil correlated with the mass collected on the gas adsorbent tubes; therefore, subsequent gas purge analyses relied on quantifying the residual sorbed on the soil. ^{14}C-Benzo[*a*]pyrene was determined at time intervals over 5 d. All experiments were conducted in triplicate, and control samples without purging were evaluated in parallel to account for volatilization. Experiments were conducted at $20° \pm 2°$ C.

Analysis.

Radioisotope analysis was performed on a Packard 2200LL scintillation counter that was calibrated to Packard-supplied standards. Benzo[*a*]pyrene concentrations were determined by shake extraction for 24 h with ethyl acetate (Tyre *et al.*, 1991) followed by analysis on a Hewlett Packard 5890A gas chromatograph equipped with a flame ionization detector (FID) and a J & W DB-5 capillary column. Chromatographic conditions included an initial temperature of 200 °C, program rate of 10 °C/min, final temperature of 310°C, injector temperature of 250 °C, and detector temperature of 350 °C. Gas chromatography/mass spectrometry (GC/MS) was performed on a Finnegan SSQ quadrapole mass spectrometer equipped with a DB-5 capillary column. The GC/MS was operated under the same chromatographic conditions used for the GC/FID analysis.

Table 7.3.3-1. Characteristics of the Palouse loess soil

Characteristic	Concentration
Organic C content (%)	0.11
Sand (%)	20.4
Clay (%)	18.8
Silt (%)	60.8
Crystalline Fe oxides (mg/kg)	33500
Amorphous Fe oxides (mg/kg	22.5
Crystalline Mn oxides (mg/kg)	7130
Amorphous Mn oxides (mg/kg)	35.5
Cation exchange capacity (cmol/kg)	22.5

Table 7.3.3-2. Experimental conditions used in central composite rotatable designs

Silica Sand				
[H2O2] (mM)	Slurry Volume (x Field Capacity)	Iron (II) (mM)	Experimental Design Code	No. of Trials
2,400	0.3	6.5	-	1
~.	~	~	1	
~.	~	.1	~	
~1	~	.1	1	
1 ~.	~	~	.	1
Palouse Loess				
[H2O2] (mM)	Slurry Volume (x Field Capacity)	pH	Experimental Design Code	No. of Trials
1,500	1.0	2.0	-	1
~.	~1	~	1	
~.	~.	~	~	
1 .1~	1~	~1	.1	
1~.	~	~	.	1

7.3.4 Mineralization of Sorbed and NAPL-Phase Hexadecane by Catalyzed Hydrogen Peroxide

Materials

Silica sand (143±179 mm), used as a model sorbent, was purchased from Fisher Scientific. ^{14}C-labeled and unlabeled hexadecane was obtained from Aldrich. The [14]C- labeled hexadecane was characterized by a specific activity of 2.2 mCi mmol^{-1}.

Hexadecane partitioning

To determine the distribution of hexadecane in silica sand slurries, 2.5 g of silica sand were spiked with 0.1 mmol kg^{-1} hexadecane by adding 1 ml of 2500 mM hexadecane in pentane and allowing the pentane to evaporate. The three possible phases (i.e. sorbed, nonaqueous liquid and aqueous) were analyzed to determine the concentration of hexadecane by first adding 10 ml of deionized water to the 2.5 g of spiked silica sand; the silica sand was then placed on a wrist action shaker for 4 h. The nonaqueous hexadecane liquid droplets rose to the surface of the slurry (specific gravity= 0.77), which were then collected. In a parallel sample, the supernatant was passed through a 0.45 mm membrane filter; the filter and the filtrate were each extracted five times with hexane to determine hexadecane concentrations in the aqueous phase. In addition, the silica sand was shake extracted five times with ethyl acetate to determine the concentration of sorbed hexadecane. The rate of hexadecane desorption was determined by gas-purge methodology (Brusseau et al., 1990; Sedlak and Andren, 1994) using nitrogen as the purge gas.

Experimental design

A central composite rotatable experimental design was used to investigate the effects of H_2O_2 concentration, slurry volume and iron (II) concentration as well as to characterize potential interactions between the three variables. The final matrix used in the experimental design was determined by conducting preliminary experiments to limit the range of each variable. Hydrogen peroxide concentrations ranged from 1,500 to 15,000 mM. Slurry volume was based on the field capacity (FC) of the silica sand (1.1 ml 2.5 g^{-1}) and varied between 0.25 FC and 4 FC. The slurries were amended with iron (II) sulfate at concentrations ranging from 5 to 25 mM. The central composite design was characterized by the three variables at five levels with five center points for statistical validity (Box and Draper, 1987). The six star points that lie outside of the central region were calculated using a factor of 1.680 to achieve complete rotatability (Figure 7.3.4-1). The experimental data were used to develop regression equations to quantitatively describe the system using least squares analysis. Each term was evaluated based on the 90% interval of a single sided t-distribution; the terms that did not meet this criterion were eliminated from the regression equation. In addition, the data fit was evaluated based on the R^2 of the final regression equation. The resulting regression equation was then used to develop contour plots with SYSTAT software.

Parent compound degradation

Hydrogen peroxide was added to the silica sand spiked with hexadecane followed by the addition of the iron (II) sulfate; the pH was then adjusted to 3.0 with 0.1M H_2SO_4. Reactions were allowed to proceed until completion (2±24 h), which was confirmed by undetectable concentrations of H_2O_2. Four replicates of each experimental unit were used; control experiments were conducted in parallel with deionized water in place of hydrogen peroxide. The slurries were shake extracted with 10 ml of ethyl acetate for 24 h and centrifuged for 15 min; the extract was

then analyzed by gas chromatography. Selected aliquots were also analyzed by gas chromatography/mass spectrometry.

Degradation of ^{14}C-hexadecane

Parallel reactions using ^{14}C-hexadecane were conducted in a closed system consisting of a reaction vial fit with a trap for collecting evolved CO_2. Gas collection was accomplished by 0.18 mm diameter fused silica capillary tubing with evolved ^{14}C-CO_2 trapped in 10 ml of a 20% (v/v) solution of Carbosorb and S¢intA-XF scintillation cocktail (Figure 7.3.4-2). The reaction vessels were then extracted with 10 ml of ethyl acetate; 5 ml of the extract was added to a scintillation vial containing Scintallene counting cocktail. The aqueous phase was sampled by removing 1 ml and adding it to 10 ml of S¢intA-XF counting cocktail. A mass balance was then constructed based on the ^{14}C recovered from the three phases.

Analysis

Hexadecane concentrations were quantified on a Hewlett Packard 5890A gas chromatograph equipped with a flame ionization detector (FID) and a DB-5 capillary column. Chromatographic conditions included initial oven temperature of 150˚C, program rate of 10˚C min^{-1}, final temperature of 220˚C, injector temperature of 250˚C and detector temperature of 350˚C.

Isotope analysis was conducted using a Packard 2200LL scintillation counter calibrated to Packard-supplied standards.
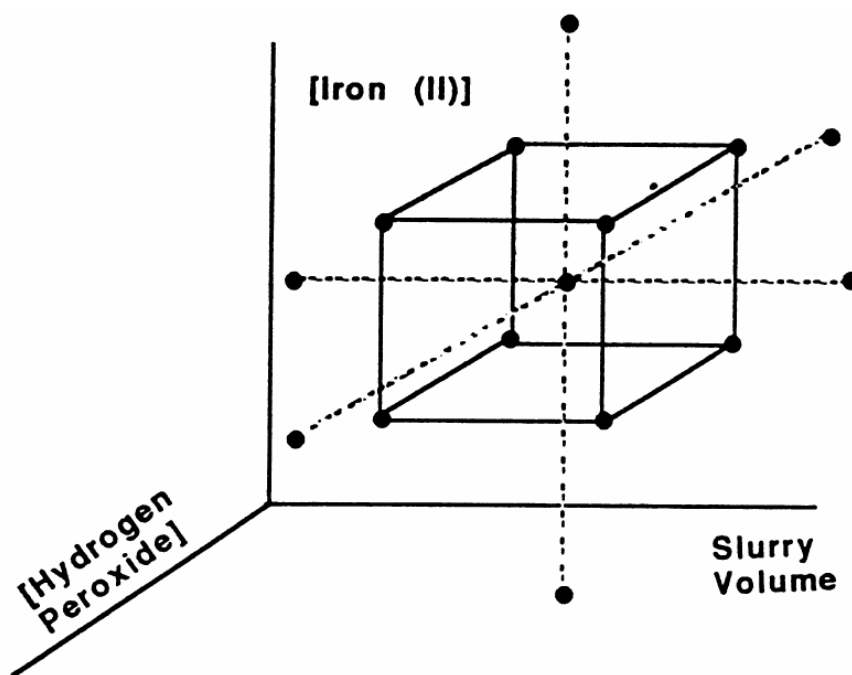
Figure 7.3.4-1. Three dimensional representation of the three-level central composite rotatable design.

24
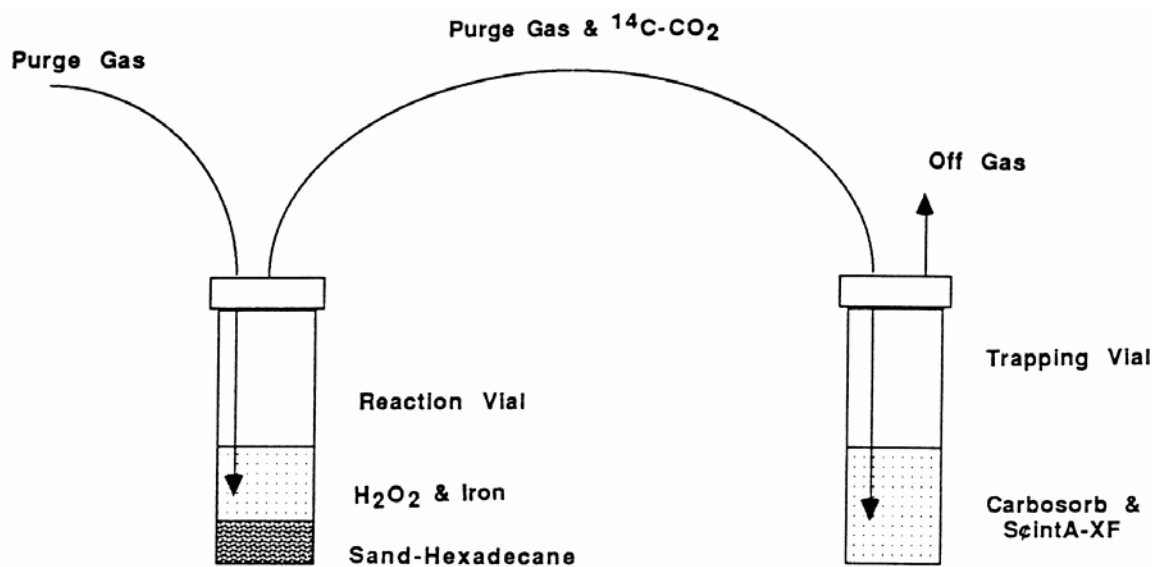
Figure 7.3.4-2. System for trapping ^{14}C-CO_2 evolved from ^{14}C-hexadecane.

7.4 DNAPL Destruction

7.4.1 Destruction of a Carbon Tetrachloride DNAPL by CHP: Proof of Concept

Mineral and probe compound

Coarse-sized pyrolusite (β-MnO$_2$) minerals (≈ 1 cm^3) were obtained from D.J. Minerals; they were crushed to a fine powder using a 150 mL capacity Spex shatter box with a hardened steel grinder. The pyrolusite surface area (5.2 m^2/g) was determined by a Coulter SA 3100 (Carter et al., 1986).

Based on the hypothesis that a reducing or nucleophilic species, not hydroxyl radical, is the reactant responsible for DNAPL destruction in CHP reactions, carbon tetrachloride (CT) was selected as a model DNAPL contaminant. Carbon tetrachloride [$k_{O_2^-} = 3.8 \pm 1.0 \times 10^3$ M^{-1} s^{-1} in aprotic dimethylformamide (DMF) (Roberts et al., 1983); $k_{e^-} = 1.6 \times 10^{10}$ M^{-1} s^{-1} (Buxton et al., 1988); $k_{OH\bullet} < 10^6$ M^{-1} s^{-1} (Buxton et al., 1988; Haag and Yao, 1992)] is unreactive with hydroxyl radicals, but as a highly oxidized organic compound is degraded by a non-hydroxyl radical species produced in CHP reactions (Teel and Watts, 2002).

Experimental procedures

All reactions were conducted in a constant temperature chamber at 20 ± 2°C in 40 mL borosilicate vials capped with PTFE-lined septa. A set of reactors was prepared for each time point for each of three parallel systems: experimental, control, and fill-and-draw. The fill-and-draw system was used to determine the maximum rate of aqueous dissolution for CT. All reactions were performed in triplicate, and the data were analyzed by averaging the results from the three replicates.

The experimental configuration consisted of a liquid injector port connected to an H$_2$O$_2$ feed, a gas sampling port connected to a gas adsorbent tube (ORBO-32, Supelco) to quantify CT loss from volatilization, a 10 ml aqueous layer containing 5 mM iron (III) sulfate at pH 3 (adjusted with 0.1 M H$_2$SO$_4$), and a CT DNAPL layer containing 1.5 g or 3.0 g of CT (Figure 7.4.1-1). The injector and sampling ports were sealed with silicone. Hydrogen peroxide decomposition over time in the iron (III)- and manganese oxide-catalyzed CHP systems is shown in Figure 7.4.1-2. These decomposition data were used to determine feed rates to maintain steady-state H$_2$O$_2$ conditions; the required H$_2$O$_2$ dosage was confirmed by iteration prior to the start of each reaction. Steady-state H$_2$O$_2$ concentrations were determined by collecting preliminary data to determine the concentrations in each system that would rapidly destroy CT DNAPLs. Injection of 16 M H$_2$O$_2$ (adjusted to pH 3 with 0.1 M H$_2$SO$_4$) was accomplished with a KD Scientific syringe pump to maintain a steady-state H$_2$O$_2$ concentration of 1470 mM (Howsawkeng et al., 2001). The total mass of H$_2$O$_2$ consumed over the 3 h reaction time was 64.6 mmol. The pH of the reactors was monitored and adjusted back to the original pH with 0.1 M H$_2$SO$_4$ or 0.1 M NaOH if any deviation from the original was found. For MnO$_2$-catalyzed CHP reactions, iron (III) sulfate was replaced by 1.0 g of pyrolusite catalyst, the pH of the aqueous phase and the H$_2$O$_2$ feed was adjusted to pH 7 (with 0.1 M H$_2$SO$_4$), and the H$_2$O$_2$ concentration was maintained at 294 mM. The total mass of H$_2$O$_2$ consumed over the 3 h reaction time was 51.1 mmol.

The rate of gas evolution during the experimental reactions was quantified using a gas-bubble flow meter. The same flow rate was then applied to the air diffusers in the fill-and-draw and the control systems. The fill-and-draw system consisted of an air stone connected to a nitrogen supply, a 10 mL aqueous layer, 1.0 g of MnO_2 catalyst, and a DNAPL layer (1.5 g or 3.0 g). At each time point, the 10 mL aqueous layer was drawn off from every vial in the fill-and-draw system and replaced by an equal volume of fresh deionized water. Aqueous aliquots from the fill-and-draw vials were shake-extracted with hexane and analyzed by gas chromatography/electron capture detection (GC/ECD) to quantify CT loss through dissolution. Control reactions were prepared in a similar manner to the fill-and-draw vials, but the aqueous layer was not removed.

Every 15 or 30 min over 3 h, reactions in the experimental, fill-and-draw, and control systems were analyzed by removing the injection and gas sampling ports from a set of reactors and weighing each vial using a Sartorius R 300 S analytical balance to determine the mass of the remaining DNAPL. The ORBO gas adsorbent tubes from all of the experimental vials were also replaced by new tubes at every time point, and the tubes collected were extracted with hexane to quantify CT loss through volatilization.

Loss of CT as a function of time was quantified by:

$$\Delta W_{adj.} = W_{adj. @ t=t} - W_{adj. @ t=0} \tag{1}$$

$$\Delta W_{EXP} = W_{EXP @ t=t} - W_{EXP @ t=0} \tag{2}$$

$$\text{Loss of CT} = \Delta W_{adj.} - \Delta W_{EXP} - \text{loss to aqueous phase} - \text{loss to gas phase} \tag{3}$$

W = Mass of the reactor

$\Delta W_{adj.}$ = Change in mass due to H_2O_2 feed

ΔW_{EXP} = Change in mass of experimental reactor
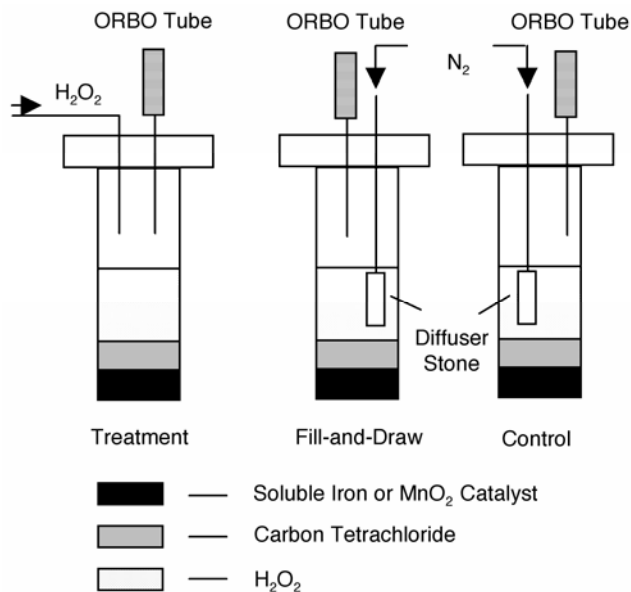
Figure 7.4.1-1. Schematic drawing of the experimental setup for the study of DNAPL destruction using soluble iron- or MnO_2-catalyzed CHP reactions.
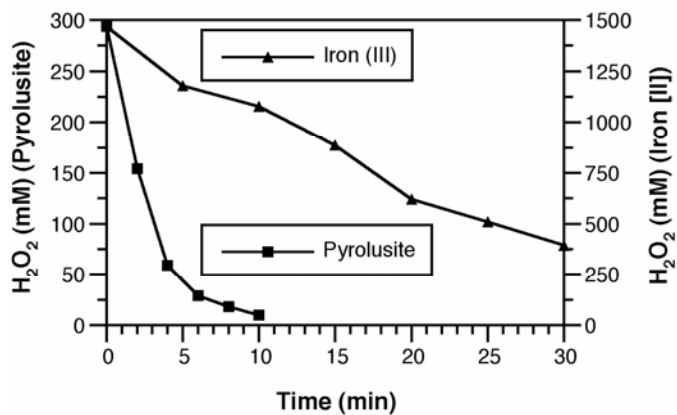
Figure 7.4.1-2. Hydrogen peroxide decomposition in and pyrolusite-catalyzed modified CHP systems. (Reaction conditions: iron (III)-catalyzed system, 5 mM $Fe_2(SO_4)_3$, 1470 mM H_2O_2, pH 3 T = 20 ± 2 ˚C; pyrolusite-catalyzed system, 1 g MnO_2, 294 mM H_2O_2, pH 7, T = 20 ± 2 ˚C).

7.4.2 Pathways for the Destruction of Carbon Tetrachloride and Chloroform DNAPLs by CHP

Reactor system.

  All reactions were conducted in 20 mL borosilicate vials capped with PTFE-lined septa. The experimental configuration (Figure 7.4.2-1) consisted of a liquid injector port connected to a reactant feed; a gas sampling port that was prepared by inserting a 4 mm diameter Teflon tube through a hole in the PTFE septum and connecting an ORBO-32 gas adsorbent tube to quantify contaminant losses from volatilization; a 10 ml aqueous layer containing the reactants; and a DNAPL layer containing 0.5 mL of carbon tetrachloride or chloroform. In order to obtain fundamental information about the potential for DNAPL destruction by CHP and the associated mechanisms of destruction, all reactions were conducted without the potentially complicating presence of a solid phase (e.g. aquifer solids). A set of reactors was prepared for each time point for each of three parallel reactions: experimental, control, and gas-purge. All reactions were performed in triplicate, and the data were analyzed by averaging the results of the three replicates. All reactions were conducted under minimal light conditions in a water bath at 20 ± 1˚C.

Gas purge dissolution.

  A gas purge system was used to determine the maximum rate of dissolution of the carbon tetrachloride and chloroform DNAPLs (Brusseau et al., 1990; Yeh et al., 2003). A flow rate of 200 mL min^{-1} nitrogen was applied to vials with 10 mL of 2 M hydrogen peroxide and 0.5 mL of a carbon tetrachloride or chloroform DNAPL. The purged compounds were trapped using ORBO® 32 adsorbent tubes.

CHP reactions.

  CHP reactions consisted of 10 mL of 2 M hydrogen peroxide and 5 mM iron (III):HKCH chelate, which was used to minimize iron precipitation over the long duration of the experiments. The pH, initially 2.0–2.1, was adjusted to 3.0 using 2 M NaOH. Quasi steady-state conditions were maintained by monitoring pH and hydrogen peroxide concentration at each time point, and adding 2 M NaOH when the pH dropped below 2.7 and 13.8 M hydrogen peroxide when the hydrogen peroxide concentrations dropped below 1.85 M. The change in the total reaction volume was less than 1% by the end of the experiment. Triplicate control reactions were conducted in parallel with double-deionized water used in place of hydrogen peroxide.

Hydroxyl radical generation system.

  Hydroxyl radical alone was generated using a standard Fenton's reaction designed to minimize the generation of superoxide (Babbs and Griffin, 1989). Twenty-four additions of 1 M hydrogen peroxide and 1 M iron (II)-citrate at pH 1.8 were performed over 48 hr to reactors containing 7 mL water and 0.5 mL of a carbon tetrachloride or chloroform DNAPL. The volume of each injection was 0.21 mL, for a total of 5 mmol each of hydrogen peroxide and iron (II) added to the system. There was no significant change in pH over the course of the experiment. Triplicate control reactions were conducted in parallel with additions of double-deionized water in place of hydrogen peroxide.

Hydroperoxide generation system.

The system used to generate hydroperoxide consisted of 2 M hydrogen peroxide raised to pH 11.7 with purified NaOH:

$$H_2O_2 \leftrightarrow H^+ + HO_2^- \qquad pK_a = 11.8 \qquad\qquad (1)$$

The NaOH was purified (Csanyi et al., 1983) to remove impurities that catalyze the generation of other transient oxygen species, and 1 mM DTPA was added to bind residual metal species. Hydrogen peroxide was added when the combined concentrations of hydrogen peroxide and hydroperoxide decreased below 1.8 M to maintain steady state conditions. There was no significant change in pH over the course of the experiment. Triplicate control reactions were conducted in parallel at pH 11.7 with double-deionized water in place of hydrogen peroxide.

Superoxide generation systems.

Two superoxide generating systems were used: 1) a hydroxyl radical-scavenged Fenton-based system at basic pH and 2) a potassium superoxide system. Superoxide was generated in the Fenton-based system by using 1 M hydrogen peroxide and 5 mM iron (III)-EDTA (1:20 molar ratio) at pH 9–9.5 (Rizkalla, et al., 1982; Francis et al., 1985). Superoxide is released after an electron transfer from the complex of iron (III), hydroperoxide, and EDTA (Francis et al., 1985). Ethanol (3 M) was used to scavenge hydroxyl radical and increase the rate of superoxide generation (Bielski and Arudi, 1983). The pH and hydrogen peroxide concentrations were tested every 30 min. Concentrated hydrogen peroxide and ethanol (1:1 molar ratio) were added when hydrogen peroxide concentrations dropped below 0.9 M to maintain steady state conditions. Sodium hydroxide (2 M) was added when the pH dropped below 8.9. The change in the total reaction volume was less than 3% by the end of the experiment. Triplicate control reactions were conducted in parallel at pH 9–9.5 by replacing hydrogen peroxide with double-deionized water.

Superoxide was also delivered to the DNAPLs by adding solutions of potassium superoxide to the reactors under conditions that increase the lifetime and reactivity of superoxide in water. A potassium superoxide stock solution (6 M) was made by dissolving potassium superoxide in 4 °C deionized water containing purified NaOH and DTPA (Marklund, 1976). The NaOH was purified using magnesium hydroxide at pH >13 to bind and remove transition metal impurities (Csanyi et al., 1983).

Superoxide is essentially unreactive with chlorinated organic contaminants in deionized water, although it is highly reactive with such compounds in aprotic solvents. The difference in superoxide reactivity in water vs. organic solvents is related to its solvation (Roberts and Sawyer, 1981). Smith et al. (2004) documented that superoxide reactivity is increased substantially in water when a cosolvent, such as acetone or hydrogen peroxide, is present. Therefore, acetone was used in one set of reactions as a cosolvent; the reactions consisted of 1 M acetone, 2 M potassium superoxide, 33 mM purified NaOH, and 1 mM DTPA (to bind and inactivate transition metals) at pH 14 to minimize the disproportionation of superoxide (Bielski et al., 1985). Hydrogen peroxide was used as a cosolvent in another set of reactions (Smith et al., 2004); the reactions consisted of 1 M hydrogen peroxide, 2 M potassium superoxide, 2.3 M purified NaOH, and 1 mM DTPA at pH 14. (A higher concentration of NaOH was required in these reactions to maintain a pH of 14 due to the weakly acidic nature of hydrogen peroxide.) The rate of superoxide decomposition under these conditions was 110 min, which was quantified

in parallel reactions by measuring the rate of oxygen evolution using a manometer attached to the reactors. Triplicate control reactions were conducted in parallel at pH 14 using deionized water in place of the potassium superoxide solution.

Extraction

At each time point, triplicate reactors were sacrificed and the DNAPL and aqueous phases were immediately separated for analysis by removing the aqueous phase with a Pasteur pipette. The aqueous and DNAPL phases were shake-extracted with decane and toluene, respectively, and ORBO® 32 tubes were extracted with decane for 30 min.
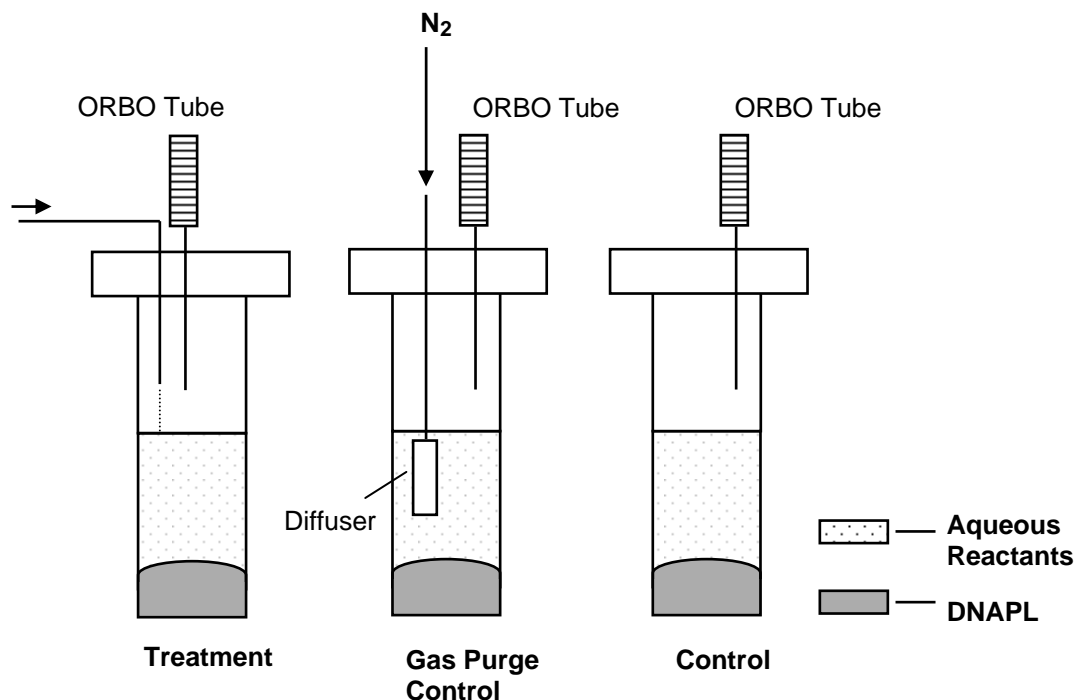
Figure 7.4.2-1. Experimental apparatus for evaluating the destruction of TCE and PCE DNAPLs.

7.4.3 Destruction of 1,1,1-Trichloroethane and 1,2-Dichloroethane DNAPLs by CHP

Methodology for investigating the destruction of 1,1,1-TCA and 1,2-DCA DNAPLs by CHP reactions followed the same procedures described in Section 7.4.2 with the exception of GC/MS analysis, which is described below.

GC/MS Analysis.

An Agilent 6890 gas chromatograph coupled with an Agilent 5973N mass selective detector fitted with a 100 m x 0.32 mm i.d. DB-5MS column was used to analyze off gas collected in Carbotrap 300 gas adsorbent tubes. Thermal desorption was used to release compounds sorbed on the Carbotrap; prior to injection they were held in a liquid oxygen cooled cryogenic loop attached to the injection valve. The initial oven temperature was $-50\degree C$ with a program rate of $10\degree C$ min^{-1}. The final temperature was $240\degree C$ with a final time of 4 min.

7.4.4 Destruction of Trichloroethylene and Perchloroethylene DNAPLs by CHP Reactions

Methodology for investigating the destruction of TCE and PCE DNAPLs by CHP reactions followed the same procedures described in Section 7.4.2.

7.5 Enhanced Destruction of Sorbed Contaminants

7.5.1 Effect of Contaminant Hydrophobicity on H_2O_2 Dosage Requirements in the CHP Treatment of Soils

Soil

The soil used was a grayish-brown gravelly loamy sand, mixed, mesic Torriothentic Haploxeroll, sampled from an alluvial fan above Carson Valley, Nevada. It was characterized for particle size distribution by the pipette method (Gee and Bauder, 1986). Organic carbon was determined by combustion at 900 °C with evolved CO_2 trapped in KOH and measured by back-titration of unreacted KOH (Nelson et al., 1982). Cation exchange capacity was established by saturation with sodium acetate at pH 8.2 (Soil Conservation Science, 1986). Crystalline and amorphous iron and manganese oxyhydroxides were determined by citrate–bicarbonate–dithionite extraction (Jackson et al., 1986). The soil characteristics are listed in Table 7.5.1-1.

Confirmation of equal reactivity of probe compounds with hydroxyl radicals

A series of *n*-alcohols was chosen for use as probe compounds. Rate constants for 1-hexanol, 1-heptanol, 1-octanol, 1-nonanol, and 1-decanol with hydroxyl radicals were determined using an optimized Fenton's procedure that produces a maximum stoichiometric yield of hydroxyl radicals (Steiner and Babbs, 1990). Reactions for each probe compound were carried out in triplicate in 250 ml Erlenmeyer flasks containing 50 ml of a 0.2 mM probe and 30 mM iron (II) perchlorate solution, which was nitrogen purged for 10 minutes prior to starting the reaction. The probe concentration of 0.2 mM was based on the water solubility of 1-decanol, the least water-soluble of the probe compounds. Hydrogen peroxide (0.5 mM) was added to the rapidly-stirred probe–iron (II) solution at a rate of 1 ml min^{-1}. Aliquots were collected at one-minute intervals, extracted with mixed hexanes, and analyzed by gas chromatography. Control experiments were conducted in parallel using deionized water in place of hydrogen peroxide. The data were analyzed by normalizing the concentration for dilution and then plotting the normalized concentration as a function of mol hydrogen peroxide added per mol of probe compound degraded.

Experimental design

Central composite rotatable experimental designs (Diamond, 1989) were used to determine the optimum concentrations of hydrogen peroxide and iron (III) for degradation of probe compounds sorbed to Carson Valley soil. Iron (III) was chosen for this system rather than iron (II) because, with the high relatively high concentrations of H_2O_2 used, iron (II) is rapidly oxidized to iron (III) with a resulting initial demand on the H_2O_2 in the system (Watts and Dilly, 1996). Therefore, the more efficient perhydroxyl-driven initiation reaction was used to initiate the CHP process chemistry:

$$H_2O_2 + Fe^{3+} \rightarrow HO_2\bullet + H^+ + Fe^{2+} \qquad [1]$$

Hydrogen peroxide concentrations ranged from 7 to 442 mM and iron (III) sulfate concentrations ranged from 1.5 to 7 mM. The central composite matrix was characterized by five center points and four star points, or vertices, set at a factor of ± 1.4142 on the far ends of

the coded scale to achieve complete rotatability (Diamond, 1989). Linear regression using least squares analysis was used to derive regression equations from the experimental data. A single sided t-distribution ($\alpha = 0.10$) was used to evaluate each term in the regression equation; the terms that were not significant at the 90% interval were eliminated. Correlation (R^2) values were determined by comparing experimental values to values calculated using the regression equations. Corresponding three-dimensional response surfaces, representing the effect of hydrogen peroxide and soluble iron concentration on probe compound degradation in the soil slurries, were generated from the regression equations using SYSTAT® software.

Procedures

Reactions were conducted in batch reactors consisting of 30-mL borosilicate vials fitted with PTFE-lined caps. All reactions were conducted in triplicate. Each vial contained 5 g ± 0.01 g of Carson Valley soil to which a probe compound was added in pentane. The pentane was allowed to evaporate, resulting in a probe concentration of 0.25 mmol kg^{-1}. The reactions were conducted using reagent volumes of 1.2 times the soil field capacity. The pH was adjusted to pH 3 using 0.1 N solutions of NaOH or H_2SO_4. Upon addition of reagents and adjustment of pH, the vials were mixed at 250 rpm on an orbital shaker to ensure homogeneity of the catalyst and hydrogen peroxide. The reactions were allowed to proceed until the hydrogen peroxide was consumed (9 to 30 h). The entire vial contents were then extracted with mixed hexanes and analyzed by gas chromatography. The extraction efficiencies for 1-hexanol, 2-heptanol, 3-octanol, 4-nonanol, and 5-decanol into ethyl acetate were 84%, 85%, 87%, 87% and 89%, respectively. Control reactions were conducted in parallel using deionized water in place of hydrogen peroxide.

Analysis

Probe compound residuals were determined using a Hewlett-Packard 5890 Series II gas chromatograph fitted with a Supelco SPB-5 0.53 mm i.d. × 15 m fused silica capillary column and flame ionization detector. The injector port and detector port temperatures were 280 ˚C and 300 ˚C, respectively. The initial temperatures were 45 ˚C for 1-hexanol, 55 ˚C for 1-heptanol, 75 ˚C for 1-octanol, 90 ˚C for 1-nonanol, and 105 ˚C for 1-decanol. The program rate was 15 ˚C min^{-1} for hexanol and 20 ˚C min^{-1} for all other probe compounds; the final temperature was 280 ˚C.

Table 7.5.1-1. Characteristics of the Carson Valley Soil

Organic carbon content (mg kg^{-1})	3700
Sand (%)	86.5
Silt (%)	11.0
Clay (%)	2.5
Crystalline Fe oxides (mg kg^{-1})	4400
Crystalline Mn oxides (mg kg^{-1})	100
Amorphous Fe oxides (mg kg^{-1})	4400
Amorphous Mn oxides (mg kg^{-1})	100
Cation exchange capacity (cmol kg^{-1})	4.28
pH	6.4

7.5.2 Reactive Oxygen Species Responsible for the Enhanced Desorption of Dodecane in CHP Systems

Probe compound.

Dodecane was used as a probe compound to evaluate enhanced desorption because of its high hydrophobicity and sorptivity (log K_{ow} = 6.44), high potential for gas-purge analysis (Henry's law constant = 24.2 atm-m^3/mole @ 25°C [Verschueren, 1983]), and low reactivity with superoxide and hydroperoxide anion in aqueous solution (Bielski et al., 1985).

Adsorption of dodecane.

Silica sand was used because it is a simple and well-defined sorbent (Goss, 1992). Furthermore, use of an inorganic sorbent eliminates contaminant release resulting from soil organic matter destruction in CHP reactions, which can be a complicating factor in elucidating the reactive oxygen species. Vapor deposition was used to sorb dodecane to silica sand (Ong and Lion, 1991; Unger et al., 1996; Steinberg et al., 1999). Dodecane was applied to 50 g of purified silica sand in 100 ml Pyrex media bottles to provide a concentration of 2.5 mmol/kg sand. The bottles were capped using aluminum foil as a liner and heated at 80°C for 3 h.

Gas purge desorption.

Gas-purge desorption was conducted in 100 ml media bottles fitted with one sparger for purging the reaction solution above the sand and a second sparger for purging the sand saturated with aqueous-phase reagents (Figure 7.5.2-1). The nitrogen flow rate to the aqueous-phase sparger was 500 ml/min. Gas production rates in the experimental systems (e.g. CHP, KO_2, etc.) were measured using a bubble meter attached to a port on the reaction bottle; the flow rate to the sand sparger was equal to the gas production rate in the parallel experimental reactions. An additional port on each bottle was used to hold an ORBO-32 gas adsorbent tube. The ORBO tubes were sampled and replaced at selected time points, then extracted with an ethyl acetate-water mixture (2:1 vol/vol) followed by analysis of the extract by gas chromatography.

Measurement of enhanced desorption by CHP and specific reactive oxygen species.
After the gas-purge desorption of dodecane in deionized water was quantified, potential enhanced desorption by hydroxyl radical, superoxide anion, and hydroperoxide was evaluated by generating each of these reactive oxygen species separately in dodecane-sand systems with simultaneous gas-purge desorption. All reactions were conducted in triplicate in 100 ml media bottles containing 50 g of dodecane-spiked sand and 50 ml of reaction solution with continuous N_2 gas purging in a constant temperature chamber at $20 \pm 2°C$, except superoxide reactions, which were conducted at $4 \pm 1°C$. Triplicate control reactions were conducted in parallel using deionized water in place of the reaction solution. The ORBO tubes and sand were each extracted at selected time points over 180 min and analyzed by gas chromatography to quantify residual dodecane concentrations.

CHP reaction. Enhanced desorption in CHP systems was evaluated in separate reactors using initial concentrations of 0.5 M or 3.0 M H_2O_2 catalyzed by 5 mM iron (III).

Enhanced desorption by hydroxyl radicals. A standard Fenton's reaction was used for generating hydroxyl radicals as the sole reactant. The stoichiometrically-efficient Fenton's system was based on the conditions provided by Babbs and Griffin (1989). To 50 ml of a 5 mM iron (II) solution, 0.1 ml of 100 mM H_2O_2 was added every 10 min over 180 min.

Enhanced desorption by hydroperoxide. Hydroperoxide was generated by adding a 150 mM solution of sodium perborate to the reactors. Sodium perborate decomposes to hydroperoxide anion in water (David and Seiber, 1999)

$$2H_2O + BO_3^- \leftrightarrows HO_2^- + B(OH)_3 \quad (5)$$

Enhanced desorption by superoxide. Potassium superoxide in deionized water was used to generate $O_2•^-$ as the sole reactive oxygen species based on the methodology of Marklund (1976). Reactions were conducted in triplicate and consisted of 1 M or 3 M KO_2, 0.1 M purified NaOH, and 1 mM DTPA (to bind and inactivate transition metals) at pH 14 to minimize the disproportionation of $O_2•^-$ (Csanyi et al., 1983). The KO_2 was mixed into a 4°C NaOH-DTPA solution; under these conditions, the half-life of $O_2•^-$ was 110 min, which was quantified by measuring the rate of oxygen evolution using a manometer attached to a reaction vessel.

Analysis.
Sand extracts and ORBO tube extracts were analyzed using a Hewlett-Packard 5890 gas chromatograph fitted with a 0.53 mm (i.d.) x 15 m DB-1 capillary column and a flame ionization detector (FID). The injector port and detector port temperatures were 200°C and 300°C, respectively. The oven temperature was 110°C (isothermal). Hydrogen peroxide concentrations were quantified by iodometric titration with 0.1 N sodium thiosulfate (Schumb et al., 1955). Solution pH was measured using a Fisher Accumet pH meter.
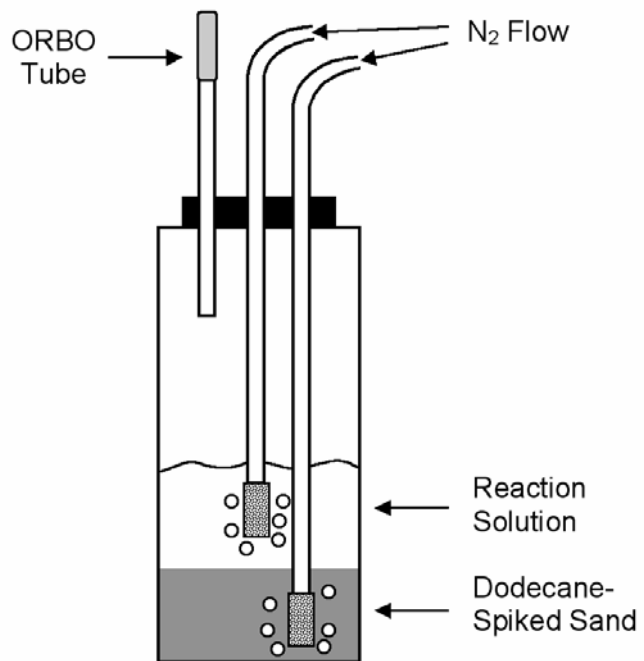
Figure 7.5.2-1. Experimental reactor used for desorption experiments.

7.6 Delivery of Peroxide

7.6.1 Soil Organic Matter–Hydrogen Peroxide Dynamics in the Treatment of Contaminated Soils and Groundwater using CHP

Soil sampling, preparation, and analysis.

The soil used was a silt loam sampled from the Palouse Silt Loam soil series located near Johnson, WA. Three soil horizons were sampled and used in CHP reactions. Soil depth A was collected from a depth of 0-75 cm; it was placed in a soil splitter to provide homogeneity during CHP reactions. Soil depth B was sampled from a depth of 45-60 cm, and soil depth C was sampled from a depth of 105-120. Samples were collected using a hand auger and were stored in 4-L polyethylene bags. Each soil horizon was characterized for particle size distribution by the pipette method (Gee and Bauder, 1986). Organic carbon was determined by combustion at 900˚C with evolved CO_2 trapped in KOH and measured by back-titration of unreacted KOH (Nelson et al., 1982). Cation exchange capacity was established by saturation with sodium acetate at pH 8.2 (SCS, 1986). Crystalline and amorphous iron and manganese oxyhydroxides were determined by citrate–bicarbonate–dithionite extraction (Jackson et al., 1986). Characteristics of the soil horizons are listed in Table 7.6.1-1.

CHP reactions.

Soil depth A was treated with six different CHP process conditions in which the catalyst and the pH were varied. Reaction conditions consisted of 5 mM and 10 mM soluble iron (III) at pH 3, 5 mM and 10 mM iron (III)-EDTA chelate at neutral pH, and no iron amendment at pH 3 and neutral soil pH with catalysis by naturally-occurring soil minerals. Sulfuric acid (25% H_2SO_4) was used to adjust the pH to 3; the slurries were then allowed to equilibrate for 1 hr. In each CHP system, hydrogen peroxide concentrations ranged from 0.5 M to 3 M. CHP reactions were conducted in 250 mL borosilicate glass batch reactors with 20 grams of soil and 20 mL of reactant solution at 20°C. After addition of the hydrogen peroxide, catalyst, and acid for pH adjustment, the suspensions were mixed for 1 min on a vortex. Reactions proceeded until the hydrogen peroxide decomposed to undetectable concentrations. All reactions were conducted in triplicate, and control reactions were conducted in parallel using deionized water in place of hydrogen peroxide.

Soil fractionation and carbon analysis.

After the CHP reactions proceeded to completion, the soils were dried at 40°C; 5 g of the dried soil were then ground and analyzed for total organic carbon on a LECO CNS-2000 carbon analyzer. The remaining 15 g of soil were fractionated using the methodology described by Cambardella and Elliott (1992) and Gill et al. (1999). A 0.5 M sodium hexametaphosphate solution (150 mL) was added to the remaining 15 g of soil, which was then placed on an orbital shaker at 120 rpm for 18 hours. The soil slurry was then passed through a 53 µm sieve and rinsed with deionized water until the rinse water from the sieve was clear. Particles caught in the sieve were dried at 40°C, ground, and analyzed for organic carbon content. The organic carbon of the soil fraction > 53 µm is classified as particulate organic matter (POM), and the organic carbon of the soil fraction < 53 µm (obtained by the difference of total carbon and POM) is classified as non-particulate organic matter (NPOM).

Hydrogen peroxide stability.

Hydrogen peroxide concentrations were monitored during CHP reactions in two different horizons of the Palouse silt loam (soil depths B and C) to evaluate the effect of SOM content on hydrogen peroxide stability. CHP reactions with 5 mL total liquid volume and 5 g soil were conducted in 40 mL borosilicate glass vials containing 3 M hydrogen peroxide at pH 3 catalyzed by naturally occurring soil minerals. Hydrogen peroxide was analyzed by iodometric titration in triplicate at eight time points over the course of the reactions.

Relative rates of hydroxyl radical activity.

1-Hexanol was used as a hydroxyl radical probe in two horizons of the Palouse silt loam (soil depths B and C) to evaluate potential scavenging of hydroxyl radical by SOM. 1-Hexanol is rapidly oxidized by hydroxyl radicals ($k_{OH\bullet} = 3 \times 10^9$ M^{-1} s^{-1}) but is not reactive with superoxide, perhydroxyl, or hydroperoxide anion (Watts et al., 2001). CHP reactions were conducted with 5 g of soil and 5 mL liquid volume in 40 mL vials closed to the atmosphere and fitted with ORBO-32$^{©}$ gas adsorbent tubes to capture any hexanol that could potentially escape through volatilization. The reactions consisted of 2 mM hexanol and 3 M hydrogen peroxide at pH 3 and were catalyzed by naturally occurring soil minerals. Triplicate sets of reactions were shake extracted with hexane at eight time points over the course of the reaction. Triplicate control systems were performed in parallel using deionized water in place of hydrogen peroxide.

Analysis.

The organic carbon content of the soils and of the POM and NPOM fractions was quantified using a LECO-CNS 2000 carbon analyzer with oxygen combustion at 1350°C and an infrared (IR) cell detector.

Table 7.6.1-1. Soil characteristics of Palouse Silt Loam soils A, B, and C.

	Soil A	Soil B	Soil C
Depth (cm)	0–75	45–60	105–120
pH	6.9	7.0	7.1
Organic Carbon (%)	1.6	1.6	0.2
Amorphous Oxides			
Fe (μg/g)	1800	1600	830
Mn (μg/g)	410	650	410
Crystalline Oxides			
Fe (μg/g)	7100	7200	6800
Mn (μg/g)	400	410	340
Cation Exchange Capacity (cmol(+)/kg)	22	22	22
Particle Size Distribution			
Sand (%)	21.2	21.2	19.2
Clay (%)	14.8	14.8	10.8
Silt (%)	64.0	64.0	70.0
Texture (USDA, 1950)	Silt Loam	Silt Loam	Silt Loam

7.6.2 Displacement of Five Metals Sorbed on Kaolinite During Treatment with CHP

Sorbent.

Kaolinite was used as a simple model sorbent for investigating metals release in CHP reactions because 1) it has minimal catalytic activity in CHP reactions, 2) it contains minimal concentrations of organic matter, which would potentially release sorbed metals as the organic matter is destroyed, and 3) it has sufficient cation exchange capacity to sorb most metals. Kaolinite was purchased from Ward's Geology (Rochester, N.Y). The surface area was 17.8 m^2/g. Kaolinite was characterized for particle size distribution using the pipette method (Gee et al., 1986); it was characterized under USDA textural classes as a clay. Organic carbon was 0.16% as determined by combustion at 900°C with evolved CO_2 trapped in KOH and measured by back titration of unreacted KOH (Nelson et al., 1982). The cation exchange capacity (CEC) of 3.0 cmol/kg was established by saturation with sodium acetate at pH 8.2 (Soil Conservation Service, 1986).

Sample preparation and exchange of metals.

Oxidation studies employed kaolinite as a model sorbent for five metals. A mass of 1 g ± 0.05 g of kaolinite was weighed into 40 ml borosilicate vials fitted with PTFE-lined caps.

Twenty-five mL of a solution containing 2 mM of a metal ($NiSO_4$, $Pb(NO_3)_2$, $CdSO_4$, $ZnSO_4$ or $CuCl_2$) was added to each borosilicate vial containing kaolinite for a concentration of 100 meq/kg kaolinite, and the slurries were placed on an orbit shaker at 200 rpm for 48 h. After the metals were exchanged, a 10 mL aliquot of the aqueous phase was passed through a 0.22 µm filter, which ensures capture of both dissolved and mobile colloidal particles (Gschwend and Reynolds, 1987); the filtrates were then analyzed by atomic absorption spectroscopy. Initial average aqueous phase concentrations for cadmium, copper, lead, nickel and zinc were 0.68 meq/L, 0.42 meq/L, 1.16 meq/L, 0.36 meq/L and 0.34 meq/L, respectively, indicating that 71%–92% of each metal was exchanged on the kaolinite.

The iron (III) CHP catalyst stock solution consisted of 5 mM $Fe(ClO_4)_3$. In addition, a 5 mM iron (III) chelate CHP catalyst was prepared by dissolving NTA in deionized water with 1.0 M NaOH prior to combining with an equimolar concentration of $Fe(ClO_4)_3$, followed by pH adjustment to 6.0 with 0.1 M NaOH (Pignatello and Baehr, 1994).

Experimental procedures.
Kaolinite-metal slurries were evaluated for changes in the aqueous-phase concentration of metals during treatment with CHP using two different soluble iron catalysts and three H_2O_2 concentrations. Each vial of kaolinite-metal slurry (1 g kaolinite and 15 mL remaining metals solution) received 10 mL of catalyst solution, followed by 10 mL of H_2O_2 (or deionized water for control reactions) for a final aqueous volume of 35 mL, which was adjusted to pH 3 or pH 6 using 0.1 M H_2SO_4 or 0.1 M NaOH. Final catalyst concentrations were 1 mM iron (III) at pH 3 and 1 mM iron (III)–NTA chelate at pH 6; final H_2O_2 concentrations used with each catalyst were 0.9 M (3%), 1.8 M (6%), and 2.7 M (9%). Reactions were allowed to proceed for 120 min, with 3 mL aliquots collected every 15 min. The pH remained at 3.0 ± 0.1 in the iron (III)-catalyzed pH 3 reactions, and increased by < 0.5 in the iron (III)–NTA-catalyzed pH 6 reactions. The aliquots were passed through a 0.22 µm Millipore Millex PTFE filter and analyzed for metal concentrations by atomic absorption spectrophotometry. All reactions were conducted in triplicate, and control reactions were performed in parallel using deionized water in place of H_2O_2.

Statistical analysis.
Analysis of sample means was performed using analysis of variance (ANOVA) over the treatment time. A completely randomized design with one-way treatment structure with repeated measures using four treatments (0 M, 0.9 M, 1.8 M, and 2.7 M H_2O_2) and three replicates with eight repeated measures (0, 15, 30, 45, 60, 75, 90 and 120 min) was used with $\alpha = 0.05$ and 9 degrees of freedom (Freund, 1992). Fisher's least significant difference (LSD) procedure was used to separate means for treatments. Analysis was performed for the average of each concentration of H_2O_2 over the entire experimental time period. All statistics were computed using SAS[®] statistical software.

7.6.3 Fate of Sorbed Lead During Treatment of Contaminated Soils by CHP

Soils.

Three natural soils were used as lead sorbents. Hanford soil was collected from an alluvial deposit on the US Department of Energy Hanford Reservation, WA. Kamiak Butte soil was selected from the B horizon of a road cut near Kamiak Butte, WA. Colorado soil was collected from the front range near Golden, Colorado. Each of the soils was sieved to capture mesh sizes between 50 and 100 (300 μm–150 μm). Soils were characterized for particle size distribution using the pipette method (Gee et al., 1986). Organic carbon content was determined by combustion at 900°C with evolved CO_2 trapped in KOH and measured by back titration of unreacted KOH (Nelson et al., 1982). Cation exchange capacity (CEC) was established by saturation with sodium acetate at pH 8.2 (Soil Conservation Service, 1986). Trace analysis was performed using method x-ray fluorescent spectroscopy (Karathanasis and Hajaek, 1996). Characteristics of the three soils are listed in Table 7.6.3-1.

Sample preparation and exchange of metals.

Preliminary experiments were conducted to obtain data on kinetics of metal sorption onto the three soils. The Colorado and Kamiak Butte soils sorbed lead more rapidly and sorbed more total lead than did Hanford; therefore, a higher initial concentration of lead was added to CHP desorption experiments using Colorado and Kamiak Butte soils. A mass of 1 g ± 0.05 g of soils was weighed into 40 ml borosilicate vials fitted with PTFE-lined caps. Twenty mL of a solution containing 3 mM (Hanford soil) or 5 mM (Colorado and Kamiak Butte soils) lead (II) nitrate were added to each borosilicate vial containing soils, and the slurries were placed on an orbit shaker at 200 rpm for 48 h. After the lead was exchanged, a 5 mL aliquot of the aqueous phase was passed through a 0.22 μm filter, which ensures capture of both dissolved and mobile colloidal particles (Gschwend and Reynolds, 1987); the filtrates were then analyzed by atomic absorption spectroscopy. For all three soils, >95% of the lead was sorbed after 48 hr.

The iron (III) CHP catalyst stock solution for pH 3 reactions consisted of 120 mM $Fe(ClO_4)_3$. For reactions conducted at pH 7, a 120 mM iron (III) chelate CHP catalyst was prepared by dissolving NTA in deionized water with 1.0 M NaOH prior to combining with an equimolar concentration of $Fe(ClO_4)_3$, followed by pH adjustment to 7.0 with 0.1 M NaOH (Pignatello and Baehr, 1994).

Experimental procedures.

Soil slurries were evaluated for changes in the aqueous-phase concentration of lead during treatment with CHP at two pH regimes using two soluble iron catalysts. Each vial, which contained a slurry of 1 g soil and 15 mL lead solution remaining from the sorption procedure, received 0.75 mL of catalyst solution, followed by 2.25 mL of 40% H_2O_2 (or deionized water for the control reactions) for a final aqueous volume of 18 mL, which was adjusted to pH 3 or pH 7 using 0.1 M H_2SO_4 or 0.1 M NaOH. Final catalyst concentrations were 5 mM iron (III) at pH 3 and 5 mM iron (III)–NTA chelate at pH 7, and the final H_2O_2 concentration used with each catalyst was 1.5 M (5%). The reactions were allowed to proceed for 120 min. A triplicate set of vials was sacrificed every 10 min and 3 mL aliquots were collected for analysis. The pH of each remaining vial was evaluated at every time point and was maintained at 3.0 ± 0.1 in the iron (III)-catalyzed pH 3 reactions, and at 7.0 ± 0.1 in the iron (III)–NTA-catalyzed pH 7 reactions. The aliquots were passed through a 0.22 μm Millipore Millex PTFE filter and analyzed for lead

42

concentrations by atomic absorption spectrophotometry. All reactions were conducted in triplicate, and control reactions were performed in parallel using deionized water in place of H_2O_2.

Experiments investigating the role of hydroxyl radical in lead sorption to Hanford soil used isopropanol as a hydroxyl radical scavenger. Each vial containing 15 mL of solids slurry received 0.9 mL of catalyst solution (iron (III) or iron (III)-NTA) and 2 mL of 100% isopropanol, followed by 2 mL of 50% H_2O_2 for a final volume of 19.9 mL. The final catalyst and H_2O_2 concentrations were 5 mM and 1.5 M, respectively, and the final isopropanol concentration was 10% (1.3 M).

Table 7.6.3-1. Soil Characteristics of Hanford, Kamiak Butte, and Colorado Soils

| | Soil | | |
	Hanford	Kamiak Butte	Colorado
Organic matter (%)	0.32	0.76	1.7
Sand (%)	48.4	22.4	68.7
Clay (%)	5.6	13.6	11.8
Silt (%)	46.0	64.0	19.5
Texture (USDA, 1950)	Sandy loam	Silt loam	Sandy loam
Trace Elements (μg/g)			
As	9.9	12	n.d.
Ba	160	280	190
Be	0.68	0.96	1.1
Ca	17,000	6900	3300
Cd	n.d.	n.d.	n.d.
Co	15	27	8.0
Cr	27	75	40
Cu	24	22	53
Fe	28,000	34000	36000
K	3300	2700	8300
Mg	8100	6900	6400
Mn	500	1400	340
Mo	n.d.	n.d.	4.2
Na	240	320	n.d.
Ni	22	43	19
P	800	880	470
Pb	20	13	16
S	380	370	370
V	59	76	42
Zn	79	74	85

7.6.4 Fate of Sorbed Cadmium During Treatment of Contaminated Soils by CHP

Sorbents.

   One clay mineral and three natural soils were used as cadmium sorbents. Illite was purchased from Ward's Geology (Rochester, N.Y). The Hanford, Kamiak Butte, and Colorado soils are described in section 7.6.3, and characteristics of the three soils are presented in Table 7.6.3-1.

Sample preparation and exchange of metals.

   Preliminary experiments were conducted to obtain data on kinetics of cadmium sorption onto the four sorbents. A mass of 1 g ± 0.05 g of sorbents was weighed into 40 ml borosilicate vials fitted with PTFE-lined caps. Twenty mL of a solution containing 2 mM cadmium chloride (for a total of 40 µmol cadmium) were added to each borosilicate vial containing sorbents, and the slurries were placed on an orbit shaker at 200 rpm for 48 h. After the cadmium was exchanged, a 5 mL aliquot of the aqueous phase was passed through a 0.22 µm filter, which ensures capture of both dissolved and mobile colloidal particles (Gschwend and Reynolds, 1987); the filtrates were then analyzed by atomic absorption spectroscopy. The percent of the cadmium sorbed after 48 hr varied between the sorbents and was 52% for illite, 73% for the Hanford soil, 85% for the Kamiak Butte soil, and 79% for the Colorado soil.

   The iron (III) CHP catalyst stock solution for pH 3 reactions consisted of 120 mM $Fe(ClO_4)_3$. For reactions conducted at pH 7, a 120 mM iron (III) chelate CHP catalyst was prepared by dissolving NTA in deionized water with 1.0 M NaOH prior to combining with an equimolar concentration of $Fe(ClO_4)_3$, followed by pH adjustment to 7.0 with 0.1 M NaOH (Pignatello and Baehr, 1994).

Experimental procedures.

   Solids slurries were evaluated for changes in the aqueous-phase concentration of cadmium during treatment with CHP at two pH regimes using two soluble iron catalysts. Each vial, containing 1 g sorbent and 15 mL cadmium solution remaining from the sorption procedure, received 0.75 mL of catalyst solution, followed by 2.25 mL of 40% H_2O_2 (or deionized water for control reactions) for a final aqueous volume of 18 mL, which was adjusted to pH 3 or pH 7 using 0.1 M H_2SO_4 or 0.1 M NaOH. The final catalyst concentrations were 5 mM iron (III) at pH 3 and 5 mM iron (III)–NTA chelate at pH 7, and the final H_2O_2 concentration used with each catalyst was 1.5 M (5%). The reactions were allowed to proceed for 120 min. A triplicate set of vials was sacrificed every 10 min and 3 mL aliquots were collected for analysis. The pH of each remaining vial was evaluated at each time point and was maintained at 3.0 ± 0.1 in the iron (III)-catalyzed pH 3 reactions, and at 7.0 ± 0.1 in the iron (III)–NTA-catalyzed pH 7 reactions. The aliquots were passed through a 0.22 µm Millipore Millex PTFE filter and analyzed for cadmium concentrations by atomic absorption spectrophotometry. All reactions were conducted in triplicate, and control reactions were performed in parallel using deionized water in place of H_2O_2.

   Experiments investigating the role of hydroxyl radical in cadmium sorption used isopropanol as a hydroxyl radical scavenger. Each vial containing 15 mL of solids slurry received 0.9 mL of catalyst solution (iron (III) or iron (III)-NTA) and 2 mL of 100% isopropanol, followed by 2 mL of 50% H_2O_2 for a final volume of 19.9 mL. The final catalyst

and H_2O_2 concentrations were 5 mM and 1.5 M, respectively, and the final isopropanol concentration was 10% (1.3 M).

7.6.5 Hydrogen Peroxide Stabilization in Minerals and Soils

Minerals and soils.

Two iron oxide minerals (goethite and hematite) and two manganese oxide minerals (manganite and pyrolusite) were used to evaluate mineral-mediated hydrogen peroxide decomposition. Four soils and subsurface solids were also used to evaluate soil-mediated hydrogen peroxide decomposition. The characteristics of the four soils are listed in Table 7.6.5-1.

Screening of stabilizers.

The ten potential stabilizers were screened by adding each stabilizer to 5 ml of a 2% solution of hydrogen peroxide, mixing the hydrogen peroxide-stabilizer solution containing 1 g of each of goethite, hematite, manganite, or pyrolusite; hydrogen peroxide residuals were then quantified over several days. The rates of hydrogen peroxide decomposition were then compared to rates in parallel systems with no stabilizers. The results of initial screening efforts showed that malonate, citrate, and phytate are the most effective stabilizers.

Evaluation of the hydrogen peroxide stabilization ability of the most effective stabilizers.

The stabilizers citrate, malonate, and phytate were subsequently investigated in further detail. The potential for the compounds to stabilize hydrogen peroxide was investigated in the four mineral systems and four soils and subsurface solids. Each of the stabilizers added to 2% hydrogen peroxide at a concentration of 10 mM and 1 M (250 mM for phytate); 5 ml of the stabilized solution was then added to 1 g of the mineral or soil/subsurface solid. Aliquots were then collected over time and analyzed for hydrogen peroxide residuals.

Probe compounds and measurement of relative hydroxyl radical and superoxide activity.

The probe compounds were selected based on their ability to react solely through either oxidation or reduction. Carbon tetrachloride (CT) was used as a reductant probe (Peyton et al., 1995) because it is readily reduced (k_{e-} = 1.6 x 10^{10} $M^{-1}s^{-1}$) (Buxton et al., 1988) but is not oxidized by hydroxyl radicals ($k_{OH\bullet}$ < 6 x 10^6 $M^{-1}s^{-1}$) (Buxton et al., 1988). In contrast, 1-hexanol was used as an oxidant probe because it is readily oxidized by hydroxyl radicals ($k_{OH\bullet}$ = 3 x 10^9 $M^{-1}s^{-1}$) but is not readily reduced (k_{e-} = 2 x 10^7 $M^{-1}s^{-1}$) (Buxton et al., 1988). Based on the linear range of analysis, initial concentrations of CT and 1-hexanol were 10 μM and 2 mM, respectively.

Each of the probes was added to stabilizer-2% hydrogen peroxide solutions. Using a volume of 5 ml, the solutions containing the probe, stabilizer, and hydrogen peroxide were added to 1 g of each of the soils or subsurface solids. Aliquots were collected over 4 hr, extracted with hexane, and analyzed for residual probe compound concentration.

Table 7.6.5-1. Characteristics of the Georgia, Maine, California and Washington soils.

	Soil			
	Georgia	Maine	California	Washington
Sand (%)	47.4	54.0	78.7	32.4
Silt (%)	14.3	33.5	8.0	15.6
Clay (%)	38.3	12.5	13.3	52.0
Crystalline iron oxides (mg/kg)	4,300	7,200	11,000	6,900
Crystalline manganese oxides (mg/kg)	170	183	340	380
Amorphous iron oxides (mg/kg)	16	8	780	150
Amorphous manganese oxides (mg/kg)	160	250	330	360
Organic carbon (%)	0.062	0.51	0.08	1.08
Surface area (m^2/g)	5.5	2.5	1.5	6.3
Cation exchange capacity (cmol/kg)	7.9	3.6	22.0	25.0

7.6.6 Hydrogen Peroxide Stabilization in One-Dimensional Flow Columns

Probe compound.

Hexachlorobenzene (HCB) was used as a probe because it is readily oxidized by hydroxyl radicals ($k_{OH\bullet}$ = 3.7 X 10^9) (Haag and Yao, 1992) and degraded by superoxide (Bielski et al, 1991); HCB is also highly hydrophobic (log K_{ow} = 5.65), and therefore provides a measure of local degradation by CHP reactions. HCB is also characterized by low volatility (H=0.0017 atm*m^3/mole). Based on the linear range of analysis, the initial concentration sorbed onto the mineral coated sand was 10 mg HCB/kg sand.

Mineral coated sand preparation .

Prior to coating with minerals, the sand was acid washed for 24 hours in 30% nitric acid and then continuously rinsed with deionized water until there was no change in pH between the influent and the effluent wash water. The rinsed sand was then oven dried at 93ºC. After drying, iron-coated sand (ICS) was prepared by adding 3 L of 30g/L aqueous ferric nitrate to 5500 ml of acid washed sand. The sand was then stirred until evenly coated and placed in an oven at 93º C until dry (Stenkamp and Benjamin, 1994). Manganese coated sand (MCS) was prepared by combining 585 ml of 1 mM manganese chloride, 1.5 ml 5.5 M sodium hydroxide, and 726 ml of deionized water. After the compounds dissolved, the solution was added to 3.75 kg of acid

washed sand. The sand was then stirred until evenly coated and placed in an oven at 40º C until the water evaporated (Stahl and James,1991). HCB coated sand was prepared by dissolving HCB in toluene and adding to ICS or MCS to a concentration of 10 mg HCB/kg sand. The toluene was allowed to evaporate, leaving the HCB sorbed to the sand.

CHP reactions in batch systems.

Initial experiments were conducted in batch systems to determine 1) the lowest concentration of stabilizer required to maintain extended hydrogen peroxide lifetimes and 2) the amount of iron and manganese used to coat the sand to provide similar decomposition rates of unstabilized hydrogen peroxide for the two coated sands.

Batch reactions were conducted with 100 g of ICS or MCS with sorbed HCB in 250 ml Erlenmeyer flasks and 60 ml hydrogen peroxide-stabilizer solution. The pH was adjusted to 7.0 with 1.0 N sulfuric acid or 1.0 N sodium hydroxide. Control reactions were evaluated in parallel with no stabilizer addition and with a stabilizer but no hydrogen peroxide. The reactions were conducted over six hr., and aliquots were collected at 0, 1, 2, 3, 4, and 6 hr. Sand samples were collected at the beginning and at the end of each reaction, extracted with toluene, and analyzed by gas chromatography to determine the initial and final concentrations of HCB on the sand. The batch experiments were conducted in triplicate and the optimum results from the batch reactions were applied to the one-dimensional columns.

CHP stabilization in one-dimensional columns.

The most effective process conditions determined in the batch reactors were used in the one-dimensional columns in order to evaluate hydrogen peroxide decomposition dynamics and potential for contaminant destruction in a dynamic environment. ICS or MCS was loaded into a Plexiglas column 125 cm high x 7.5 cm in diameter fitted with ports at 12.7 cm intervals. The bottom 6.4 cm of the column was filled with 0.74 mm mesh size sand to promote drainage; as a result, the total depth of experimental sand in the column was 102 cm. The column was filled with the HCB-sorbed sand, double deionized water was then applied using a peristaltic pump and a head of 6.4-7.5 cm was maintained above the sand in the column for the duration of the experiments. After the column reached steady state (i.e., the influent flow rate was equal to the effluent flow rate), a pulse of hydrogen peroxide-stabilizer mix was applied. The volume of the pulse was equal to one-half the pore space of the sand in the column (1.95 L). The pulse consisted of 5.0% hydrogen peroxide and 25 mM stabilizer at pH 7.0. Following dosing with the hydrogen peroxide and stabilizer, double deionized water was added to the column until the hydrogen peroxide concentration in the lowest port (port 8) was below the level of detection. Sand samples were collected from each port using a syringe, weighed, and analyzed for residual HCB concentration.

Liquid samples were taken from each port every 10 minutes and were analyzed for hydrogen peroxide and stabilizer concentrations. The experiments were terminated when the concentration of hydrogen peroxide in the effluent of the lowest port fell below the level of detection.

Analysis.

 HCB extracts were analyzed using a Hewlett-Packard 5890A gas chromatograph with a 30 mm (i.d.) x 0.53 mm DB-5 capillary column and electron capture detector. The injector port

and detector port temperatures were 300° C and 325° C, respectively. The initial temperature was 40° C and the program rate was 30° C min^{-1}. Sodium citrate concentrations were measured by UV spectrophotometry after color development by lyophilizate, glycylglycine buffer, L-malate dehydrogenase, L-lactate dehydrogenase, NADH, and lyophilizate citrate lyase (Möllering and Gruber, 1966). Sodium phytate concentrations were measured by UV spectrophotometry after color development by Wade's Reagent (Vaintraub and Lapteva, 1988).

8. RESULTS AND ACCOMPLISHMENTS

8.1 Factors That Control Hydrogen Peroxide Decomposition

Information on the soil and subsurface properties that control the rate of hydrogen peroxide decomposition is essential to the effective and economical application of CHP. Soil and subsurface properties that can potentially influence the decomposition rate of hydrogen peroxide include surface area, soil organic matter, iron oxides, manganese oxides, and trace minerals. Elucidation of the factors that mediate hydrogen peroxide decomposition will provide valuable information on possible pathways of generation of reactive oxygen species and mechanisms for the stabilization of hydrogen peroxide.

Mineral mediated decomposition of hydrogen peroxide. Numerous catalysts have been used in CHP reactions, including soluble iron, iron chelates, and solid metal oxides. Naturally occurring iron oxides and manganese oxides have the advantage of mediating the decomposition of H_2O_2 to reactive oxygen species without the addition of soluble iron salts to the subsurface. Manganese oxides and oxyhydroxides have been considered the most important inorganic catalysts for H_2O_2 decomposition in the subsurface (Watts et al., 1993, Watts et al., 1997, Lin and Gurol, 1998, Valentine and Wang, 1998, Teel et al., 2001). However, the relative contribution of iron and manganese oxides and trace minerals in promoting the decomposition of H_2O_2 has not been investigated. The purpose of this segment of research was to investigate rates of H_2O_2 decomposition mediated by two iron oxide minerals, two manganese oxide minerals, and seven different trace minerals.

Soil and subsurface mediated decomposition of hydrogen peroxide. Common parameters used to characterize soils and subsurface solids include surface area, soil organic carbon, and crystalline and amorphous iron and manganese oxides. After investigating rates of hydrogen peroxide decomposition mediated by individual minerals, the purpose of this segment of research was to correlate hydrogen peroxide decomposition rates with commonly analyzed soil properties.

8.1.1 Rates of Hydrogen Peroxide Decomposition Mediated by Iron Oxides, Manganese Oxides, and Trace Minerals

A significant shortcoming of CHP ISCO is the rapid decomposition of H_2O_2 in the subsurface, which limits its potential for transport downgradient. Although iron and manganese oxides and oxyhydroxides are considered the most important inorganic catalysts for H_2O_2 decomposition in the subsurface (Watts et al., 1993, Watts et al., 1997, Lin and Gurol, 1998, Valentine and Wang ,1998, Teel et al., 2001), the contribution of trace minerals in catalyzing the decomposition of H_2O_2 has not been investigated. The purpose of this research was to investigate rates of H_2O_2 decomposition mediated by seven different trace minerals and to compare these rates to those mediated by iron and manganese oxides.

The mineral-mediated decomposition of H_2O_2 using initial H_2O_2 concentrations of 0.5% and 2% each at pH 3 and pH 7 is shown in Figure 8.1.1-1a–d. Under all four conditions, the slowest rates of H_2O_2 decomposition occurred in the presence of anatase, bauxite, magnesite, and wilmenite. Hydrogen peroxide in the presence of anatase decomposed very slowly, with >75% of the H_2O_2 remaining after 2800 min, with the exception of the 0.5% H_2O_2 pH 7 system, in which H_2O_2 decomposed more rapidly toward the end of the experiment. Hydrogen peroxide also decomposed slowly in the presence of bauxite and magnesite, with approximately 20–40% of the initial H_2O_2 remaining after 2800 min. Willmenite- and ilmenite-mediated H_2O_2 decomposition rates were in the intermediate range, while the remainder of the minerals (cuprite, goethite, hematite, manganite, and pyrolusite) promoted more rapid H_2O_2 decomposition.

The slope of the initial rates of H_2O_2 decomposition, the surface areas of each of the minerals, and the H_2O_2 decomposition rates normalized for mineral surface area are listed in Table 8.1.1-1. A comparison of H_2O_2 decomposition rates at two pH regimes and two H_2O_2 concentrations, normalized for mineral surface area, is shown in Figure 8.1.1-2. The dominant catalysts in the decomposition of H_2O_2 were pyrolusite, goethite, and hematite. The rates of H_2O_2 decomposition mediated by pyrolusite, goethite, and hematite were nearly equal at pH 3. However, H_2O_2 decomposition rates are significantly higher for pyrolusite at pH 7; in addition, the hematite-mediated decomposition of H_2O_2 was higher at pH 3 compared to pH 7. In general, H_2O_2 decomposition mediated by the trace minerals (siderite, willemite, ilmenite, cuprite, anatase, magnesite, bauxite) was not affected by pH, although there were some differences in pH effects among each of the different minerals. Hydrogen peroxide decomposition rates mediated by the trace minerals siderite, ilmenite, cuprite, anatase, magnesite, and bauxite increased slightly (approximately 1.5–2 fold) at pH 7 compared to pH 3. However, rates of willmenite mediated H_2O_2 decomposition at pH 7 increased by approximately 7.5 times the rate at pH 3.

As with changes in pH, the initial H_2O_2 concentration had minimal effect on H_2O_2 decomposition rates mediated by trace minerals. There was no significant change in rates of siderite- and bauxite-mediated decomposition of H_2O_2 when its concentration was increased from 0.5% to 2%. Slight rate increases of 1.1 to 1.5 fold were noted for ilmenite and cuprite when the H_2O_2 concentration was increased from 0.5% to 2%. Conversely, H_2O_2 decomposition rates for anatase and magnesite decreased 1.5 to 2 times as the H_2O_2 concentration was increased from 0.5% to 2%.

The effect of H_2O_2 concentration on rates of H_2O_2 decomposition for the major iron and manganese oxide minerals was small, with the exception of pyrolusite. Hydrogen peroxide decomposition rates increased 1.2 to 2 times with the increase of H_2O_2 concentration from 0.5% to 2%. However, pyrolusite-mediated H_2O_2 decomposition rates increased significantly with an 8.4 fold increase in the decomposition rate at pH 3 and a 6.6 fold increase in the decomposition rate at pH 7.

The results shown in Figures 8.1.1-1 and 8.1.1-2 demonstrate that of the minerals studied, iron oxide and manganese oxide minerals are the dominant mediators of H_2O_2 decomposition. The trace minerals anatase, bauxite, calcite, cuprite, ilmenite, magnesite, pyrite, siderite and willemite provided minimal activity for decomposing H_2O_2 on a per surface area basis. Furthermore, these trace minerals are present in significantly smaller concentrations in soils and

the subsurface relative to iron and manganese oxides (Dixon and Schulze, 2002). As a result, trace minerals likely contribute minimally to H_2O_2 decomposition during CHP ISCO.

Hydrogen peroxide decomposition mediated by iron oxide minerals has been studied extensively (Tyre et al., 1991, Miller and Valentine, 1995, Lin and Gurol, 1998, Teel et al., 2001). Iron oxide-mediated decomposition of H_2O_2 generates hydroxyl radicals and may provide some direct oxidations on mineral surfaces (Watts et al., 1997, Valentine and Wang, 1998). The manganese oxide-mediated decomposition of H_2O_2 does not generate hydroxyl radicals, but produces significant quantities of superoxide and molecular oxygen (Watts et al., 2005). Based on the slow rates of reaction of trace minerals with H_2O_2, a large flux of reactive oxygen species is not expected from their decomposition of H_2O_2.

Hydrogen peroxide stability is the primary limitation to the successful field implementation of CHP ISCO (Watts and Teel, 2006). Hydrogen peroxide residuals are usually maintained for no more than a few days, and in many cases H_2O_2 decomposes to undetectable concentrations within hours. The results of this research document that the trace minerals anatase, bauxite, calcite, cuprite, ilmenite, magnesite, pyrite, siderite and willemite do not provide high potential for the decomposition of H_2O_2. The results of this segment of research provide the basis for correlating soil physical and chemical properties, including different classes of iron and manganese oxides, with rates of hydrogen peroxide decomposition.

Table 8.1.1-1. Surface areas of trace minerals and iron and manganese oxides and slopes of first order hydrogen peroxide decomposition rates in the presence of the minerals

Mineral	Surface Area	0.5% pH 3		0.5% pH 7		2% pH 3		2% pH 7	
		Slope	Slope/SA	Slope	Slope/SA	Slope	Slope/SA	Slope	Slope/SA
Anatase	9.1	0.0002	2.20×10^{-5}	0.0004	4.40×10^{-5}	0.0001	1.10×10^{-5}	0.0002	2.20×10^{-5}
Bauxite	288.8	0.0004	1.39×10^{-6}	0.0007	2.42×10^{-6}	0.0004	1.39×10^{-6}	0.0008	2.77×10^{-6}
Cuprite	49.5	0.0074	1.49×10^{-4}	0.0101	2.04×10^{-4}	0.0069	1.39×10^{-4}	0.0109	2.20×10^{-4}
Goethite	1.4	0.1540	1.11×10^{-1}	0.0156	1.12×10^{-2}	0.1896	1.36×10^{-1}	0.0203	1.46×10^{-2}
Hematite	0.3	0.0231	7.91×10^{-2}	0.7559	2.59×10^{-0}	0.0156	5.34×10^{-2}	0.5452	1.87×10^{-0}
Ilmenite	1.7	0.0027	1.57×10^{-3}	0.0022	1.28×10^{-3}	0.0024	1.39×10^{-3}	0.0014	8.12×10^{-4}
Magnesite	38.0	0.0006	1.58×10^{-5}	0.0011	2.89×10^{-5}	0.0004	1.05×10^{-5}	0.0008	2.10×10^{-5}
Manganite	15.9	0.0476	3.00×10^{-3}	0.3127	1.97×10^{-2}	0.0275	1.73×10^{-3}	0.1505	9.48×10^{-3}
Pyrolusite	5.2	0.9357	1.80×10^{-1}	1.4360	2.76×10^{-1}	7.8715	1.51×10^{-0}	9.4907	1.83×10^{-0}
Siderite	6.8	0.0282	4.12×10^{-3}	0.0452	6.60×10^{-3}	0.0247	3.61×10^{-3}	0.0450	6.57×10^{-3}
Willemite	1.8	0.0006	3.25×10^{-4}	0.0045	2.44×10^{-3}	0.0006	3.25×10^{-4}	0.0045	2.44×10^{-3}

Figure 8.1.1-1. Decomposition of 0.5% and 2% hydrogen peroxide at pH 3 and pH 7 in the presence of trace minerals and iron and manganese oxides.
(Reaction conditions: 10 mL of 0.5% or 2% H_2O_2 and 1 g of crushed anatase, bauxite, cuprite, ilmenite, magnesite, siderite, willemite, hematite, goethite, manganite, or pyrolusite, pH 3 or 7, T = 25 ± 2°C). a: 0.5% hydrogen peroxide at pH 3; b: 0.5% hydrogen peroxide at pH 7; c: 2.0% hydrogen peroxide at pH 3; d: 2.0% hydrogen peroxide at pH 7.
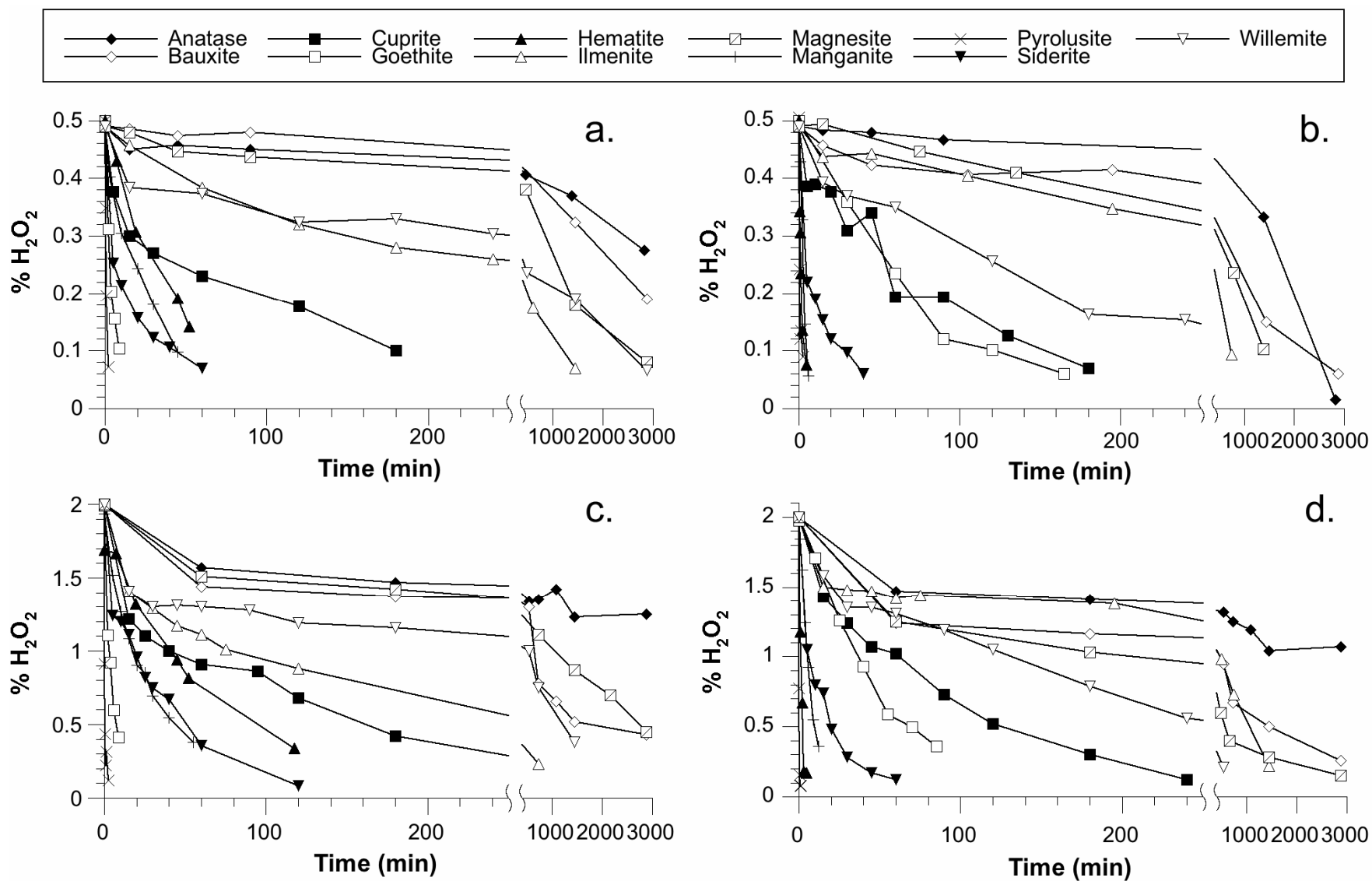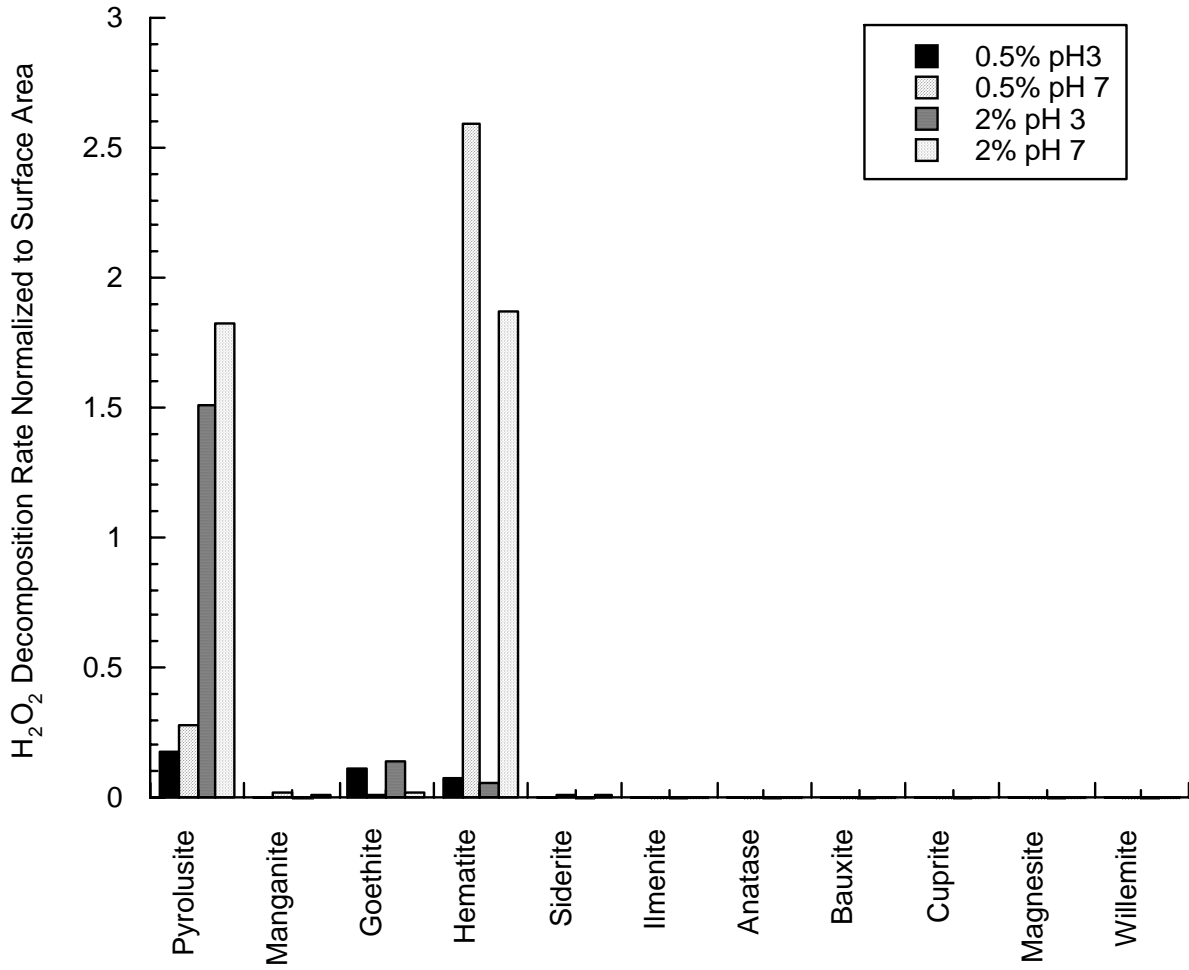
Figure 8.1.1-2. Slopes of first order hydrogen peroxide decomposition rates in the presence of trace minerals and iron and manganese oxides, normalized to mineral surface areas

8.1.2 Correlation of Hydrogen Peroxide Decomposition Rates with Soil Properties

Correlation of hydrogen peroxide decomposition at pH 7 with soil properties.

Hydrogen peroxide concentrations at pH 7 as a function of time were fit to first order kinetics by plotting ln C/C_0 as a function of time; the –slope from the plot was the first order rate constant. First order rate constants for each of the 11 soils and subsurface solids were then plotted as a function of six soil properties. First order rate constants plotted as a function of soil surface area, soil organic carbon, crystalline iron oxides, crystalline manganese oxides, amorphous iron oxides, and amorphous manganese oxides are shown in Figures 8.1.2-1–6. Low correlation between hydrogen peroxide decomposition rates and surface area and organic carbon content were observed with $R^2 = 0.0076$ and 0.023, respectively. Higher correlations were found with amorphous iron and manganese oxides with $R^2 = 0.33$ and 0.60, respectively. The highest correlations with hydrogen peroxide decomposition rates were with crystalline iron and manganese oxides with $R^2 = 0.82$ and 0.71, respectively. Manganese oxides have traditionally been considered as the dominant mineral in promoting hydrogen peroxide decomposition, which is confirmed by the data shown in Figure 8.1.2-4. However, iron oxides are usually present in soils and subsurface solids in significantly higher concentrations compared to manganese oxides. Therefore, both of these species are important in promoting the decomposition of hydrogen peroxide.

Correlation of hydrogen peroxide decomposition at pH 3 with soil properties.

First order rate constants for the decomposition of hydrogen peroxide as a function of soil surface area, soil organic carbon, crystalline iron oxides, crystalline manganese oxides, amorphous iron oxides, and amorphous manganese oxides are shown in Figures 8.1.2-7–12. The correlation of hydrogen peroxide rate constants with soil surface area was minimal, with $R^2 = 0.016$. In a similar manner, soil organic carbon content did not correlate well with the hydrogen peroxide decomposition rate constants ($R^2 = 0.22$). There was low correlation between hydrogen peroxide decomposition rate constants and crystalline iron and manganese oxide contents with $R^2 = 0.47$ and $R^2 = 0.16$, respectively. However, amorphous iron and manganese oxides were correlated more highly with hydrogen peroxide decomposition rate constants, with $R^2 = 0.63$ for iron oxides and $R^2 = 0.41$ for manganese oxides. The conceptual basis for the results obtained at pH 3 is dissolution of a portion of the crystalline iron and manganese oxides, minimizing their potential to catalyze hydrogen peroxide decomposition. The amorphous iron and manganese oxides would then be the more dominant catalysts for hydrogen peroxide decomposition after the dissolution of the crystalline forms of the minerals.

Summary and Conclusions

The results of Section 8.1 demonstrate that iron and manganese oxide are the dominant mediators of hydrogen peroxide decomposition by soils and subsurface solids. In almost all CHP ISCO applications, hydrogen peroxide is consumed more rapidly than desired. Therefore, the key to providing effective and economical CHP ISCO will be the control the catalytic activity of iron and manganese oxides.
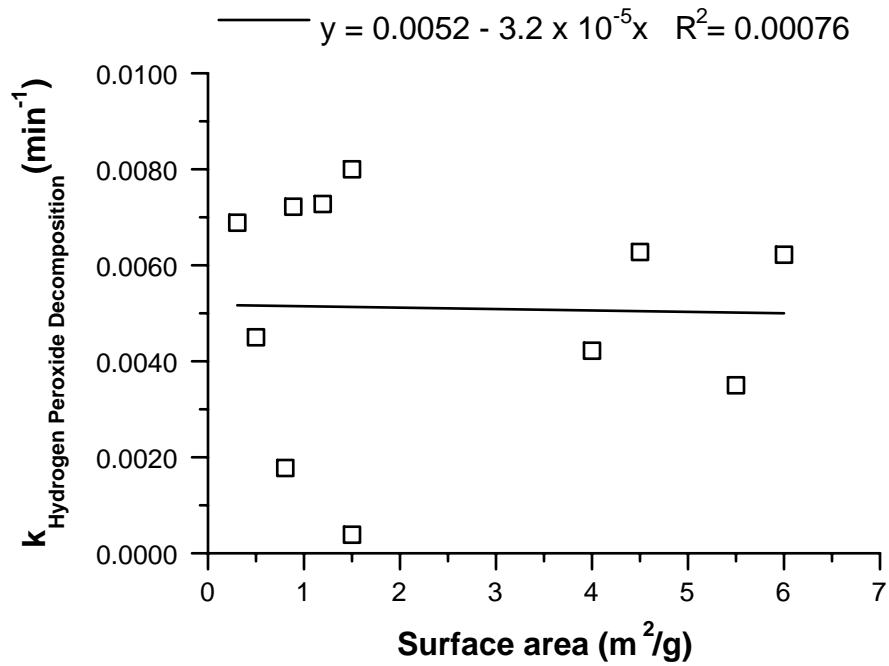
Figure 8.1.2-1. Correlation of hydrogen peroxide decomposition in soils at pH 7 to soil surface area.
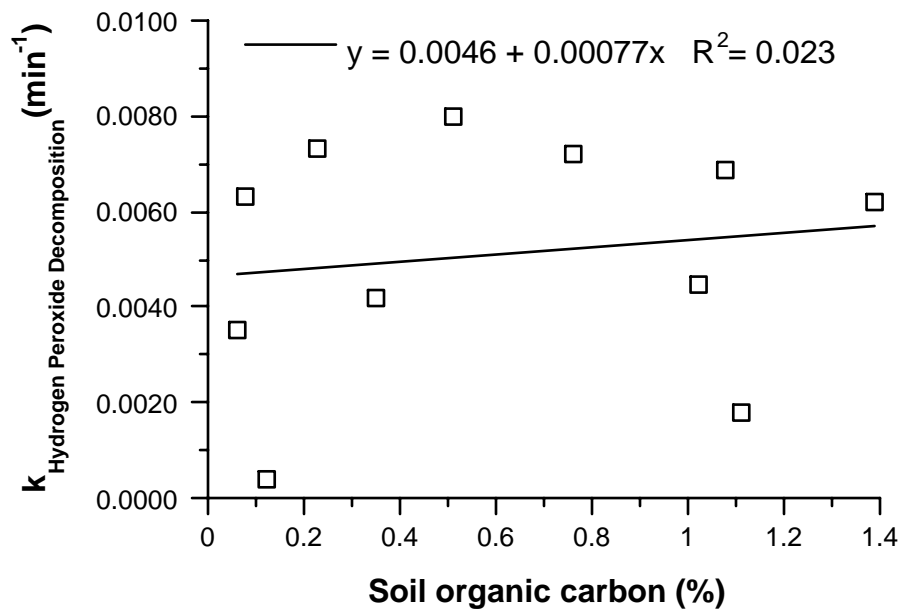
Figure 8.1.2-2. Correlation of hydrogen peroxide decomposition in soils at pH 7 to soil organic carbon.
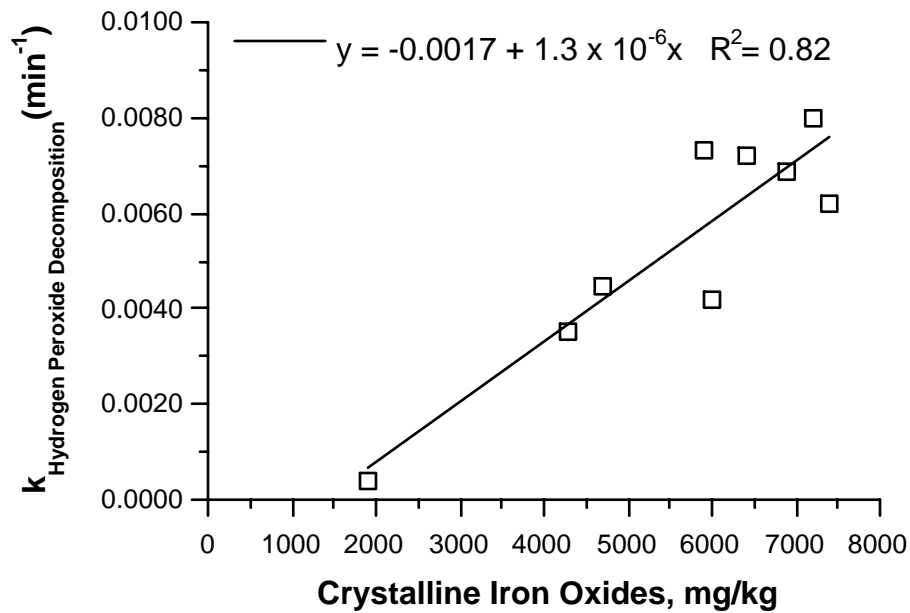
Figure 8.1.2-3. Correlation of hydrogen peroxide decomposition in soils at pH 7 to soil crystalline iron oxide content.
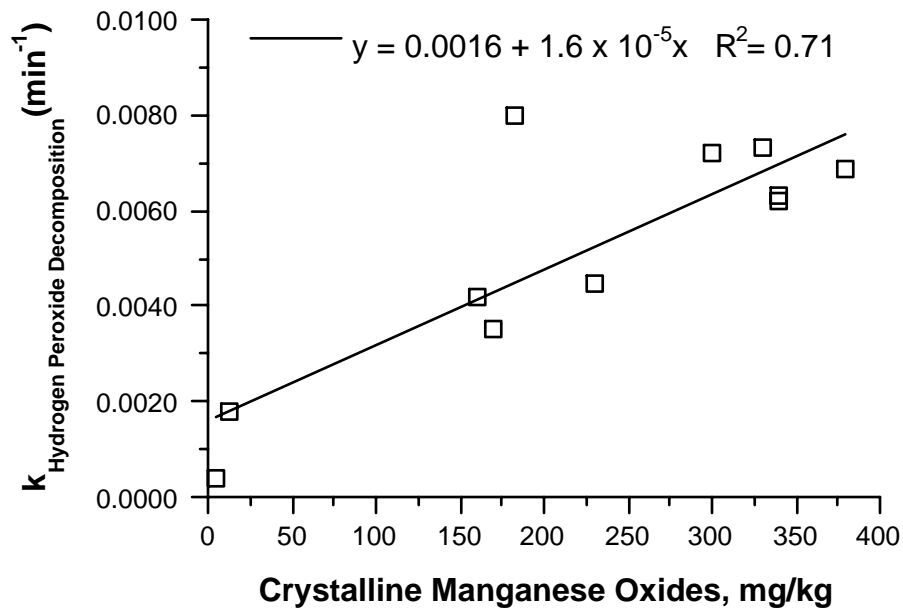
Figure 8.1.2-4. Correlation of hydrogen peroxide decomposition in soils at pH 7 to soil crystalline manganese oxide content.
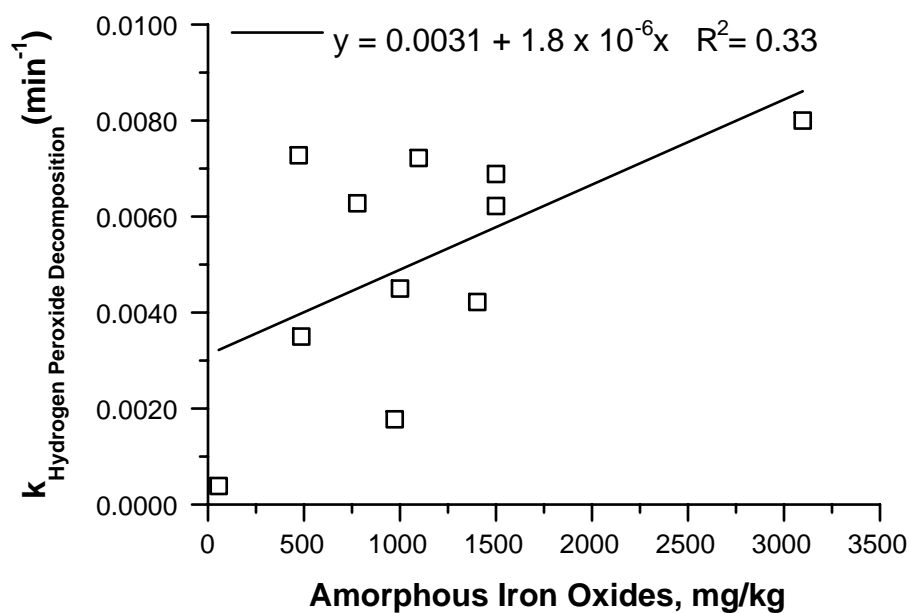
Figure 8.1.2-5. Correlation of hydrogen peroxide decomposition in soils at pH 7 to soil amorphous iron oxide content.
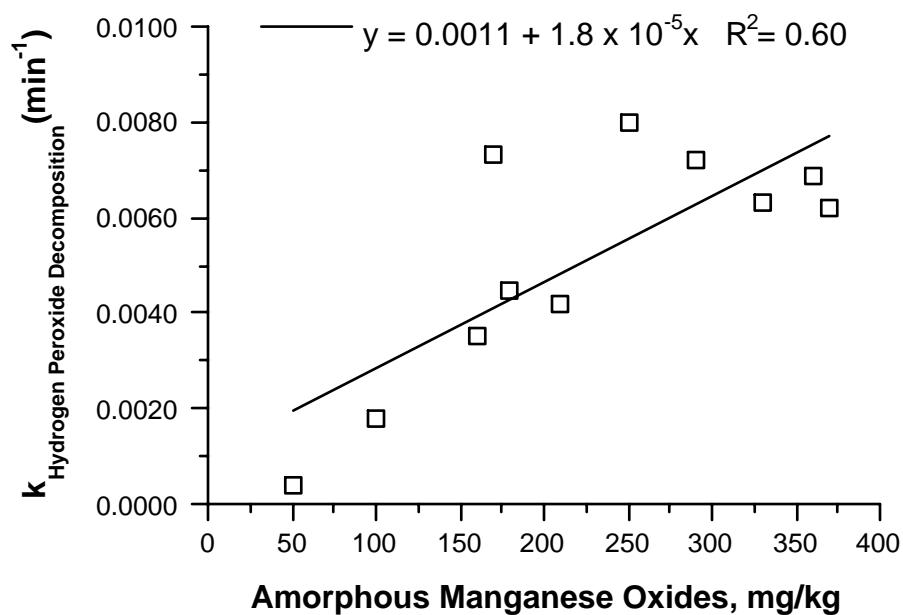
Figure 8.1.2-6. Correlation of hydrogen peroxide decomposition in soils at pH 7 to soil amorphous manganese oxide content.
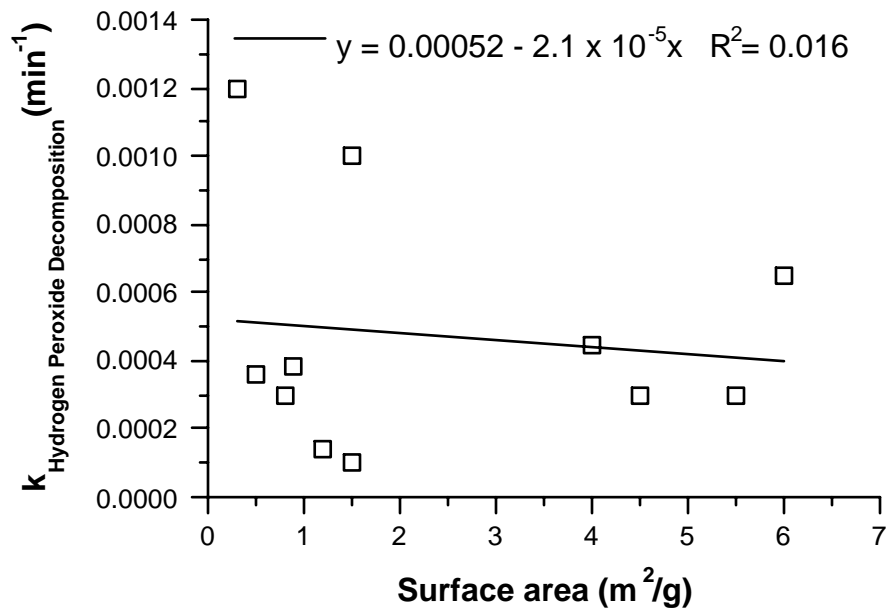
Figure 8.1.2-7. Correlation of hydrogen peroxide decomposition in soils at pH 3 to soil surface area.
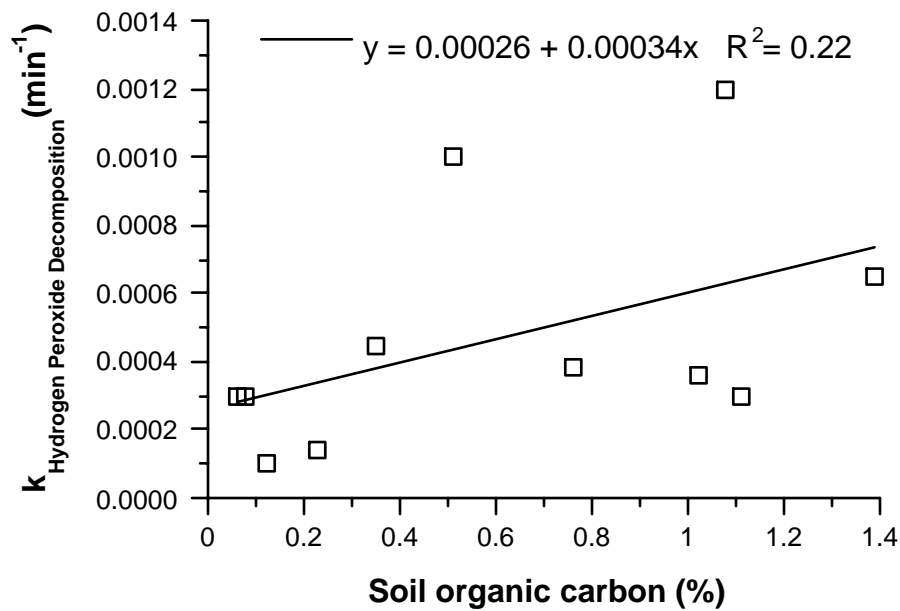
Figure 8.1.2-8. Correlation of hydrogen peroxide decomposition in soils at pH 3 to soil organic carbon.
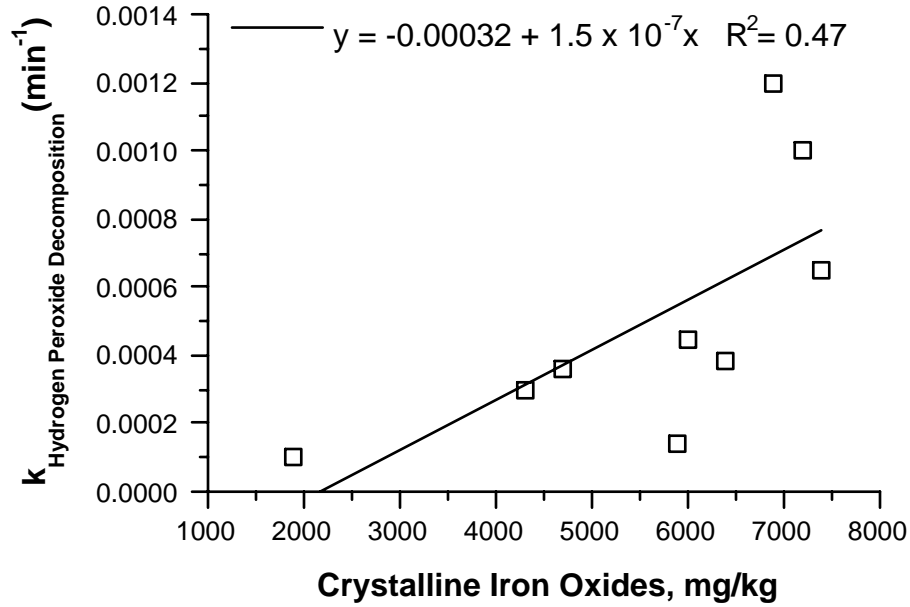
Figure 8.1.2-9. Correlation of hydrogen peroxide decomposition in soils at pH 3 to soil crystalline iron oxide content.
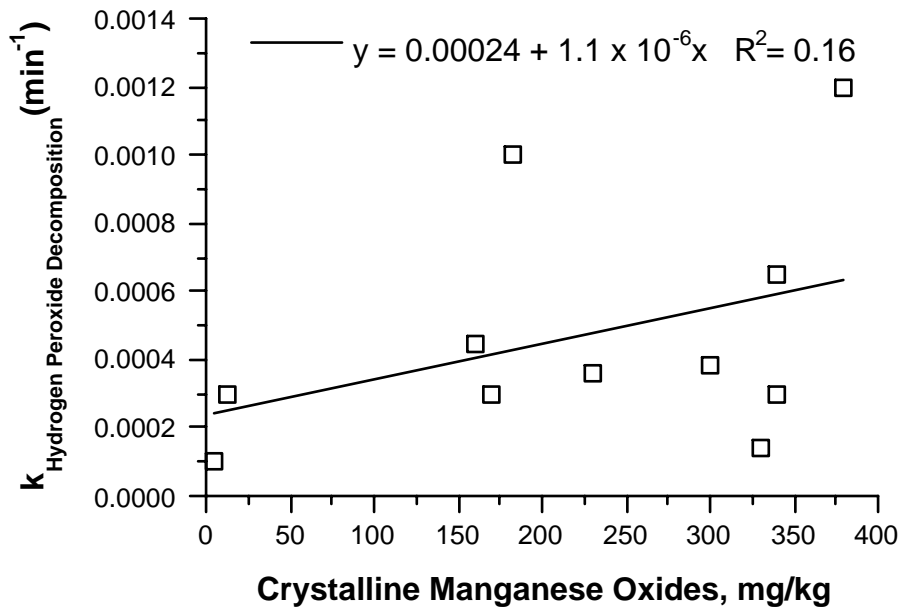
Figure 8.1.2-10. Correlation of hydrogen peroxide decomposition in soils at pH 3 to soil crystalline manganese oxide content.
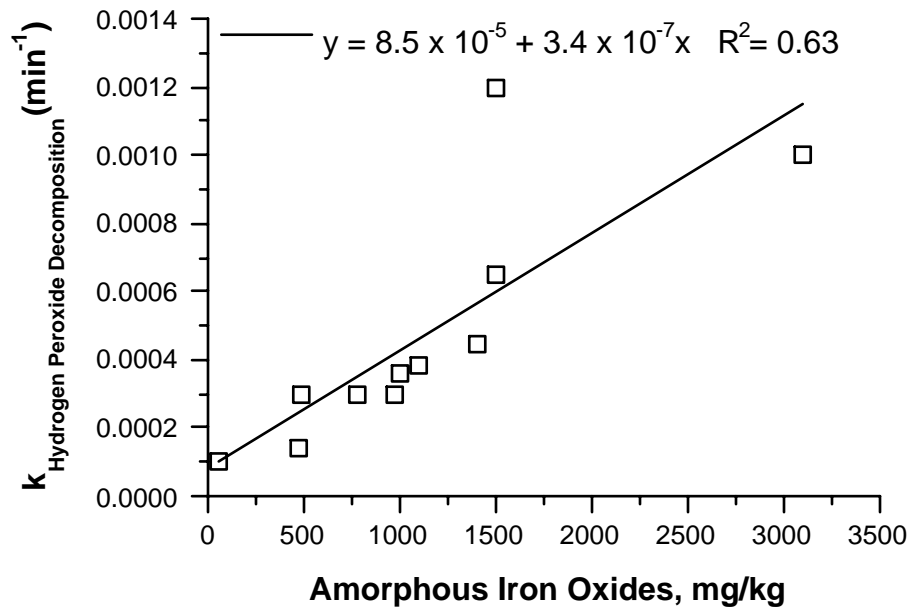
Figure 8.1.2-11. Correlation of hydrogen peroxide decomposition in soils at pH 3 to soil amorphous iron oxide content.
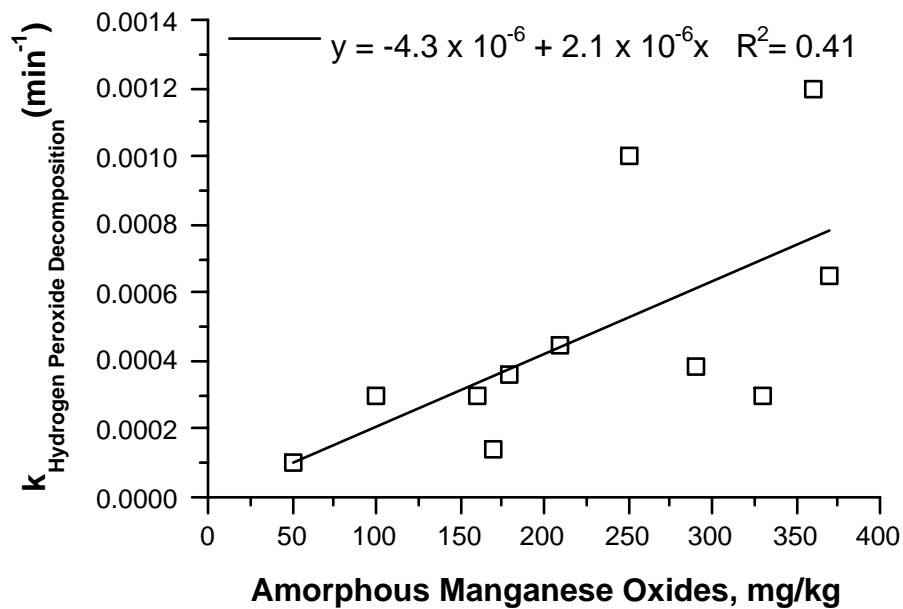
Figure 8.1.2-12. Correlation of hydrogen peroxide decomposition in soils at pH 3 to soil amorphous manganese oxide content.

8.2 Reactive Oxygen Species Generation by Different CHP Systems

Soluble iron, soluble manganese, and various iron, manganese, and trace minerals decompose hydrogen peroxide at different rates; in addition, these metals and minerals likely generate reactive oxygen species in varying proportions because of different oxidation-reduction couples between valence states of the species initiating hydrogen peroxide decomposition.

Naturally-occurring iron minerals have been studied extensively for catalyzing the decomposition of hydrogen peroxide (Tyre et al., 1991; Watts et al., 1993; Miller and Valentine, 1995; Khan and Watts, 1996; Lin and Gurol, 1998). In many cases, CHP reactions are more stoichiometrically efficient when iron minerals are used as the catalyst, suggesting that injection of soluble forms of iron may not be needed for *in situ* treatment. Sun and Pignatello (1992) and Pignatello and Baehr (1994) developed iron catalysts chelated with organic ligands, such as ethylenediaminetetraacetic acid (EDTA) and nitrilotriacetic acid (NTA), to catalyze CHP reactions. Wang and Brusseau (1998) used an inorganic ligand system consisting of pyrophosphate, which promoted CHP reactions at neutral pH. These iron ligands allow CHP reactions to proceed at neutral pH by minimizing the precipitation of iron and may eliminate the need to acidify the subsurface during *in situ* remediation. Research on CHP catalysts has provided more effective process conditions for contaminant degradation, and investigation of new catalysts will likely provide further improvements in the CHP treatment of soils and groundwater.

Radical generation in soluble and crystalline manganese catalyzed CHP systems. Transition elements other than iron, such as manganese, also catalyze CHP reactions but have not been studied to the extent of iron catalysts. Manganese is a transition metal that exists naturally in the (+II) and (+IV) oxidation states, although other valence states, such as (+III) and (+VII), also occur. Similar to iron, manganese is found in the geosphere as amorphous and crystalline oxides and oxyhydroxides. Manganese oxides occur in soils and subsurface solids as coatings on particles, as well as deposited in cracks, veins, and nodules up to 2 cm in diameter. The nodules often exhibit a concentric layering, and may contain oxides of both iron and manganese as well as other transition elements (Sposito, 1989). Using selective removal of manganese from aquifer solids, Valentine and Wang (1998) found that the manganese oxide fraction was significantly more reactive than iron oxides in promoting the decomposition of hydrogen peroxide; the authors also suggested that manganese oxides may be important in the catalytic decomposition of hydrogen peroxide when it is injected into the subsurface. The ability of soluble manganese and manganese oxides to catalyze CHP reactions has not been studied in depth. Therefore, one purpose of this segment of research was to investigate the occurrence of chemical oxidation and reduction reactions in soluble manganese- and manganese oxide-catalyzed CHP reactions.

Radical generation in soluble iron catalyzed CHP systems at neutral pH. CHP is usually most effective at acidic pH. Watts et al. (1990) and Leung et al. (1992) documented that PCP and PCE degradation through CHP reactions were optimized at pH 3. The need to adjust pH for effective CHP treatment in subsurface systems is often impractical (Chen, 1992). Lowering the pH of the subsurface often creates additional problems such as percolation of acidic water and toxic heavy metals into groundwater. To limit the practical implications of lowering pH for CHP effectiveness, Pignatello and Baehr (1994) studied the use of chelates that could keep iron

soluble at neutral pH regimes. The iron chelates were observed to catalyze CHP reactions and degrade two common pesticides, dichlorophenoxyacetic acid (2-4 D) and methoxychlor. Motekaitis and Martell (1994) demonstrated that a chelating agent, nitrilotriacetic acid (NTA), can potentially keep ferric iron in solution up to pH 9.3 before the cation precipitated. Chelated iron-mediated reactions have become one of the most common pathways of promoting CHP remediation in the subsurface; therefore, the reactive oxygen species generated in these reactions is an important area of investigation. The other purpose of the this segment of research was to investigate the mechanisms of oxidation and reduction in CHP reactions at different pH regimes using NTA as an iron chelating agent.

8.2.1 Oxidative and Reductive Pathways in Manganese-Catalyzed CHP Reactions

Transition elements other than iron, such as manganese, also catalyze CHP reactions but have not been studied to the extent of iron catalysts. Manganese is a transition metal that exists naturally in the (+II) and (+IV) oxidation states, although other valence states, such as (+III) and (+VII), also occur. Similar to iron, manganese is found in the geosphere as amorphous and crystalline oxides and oxyhydroxides. Valentine and Wang (1998) found that manganese oxide was significantly more reactive than iron oxides in promoting the decomposition of hydrogen peroxide and suggested that manganese oxides may be important in the catalytic decomposition of hydrogen peroxide when it is injected into the subsurface. The ability of soluble manganese and manganese oxides to catalyze CHP reactions has not been studied in depth. Therefore, the purpose of this research was to investigate the occurrence of chemical oxidation and reduction reactions in soluble manganese- and manganese oxide-catalyzed CHP reactions.

Oxidant production in soluble manganese (II)-catalyzed CHP reactions.

To investigate the potential of soluble manganese (II) to catalyze the generation of hydroxyl radicals, CHP reactions (600 mM H_2O_2 and 200 mM $MnSO_4$) were conducted at a range of pH regimes using 1-hexanol as a hydroxyl radical probe. The oxidation of 1-hexanol and the corresponding hydrogen peroxide residuals at pH 4, 6, 6.4, and 6.8 are shown in Figures 8.2.1-1a-d. Although the CHP reactions were also conducted at pH 3 and 5, the data shown in Figures 8.2.1-1a-d demonstrate the minimal changes from pH 3 to pH 6 and the dramatic change in pathways that occurs above pH 6. Greater than 99% of the 1-hexanol was oxidized within 48 h at pH 4, while the consumption of hydrogen peroxide was minimal (Figure 8.2.1-1a); similar results were observed at pH 3 and 5. These data demonstrate that soluble manganese promotes hydroxyl radical production at acidic pH regimes; however, significant concentrations of catalyst are required compared to iron-catalyzed reactions. For example, iron (III)-catalyzed CHP reactions using the same concentrations of hydrogen peroxide and 5 mM iron were complete within 2 h (Watts et al., 1993). As the system pH was increased, a significant change in reaction pathways was observed. The rate of hydroxyl radical generation, as measured by 1-hexanol oxidation, decreased at pH 6 (Figure 8.2.1-1b) and became near-undetectable at pH 6.4 and pH 6.8 (Figure 8.2.1-1c and d). Hydrogen peroxide decomposition rates were higher at pH 6 and increased further at pH 6.4 and 6.8. The increase in hydrogen peroxide consumption was accompanied by significant gas evolution and the formation of a precipitate, which was likely an amorphous manganese oxide, because the pH adjustment procedure is similar to that used by Stone and Morgan (1984) to generate amorphous manganese oxides. The reaction stoichiometry

at pH 4 was highly efficient, with 21.5 mol of H_2O_2 consumed/mol of 1-hexanol oxidized, because hydrogen peroxide consumption was minimal over the 48 h reaction period. However, reaction stoichiometry became significantly less efficient as the system pH was increased to 6.8, with 5.8 mmol of H_2O_2 consumed in 30 min and no measurable oxidation of 1-hexanol relative to the control reactions. In summary, the data of Figure 8.2.1-1 show that soluble manganese (II) is a stoichiometrically-efficient catalyst for the generation of hydroxyl radicals at acidic pH, but not at the near-neutral pH regime of pH 6.4-6.8.

Reductant production in soluble manganese-catalyzed CHP reactions.

To investigate the potential of soluble manganese (II) to catalyze the decomposition of hydrogen peroxide into reducing species, CHP reactions (600 mM H_2O_2 and 200 mM $MnSO_4$) were conducted at the same pH regimes used with 1-hexanol, but with CT as a reductant probe. Transformation of CT and corresponding hydrogen peroxide residuals at pH 4, 6, 6.4, and 6.8 are shown in Figures 8.2.1-2a-d. Similar to the data of Figures 8.2.1-1a-d, CT and hydrogen peroxide decomposition rates were characterized by minimal changes from pH 3 to 6, with dramatic changes above pH 6. No measurable reducing activity was found at pH 4 over 72 h compared to control reactions, and the decomposition of hydrogen peroxide was negligible (Figure 8.2.1-2a), as it was in the parallel reactions in which 1-hexanol was used as a probe (Figure 8.2.1-1a). Similar minimal reducing activity was found over 24 h in reactions conducted at pH regimes up to pH 6, although the hydrogen peroxide decomposition rate increased at pH 6 (Figure 8.2.1-2b). As the pH of the CHP system was raised to pH 6.4 and 6.8, the rates of both hydrogen peroxide decomposition and CT transformation increased significantly. Degradation of CT was 66% at pH 6.4 within 8 h (Figure 8.2.1-2c) and increased to 89% at pH 6.8 within 60 min (Figure 8.2.1-2d). These data show a relationship between the pH of the system and the generation of reductants, with the reduction of CT increasing from undetectable to 89% as the pH was increased from 3 to 6.8.

Visual inspection of the reactions showed that as the pH of the manganese-catalyzed systems approached 6.8, an amorphous precipitate formed. The increased rates of CHP reductions correlated with the presence of the manganese precipitate, suggesting that the solid material may catalyze the generation of reductants.

Reductant and oxidant generation in manganese oxide precipitate–catalyzed CHP reactions.

To determine the role of the amorphous manganese solid in catalyzing the decomposition of hydrogen peroxide into reducing species, an amorphous manganese oxide was generated in a separate reactor, washed and dried, and employed as the catalyst in CHP reactions (10 ml of 600 mM H_2O_2 and 25 mg manganese precipitate). Using these conditions, 70% CT transformation occurred within 10 min at pH 6.8 (Figure 8.2.1-3), which is similar to the results shown in Figure 8.2.1-2d. Carbon tetrachloride degradation was verified by monitoring chloride release in parallel reactions. Chloride was released from CT in the ratio of 2 mol chloride per mol CT lost over the 60 min reaction, confirming degradation of CT (Figure 8.2.1-4). Because CT is not reactive with hydroxyl radicals (Buxton et al., 1987), its degradation is likely due to a non-hydroxyl radical mechanism. Teel and Watts (2002) also found degradation of CT in iron-catalyzed CHP reactions (600 mM H_2O_2 and 1 mM iron [III]) and, through a series of scavenging experiments, confirmed a reductive pathway for the degradation of CT. Similar reductive mechanisms are likely occurring in the CHP system catalyzed by the amorphous manganese oxide precipitate.

The reductants formed in manganese-oxide catalyzed reactions may include superoxide radical anion ($O_2\bullet^-$), hydroperoxide anion (HO_2^-), and hydrogen atoms ($H\bullet$). Superoxide anion has been shown to reduce quinones (Wilson, 1971), nitrobenzenes (Poupko and Rosenthal, 1973), and nitrogen heterocycles (Bielski et al., 1980). Hydroperoxide anion is a reductant and a nucleophile that can reduce organic compounds via one-electron transfers (Afanas'ev, 1989); it has been shown to reduce benzoquinones (Afanas'ev, 1989) and 5-aminophthalazine-1,4-dione (Merenyi et al., 1984). Kitajima et al. (1978) documented the formation of superoxide in the metal oxide-catalyzed decomposition of hydrogen peroxide, a mechanism that was confirmed by electron spin resonance (ESR) spectra. Miller and Valentine (1999) investigated hydrogen peroxide decomposition and contaminant degradation in the presence of natural metal oxide-coated sand, and found that both superoxide and hydroxyl radical were generated in the system. They proposed a mechanism in which the positively-charged surface catalyzes the decomposition of hydrogen peroxide to a proton and perhydroxyl radical ($HO_2\bullet$), which can dissociate to superoxide or react with the reduced surface to form hydroperoxide anion. Hasan et al. (1999) postulated that manganese oxides catalyze the decomposition of hydrogen peroxide to hydroperoxide and a proton, followed by an electron transfer from hydroperoxide to the proton to yield perhydroxyl radical (and its conjugate base superoxide) and a hydrogen atom. Thus, one or more reductants may be generated in the manganese oxide-catalyzed decomposition of hydrogen peroxide.

CHP reactions catalyzed by the manganese oxide precipitate were repeated using 1-hexanol in place of CT to determine if hydroxyl radicals are generated in addition to reductants. In reactions conducted at pH 6.8 (10 ml of 600 mM H_2O_2 and 25 mg manganese precipitate), no measurable oxidation of 1-hexanol was found; however, hydrogen peroxide decomposed by 97% within 10 min (Figure 8.2.1-5). These results demonstrate that, although amorphous manganese oxide-catalyzed CHP reactions generate reductants, they do not generate hydroxyl radicals. The results are in agreement with the findings of Valentine and Wang (1998), who showed that the removal of manganese oxides from mineral conglomerates used as CHP catalysts lowered hydrogen peroxide decomposition by 90% and increased quinoline degradation from 15% to 50%. Quinoline is reactive with hydroxyl radicals but not with reductants; eliminating the rapid manganese oxide-catalyzed decomposition of hydrogen peroxide to reductants resulted in a hydrogen peroxide residual that could be catalyzed by the iron oxide fraction to generate hydroxyl radicals and degrade the quinoline. In summary, amorphous manganese oxides catalyze the decomposition of hydrogen peroxide to generate reductants, but not oxidants.

Reductant and oxidant generation by crystalline manganese oxide-catalyzed CHP reactions.
The high rates of CT degradation and hydrogen peroxide decomposition found in amorphous manganese oxide-catalyzed CHP reactions suggested that crystalline manganese oxides, such as pyrolusite, may also catalyze the generation of reductants. Therefore, CT was used as a reductant probe in CHP reactions catalyzed by 25 mg pyrolusite using 600 mM hydrogen peroxide at pH 6.8. Carbon tetrachloride was degraded by 82% with 96% consumption of the hydrogen peroxide within 60 min (Figure 8.2.1-6). Similar to the data shown in Figure 8.2.1-4, degradation of CT was verified by monitoring the release of chloride in parallel reactions, with 2 moles of chloride formed per mole of CT degraded.

The generation of hydroxyl radicals in the pyrolusite-catalyzed decomposition of hydrogen peroxide, measured by the oxidation of 1-hexanol, is shown in Figure 8.2.1-7. As in

the results shown in Figures 8.2.1-2d and 8.2.1-5, the oxidation of 1-hexanol was negligible, indicating that hydroxyl radicals are not generated when manganese oxides catalyze the decomposition of hydrogen peroxide.

The results of this research demonstrate that soluble manganese (II) catalyzes the decomposition of hydrogen peroxide to hydroxyl radicals, and amorphous and crystalline manganese oxides catalyze its decomposition to reductants. The occurrence of manganese oxides in the subsurface varies both locally and regionally. Although not found in high concentrations in the geosphere, manganese oxides are present in the subsurface as nodules with high surface areas. The high rate of hydrogen peroxide decomposition catalyzed by manganese oxides may compete with hydroxyl radical production when hydrogen peroxide is injected into the subsurface as an oxidant source for *in situ* CHP reactions. However, many groundwater contaminants, such as CT and perchloroethylene, may be reduced by the reductants formed (Teel and Watts, 2002). Furthermore, the reductants generated in CHP reactions are likely responsible for enhanced desorption of hydrophobic contaminants, in which soils and the subsurface are treated more rapidly than the rate of contaminant desorption (Watts et al., 1999). However, if the contaminants that are desorbed are not reactive with reductants, they may be transported downgradient if hydroxyl radicals are not generated in sufficient quantities to transform them.

The formation of reductants and the rapid decomposition of hydrogen peroxide catalyzed by manganese oxides at near-neutral pH has important implications for applications in which hydrogen peroxide is injected into groundwater as an oxygen source for *in situ* bioremediation. Stabilized hydrogen peroxide was once used extensively as an oxygen source for *in situ* bioremediation (Spain et al., 1989). Little was known of the mechanisms of hydrogen peroxide decomposition in the subsurface at the time when it was commonly used. For example, recent studies have shown that both abiotic oxidations and aerobic heterotrophic bacterial metabolism can coexist when hydrogen peroxide is injected into the subsurface (Howsawkeng et al., 2001). Similarly, the potential for abiotic reductions and aerobic biotic oxidations may exist when manganese oxides are present in the subsurface, because superoxide is less toxic to microorganisms than hydrogen peroxide and hydroxyl radicals (Watts et al., 2002). The results of this research demonstrate that oxidative and reductive pathways occur during the manganese oxide-catalyzed decomposition of hydrogen peroxide. Furthermore, because of the complexity of the subsurface and the intricacies of hydrogen peroxide–mineral reactions, extensive research efforts are needed to provide fundamental understanding of processes that serve as the basis for the design and operation of *in situ* chemical oxidation (ISCO) systems. Subsequent research will focus on elucidating the reductants formed by the manganese oxide-catalyzed decomposition of hydrogen peroxide with emphasis on superoxide, hydroperoxide, and hydrogen atoms.

Summary and Conclusions

The effect of pH on reaction pathways in the soluble manganese (II)-catalyzed decomposition of hydrogen peroxide was investigated. Soluble manganese (II) at pH ≤ 5 catalyzed hydrogen peroxide decomposition very slowly; after 72 h, only 7% of the hydrogen peroxide was consumed. However, the hydroxyl radical probe 1-hexanol was oxidized to undetectable concentrations within 48 h. Reductant generation by manganese (II)-catalyzed CHP reactions was undetectable as measured by the loss of the reductant probe CT.

When reactions were conducted at pH ≥ 6, an amorphous manganese oxide precipitate formed which resulted in a significant change in reaction pathways. Hydroxyl radical oxidation decreased significantly to undetectable as the pH was elevated from 6.0 to 6.8; in contrast, the generation of reductants increased substantially as the reaction pH was raised above pH 6. Isolating the amorphous manganese oxide precipitate from separate reactors and using it as a catalyst with CT as a probe compound confirmed its role as the catalyst for reductant generation. The crystalline manganese oxide pyrolusite had catalytic properties similar to those of the amorphous precipitate, causing rapid decomposition of hydrogen peroxide and rapid transformation of carbon tetrachloride. The presence of manganese oxides in the subsurface may decompose hydrogen peroxide rapidly, providing a pathway to reduce chloroaliphatic contaminants when hydrogen peroxide is injected into the subsurface as a supplemental oxygen source for bioremediation or as an oxidant source for *in situ* chemical oxidation (ISCO).
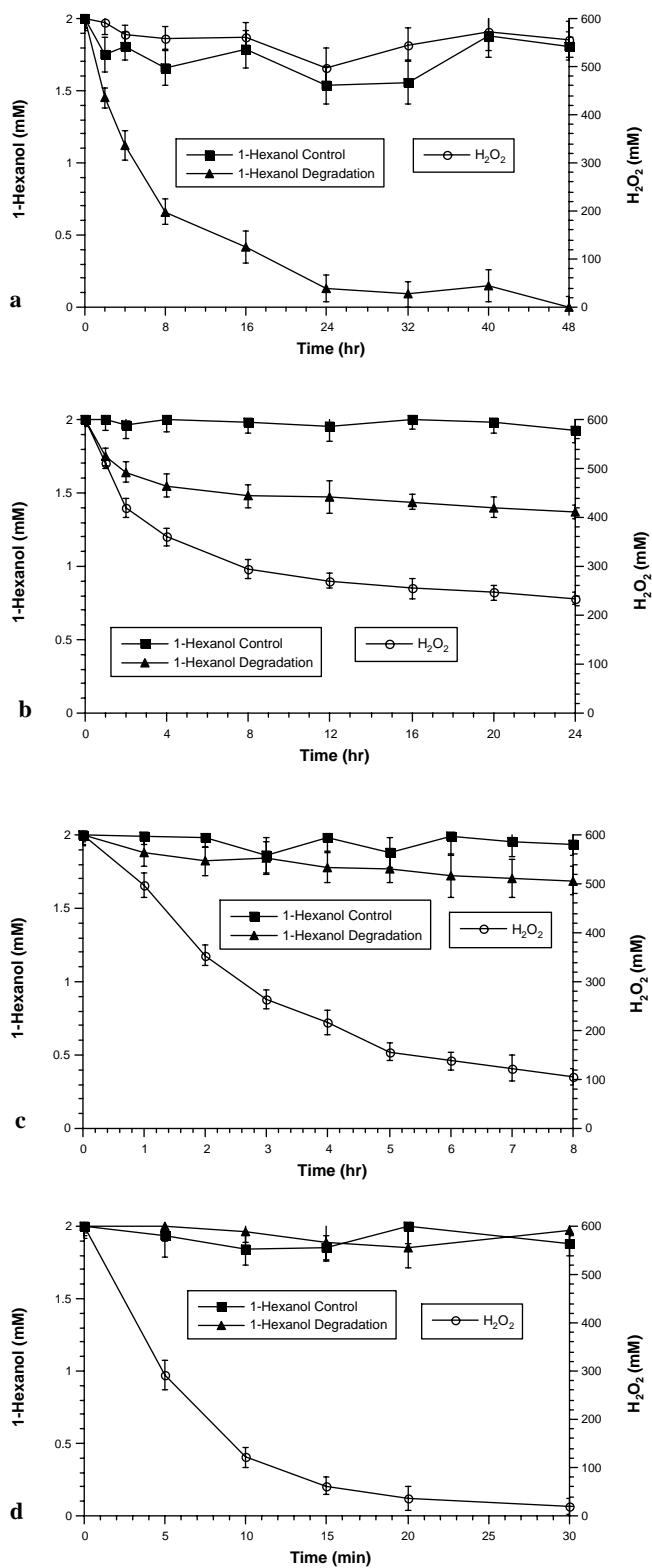
Figure 8.2.1-1. 1-Hexanol and hydrogen peroxide concentrations in manganese (II)-catalyzed CHP reactions (600 mM hydrogen peroxide and 200 mM manganese sulfate).
(a) pH 4.0; (b) pH 6.0; (c) pH 6.4; (d) pH 6.8

69
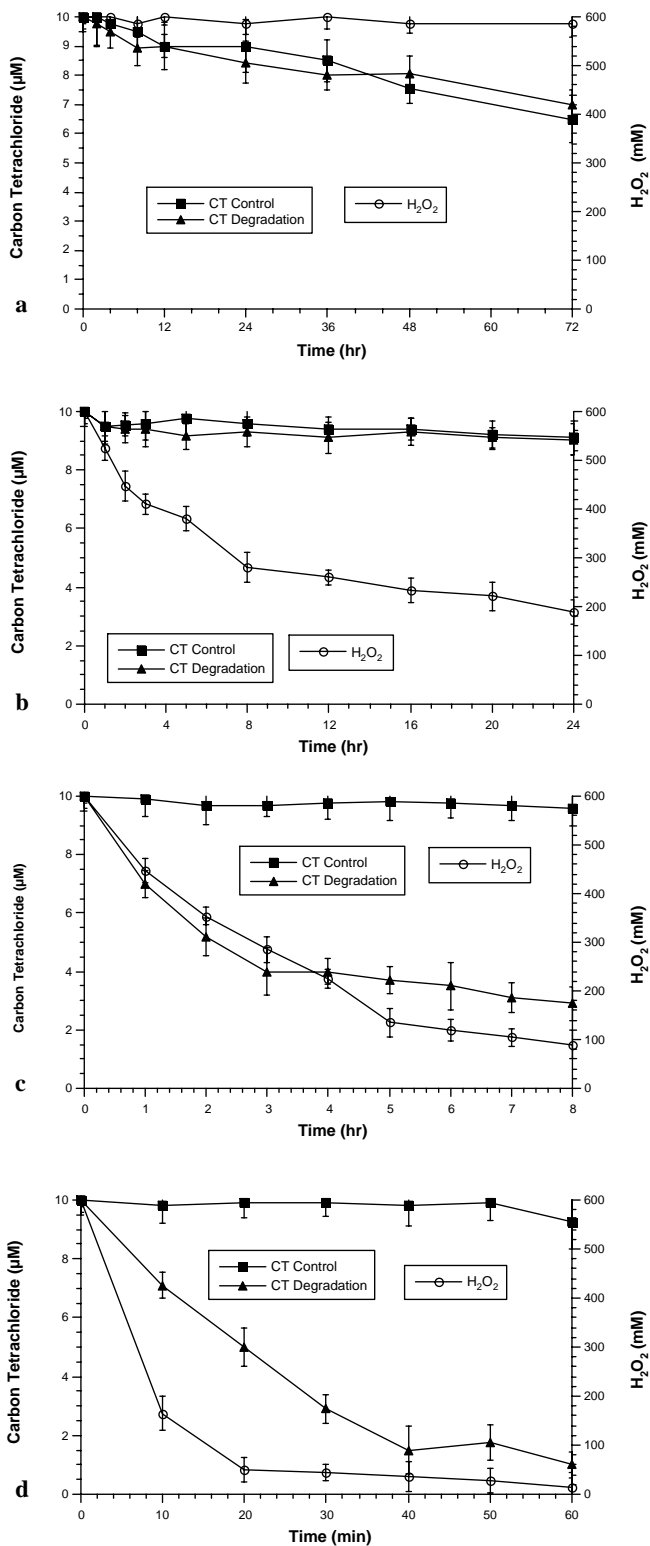
Figure 8.2.1-2. Carbon tetrachloride and hydrogen peroxide concentrations in manganese (II)-catalyzed CHP reactions (600 mM hydrogen peroxide and 200 mM manganese sulfate).
(a) pH 4.0; (b) pH 6.0; (c) pH 6.4; (d) pH 6.8
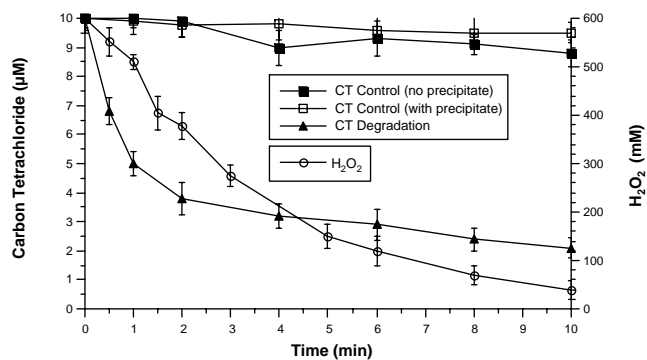
Figure 8.2.1-3. Carbon tetrachloride and hydrogen peroxide concentrations in CHP reactions catalyzed by amorphous manganese oxide precipitate (600 mM hydrogen peroxide and 25 mg manganese precipitate at pH 6.8)
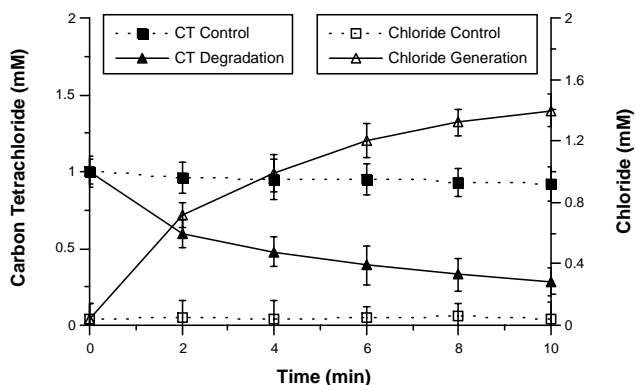
Figure 8.2.1-4. Chloride generation from the degradation of 1 mM carbon tetrachloride during in CHP reactions catalyzed by amorphous manganese oxide precipitate (600 mM hydrogen peroxide and 25 mg manganese precipitate at pH 6.8)
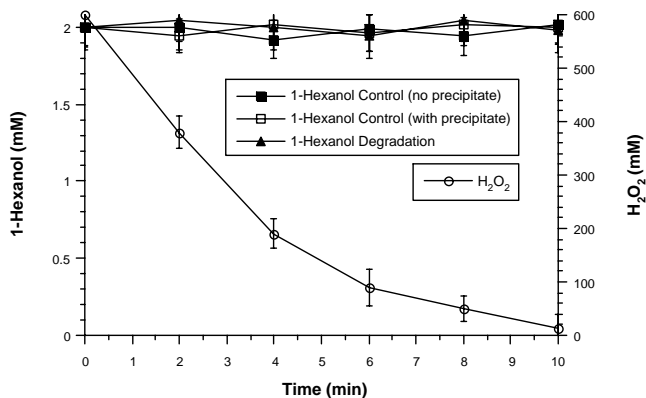
Figure 8.2.1-5.   Hexanol and hydrogen peroxide concentrations in CHP reactions catalyzed by amorphous manganese oxide precipitate (600 mM hydrogen peroxide and 25 mg manganese precipitate at pH 6.8)

71
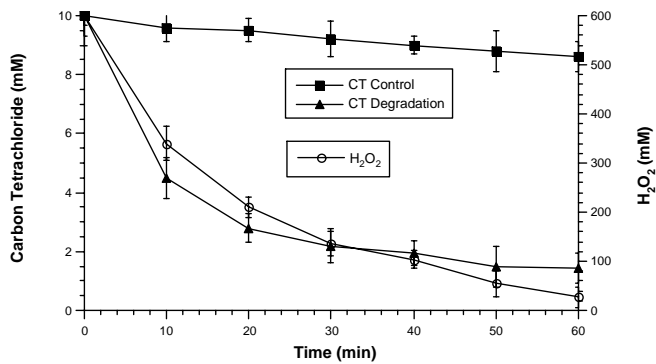
Figure 8.2.1-6. Carbon tetrachloride and hydrogen peroxide concentrations in CHP reactions catalyzed by pyrolusite (600 mM hydrogen peroxide and 25 mg pyrolusite at pH 6.8)
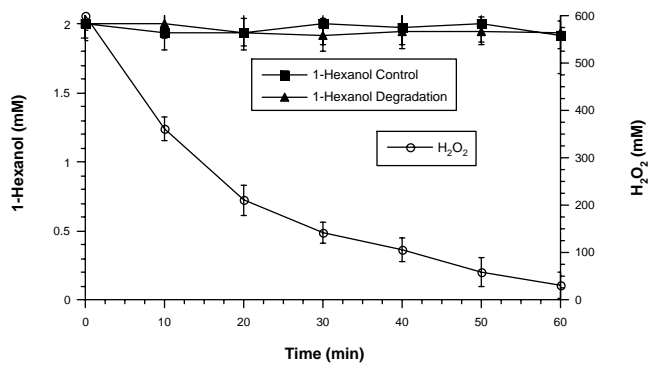
Figure 8.2.1-7. Hexanol and hydrogen peroxide concentrations in CHP reactions catalyzed by pyrolusite (600 mM hydrogen peroxide and 25 mg pyrolusite at pH 6.8)

8.2.2 Mechanisms of Oxidation and Reduction in CHP Reactions Catalyzed by Soluble Iron at Different pH Regimes

Relative hydroxyl radical production rate.

The results obtained for the relative rate of hydroxyl radical production, quantified by *n*-hexanol oxidation, under varying pH regimes are shown in Figures 8.2.2-1 to 8.2.2-4. In Figure 8.2.2-1, reactions conducted at pH 3 showed that after 3 hours, *n*-hexanol oxidation ranged from 10% (with 14.7 mM H_2O_2) to 90% (with 1470 mM H_2O_2). As the pH was raised to 5, 7, and 9, hydroxyl radical generation rates increased significantly. The data of Figure 8.2.2-2 show that at pH 5, greater than 99.99% *n*-hexanol oxidation was achieved over a time period of 3 hours with hydrogen peroxide concentrations exceeding 294 mM. As the pH was further adjusted to 7 and subsequently 9, 99.99% *n*-hexanol destruction was observed within minutes even at the lowest concentration of hydrogen peroxide (Figures 8.2.2-3 and 8.2.2-4) with the highest oxidation rates occurring at pH 9. The proposed pathway of *n*-hexanol oxidation is illustrated below; hexanoic acid transformation into CO_2 and H_2O is hypothesized to be the rate limiting step.

$$n\text{-Hexanol} + OH\bullet \rightarrow \text{Hexanal} + OH\bullet \rightarrow \text{Hexanoic acid} \qquad [1]$$
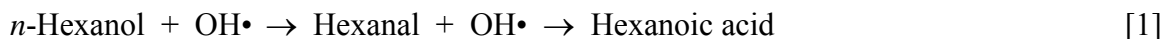
Increased hydroxyl radical generation rates at higher pH regimes were likely the result of increased hydrogen peroxide destabilization.

$$H_2O_2 + H_2O \leftrightarrow H_3O^+ + HO_2^- \quad (pK_a = 11.8) \qquad [2]$$
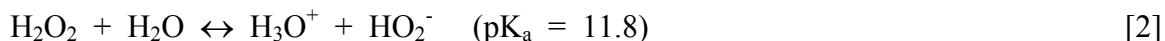
Schumb et al. (1955) postulated that hydrogen peroxide behaves as a weak acid. They later showed that increasing the pH from 5 to 7 would destabilize hydrogen peroxide by 8 fold. By Le Chatelier's principle, the increased concentration of OH^- ions at higher pH would tend to shift the equilibrium position to the right, hence destabilizing H_2O_2 (see equation [2]). As a result, hydroxyl radicals produced during CHP reactions will not be quenched by an excess of hydrogen peroxide in the system.

In the absence of the chelator nitrilotriacetic acid (NTA), the unadjusted pH of 1 mM soluble ferric iron was ~ 2.5. The data in Figure 8.2.2-5 indicate that experiments conducted without addition of NTA yielded faster degradation rates compared to those performed with iron-NTA at pH 3. *n*-Hexanol oxidation ranged from 70% (with $[H_2O_2]$ at 14.7 mM) to 99.99% (with $[H_2O_2] > 294$ mM). These results contradict the trend that higher pH is usually accompanied by an increase in hydroxyl radical generation and oxidation of *n*-hexanol. However, since the ferric-NTA chelates are very stable over a pH range of 1.5 to 3 (Gussets and Opgenorth, 1996), NTA may out compete hydrogen peroxide and bind strongly with soluble iron at pH 3, thus reducing the availability of the soluble iron for catalytic decomposition of hydrogen peroxide. As NaOH is added to raise the pH above 3, the hydroxide neutralizes the protons before destabilizing the chelate complex and compete for the soluble iron in equation 3 below. As the complex is destabilized, the availability of iron to initiate the CHP reaction may increase. Therefore, both pH and availability of soluble iron play an important role in achieving a high rate of oxidation.

$$Fe[III] + \begin{array}{c} CH_2COOH \\ N\check{S}CH_2COOH \\ CH_2COOH \end{array} \rightleftharpoons \quad \text{[Fe-NTA complex]} \quad + \quad 3\,H^+ \qquad [3]$$
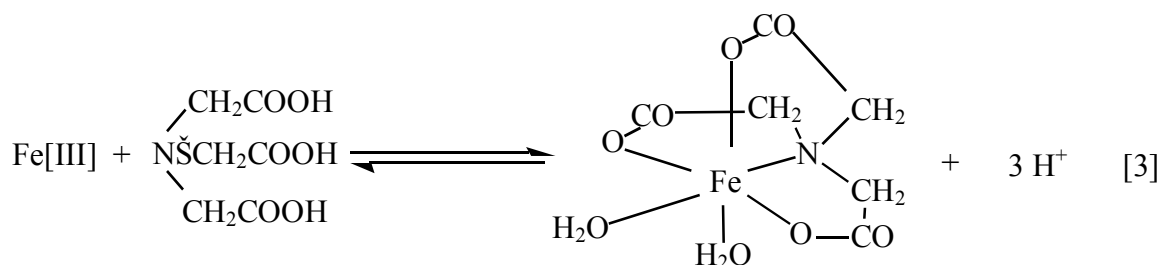
Another aspect of the lifetimes of soluble iron at different pH regimes is shown in Figure 8.2.2-6. In CHP reactions, the soluble iron will eventually precipitate as ferric hydroxide, which slows the homogeneous catalytic decomposition of hydrogen peroxide, as shown in equations [4] and [5] (Watts et al., 1990).

$$Fe^{3+} + 3OH^- \rightarrow Fe(OH)_{3(s)} \qquad\qquad [4]$$

$$Fe(OH)_{3(s)} + H_2O_2 \rightarrow \text{no hydroxyl radicals} \qquad\qquad [5]$$

In addition, the lifetime of soluble iron decreases at higher pH regimes, which is due to the unstable nature of hydrogen peroxide and iron chelate complexes at those conditions.

Scavenging of hydroxyl radical.
To verify hydroxyl radical production, various scavenging compounds were added in excess of *n*-hexanol in the presence of 1 mM Fe (III) and 294 mM (1%) hydrogen peroxide. Competition reactions were not studied at pH 7 and 9 due to the high rates of *n*-hexanol degradation at those conditions, which made detection of hexanol impractical. An excess of isopropanol or tert-butyl alcohol in the ratio of 2.5:1 relative to initial hydrogen peroxide concentration was introduced to the samples and run parallel to the experiments to quench hydroxyl radical. The scavengers were added in excess in relation to hydrogen peroxide instead of *n*-hexanol due to the fact that hydrogen peroxide is the main OH• competitor (Watts et al., 1999). Finally, an excess of chloroform in the ratio 4:1 relative to the initial *n*-hexanol concentration was also studied in parallel to scavenge any reductants. Figures 8.2.2-7 and 8.2.2-8 show similar results obtained for experiments conducted at pH 3 and 5. Isopropanol and *tert*-butyl alcohol were observed to significantly decrease the degradation of *n*-hexanol. *n*-Hexanol has the same characteristics as isopropanol, which has a readily oxidizable functional -OH group. Rush and Koppenol (1986) documented that isopropanol and tert-butyl alcohol are readily oxidized by hydroxyl radicals. They hypothesized the existence of a secondary oxidizing intermediate like ferryl ion (FeO^{2+}) that was also scavenged by isopropanol but not by bulky compounds such as tert-butyl alcohol (see equations [6] and [7]).

$$Fe(II)\text{-}NTA + H_2O_2 \rightarrow P \qquad\qquad [6]$$

$$P + Fe(II)\text{-}NTA \rightarrow 2\,Fe(III)\text{-}NTA + 2OH^- \qquad\qquad [7]$$

$$P = FeO^{2+} + H_2O \quad \text{or} \quad P = Fe\text{-}NTA + OH\bullet + OH^-$$
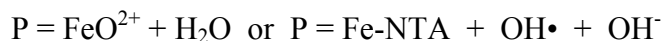
The data shown in Figures 8.2.2-7 and 8.2.2-8, however, exclude the minimal role of ferryl ions and confirm that hydroxyl radicals were the main oxidants for *n*-hexanol oxidation. Furthermore, experiments run with an addition of excess chloroform indicate that reductants have little effect on *n*-hexanol degradation, again confirming that oxidation by hydroxyl radicals were the primary mechanism for *n*-hexanol degradation.

Rates of superoxide generation.

The same conditions used for hydroxyl radical generation experiments were applied to superoxide generation. Figures 8.2.2-9–12 show CT degradation under different pH conditions. After 60 minutes, CT destruction ranged from less than 1% (with 14.7 mM H_2O_2) to 50% (with 1470 mM H_2O_2). As the pH was raised, no significant increase in the rate of CT degradation was observed, except for the first 15 minutes in which the destruction rate was slightly higher at high pH regimes. These data indicate that CT was degraded in a CHP reaction using high hydrogen peroxide concentrations, but pH conditions had minimal effect on the CT degradation rate. Smith et al. (2004) demonstrated the existence of superoxide anions as the primary reducing species for CT in CHP reactions.

The propagation reactions resulting from the iron (III) catalyzed decomposition of hydrogen peroxide were first reported by Barb et al. (1951) and later reviewed by Walling and Weil (1975). The propagation reactions were described as:

$$Fe^{3+} + H_2O_2 \rightarrow Fe^{2+} + HO_2\bullet + H^+ \tag{8}$$

$$Fe^{2+} + H_2O_2 \rightarrow Fe^{3+} + OH\bullet + OH^- \tag{9}$$

$$OH\bullet + H_2O_2 \rightarrow H_2O + HO_2\bullet \tag{10}$$

$$HO_2\bullet + Fe^{3+} \rightarrow Fe^{2+} + H^+ + O_2 \tag{11}$$

$$HO_2\bullet + Fe^{2+} \rightarrow HO_2^- + Fe^{3+} \tag{12}$$

$$OH\bullet + Fe^{2+} \rightarrow Fe^{3+} + OH^- \tag{13}$$

Barb et al. (1951) suggested that an excess of hydrogen peroxide would favor equations [8] through [12] to proceed favoring the production of superoxide. Excess hydrogen peroxide will compete for hydroxyl radicals formed in reaction [16]. Iron (II) and iron (III) are constantly cycled in the two initiation reactions [8] and [9] while the evolution of oxygen is best described by reaction [11]. In contrast, with a low $[H_2O_2]/[Fe^{3+}]$ ratio, equation [13] would replace [12] as the termination reaction. An excess Fe^{2+} produced in equation [8], as a result of a high $[Fe^{3+}]$ concentration, would compete for $OH\bullet$ formed in equation [9]. Therefore, a local excess of Fe^{3+} would limit the propagation reactions [10] through [12], thus limiting the production of superoxide.

A substantial mass of chloroform was detected during GC analyses (data not shown). An increase in concentrations of hydrogen peroxide while maintaining the initial concentration of soluble iron constant resulted in higher yield in the degradation of CT as shown in Figures 8.2.2-9–12. These results agree with the hypothesis of Barb et al. (1951) that high $[H_2O_2]/[Fe^{3+}]$ ratios

would yield more superoxide and would therefore dechlorinate more CT. However, higher pH regimes had little effect upon the overall degradation yield of CT. Unlike the results found with hydroxyl radical detection experiments using *n*-hexanol, pH regimes above 3 slightly increased CT degradation rates in the first 15 min of the reaction but did not improve the overall amount of CT degradation.

Confirmation of CT degradation.

Chloride was analyzed to verify that CT is destroyed via reductive dehalogenation,. The release of Cl$^-$ as a function of time is shown in Figure 8.2.2-13. An increase in chloride concentrations (0.05 mM to 0.2 mM) was accompanied by a 20% reduction of CT in the first 60 minutes. After 60 min, as CT degradation slowed, the chloride ion concentration fell steadily from 0.2 mM to 0.02 mM. Chloride ions released into solution during that period were likely oxidized by hydroxyl radicals ($k_{OH.}$ = 4.3 x 10^9 M^{-1} S^{-1}; Buxton et al., 1988) to chlorine.

Scavenging analyses in CT systems.

Competition reactions for CT were performed at pH 3 and 7 using isopropanol as an oxidant scavenger, nitrate to quench hydrated electrons, and chloroform to scavenge reductants. The CHP conditions included 1 mM Fe-NTA and 294 mM hydrogen peroxide. The data for the scavenging analyses are displayed in Figures 8.2.2-14 and 8.2.2-15. At both pH conditions, chloroform was the only compound that inhibited CT destruction. Experiments conducted with CT in the presence of excess isopropanol confirm a non-hydroxyl radical mechanism.

Summary and Conclusions

Relative rates of hydroxyl radical generation and superoxide generation were evaluated in CHP reactions using different hydrogen peroxide concentrations at varying pH regimes. Evidence of oxidants and reductants in CHP systems was confirmed by the use of scavenging analysis. The higher pH likely destabilized hydrogen peroxide and the iron chelate complex, resulting in rapid rates of hydroxyl radical generation at the higher pH regimes.

Results from CT experiments have shown that high (H$_2$O$_2$/Fe^{3+}) ratios may generate superoxide as postulated by Barb et al. (1951) and later by Walling and Weil (1975). Reduction of CT was confirmed by the release of chloride ions in the batch systems and by the addition of excess chloroform, which hindered CT destruction. Furthermore, the data showed that CT destruction relies primarily on (H$_2$O$_2$/Fe^{3+}) ratios. The results from this segment of research confirmed oxidative and reductive mechanisms in soluble iron-mediated CHP reactions, and provided the foundation for evaluating the evaluation of the CHP conditions that promote oxidations and reductions using response surface methodology.
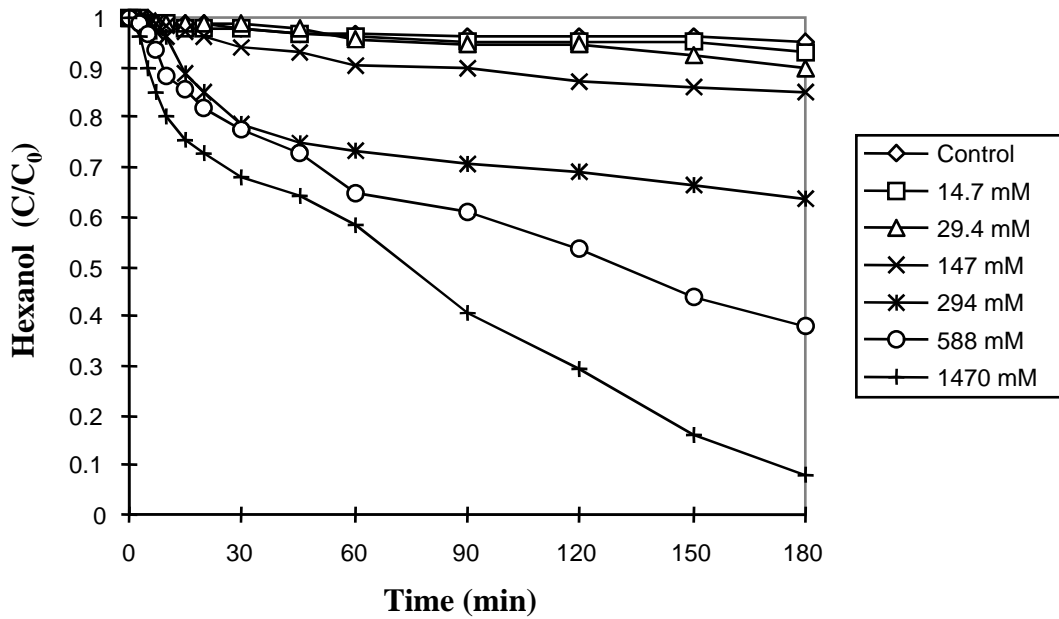
Figure 8.2.2-1. *n*-Hexanol degradation with 1 mM Fe[III] - NTA and varying hydrogen peroxide concentrations at pH 3
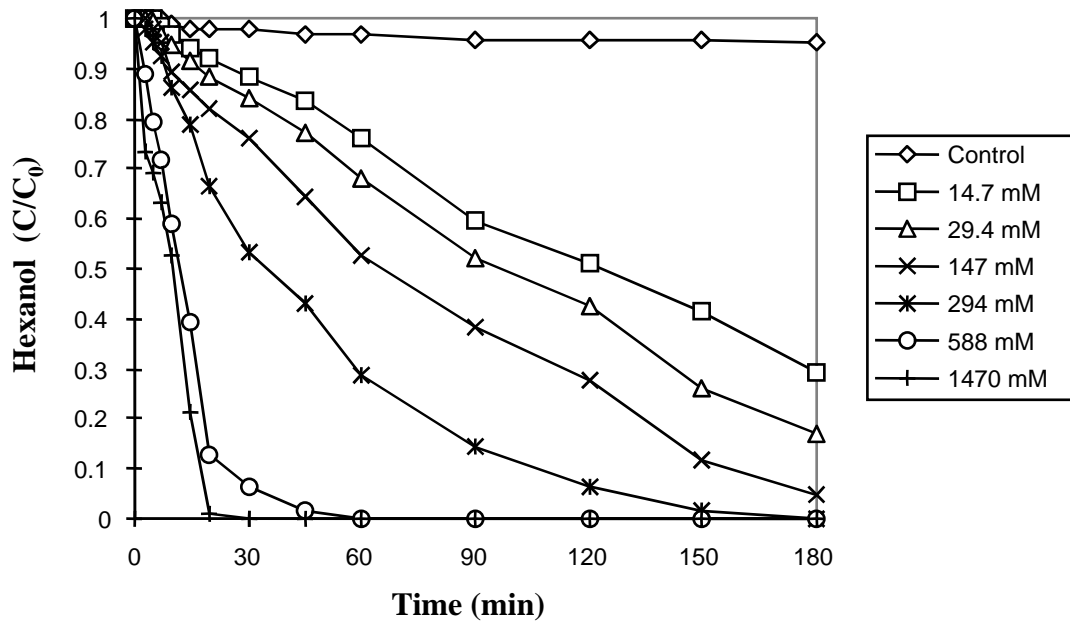
Figure 8.2.2-2. *n*-Hexanol degradation using 1 mM Fe[III] - NTA with varying hydrogen peroxide concentrations at pH 5

77
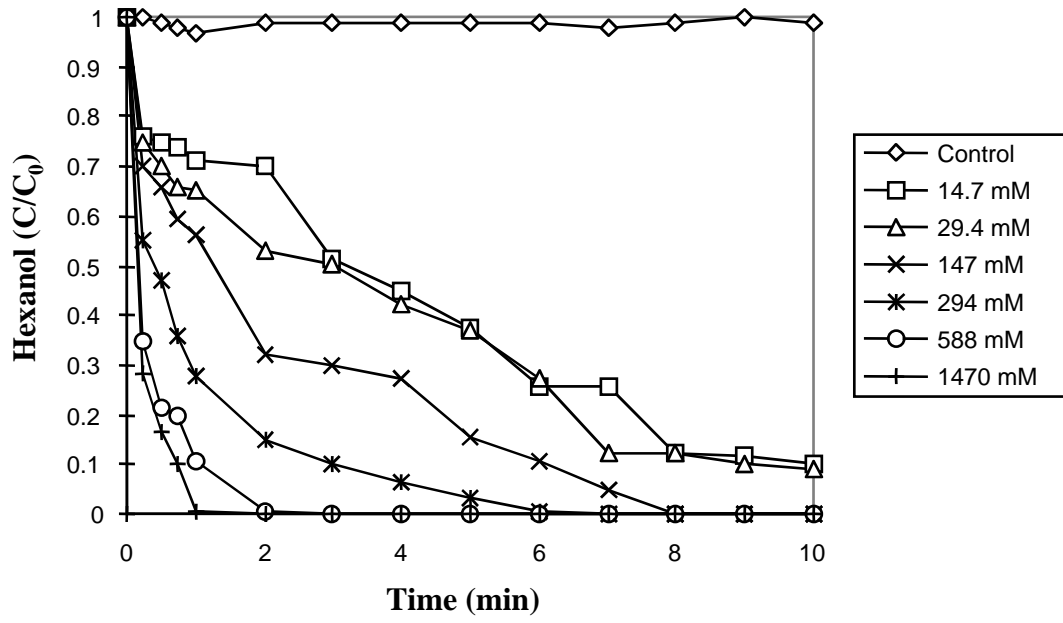
Figure 8.2.2-3. *n*-Hexanol degradation using 1 mM Fe[III] - NTA with varying hydrogen peroxide concentrations at pH 7
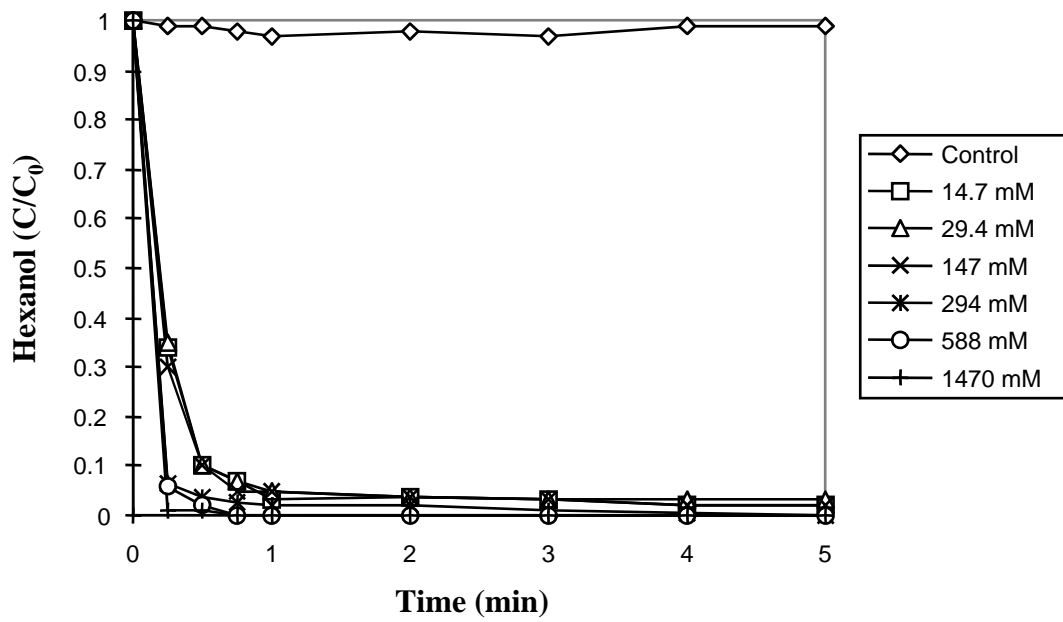
Figure 8.2.2-4. *n*-Hexanol degradation using 1 mM Fe[III] - NTA with varying hydrogen peroxide concentrations at pH 9
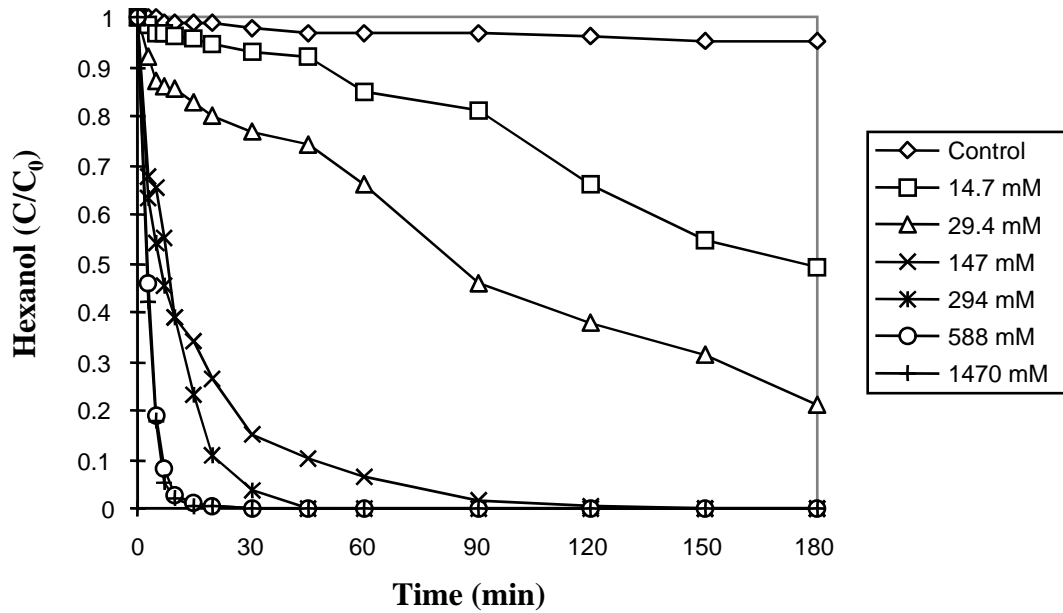
Figure 8.2.2-5. *n*-Hexanol degradation using 1 mM Fe[III] and varying hydrogen peroxide concentrations (unadjusted pH ~ 2.5)
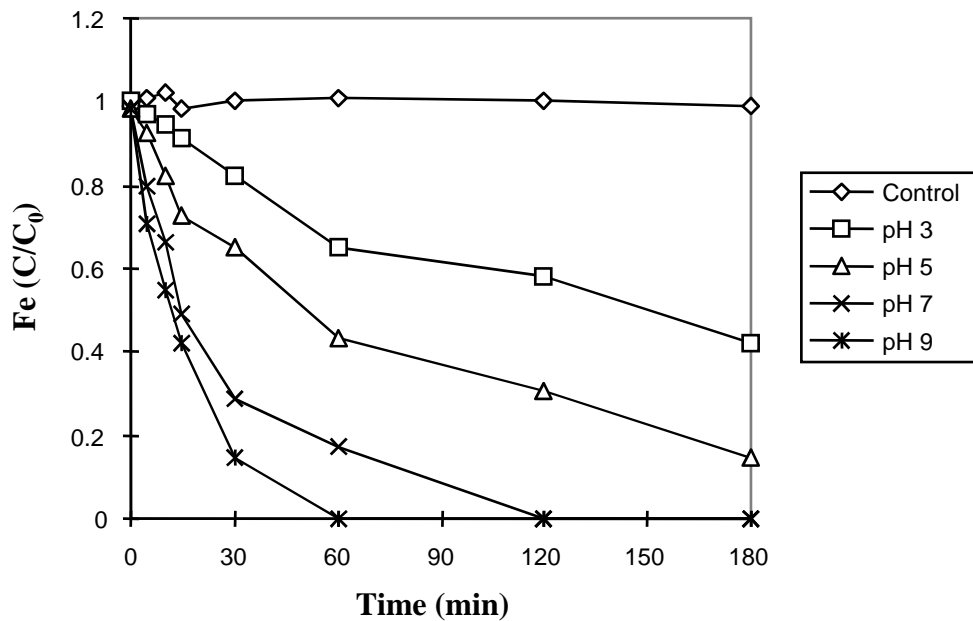
Figure 8.2.2-6. Soluble (Fe^{2+}/Fe^{3+}) - NTA concentrations with 294 mM hydrogen peroxide at varying pH
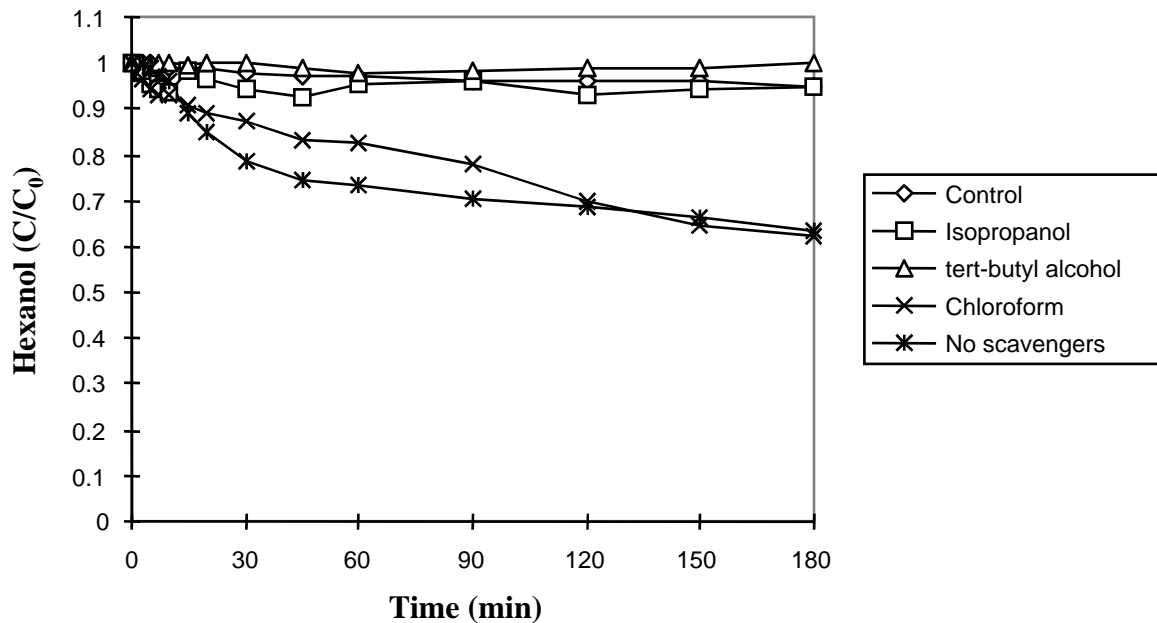
Figure 8.2.2-7. Effect of scavengers on *n*-hexanol degradation using 1 mM Fe[III] - NTA and 294 mM hydrogen peroxide at pH 3
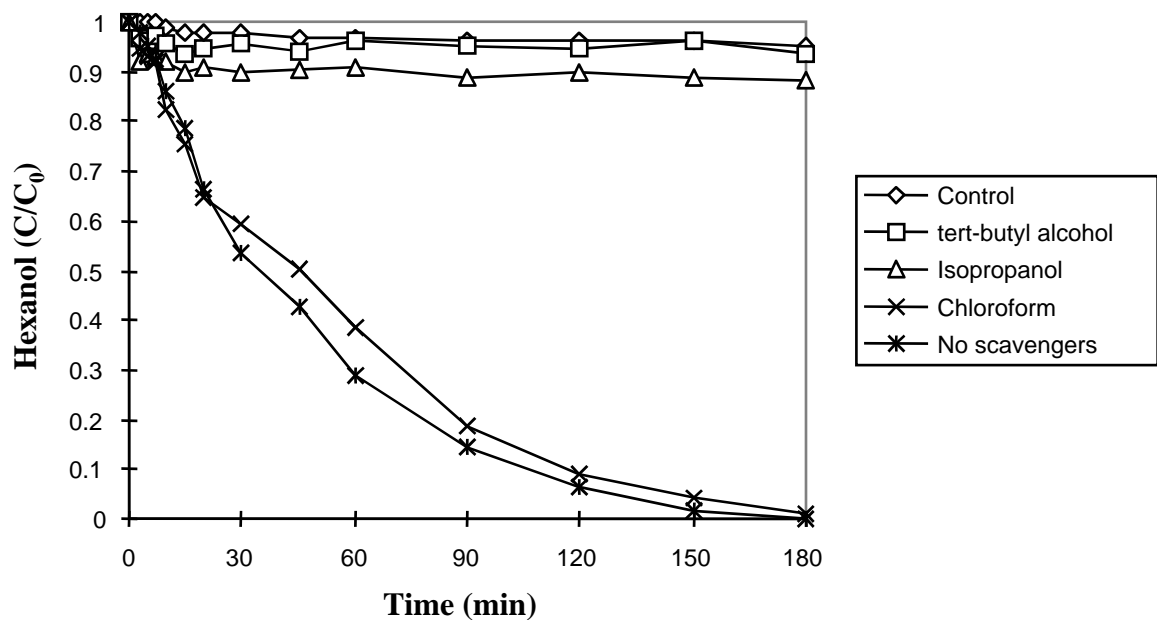
Figure 8.2.2-8. Effect of scavengers on *n*-hexanol degradation using 1 mM Fe[III] - NTA and 294 mM hydrogen peroxide at pH 5
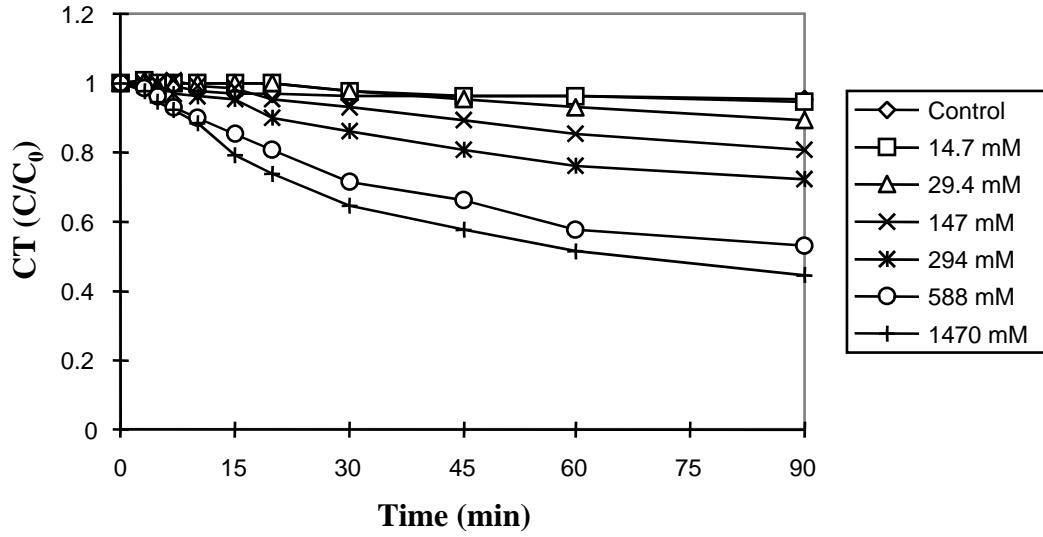
Figure 8.2.2-9. Degradation of CT with 1 mM Fe[III] - NTA and varying hydrogen peroxide concentrations at pH 3
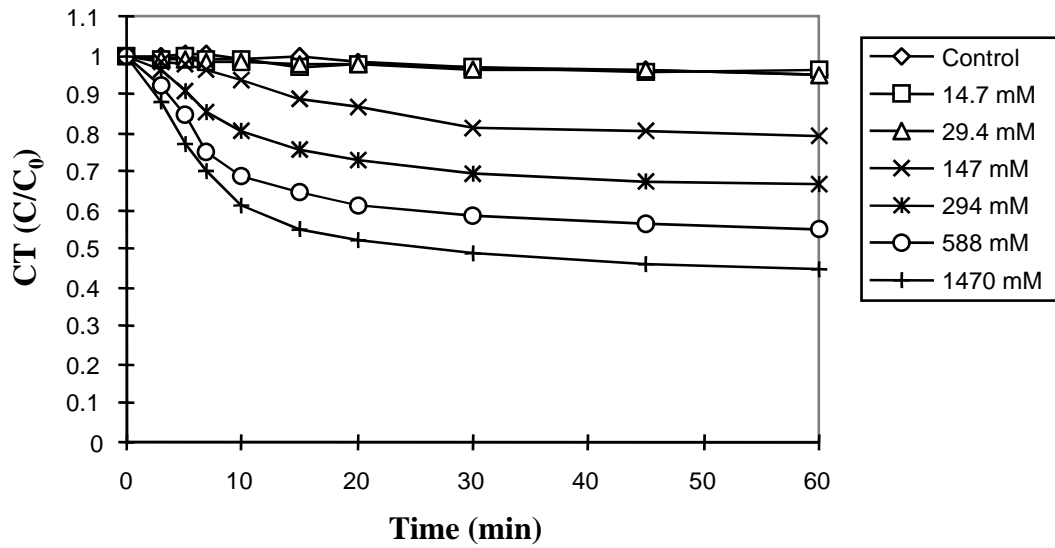
Figure 8.2.2-10. CT degradation with 1 mM Fe[III] - NTA and varying hydrogen peroxide concentrations at pH 5

81
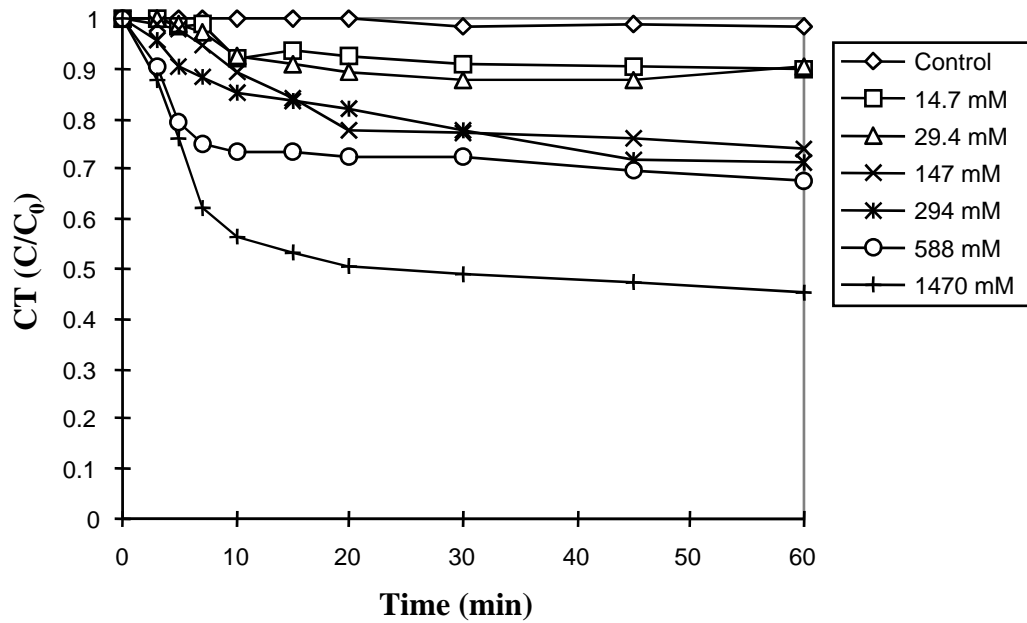
Figure 8.2.2-11. CT degradation using 1 mM Fe [III] - NTA with varying hydrogen peroxide concentrations at pH 7
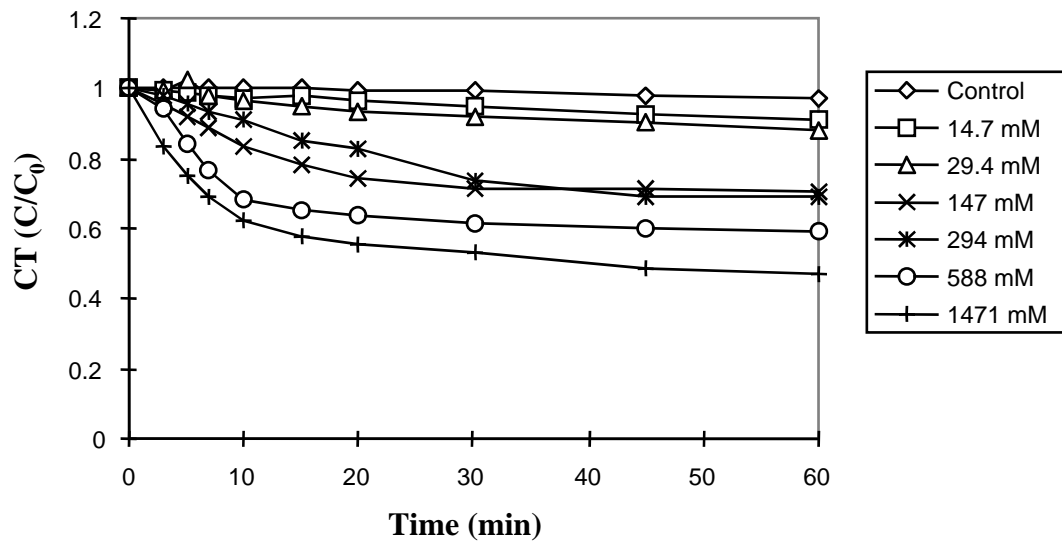
Figure 8.2.2-12. CT degradation using 1 mM Fe[III] - NTA with varying hydrogen peroxide concentrations at pH 9
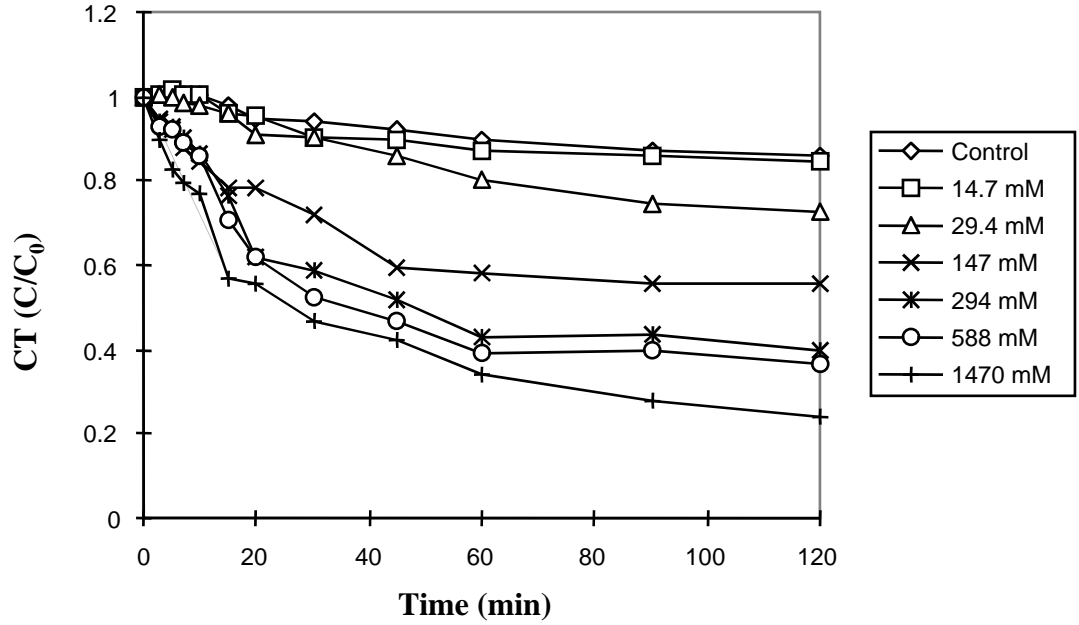
Figure 8.2.2-13. CT degradation with 1 mM Fe[III] and varying concentrations of hydrogen peroxide (unadjusted pH ~ 2.5)
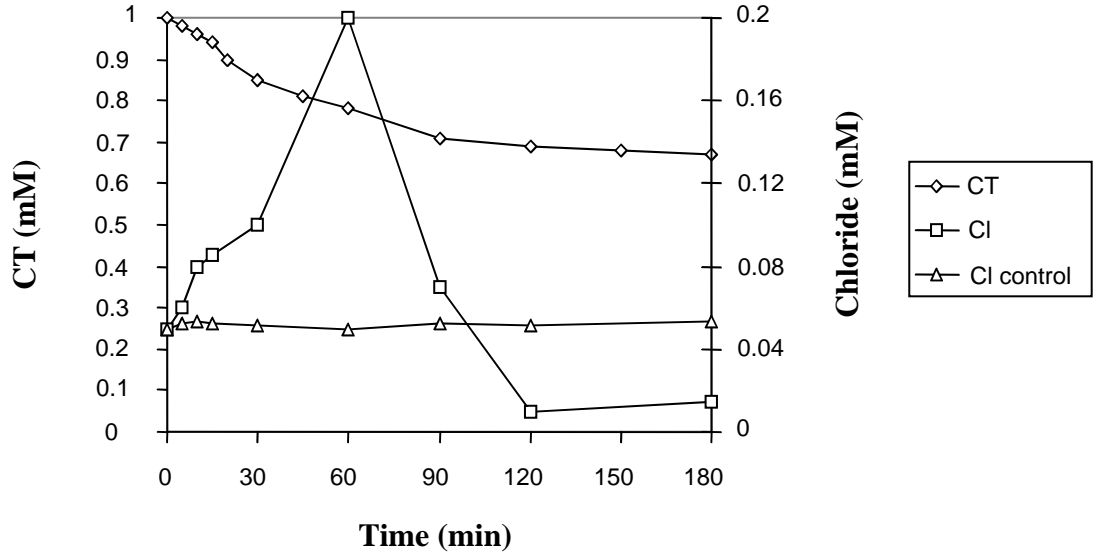
Figure 8.2.2-14. Chloride release with CT degradation
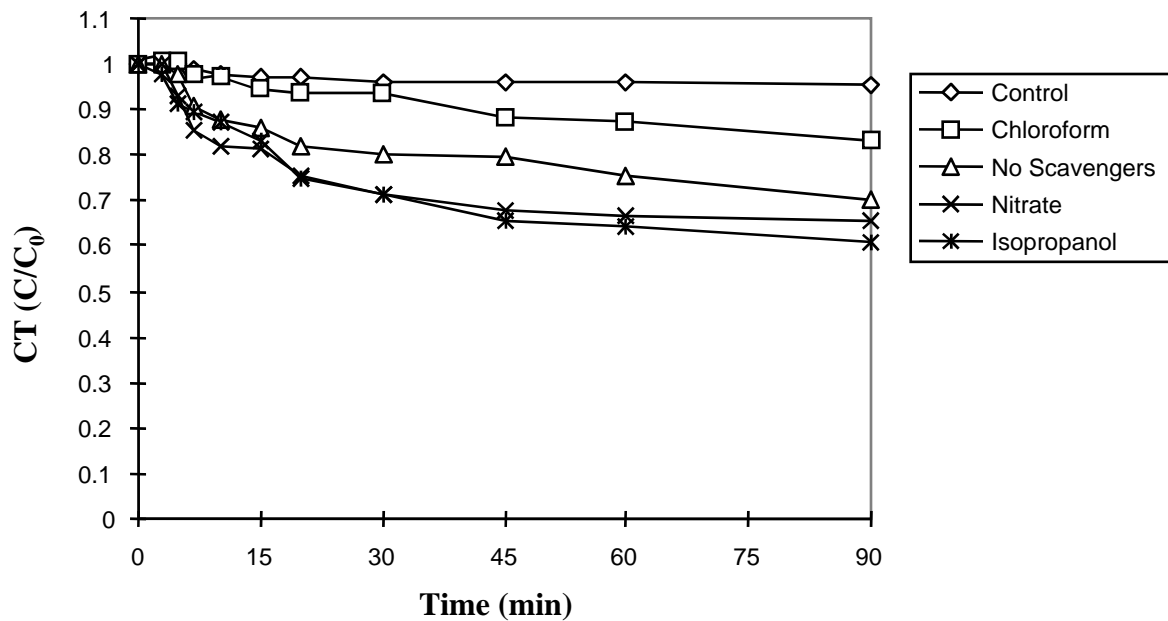
Figure 8.2.2-15. Effect of scavengers on CT degradation using 1 mM Fe[III] - NTA and 294 mM hydrogen peroxide at pH 3
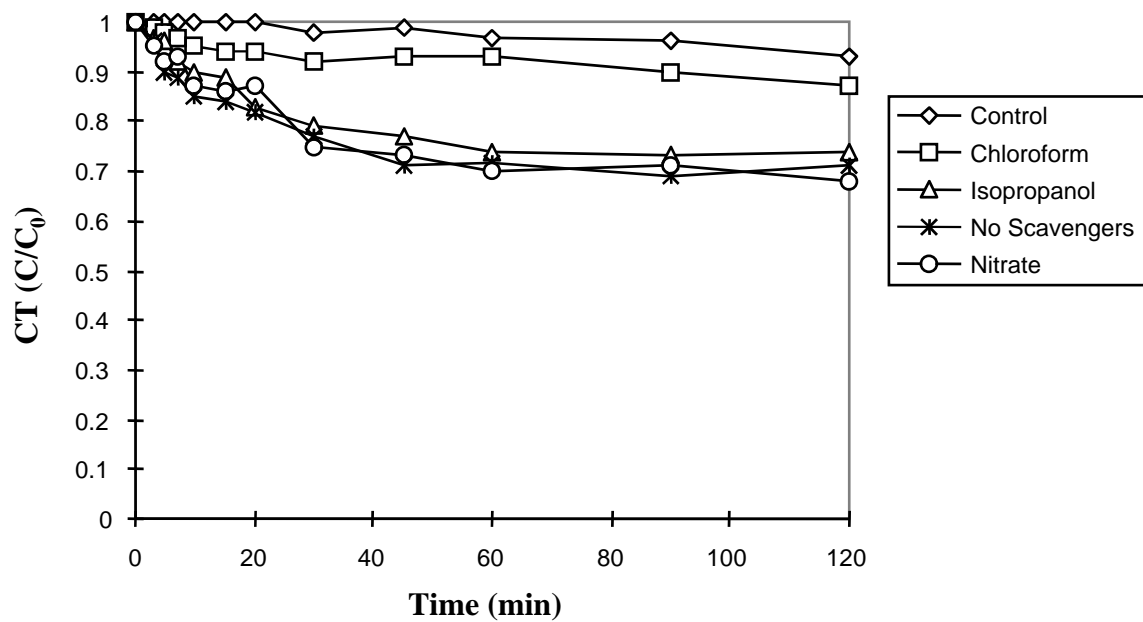
Figure 8.2.2-16. Effect of scavengers on CT degradation using 1 mM Fe[III] - NTA and 294 mM hydrogen peroxide at pH 7

8.2.3 Evaluation of Oxidation and Reduction Processes in CHP Reactions Catalyzed by Soluble Iron at Different pH Regimes

Relative rates of hydroxyl radical generation.

Response surfaces for relative hydroxyl radical production, measured by the corresponding relative rates of *n*-hexanol oxidation at pH 3 and 5, are shown in Figures 8.2.3-1 and 8.2.3-2, respectively. The isoconcentration lines represent the percentage oxidation of *n*-hexanol. At pH 3, complete oxidation occurred at hydrogen peroxide concentrations greater than 1250 mM and Fe-NTA concentrations above 4.5 mM within a 3 hr period. Ferric-NTA chelates are reported to be very stable over a pH range of 1.5 - 3 (Gousetis and Opgenorth, 1996). Under those conditions, availability of soluble iron to catalyze CHP reactions is limited, which explains the relatively slow rate of the reaction. At pH 5, the maximum rate of hydroxyl radical generation occurred with Fe-NTA concentrations of > 2.5 mM and hydrogen peroxide concentrations > 250 mM. The *n*-hexanol oxidation rate was observed to be faster as the iron-NTA complex is destabilized and soluble iron is released into solution. Unlike the pH 3 conditions in which a large dosage of hydrogen peroxide is needed for optimum oxidation, the response surface at pH 5 suggests that a high rate of oxidation can be achieved with a low concentration of hydrogen peroxide. The regression equations for the two central composites were derived as:

$$D_{pH3} = 70.31 + 11.2 \, (Fe\text{-}NTA - 2.5) + 0.04 \, (H_2O_2 - 750) - 2.08 \, (Fe\text{-}NTA - 2.5)^2 - 2.46 \times 10^{-5} \, (H_2O_2 - 750)^2 + 4.24 \times 10^{-3} \, (Fe\text{-}NTA - 2.5) \, (H_2O_2 - 750)$$

$$R^2 = 0.969 \qquad [1]$$

$$D_{pH5} = 99.99 + 8.54 \, (Fe\text{-}NTA - 2.5) + 0.01 \, (H_2O_2 - 750) - 3.99 \, (Fe\text{-}NTA - 2.5)^2 - 5.65 \times 10^{-6} \, (H_2O_2 - 750)^2 - 7.35 \times 10^{-3} \, (Fe\text{-}NTA - 2.5)(H_2O_2 - 750)$$

$$R^2 = 0.598 \qquad [2]$$

Where D = *n*-hexanol degradation (%)

Fe-NTA = Catalyst concentration (mM)

H_2O_2 = Hydrogen peroxide concentration (mM)

Hydroxyl radical generation stoichiometry.

As shown in Table 8.2.3-1, the oxidation reactions became more stoichiometrically efficient as the pH was increased. The most effective oxidation stoichiometry was achieved at pH 9 where hydrogen peroxide and Fe-NTA are most unstable.

$$H_2O_2 + H_2O \leftrightarrow H_3O^+ + HO_2^- \qquad (pK_a = 11.8) \qquad [3]$$

$$H_2O_2 + OH\bullet \rightarrow H_2O + HO_2\bullet \qquad [4]$$

Hydrogen peroxide is characterized as a weak acid with a pK_a of 11.8. As the pH is raised, the equilibrium shifts to the right in equations 3–4, which reduces the amount of H_2O_2, the major hydroxyl radical scavenger. Therefore, the most efficient stoichiometries were

observed at high pH regimes (pH 9) (< 10 moles H_2O_2 per mole of *n*-hexanol degraded). The most inefficient stoichiometries were observed at low pH regimes and high initial hydrogen peroxide concentrations. Furthermore, a decrease in the concentration of hydrogen peroxide was usually accompanied by an increase in stoichiometric efficiency. Watts and Dilly (1995) documented near stoichiometric production of hydroxyl radicals when low dosages of hydrogen peroxide were used.

Relative rates of superoxide generation.

Response surfaces for the relative rates of superoxide generation, quantified using the probe molecule carbon tetrachloride (CT), are shown in Figures 8.2.3-3 through 8.2.3-6.

Response surfaces for the reactions conducted without NTA showed greater destruction of CT and corresponding increases in superoxide generation. Nearly 80% reduction of CT was observed under optimum conditions. The presence of NTA ($k_{OH.} = 2.1 \times 10^9$ M^{-1} S^{-1}, $k_{e-} = 3.6 \times 10^7$) in these systems could limit the propagation reactions [9] - [10] by quenching hydroxyl radicals, and scavenging superoxide. CT reduction as a function of H_2O_2 and iron catalyst were quantified by the regression equations [5] - [9] derived from the experimental results:

$$D_{pH3} = 44.20 + 6.27 \,(Fe\text{-}NTA - 2.5) + 0.03 \,(H_2O_2 - 750) - 0.09 \,(Fe\text{-}NTA - 2.5)^2 - 2.03 \times 10^{-6} \,(H_2O_2 - 750)^2 + 2.97 \times 10^{-3} \,(Fe\text{-}NTA - 2.5)(H_2O_2 - 750)$$

$$R^2 = 0.936 \qquad [5]$$

$$D_{pH5} = 58.06 + 6.91 \,(Fe\text{-}NTA - 2.5) + 0.03 \,(H_2O_2 - 750) - 1.9 \,(Fe\text{-}NTA - 2.5)^2 - 2.83 \times 10^{-5} \,(H_2O_2 - 750)^2 + 4.27 \times 10^{-3} \,(Fe\text{-}NTA - 2.5)(H_2O_2 - 750)$$

$$R^2 = 0.886 \qquad [6]$$

$$D_{pH7} = 59.27 + 5.54 \,(Fe\text{-}NTA - 2.5) + 0.02 \,(H_2O_2 - 750) - 1.84 \,(Fe\text{-}NTA - 2.5)^2 - 1.71 \times 10^{-5} \,(H_2O_2 - 750)^2 + 1.35 \times 10^{-3} \,(Fe\text{-}NTA - 2.5)(H_2O_2 - 750)$$

$$R^2 = 0.895 \qquad [7]$$

$$D_{pH9} = 64.54 + 4.45 \,(Fe\text{-}NTA - 2.5) + 0.02 \,(H_2O_2 - 750) - 1.32 \,(Fe\text{-}NTA - 2.5)^2 - 2.02 \times 10^{-5}(H_2O_2 - 750)^2 + 4.89 \times 10^{-3}(Fe\text{-}NTA - 2.5)(H_2O_2 - 750)$$

$$R^2 = 0.798 \qquad [8]$$

$$D_{(no\ NTA)} = 80.63 - 1.99 \,(Fe\text{-}NTA - 2.5) + 0.03 \,(H_2O_2 - 750) - 1.65 \,(Fe\text{-}NTA - 2.5)^2\ 4.06 \times 10^{-5} \,(H_2O_2 - 750)^2 - 3.16 \times 10^{-3} \,(Fe\text{-}NTA - 2.5)(H_2O_2 - 750)$$

$$R^2 = 0.603 \qquad [9]$$

Where D = CT degradation (%)

Fe-NTA = Catalyst concentration (mM)

H_2O_2 = Hydrogen peroxide concentration (mM)

Superoxide generation stoichiometry.

The stoichiometry of superoxide generation was most effective when the concentrations of hydrogen peroxide ranged between 30 to 294 mM (Table 8.2.3-2). Absence of NTA improved the stoichiometric efficiency of superoxide generation, with ~150 moles to 190 moles H_2O_2 per mole of CT destroyed. Unlike the relative rates of hydroxyl radical generation, pH had a minimal effect on the overall stoichiometry. A large amount of oxidants produced in CHP systems would neutralize most hydroperoxide anions, explaining the relatively high H_2O_2 consumed per CT degraded. Moreover, chain propagations, complex intermediates and NTA may also limit the formation of hydroperoxide anions thus further lowering the stoichiometric efficiency of CT destruction. Although more superoxide is generated at high hydrogen peroxide concentrations, more hydrogen peroxide is also consumed, lowering the stoichiometric efficiency of superoxide generation.

Summary and Conclusions

Central composite rotatable designs were developed to investigate process optimization of CHP systems for the degradation of two probe compounds to quantify relative rates of hydroxyl radical and superoxide generation. The relative rate of destruction of *n*-hexanol and associated relative rate of hydroxyl radical was most rapid at high pH regimes. Complete oxidation of *n*-hexanol under optimum conditions was achieved over 30 minutes. Results also showed that the reaction stoichiometry was most efficient at high pH regimes with < 10 moles of H_2O_2 consumed per mole of *n*-hexanol degraded.

Response surfaces for CT destruction and associated superoxide generation by CHP reactions confirmed the existence of reductants which reduced up to 70% of the initial concentration of CT over 3 hr. Increasing pH had a minimal effect on the generation of superoxide. Treatment of CT was most efficient in the absence of NTA. The reaction stoichiometry was 150 moles of hydrogen peroxide consumed per mole of CT degraded under optimum conditions.

The results of Section 8.2 confirm that oxidative and reductive pathways are common in CHP systems, and that different catalysts promote the generation of different reactive oxygen species. The generation of superoxide in CHP systems is an important pathway for subsurface remediation, and the catalysts required for its generation will be an important component of CHP process design.

Table 8.2.3-1. Oxidation stoichiometry for n-hexanol oxidation at various hydrogen peroxide concentrations and pH regimes with 1 mM Fe.

	1471 mM	588 mM	294 mM	147 mM	30 mM	15 mM
pH 3	303*	312	275	352	333	400
pH 5	179	153	103	59	37	23
pH 7	59	29	38	15	20	16
pH 9	<10	<10	<10	<10	<10	<10
No NTA	150	117	88	50	12	11

pH 3 (3 hr); pH 5, no NTA (30 min); pH 7, pH 9 (10 min).

* refers to the number of moles of H_2O_2 consumed per mole of contaminant destroyed.

Table 8.2.3-2. Reduction stoichiometry for CT degradation at various hydrogen peroxide concentrations and pH regimes with 1 mM Fe.

	1471 mM	588 mM	294 mM	147 mM	30 mM	15 mM
pH 3 (1hr)	552	490	395	440	490	588
pH 5 (1 hr)	433	373	122	238	1175	735
pH 7 (1 hr)	673	507	404	166	330	184
pH 9 (1 hr)	638	426	346	157	368	294
No NTA (1hr)	547	322	190	156	161	220
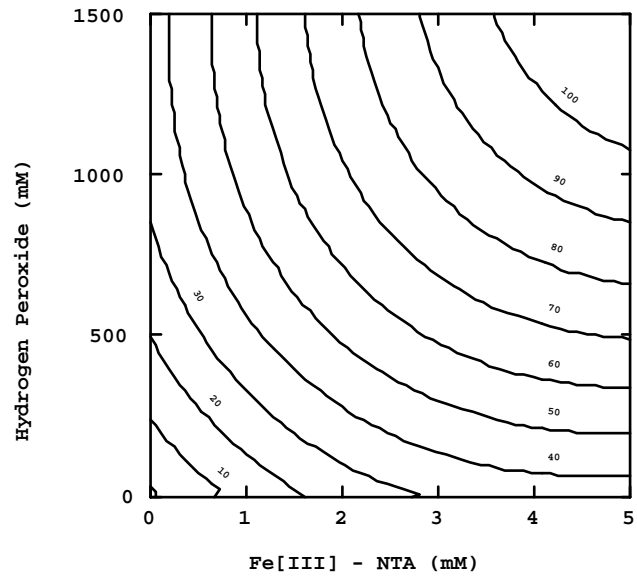
Figure 8.2.3-1. Response surface for relative hydroxyl radical generation quantified by *n*-hexanol oxidation as a function of Fe[III] - NTA concentration and hydrogen peroxide concentration at pH 3 (3 hr)
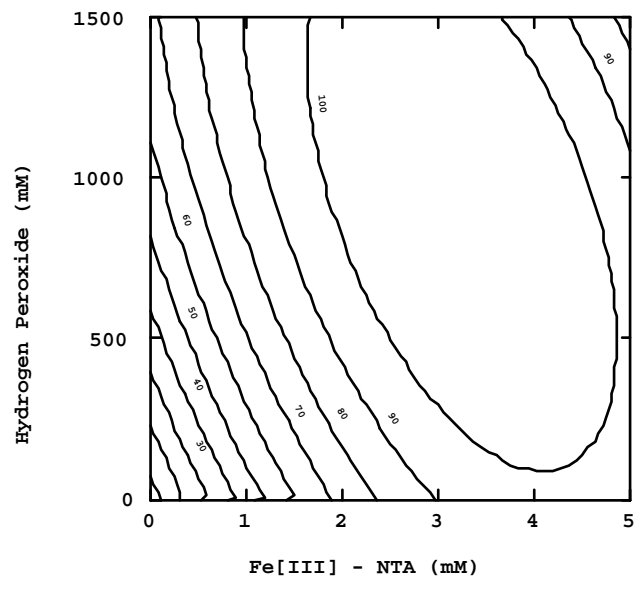
Figure 8.2.3-2. Response surface for relative hydroxyl radical generation quantified by *n*-hexanol oxidation as a function of Fe[III] - NTA concentration and hydrogen peroxide concentration at pH 5 (30 min)

89
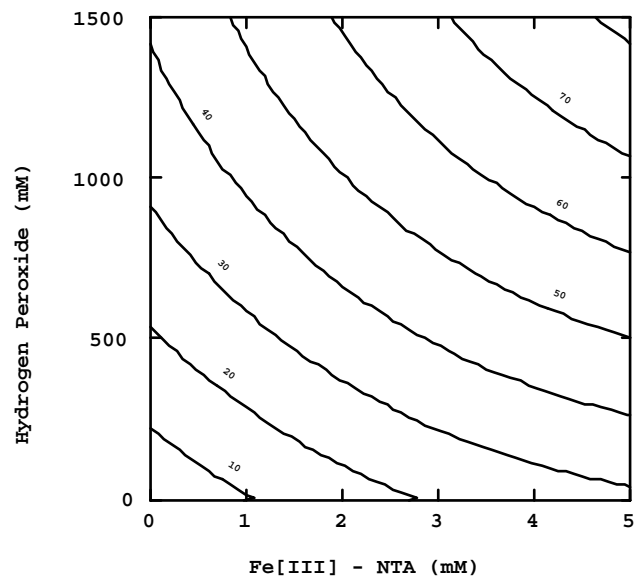
Figure 8.2.3-3. Response surface for relative superoxide generation quantified by CT degradation as a function of Fe[III] - NTA concentration and hydrogen peroxide concentration at pH 3 (3 hr)
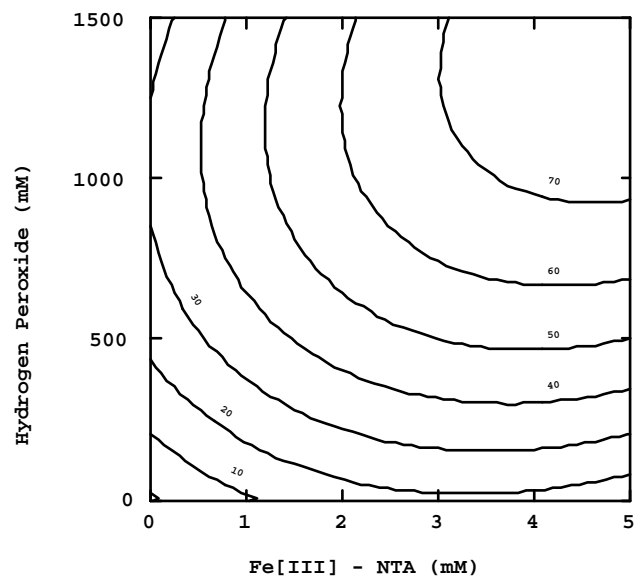
Figure 8.2.3-4. Response surface for relative superoxide generation quantified by CT degradation as a function of Fe[III] - NTA concentration and hydrogen peroxide concentration at pH 5 (3 hr)
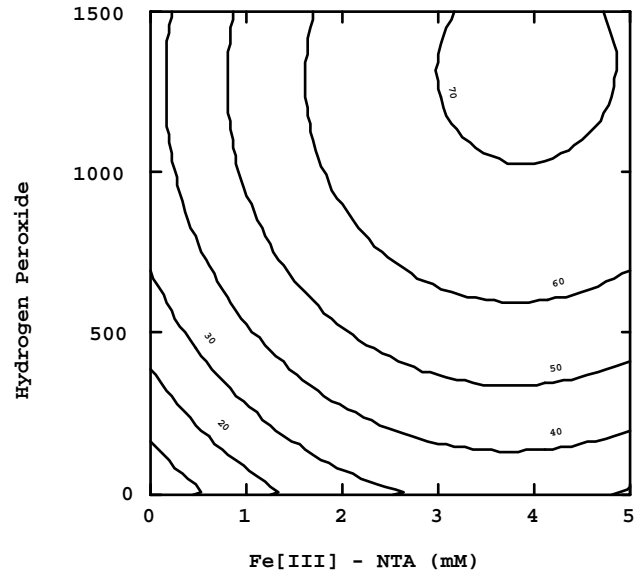
Figure 8.2.3-5. Response surface for relative superoxide generation quantified by CT degradation as a function of Fe[III] - NTA concentration and hydrogen peroxide concentration at pH 7 (3 hr)
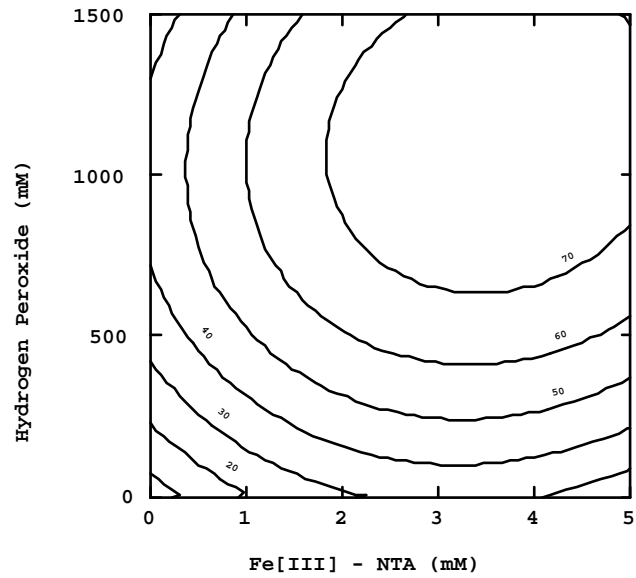
Figure 8.2.3-6. Response surface for relative superoxide generation quantified by CT degradation as a function of Fe[III] - NTA concentration and hydrogen peroxide concentration at pH 9 (3 hr)
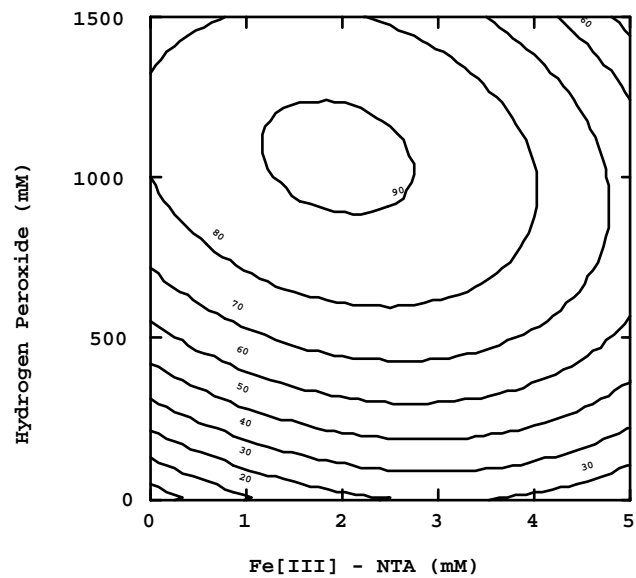
Figure 8.2.3-7. Response surface for relative superoxide generation quantified by CT degradation as a function of Fe[III] concentration (no NTA; unadjusted pH ~ 2.5) and hydrogen peroxide concentration (3 hr)

8.3 Degradation Products

The suite of reactive oxygen species generated by CHP provides a treatment matrix with greater reactivity than the standard Fenton's system, allowing contaminants to be oxidized, reduced, and attacked by nucleophiles in a single system. Products formed during the reduction of a chlorinated alkane, carbon tetrachloride, and the oxidation of a chlorinated alkene, perchloroethylene, were investigated during CHP reactions. In addition, the mineralization of two hydrocarbons, benzo[*a*]pyrene and hexadecane, was investigated in CHP reactions. Additional results on the formation of degradation products formed during DNAPL destruction by CHP are presented in Section 8.4

Chlorinated Aliphatics. Alkenes and aromatic compounds, even those with a high degree of chlorination, react rapidly with hydroxyl radical. Therefore, perchloroethylene provides an appropriate model compound for evaluating the oxidation products during CHP reactions. Alternatively, a potential reductive pathway of CHP was demonstrated by its destruction of carbon tetrachloride (Teel and Watts, 2002); the authors proposed that CT is degraded through a non-hydroxyl mechanism, and suggested that superoxide may be the species responsible. However, the results and proposed pathway described were inconsistent with previous findings of superoxide reactivity in water (Pignatello, 1992). Although superoxide is highly reactive with CT in aprotic solvents, such as dimethylsulfoxide (DMSO) and dimethylformamide (DMF) (Roberts et al., 1983), it is considered unreactive with CT in water (Monig et al., 1983). Evidence to date demonstrates that CT is degraded by CHP reactions with H_2O_2 concentrations >0.1 M (Watts et al., 1999). The purpose of this segment of research was to 1) identify the products formed in the oxidation of perchloroethylene during CHP reactions, and 2) to determine the reactive species in CHP systems that is responsible for carbon tetrachloride degradation and to identify its degradation products in CHP systems.

Hydrocarbons. Numerous studies have shown that Fenton's reactions using dilute H_2O_2 result in incomplete mineralization of organic compounds (Davidson and Busch, 1966; Ronen et al., 1994), a conclusion that is expected because many degradation products, such as β-keto acids, are not reactive with hydroxyl radicals (Buxton et al., 1987). However, the mix of oxidants, reductants, and nucleophiles generated using H_2O_2 concentrations > 0.3 M may not only provide the reactants necessary to promote the enhanced treatment of sorbed contaminants, but these same conditions may also provide the added benefit (via the same matrix of reactants) of mineralizing degradation products. Therefore, the purpose of this segment of research was to investigate the process conditions that not only provide enhanced treatment of sorbed benzo[*a*]pyrene (BaP) and hexadecane, but also mineralize the degradation products in the CHP treatment of two contaminated soils.

8.3.1 Identification of the Reactive Oxygen Species Responsible for Carbon Tetrachloride Degradation in CHP Systems

The purpose of this research was to determine the reactive species in CHP systems that is responsible for carbon tetrachloride (CT) degradation.

CT degradation in CHP reactions

The degradation of CT in a soluble iron (III)-catalyzed CHP reaction is shown in Figure 8.3.1-1. Carbon tetrachloride transformation increased with greater concentrations of H_2O_2, with 1 M H_2O_2 providing 79% CT degradation after 2 h; the corresponding CT loss in control systems was 19% due to volatilization. A similar increase in CT degradation as a function of H_2O_2 concentration in CHP systems was reported by Teel and Watts (2002), who suggested that CT was degraded by a non-OH• species, possibly $O_2•^-$. The degradation of CT by $O_2•^-$ was also proposed in a TiO_2–mediated photocatalytic system (Stark and Rabani, 1999). This mechanism is in opposition to the well-documented negligible reactivity of $O_2•^-$ in aqueous solutions (Pignatello, 1992, Halliwell, and Gutterridge, 1985) and specific findings that $O_2•^-$ is not reactive with CT in aqueous solutions (Asmus, 1988, Monig et al., 1983).

As the first step in elucidating the reactive oxygen species responsible for CT degradation, CHP reactions were repeated with the addition of isopropanol as an OH• scavenger (8.3.1-2). Carbon tetrachloride loss was 79% without isopropanol and 67% with the isopropanol amendment, demonstrating that OH• does not play a significant role in CT degradation. With OH• scavenged, the effective reaction in the system is the iron (III)-catalyzed decomposition of hydrogen peroxide to $HO_2•$, which is in equilibrium with $O_2•^-$. As a result, $HO_2•$ and $O_2•^-$ are the reactive oxygen species available for CT degradation in the scavenged system. Perhydroxyl radical is an oxidant with an oxidation potential of 1.78 V (Bielski, 1978) and therefore, like OH•, is unlikely to react with CT. Consequently, the weak reductant and nucleophile $O_2•^-$ was evaluated further as the species potentially responsible for the transformation of CT.

Degradation products of CT were analyzed to confirm its transformation in CHP reactions and to begin investigating its mechanism of transformation. Using gas adsorbent tubes collected after 120 min from reactions using 0.1 M, 0.5 M, and 1 M H_2O_2, phosgene was identified as an intermediate product in the CHP transformation of CT, and carbon dioxide was also collected in the off gas. In addition, carbonate was found in the aqueous phase of the CHP reactions. The generation of these degradation products in CHP reactions is consistent with the products formed from the nucleophilic attack of $O_2•^-$ on CT (Roberts and Sawyer, 1981, Stark and Rabani, 1999). These data suggest that $O_2•^-$ is somehow reactive in CHP systems.

CT degradation in $O_2•^-$ reactions

A KO_2 reaction was used to investigate the reactivity of CT with $O_2•^-$ in aqueous systems (Figure 8.3.1-3). The 25% loss of CT in the presence of KO_2 was not significantly different from its loss in control reactions, confirming that $O_2•^-$ is minimally reactive with CT in aqueous solutions (Monig et al., 1983). In contrast with the data of Figure 8.3.1-2, these results initially appeared to indicate that $O_2•^-$ is not the species responsible for CT degradation in CHP systems; however, comparison of the constituents of the CHP reaction to those of the KO_2 reaction shows a major difference between the two: the presence of H_2O_2.

To provide reaction conditions in the KO_2 system that more closely represent those of the CHP reactions, the KO_2–CT reactions were repeated with the addition of a range of H_2O_2 concentrations (Figure 8.3.1-4). At the high pH regime of the KO_2 system (pH 14), essentially all of the H_2O_2 exists as its conjugate base, HO_2^- ($pK_a = 11.8$) (Schumb et al., 2005). Over 2 h, 27%, 40%, and 48% of the CT was lost in the presence of 0.1 M, 0.5 M, and 1 M HO_2^-, respectively. Over the same time period, 24% of the CT was lost from control reactions

containing equivalent concentrations of HO_2^- and no KO_2. Phosgene and carbonate were detected as degradation products in the 0.5 M and 1 M HO_2^- reactions, identical to the products formed in the CHP reactions and consistent with transformation of CT by $O_2 \bullet^-$. These results demonstrate that 1) HO_2^- does not degrade CT, and 2) the presence of HO_2^- increases the reactivity of $O_2 \bullet^-$ with CT in aqueous solutions. Carbon tetrachloride transformation in control reactions was not significantly different from that in KO_2 reactions containing 0.1 M HO_2^- ($\alpha = 0.05$), indicating that >0.1 M HO_2^- is required to promote the reaction between $O_2 \bullet^-$ and CT.

Superoxide is characterized by low reactivity in water due to its high degree of solvation by water molecules, which increases its one-electron reduction potential E^0 ($O_2/O_2 \bullet^-$) to –0.33 V (Afanas'ev, 1989) compared to –0.86 V in DMF and –0.78 V in DMSO (Sawyer et al., 1982). The only difference between the KO_2 reactions that promoted CT transformation and those that did not was the addition of >0.1 M HO_2^-, suggesting that HO_2^-, as well as H_2O_2 in CHP systems, may influence the solvation state of $O_2 \bullet^-$ and enhance its reactivity with CT.

CT degradation in $O_2 \bullet^-$ reactions containing solvents
To further investigate the effect of solvents on $O_2 \bullet^-$ reactivity in aqueous systems, the KO_2–CT reactions were repeated with the addition of equimolar concentrations of five other solvents. The degradation of CT in the presence of 1 M of each of the five solvents and HO_2^- in KO_2 systems is shown in Figure 8.3.1-5. The solvents enhanced the degradation of CT in the order acetone>isopropanol>ethanol>HO_2^->methanol>ethylene glycol. These results demonstrate that the presence of even low proportions of a species less polar than water significantly increases the reactivity of $O_2 \bullet^-$.

The lines in Figure 8.3.1-5 representing degradation of CT in the presence of the five organic solvents were fit to first-order kinetics ($R^2 > 0.95$ for each when ln (C_t/C_0) was plotted as a function of time). The observed first-order rate constant (k_{obs}) for each solvent–KO_2–CT reaction was then plotted as a function of the empirical solvent polarity (E_T^N) (Reichardt, 2003) of the added solvent (Figure 8.3.1-.6). The k_{obs} for CT degradation was inversely proportional to the E_T^N with $R^2 = 0.987$. Such a high correlation between k_{obs} and E_T^N provides further support for a solvent effect that increases the reactivity of $O_2 \bullet^-$ when species less polar than water, including H_2O_2 and HO_2^-, are added to aqueous solutions of $O_2 \bullet^-$. Because H_2O_2 is less polar than its conjugate base, HO_2^-, the H_2O_2 added in the CHP system would be expected to be more effective than HO_2^- in promoting the degradation of CT by $O_2 \bullet^-$.

Superoxide is more reactive in aprotic media than in water because its solvation by water decreases its lifetime and its reactivity (Afanas'ev, 1989). The increased reactivity of $O_2 \bullet^-$ in water–solvent systems is likely due to changes in the solvent shell surrounding $O_2 \bullet^-$. The data of Figure 8.3.1-5 and 8.3.1-6 were obtained in reactions that contained a mixture of water and less polar compounds in the bulk solution, which likely results in a mixture of water and less polar molecules in the shell surrounding $O_2 \bullet^-$; the proportion of the less polar molecules in the solvent shell may actually be higher than in the bulk solution (Reichardt, 2003). The mixed solvent shell may have characteristics of both the less polar compound and water, resulting in an increase in $O_2 \bullet^-$ reactivity relative to purely aqueous solutions.

CT degradation in CHP reactions with solvent addition

To confirm the solvent effect on the reactivity of $O_2^{\bullet-}$ in CHP reactions, CHP reactions were conducted with the addition of each of the solvents, with the exception of ethylene glycol, which behaved similarly to methanol in Figure 8.3.1-6. The reactions were conducted with 0.05 M H_2O_2, and at this low H_2O_2 concentration CT degradation was not promoted in the absence of added solvent. Each solvent had a different effect on the H_2O_2 decomposition rate of the CHP reaction. This variation was likely due to different degrees of complexation of iron (Schroeder and Schwartz, 1990, Et-Asmy et al., 1994, Yasuyoshi and Yokoi, 1994); visual inspection of the reactions showed widely varying colors of the solution, ranging from bright yellow to amber. Therefore, CT degraded in the experiments was normalized to the H_2O_2 decomposition rate. The normalized degradation rate of CT in the CHP–solvent reactions was directly proportional to E_T^N with $R^2 = 0.983$ (Figure 8.3.1-7a). When acetone was added to CHP reactions at five different concentrations, the same trend was observed; CT degradation increased as a function of acetone concentration in the CHP reaction (Figure 8.3.1-7b). These results confirm a solvent effect for the degradation of CT in CHP reactions, parallel to the effect in KO_2–CT reactions.

The effect of solvent addition on $O_2^{\bullet-}$ activity in the CHP reactions may explain some of the results previously reported in studies incorporating solvents into CHP systems. For example, Lee et al. (1998) used 1.25 mL of a solution of 60% ethanol, 80 mM iron (II), and 7.2% (2.1 M) H_2O_2 per g of soil to treat sorbed anthracene. They found that the anthracene was effectively desorbed and degraded, likely due to the activity of $O_2^{\bullet-}$ (Watts et al., 1999, Watts et al., 1994), which may have been increased by the presence of ethanol. Enhanced treatment and destruction of the PAHs were documented, but no mechanism for the increased effectiveness was proposed. Similar enhanced treatment was described for 2,4-dinitrotoluene in the presence of 20% ethanol by Miller et al. (2003). In both of these systems, the added solvents likely increased the reactivity of the $O_2^{\bullet-}$ generated in CHP reactions.

The results of this research demonstrate that CHP degrades CT through a mechanism that does not involve $OH^\bullet$ or HO_2^-. Carbon tetrachloride degradation products were consistent with degradation by $O_2^{\bullet-}$, the other predominant reactive oxygen species in CHP systems. Although CT was unreactive with $O_2^{\bullet-}$ in aqueous KO_2 reactions, the addition of solvents less polar than water, including HO_2^-, significantly increased CT degradation in the KO_2 reactions. The enhanced reactivity of $O_2^{\bullet-}$ in the presence of H_2O_2, a compound less polar than water, may result in the degradation of compounds other than CT that are not reactive with $OH^\bullet$. More importantly, the simple presence of H_2O_2 likely increases the reactivity of $O_2^{\bullet-}$ in CHP reactions. Therefore, the enhanced reactivity of $O_2^{\bullet-}$ should be considered in the use of CHP for ISCO and industrial wastewater treatment.
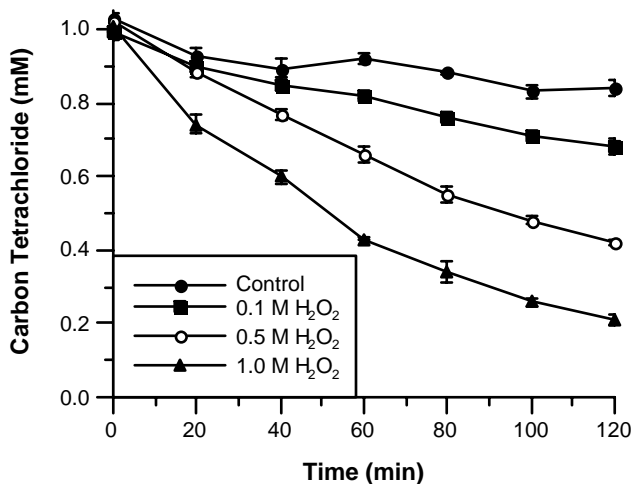
Figure 8.3.1-1. Degradation of CT in CHP reactions with varying H_2O_2 concentrations (experimental reactors: 1 mM CT, 0.5 mM iron (III), and 0.1 M, 0.5 M, or 1 M H_2O_2; 15 mL total volume at pH 3.0; control reactors: H_2O_2 substituted by deionized water; T = 20 ± 1°C).
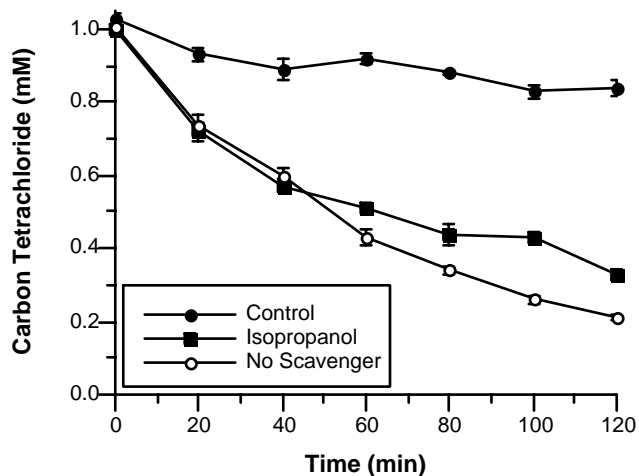
Figure 8.3.1-2. Degradation of CT in CHP reactions with and without OH• scavenging (experimental reactors: 1 mM CT, 0.5 mM iron (III), 1 M H_2O_2; 15 mL total volume at pH 3.0; scavenging reactors: 1M isopropanol added; control reactors: H_2O_2 substituted by deionized water; T = 20 ± 1°C).

97
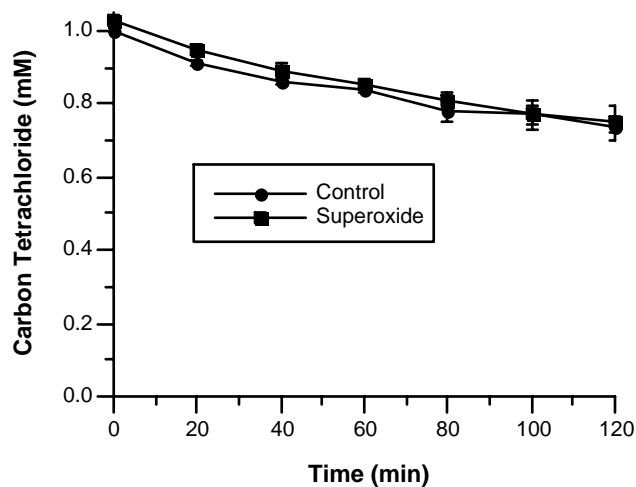
Figure 8.3.1-3. Degradation of CT in KO_2 reactions (experimental reactors: 1 mM CT, 2 M KO_2, 33 mM purified NaOH, and 1 mM DTPA; 15 mL total volume at pH 14; control reactors: KO_2 substituted by deionized water; T = 4 ± 1˚C).
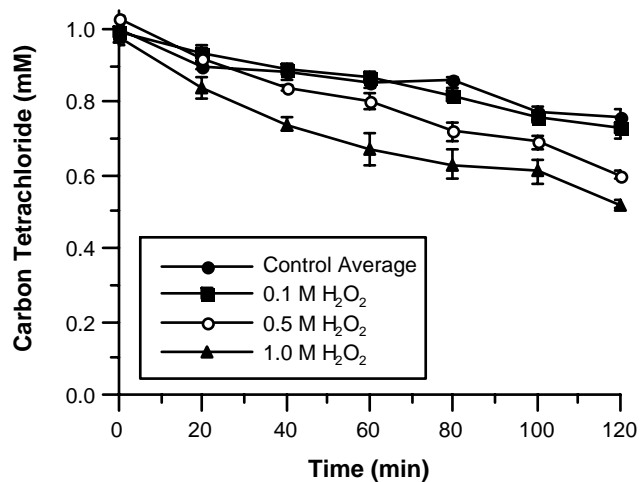
Figure 8.3.1-4. Degradation of CT in KO_2 reactions in the presence of HO_2^- (experimental reactors: 1 mM CT, 2 M KO_2, 33 mM purified NaOH, 1 mM DTPA, and 0.1, 0.5 or 1.0 M H_2O_2 (present as HO_2^-); 15 mL total volume at pH 14; control reactors: KO_2 substituted by deionized water and 0.1, 0.5 or 1.0 M H_2O_2 (present as HO_2^-); T = 4 ± 1˚C).
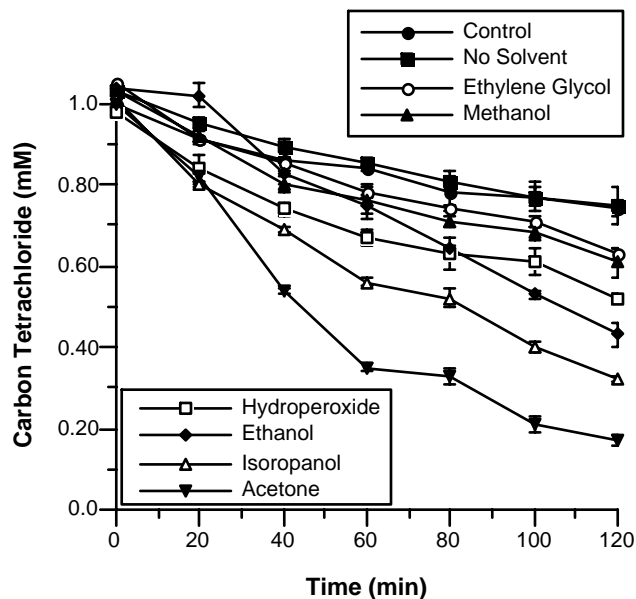
Figure 8.3.1-5. Degradation of CT in KO_2 reactions in the presence of six solvents (experimental reactors: 1 mM CT, 2 M KO_2, 33 mM purified NaOH (2 M NaOH in H_2O_2 reaction), 1 mM DTPA, and 1 M ethylene glycol, methanol, H_2O_2 (present as HO_2^-), ethanol, isopropanol, or acetone, or no added solvent; 15 mL total volume at pH 14; control reactors: KO_2 substituted by deionized water; T = 4 ± 1°C).
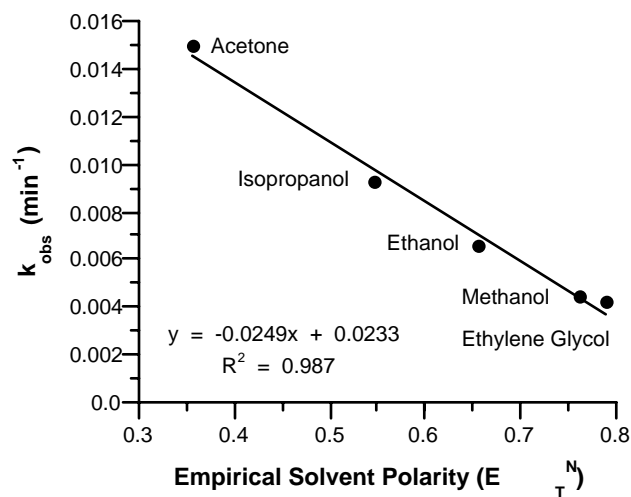
Figure 8.3.1-6: Correlation of k_{obs} for CT degradation in five KO_2–solvent systems with the empirical solvent polarity (E_T^N) of the solvents.

99
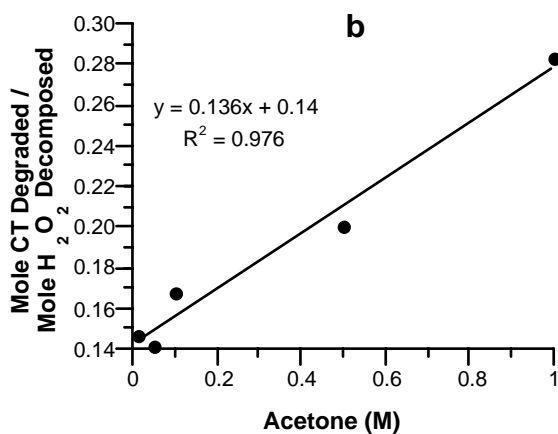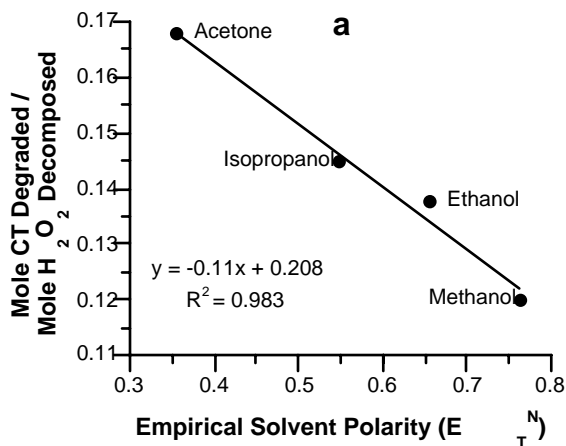
Figure 8.3.1-7. Effect of solvent addition on degradation of CT per mole of H_2O_2 lost in CHP reactions. (a) Correlation of normalized CT degradation with empirical solvent polarity (E_T^N) of four added solvents (experimental reactors: 1 mM CT, 0.5 mM iron (III), 0.05 M H_2O_2, and 1 M acetone, isopropanol, ethanol, or methanol; 15 mL total volume at pH 3.0; control reactors: H_2O_2 substituted by deionized water; T = 20 ± 1°C). (b) Correlation of normalized CT degradation with concentration of acetone added (experimental reactors: 1 mM CT, 0.5 mM iron (III), 1 M H_2O_2, and 0.01 M, 0.05 M, 0.1 M, 0.5 M, or 1 M acetone; 15 mL total volume at pH 3.0; control reactors: H_2O_2 substituted by deionized water; T = 20 ± 1°C).

100

8.3.2 Degradation of Perchloroethylene in CHP Reactions

The purpose of this segment of study was to evaluate PCE oxidation products generated in CHP systems, and to develop kinetic expressions to quantify the experimental data. PCE was rapidily oxidized in a CHP system containing 2 M hydrogen peroxide and 5 mM iron (II); more than 80% of the PCE was oxidized in the first 0.5 h, and more than 97% of the PCE was degraded within 2 h (Figure 8.3.2-1). Dechlorination of the oxidation products lagged behind PCE decomposition, which was confirmed by TOC and chloride analyses. (Figure 8.3.2-1). However, complete mineralization of the PCE was observed after 3 h. Hydrogen peroxide consumption for the CHP system is shown in Figure 8.3.2-2. These data show that sufficient hydrogen peroxide residuals were maintained over the course of the reaction to drive the oxidation of the PCE daughter products.

A brown color was observed in the CHP reactions. Dimer formation was suggested as the possible reason for color formation in the Fenton's oxidation of chlorobenzene using dilute hydrogen peroxide (Sedlak and Andren, 1990). In this study, the brown color was rapidly reversed when the pH of the solution was lowered below 2.0. This phenomena has been observed in CHP systems with aliphatic as well as aromatic compounds under the same conditions used in this study. The reversible reaction suggests formation of an iron chelate rather than dimerization.

Before a kinetic pathway for the oxidation of PCE by CHP ISCO can be proposed, the intermediate species involved in PCE decomposition require identification. Gas chromatographic analyses indicated two daughter peaks in the aqueous solution several minutes after the start of the reactions. These peaks were only detectable at pH near 3, and were undetectable above pH 6.0 when analyzed by gas chromatography using a Carbopack column with flame ionization detection. These results suggest that the degradation products are weak acids with pK_a in the range of 2 to 4. The magnitude of the peaks reached a maximum at 0.5 h and then slowly disappeared over 3 h, suggesting that the intermediates were reactive in the CHP system. Both peaks reached maximum concentration within 0.5 to 1 h within the start of the reactions. Use of authentic standards and spiked tests combined with retention time comparisons revealed that the peaks were dichloroacetic acid (DCAA) and dichloroacetyl chloride (DCAC). Although trichloroacetic acid has been identified in the oxidation of PCE, it was not detected in this study. The normalized concentration profile of DCAA and DCAC, listed as the second peak, over the course of 5 h is shown in Figure 8.3.2-3. The DCAC peak appeared to have a similar concentration profile to DCAA, which suggests that DCAC might be in pseudo-steady-state with DCAA, or is a minor product generated by a parallel mechanism.

Ollis et al. (1984) observed the formation of DCAA in their study of photoassisted TiO_2 catalyzed degradation of PCE and proposed the subsequent formation of CO_2 and a phosgene-like species in the decarboxylation of dichloroacetyl acid. Dichloroacetyl chloride (DCAC) formation was also an intermediate in the gas phase reaction of PCE with hydroxyl radicals. Generation of dichloroacetaldehyde was reported in the oxidation of TCE by hydroxyl radicals (Pruden and Ollis, 1983). Our experimental data suggest that PCE reacts with hydroxyl radical producing intermediate species similar to the gas phase reaction:

$$PCE + \bullet OH \rightarrow DCAC \tag{1}$$

DCAC then decomposes rapidly in aqueous solution to form DCAA:

$$\text{fast}$$
$$DCAC + H_2O \rightarrow DCAA + HCl \tag{2}$$

The dechlorination sequence of PCE by CHP is very different from the only route of biological degradation—reductive dechlorination. In the biological pathway under anoxic conditions, PCE undergoes reductive dechlorination leading with the formation of dichloroethylenen and vinyl chloride (Barrio-Lage et al., 1986).

Subsequent oxidation of DCAA by hydroxyl radicals may follow two different reaction pathways: Decarboxylation of DCAA may occur with the production of CO_2 and a phosgene-like species, which likely hydrolyzes rapidly into CO_2 and HCI (Pruden and Ollis, 1983). This pathway of DCAA decompositon would have resulted in dechlorination and total mineralization at about the same time, but our experimental results showed mineralization lagging behind dechlorination. An alternative pathway would be dechlorination of DCAA followed by its decarboxylation to form CO_2, HCl, and a simple organic acid (i.e., formic acid), then subsequent oxidation leading to decarboxylation of the organic acid to CO_2.

Therefore, the following PCE decomposition pathway is proposed:

$$PCE + \bullet OH \rightarrow DCAC + Cl^- \tag{3}$$

$$\text{fast}$$
$$DCAC + H_2O \rightarrow DCAA + HO \tag{4}$$

$$DCAA + 4 \bullet OH \rightarrow 2HCl + 2H_2O + 2CO_2 \tag{5}$$
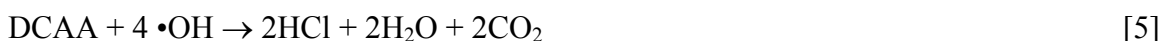
A possible route for Cl^- generated in Eq. [3] is combining with $\bullet OH$ to form HOCl. Equation [5] is based on the net stoichiometry for DCAA oxidation.

Mineralization of formaldehyde and formic acid a Fenton-like reagent was reported by Murphy et al. (1989). Draeutler and Bard (1978) described the oxidation of organic acids to CO_2 and in aqueous suspensions of TiO_2 under UV illumination. Pruden and Ollis (1983) also observed methane and CO_2 in the decomposition of acetic acid by hydroxyl radicals in a photoassisted system. The decomposition pathway of PCE by CHP was likely different from the TiO_2 photocatalyzed system reported by Pruden and Ollis (1983). In this study, TOC measurements indicated that all the organic carbib in the solution was converted into CO_2. The results also showed that dechlorination preceded mineralization of PCE, suggesting that decarboxylation occurred at the latter stage of the CHP reactions. Because PCE decomposes rapidly in CHP systems, producing no significant intermediates other than DCAC and DCAA, it is likely that hydroxyl radicals continue attacking DCAA and that reaction is the rate-limiting step to CO_2 formation (Walling and Amarnath, 1982; Cooper et al., 1989; Hoigne et al., 1989; Murphy et al., 1989). A conceivable product of this rate-limiting reaction is formaldahyde. By adopting the results of Walling and Amarnath (1982), Eq. [5] then may be viewed in two steps:

DCAA + 2 •OH → 2HCl+ CO_2 + HCOOH   [6]

                 fast

HCOOH + 2 •OH → $2H_2O$ + CO_2 [7]
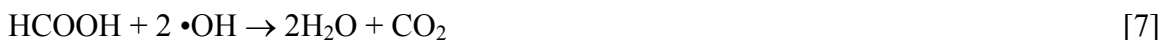
It should be noted that Eq. [6] and [7] are not necessarily the elementary equations; these proposed equations are based on overall stoichiometry and the experimental observations.

The observed degradation rates of PCE and H_2O_2 were derived from the experimental data; Figure 8.3.2-4 shows the pseudo first-order degradation of PCE. The observed degradation constant (k_{obs1}) was determined to be 1.65/h ± 0.475/h (R = 0.95, 95% CI). Combining Eq. [3] with k_{obs1} the oxidaiton of PCE can be expressed as:

$-d$[PCE]$/dt$ = k_1[PCE][•OH] = k_{obs1}[PCE]   [8]
  [•OH] = k_{obs1}/ k_1

which implies [•OH] remained constant throughout the experiment.

Similarly, as it is shown in Figure 8.3.2-5, the decomposition of H_2O_2 followed pseudo first-order kinetics with the observed decomposition constant, k_{obs2}, determined to be 0.206/h ± 0.0360/h (R = 1.0, 95% CI). Presuming the H_2O_2 decomposition follows Eq. [1], then

-d[H_2O_2]/dt = k[H_2O_2][Fe^{2+}] = k_{0bs2}[H_2O_2]   [9]

[Fe^{2+}] = k_{obs2}/ k   [10]

From Eq. [10], the concentration of Fe^{2+} is a constant and was calculated to be 7.53 x 10^{-4} mM. Compare the calculated [Fe^{2+}] with the initial Fe concentration denoted that most of the Fe remained as Fe^{3+} in the degradation process. However, the calculation has not taken into consideration that H_2O_2 can be catalyzed by Fe^{2+} to release oxygen (Sung and Morgan, 1980).

Summary
Silica sand contaminated with PCE at 1000 mg/kg was mineralized in 3 h using CHP systems with initial concentrations of 2 M of H_2O_2 and 5 mM of $FeSO_4$. Dichloroacetyl chloride and dichloroacetic acid were the only significant intermediates detected, and the formation of DCAA was believed to be the limiting step of PCE mineralization. A degradation pathway of PCE in CHP systems has been proposed based on experimental observations and reactions reported in the literature. Formic acid is proposed asthe final intermediate before it is mineralized to CO_2. Both PCE and H_2O_2 decomposition revealed pseudo first order kinetics with rate constants determined to be 1.65lh 0.475lh and 0.206lh 0.036/h, respectively.
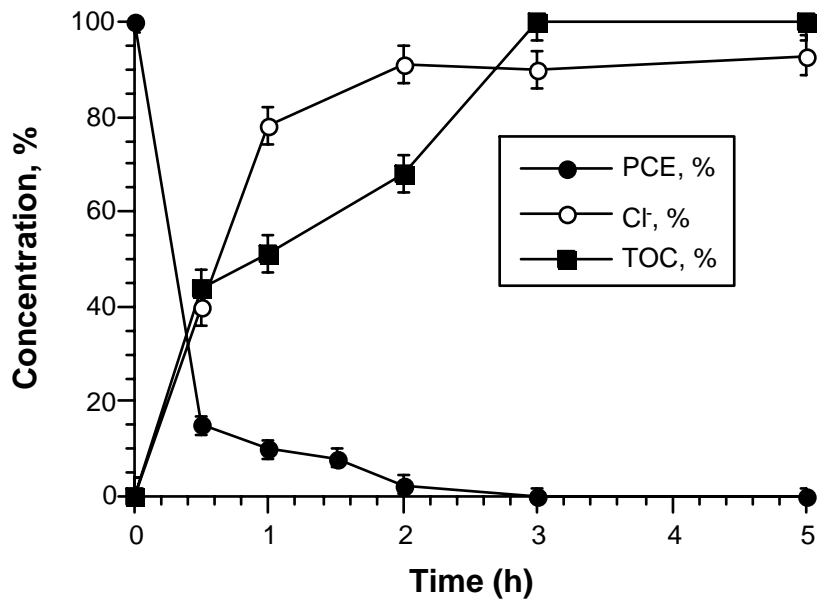
Figure 8.3.2-1. Perchloroethylene degradation by CHP over time. Initial PCE concentration: 1000 mg/kg sand. The TOC (CO_2) and Cl^- concentrations are expressed as the equivalent amount of PCE.
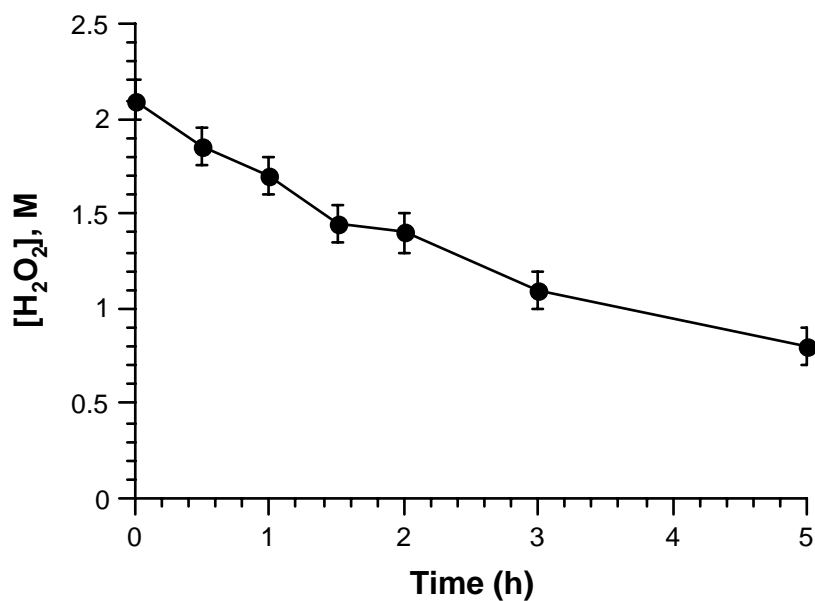
Figure 8.3.2-2. Corresponding hydrogen peroxide consumption over time.
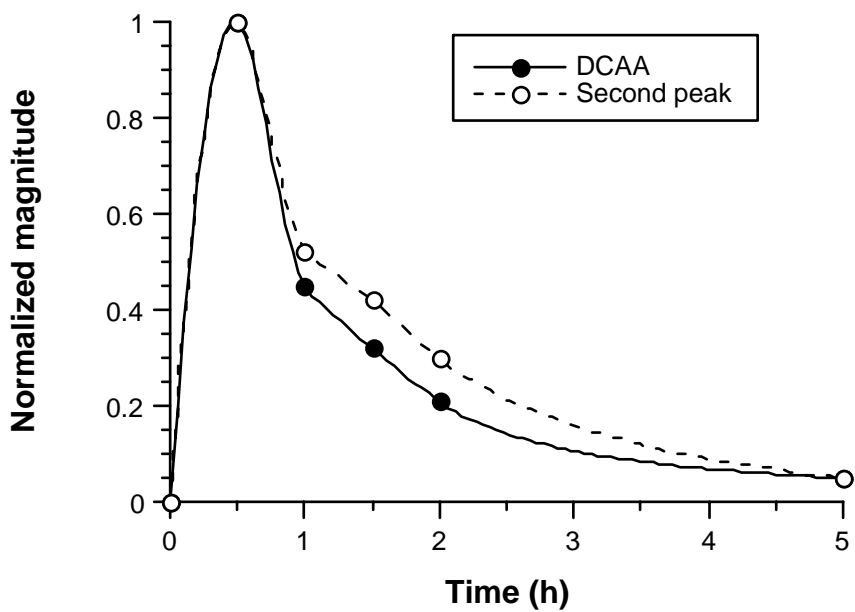
Figure 8.3.2-3. Normalized concentration profile of dichloroacetic acid (DCAA) and the unknown second peak generated during PCE degradation. The actual magnitude of the second peak was significantly smaller in comparison to DCAA.
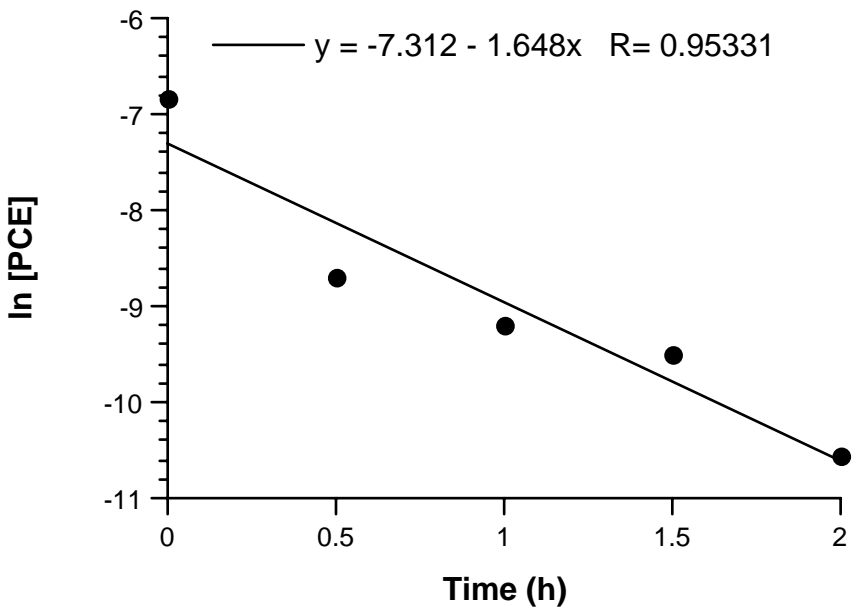
Figure 8.3.2-4. Pseudo first-order plot of PCE degradation. Data beyond 2 h were omitted because PCE degradation was near complete. PCE concentration is expressed in molarity.
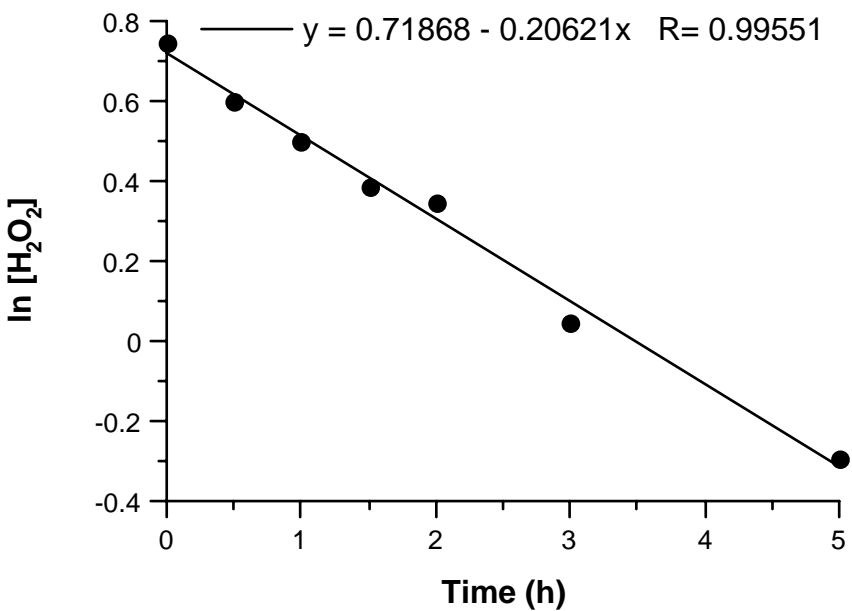
Figure 8.3.2-5. Pseudo first-order plot of hydrogen peroxide degradation. Hydrogen peroxide concentration is expressed in molarity.

8.3.3 Mineralization of a Sorbed Polycyclic Aromatic Hydrocarbon, Benzo[*a*]pyrene, in Soils Using CHP

Analysis of the data obtained through the central composite experimental design procedures first involved development of regression equations from the empirical data; secondly, response surfaces, which physically illustrate the regression equation as isoresponse lines, were generated from the regression equations.

Mineralization of BaP in silica sand.
Based on statistical analysis of the experimental data, BaP oxidation in the silica sand was described by:

$$^{14}C\text{-}CO_2 \text{ Recovery (\%)} = 40.7 + 1.47 \times 10^{-3}(H_2O_2) - 3.40(VOLUME) - \qquad (1)$$
$$2.33(IRON) + 1.07 \times 10^{-7}(H_2O_2)^2 + 3.0 \times 10^{-2}(VOLUME)^2$$
$$+4.58 \times 10^{-1}(VOLUME)(IRON)$$

where

(H_2O_2) = the hydrogen peroxide concentration (mM)

(VOLUME) = the slurry volume ($\times$ 0.31 g/ml, the silica sand field capacity)

(IRON) = the iron (II) amendment concentration (mM)

Treatment stoichiometry was quantified by:

$$\text{Stoichiometry (mole } H_2O_2/\text{mole } ^{14}C\text{-}CO_2) = [1.20 - 3.71 \times 10^{-5}(H_2O_2) \qquad (2)$$
$$-6.41 \times 10^{-1}(VOLUME) + 1.01 \times 10^{-1}(VOLUME)^2$$
$$+9.62 \times 10^{-6}(H_2O_2)(VOLUME)]^{-1} \times 1000$$

Equations 1 and 2 were characterized by R^2 of 0.88 and 0.91, respectively, when the experimental data were plotted against values generated by the equations. All terms were within the 90% confidence interval of a single sided t-distribution with 13 and 15 degrees of freedom. The materials balance accounted for 89% of the ^{14}C in the silica sand systems.

Inspection of equation 1 reveals that the relationships between H_2O_2 concentration, iron (II) amendment, and slurry volume are interactive. Graphing the n = 3 variables with the n + 1 = 4 response of $^{14}C\text{-}CO_2$ recovery is not possible because of the four dimensions involved. Therefore, the iron (II) amendment was held constant at 6.6 mM and a response surface was generated for BaP oxidation in silica sand as a function of H_2O_2 concentration and slurry volume ($\times$ the sand field capacity = 0.31 ml/g) (Figure 8.3.3-1). These data show that 59% of the BaP was mineralized in silica sand using 12,300 mM H_2O_2 at nearly all slurry volumes. Although slurry volume was not a significant factor, BaP mineralization increased from <30% to 59% as a function of H_2O_2 concentration. Although high concentrations of H_2O_2 (30%; 8850 mM) are used as a standard procedure for removing organic carbon from soils, this procedure does not result in the removal of all carbon, nor is the majority of the carbon mineralized (Griffith and Schnitzer, 1977). Therefore, the removal and mineralization of BaP in this study is likely

primarily due to reactive species produced in vigorous CHP reactions, rather than direct oxidation by H_2O_2.

The interactive effects of H_2O_2 concentration and iron (II) amendment were significantly higher than the effect of slurry volume. The oxidation of BaP as a function of H_2O_2 concentration and iron (II) concentration with a slurry volume held constant at 0.30 x the sand field capacity is shown in Figure 8.3.3-2. Benzo[a]pyrene mineralization increased as a function of H_2O_2 concentration and decreased as a function of the iron (II) amendment. A potential reason for the more effective oxidation with lower iron (II) amendments may be less quenching of reactive species by iron (Walling, 1975).

A response surface illustrating stoichiometries for the mineralization of BaP as a function of H_2O_2 concentration and slurry volume, with the iron (II) amendment held constant at 6.6 mM, is shown in Figure 8.3.3-3. The data suggest that excess slurry volume (containing H_2O_2 that is not in contact with the sorbed or NAPL-phase BaP) consumes H_2O_2 while not degrading the sorbed or NAPL contaminant. The results also document that the reactions became increasingly inefficient with increased H_2O_2 concentrations, which was likely due to an increase in quenching reactions. The molar H_2O_2 requirements for BaP mineralization are several orders of magnitude greater than those characteristic of standard Fenton's systems in which water-soluble parent compounds are oxidized with 2-10 moles H_2O_2/mole of substrate degraded. Although lower H_2O_2 concentrations have been used in some CHP soil treatment studies, such as 0.29 M (Li et al., 1997), 1 M (Watts et al., 1994), and 2 M (Miller et al., 1996), similar results to those found in this research were reported by and Kakarla and Watts (1997) and Watts et al. (1999b) in the CHP oxidation of highly hydrophobic, sorbed contaminants. One reason that for the wide range of H_2O_2 concentrations may be the degree of contaminant sorption; more strongly sorbed contaminants may require higher dosages of H_2O_2.

Mineralization of BaP in the Palouse loess soil.
Statistical analyses of the experimental data showed that BaP oxidation in the Palouse loess soil was quantified by:

$$^{14}C\text{-}CO_2 \text{ Recovery (\%)} = 53.1 + 1.13 \times 10^{-3}(H_2O_2) - 5.79(pH) - \quad\quad (3)$$
$$0.122(VOLUME)^2 - 0.360(pH)^2 + 0.838(VOLUME)(pH)$$

where

(VOLUME) = the slurry volume ($\times$ 0.42 g/ml, the silica sand field capacity)

Treatment stoichiometry for the oxidation of BaP in the Palouse loess was described by:

$$\text{Stoichiometry (mole } H_2O_2/\text{mole } ^{14}C\text{-}CO_2) = [4.18 \times 10\text{-}1 - 3.25 \times 10^{-5}(H_2O_2) \quad (4)$$
$$-2.90 \times 10^{-2}(VOLUME) + 1.42 \times 10^{-9}(H_2O_2)^2 + 6.53 \times 10^{-4}(VOLUME)^2$$
$$-2.09 \times 10^{-3}(pH)^2 + 1.63 \times 10^{-3}(VOLUME)(pH)]^{-1} \times 1000$$

Equations 3 and 4 were characterized by an R^2 of 0.89 and 0.84 when the experimental data were compared with values generated from the equations. All terms were within the 90% confidence

interval of a single sided t-distribution with 14 and 13 degrees of freedom, respectively. The materials balance accounted for 93% of the ^{14}C in the system.

The results of one of the more effective oxidation conditions in the Palouse loess with no soluble iron addition (i.e., catalysis of CHP reactions by naturally-occurring iron minerals) are shown in the response surface of Figure 8.3.3-4. Under optimum conditions consisting of 14,000 mM H_2O_2, a slurry volume of 20 × the soil field capacity (= 0.42 ml/g), and a pH of 8.0, 85% of the BaP was mineralized. Because degradation was more effective at low slurry volumes, the most effective process conditions appear to be characterized by vigorous CHP reactions (i.e., with concentrated H_2O_2) in which hydroxyl radicals and other reactive species are produced in close proximity to the sorbed or NAPL-phase BaP. Results obtained at pH 3 show that mineralization of BaP was less effective under acidic pH conditions than at pH 8, which is different from the results obtained in previous studies because hydroxyl radical generation through CHP reactions is usually more effective under acidic pH regimes (Barbeni et al., 1987: Watts et al., 1990). A possible explanation of this trend may be that the reductive pathway found in vigorous CHP reactions that is responsible for enhanced desorption and degradation of species not reactive with hydroxyl radical (Watts et al., 1999b) is favored at high pH.

The oxidation stoichiometries (moles of H_2O_2 consumed/moles of ^{14}C-CO_2 recovered) for BaP mineralization in the Palouse loess are shown in Figure 8.3.3-5. Similar to the results obtained in silica sand, these data indicate that the most efficient systems are those in which the slurry volume was low; i.e., the results suggest that the close proximity of the H_2O_2 to the sorbed or NAPL-phase BaP is an important factor in promoting a stoichiometrically-efficient reaction that enhances its desorption/dissolution and mineralization. Excess H_2O_2 that decomposed away from the soil was probably not effective in degrading and mineralizing sorbed or NAPL-phase BaP. Watts and Stanton (1999) obtained similar results in documenting the oxidation of ^{14}C-hexadecane; they found that the degradation of hexadecane required relatively high concentrations of H_2O_2 and that the most efficient stoichiometry was at low slurry volumes. In addition, scavenging of oxidants by mineral surfaces may be mechanism for the ineffective stoichiometries observed in these reactions (Miller and Valentine, 1999)

Gas chromatographic and GC/MS analyses coupled with ^{14}C measurements documented that the remaining contaminant carbon in each system (41% for the silica sand system and 15% for the Palouse loess) was undegraded BaP. Analysis of the aqueous phase by gas chromatography/mass spectrometry and ^{14}C scintillation counting showed no presence of contaminant carbon in the soil water. These results indicate that all of the ^{14}C-BaP that was degraded was rapidly converted to ^{14}C-CO_2. Polycyclic aromatic hydrocarbons, such as BaP, are oxidized by hydroxyl radicals to keto acids, such as muconic acid, pyruvate, and oxalate (Schwarzenbach et al., 1993). Most keto acids are characterized by low reactivity with hydroxyl radicals ($k_{OH\bullet} = 7.7 \times 10^6$ M^{-1} s^{-1} for oxalate; $k_{OH\bullet} = 3.1 \times 10^7$ M^{-1} s^{-1} for pyruvate); therefore, a standard Fenton's reaction producing only hydroxyl radicals would not be expected to mineralize BaP (Ronen et al., 1994). However, rapid mineralization of these species may be promoted by the generation of reductants formed in vigorous CHP reactions (Watts et al., 1999b), because these intermediates react rapidly with reductants ($k_{e^-} = 3.2 \times 10^9$ M^{-1} s^{-1} for oxalate; $k_{e^-} = 6.8 \times 10^9$ M^{-1} s^{-1} for pyruvate) (Buxton et al., 1987). As a result, PAHs, such as BaP, may be rapidly converted to carbon dioxide and water through the presence of both reductants and hydroxyl radicals in CHP systems.

Biological processes are often the most economical means of treating soils contaminated with refractory compounds. A number of investigations have documented the mineralization of organic contaminants in soils through biological metabolism (Jones and Alexander, 1986; Scow et al., 1989; Schmidt and Gier, 1989). These studies have shown that mineralization of xenobiotics ranges from 30% to 80% depending on the structure of the parent compound and the biorecalcitrance and toxicity of the degradation products. However, biological treatment is limited by the natural desorption rates of contaminants and, therefore, may take months to years. The data provided in Figures 8.3.3-1 through 8.3.3-5 show that soil remediation using CHP reactions can promote the same degree of mineralization as bioremediation in significantly shorter time periods. While the cost of the H_2O_2 is a disadvantage of CHP reactions, it may be outweighed by the advantages of rapid treatment and site closure.

Desorption of BaP from the silica sand and the Palouse Loess (i.e., the mass of sorbed BaP remaining in the GP systems over time) is shown in Figure 8.3.3-6; these data demonstrate undetectable desorption over 5 d. However, treatment of BaP using CHP reactions was complete in 2 to 24 hr resulting in 59% to 85% mineralization of the parent compound under optimum conditions. Because no GP desorption occurred over the time in which a significant amount of treatment occurred, the CHP reactions were not limited by desorption. Similar results were reported by Watts et al. (1994), Gates and Siegrist (1995), and Kakarla and Watts (1997). Furthermore, these data are consistent with the results of Watts et al. (1999b), who found that desorption of toluene was enhanced in vigorous CHP reactions, even when its degradation was prevented by addition of the hydroxyl radical scavenger isopropanol. They suggested that enhanced treatment of sorbed compounds is a two-step process: the reducing species generated in CHP reactions first desorbs contaminants, with subsequent oxidation or reduction of the contaminants in the aqueous phase.

Contaminant sorption and the presence of NAPL lenses often control the treatment of contaminated soils by chemical or biological methods. Soil washing and soil flushing are often used to overcome sorption in soil remediation (Wayt and Wilson, 1989); however, a disadvantage of soil washing is the subsequent need to treat surfactant-laden wash water (Valsaraj and Thibodeaux, 1989). The use of surfactants to disrupt NAPLs has similar disadvantages. The CHP treatment of soils contaminated with hydrophobic compounds, such as BaP, provides a mechanism in which the contaminants are desorbed/dissolved and oxidized in a single physiochemical process (i.e., a combined soil washing-oxidation process). CHP reactions, in which reductants as well as hydroxyl radicals are generated, may provide a universal treatment matrix in which contaminants are desorbed from solids and mineralized through coexisting oxidations and reductions.

Summary and Conclusions

The potential for CHP to mineralize BaP sorbed on soils was investigated. CHP treatments were conducted in silica sand and a Palouse loess soil spiked with 0.1 mmol/kg BaP, and were complete within 24 hours. Confirmation of degradation was accomplished using ^{14}C-labeled BaP and recovering evolved ^{14}C-CO_2. Experimental procedures incorporating central composite rotatable experimental designs were used to determine the most effective treatment conditions. The effects of H_2O_2 concentration, slurry volume, and iron (II) concentrations were investigated in the silica sand. In the Palouse loess soil, the variables included H_2O_2

concentration, slurry volume, and pH with CHP reactions catalyzed by iron oxyhydroxides present in the soil.

Vigorous conditions (i.e., high H_2O_2 concentrations) were required to oxidize BaP in silica sand, which was likely related to the requirement of overcoming sorption. Under optimum conditions, 59% of the ^{14}C-BaP was recovered as ^{14}C-CO_2 within 24 h using 12,300 mM H_2O_2, a slurry volume of 0.3 x the sand field capacity, and an iron (II) concentration of 6.6 mM. In the Palouse loess soil, 85% of the BaP was oxidized to CO_2 and H_2O using 14,000 mM H_2O_2, a slurry volume of 20 × field capacity, and a pH of 8.0. The oxidation stoichiometry was highly sensitive to slurry volume and less sensitive to H_2O_2 concentration, with more efficient oxidation occurring when the CHP reagents were in direct contact with the sorbed contaminants. In addition, mineral-catalyzed CHP reactions at neutral pH were found to promote greater BaP mineralization than the same reactions conducted at acidic pH regimes. Gas purge measurements confirmed negligible desorption of BaP over 5 days in the absence of treatment.

The radiolabeled carbon that was not mineralized (15-41%) remained with the soil fraction in the form of BaP; none was found in the aqueous phase, suggesting that the contaminant was degraded through enhanced desorption/dissolution with subsequent rapid degradation in the aqueous phase. The results show that under conditions of high H_2O_2 concentration, CHP reactions can enhance desorption and NAPL dissolution while simultaneously mineralizing the contaminant, resulting in the equivalent of a combined soil washing-oxidation process.
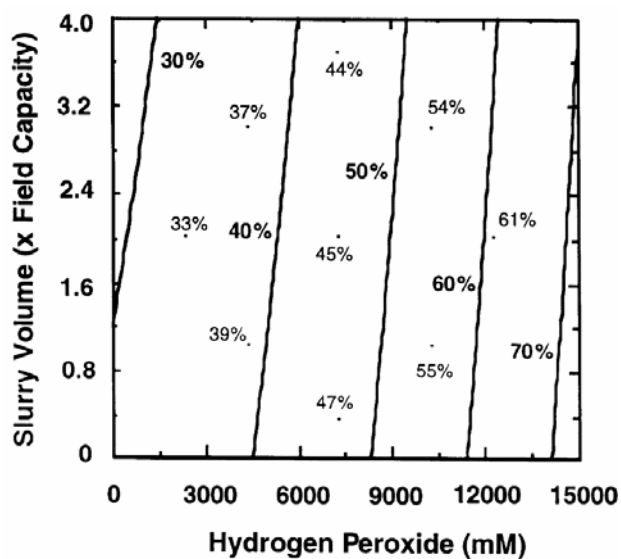
Figure 8.3.3-1. Response surface for the mineralization of ^{14}C-BaP as a function of H_2O_2 concentration and slurry volume in silica sand catalyzed by 6.6 mM iron (II). Isoconcentration lines represent the per cent BaP recovered as ^{14}C-CO_2 described by equation 5. The field capacity of the silica sand = 0.31 ml/g.
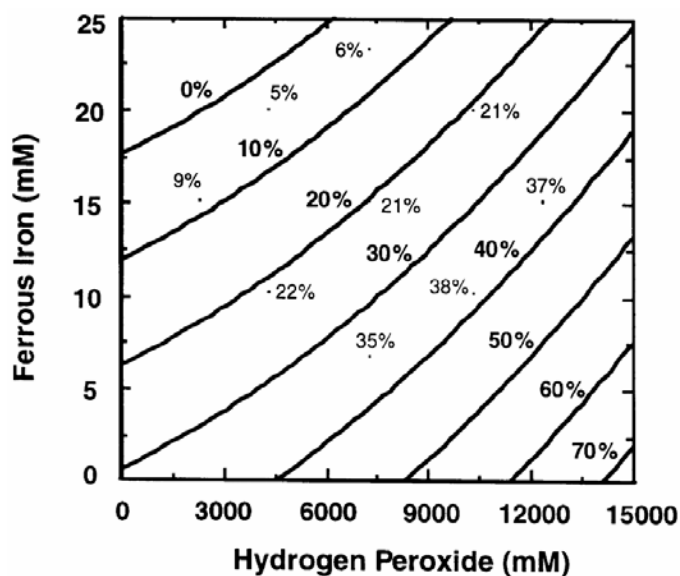
Figure 8.3.3-2. Benzo[a]pyrene oxidation in silica sand as a function of H_2O_2 concentration and iron (II) concentration at an optimal slurry volume of 0.25 x soil field capacity. Isoconcentration lines represent the per cent BaP recovered as ^{14}C-CO_2- described by equation 5.

112
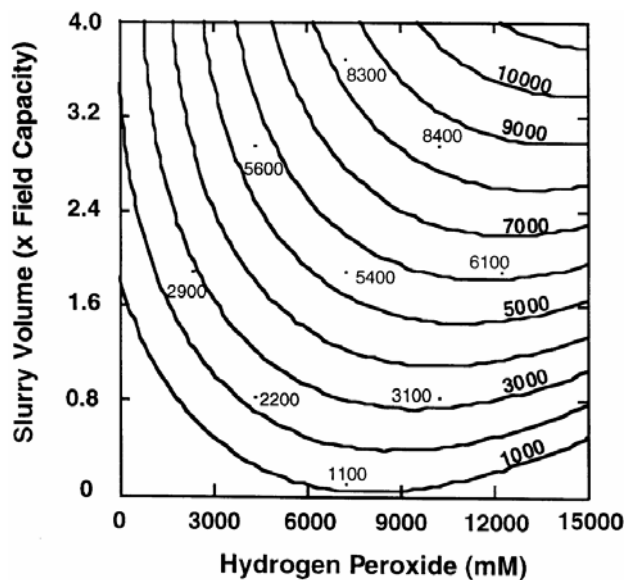
Figure 8.3.3-3. Benzo[a]pyrene oxidation stoichiometries in silica sand as a function of H_2O_2 concentration and slurry volume with a 6.6 mM iron (II) amendment. Isoconcentration lines represent the moles H_2O_2 consumed/^{14}C-CO_2 described by equation 6.
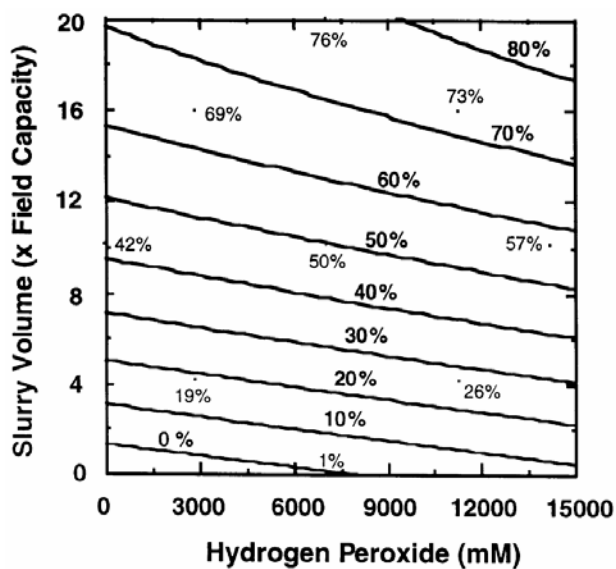
Figure 8.3.3-4. Response surface for the mineralization of ^{14}C-BaP as a function of H_2O_2 concentration and slurry volume in Palouse loess catalyzed by naturally occurring iron oxyhydroxides at pH 8. Isoconcentration lines represent the per cent BaP recovered as ^{14}C-CO_2 described by equation 7. The field capacity of the Palouse loess = 0.42 ml/g.

113
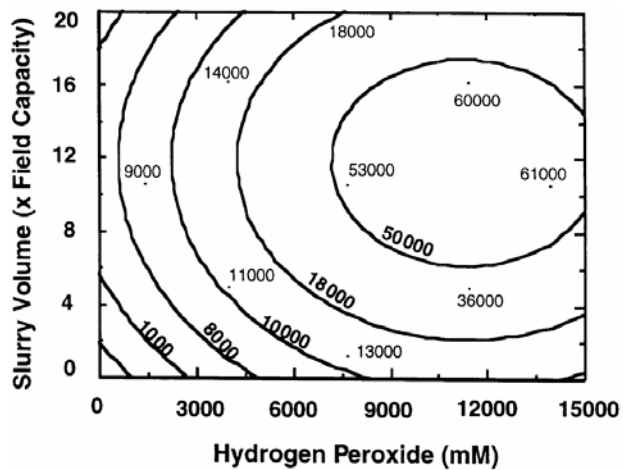
Figure 8.3.3-5. Benzo[a]pyrene oxidation stoichiometry in the Palouse loess as a function of H_2O_2 concentration and slurry volume at pH 8.0. Isoconcentration lines represent the moles H_2O_2 consumed/^{14}C-CO_2 described by equation 8.
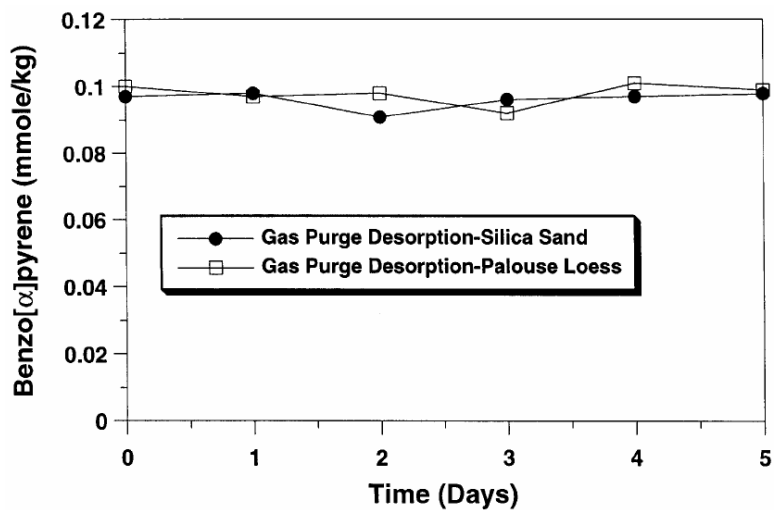
Figure 8.3.3-6. Desorption of BaP from the silica sand and the Palouse loess.

8.3.4 Mineralization of Sorbed and NAPL-Phase Hexadecane by Catalyzed Hydrogen Peroxide

Hexadecane partitioning

In aqueous silica sand suspensions, hexadecane distributed into the sorbed, nonaqueous liquid and aqueous phases. Only 0.36% of the hexadecane was found in the aqueous phase, which corresponds to its water solubility of 0.00048 mg l^{-1} (Verschueren, 1983). Nonaqueous liquid hexadecane comprised 43.3% of the total and was present due to the low water solubility of hexadecane and the limited number of sorption sites on the silica sand. The majority of the hexadecane (56.3%) was found in the sorbed state, which is a function of its high octanol–water partition coefficient (log K_{ow}=9.07) and low water solubility (Karickhoff et al., 1979).

Desorption dynamics

The data of Figure 8.3.4-1 show the degree of hexadecane desorption over 72 h relative to the concentration of control samples. These results indicate no significant difference between hexadecane loss in the gas- purge samples and control samples; therefore, desorption was negligible over the 72 h period. Minimal desorption would be expected due to the partitioning of hexadecane to the silica sand or as a nonaqueous liquid (Jury et al., 1983). Similar results were documented by Sedlak and Andren (1994) in the desorption of PCBs and Pavlostathlis and Jaglal (1991), who found that a persistent fraction of trichloroethylene desorbed slowly.

Parent compound degradation

The experimental treatment data were first analyzed to determine a second-order equation including terms for interactions of the two variables. Based on central composite design data obtained from reactions of unlabeled hexadecane treated with a three-dimensional matrix of hydrogen peroxide concentrations, slurry volumes and iron (II) concentrations, statistical analysis provided a regression equation of the experimental data:

$$\text{Hexadecane Oxidation (\%)} = -12.4 + 13.1(H_2O_2) + 19.6(\text{VOLUME}) - 6.18 \times 10^{-7}(H_2O_2)^2 - 3.72(\text{VOLUME})^2 \tag{1}$$

where H_2O_2 = hydrogen peroxide concentration (mM), and VOLUME = slurry volume (FC). A similar analysis showed that the oxidation stoichiometry of the system was represented by:

$$\text{Oxidation Stoichiometry (mol } H_2O_2 \text{ consumed x mmol hexadecane oxidized}^{-1}) =$$
$$63.31 - 1.14 \times 10^{-3}(H_2O_2) - 33.86(\text{VOLUME}) + 5.97(\text{VOLUME})^2 \tag{2}$$

Equation 1 was characterized by an R^2 of 0.94 with 15 degrees of freedom; the R^2 of equation 2 was 0.85 with 16 degrees of freedom. The original form of equations 1 and 2 was analyzed in a stepwise manner to evaluate the importance of each term by comparing the results of these equations to the experimental data and analyzing the significance of terms within the 90% confidence interval of a single sided t-distribution. Because the term for iron (II) amendment was not significant at the 90% confidence interval of a single-sided t-distribution, it was eliminated from equations 1 and 2. Therefore, the iron (II) amendment was not a significant factor in oxidation of the parent compound within the range of concentrations evaluated, which suggests that within the range of iron (II) concentrations used (5 to 25 mM), sufficient iron (II) was present for CHP reactions to occur and the relative degree of quenching was equal at all iron (II)

concentrations. CHP reactions also occur in the presence of sand without iron addition because it contains trace concentrations of iron (Ravikumar and Gurol, 1994); the rates of oxidation are lower when no soluble iron is added but the oxidation stoichiometry is often more efficient (Watts et al., 1994).

Equations 1 and 2 were transformed into three- dimensional figures (response surfaces), which physically describe the data. The response surface illustrating the effects of hydrogen peroxide concentration and slurry volume in the oxidation of hexadecane is shown in Figure 8.3.4-2. Use of 10,000 mM hydrogen peroxide and a slurry volume of 2.5 x the sand field capacity resulted in over 80% hexadecane oxidation. Control experiments using deionized water in place of H_2O_2 showed no measurable hexadecane degradation. Based on the concentric isodegradation lines shown in Figure 8.3.4-2, hydrogen peroxide concentration and slurry volume have a significant effect on hexadecane treatment. The effect of hydrogen peroxide concentration may be related to the intensity of the reaction required to oxidize nonaqueous liquid and sorbed species (Watts et al., 1994). The importance of slurry volume was likely related to the additional mass of reagents present at higher field capacities. However, at slurry volumes >3 FC at all hydrogen peroxide concentrations, there was a corresponding decrease in hexadecane oxidation. Hexadecane oxidation decreased at H_2O_2 concentrations >10,000 mM; in both cases, decreased hexadecane oxidation may be due to hydroxyl radical quenching by excess H_2O_2, OH• and iron species. The presence of oxidized iron species (e.g. ferrihydrite) in slurries may also affect the stoichiometry of CHP reactions. Similar results were obtained by Watts et al. (1990), who found that when iron (II) precipitates from solution as amorphous iron (III) species, the oxidation stoichiometry became significantly less effective. Dilute hydrogen peroxide concentrations have been used in most Fenton's studies (Sedlak and Andren, 1994), but high concentrations of hydrogen peroxide appear to be needed to oxidize sorbed contaminants. Such a trend was documented by Watts et al. (1994), who found that high concentrations of hydrogen peroxide were required to oxidize sorbed hexachlorobenzene.

The response surface describing reaction stoichiometry (mol H_2O_2 consumed mmol hexadecane oxidized^{-1}) superimposed on the corresponding response surface for hexadecane oxidation (Figure 8.3.4-2) is shown in Figure 8.3.4-3. Based on the system stoichiometry, hydrogen peroxide was inefficiently consumed under the conditions at which maximum hexadecane oxidation was achieved. The most efficient stoichiometry was found at low slurry volumes, which suggests that intimate contact between the reagents and the contaminant provides the most effective reaction conditions. Increases in slurry volume result in more inefficient stoichiometry and did not increase the degree of hexadecane oxidation. These data suggest that reactions that occur in the aqueous phase away from NAPL and sorbed hexadecane are ineffective due to the lack of contact between the hexadecane and hydroxyl radicals.

Aliquots were also analyzed by GC/MS to detect products from the oxidation of hexadecane. Small quantities of hexadecane as well as a small amount of a large (C^{14}) carboxylic acid were found. The paucity of reaction intermediates suggest that aggressive CHP reactions destroy degradation products as rapidly as they are formed.

Hexadecane mineralization
The statistical analysis of data and response surface development for the mineralization of ^{14}C-hexadecane by recovery of ^{14}C-CO_2 were described by:

116

Hexadecane Mineralization (%) = 26.04 - 1.30 x 10^{-3}(H_2O_2) - 8.59(VOLUME) - 3.13 x 10^{-2}(IRON $)^2$ + 8.23 x 10^{-4}(H_2O_2)(VOLUME) + 1.05 x 10^{-4}(H_2O_2)(IRON) + 3.45(VOLUME) (IRON) (3)

where IRON =iron (II) concentration (mM). In addition, the stoichiometry of hexadecane mineralization was:

Mineralization Stoichiometry (mol H_2O_2 consumed x mmol hexadecane oxidized$^-$ ^{1}) = 28.08 - 4.79 x 10^{-4}(H_2O_2) - 16.17(VOLUME) + 2.97(VOLUME $)^2$ (4)

Equation 3 was characterized by an R^2 of 0.85 with 16 degrees of freedom; equation 4 was described by an R^2 of 0.82 with 16 degrees of freedom with all terms lying within the 90% confidence interval of a single sided t-distribution.

The response surface describing the interaction of hydrogen peroxide concentration and slurry volume for the mineralization of hexadecane with an iron (II) concentration of 25 mM is shown in Figure 8.3.4-4. With 15,000 mM hydrogen peroxide and a slurry volume of 4 FC, 73% of the 0.1 mmol kg^{-1} hexadecane was oxidized to ^{14}C-CO_2. Unlike the results of parent compound oxidation, mineralization of hexadecane was strongly dependent on the iron (II) amendment, which suggests that a non-hydroxyl radical mechanism involving iron species may be involved (Ronen et al., 1994). From Figure 8.3.4-6, the importance of slurry volume and hydrogen peroxide concentration are nearly equal, with hexadecane mineralization increasing as a function of both the variables.

While parent compound oxidation was most effective at a specific locus on the surface response, a maximum for hexadecane mineralization was not achieved; furthermore, the data show that hexadecane mineralization is a function of an entirely different set of conditions. The surface response describing the interaction of hydrogen peroxide concentration and iron (II) concentration at a slurry volume of 20 ˚C is illustrated in Figure 8.3.4-5. These data show the same trends as Figure 8.3.4-4, in which increased concentrations of hydrogen peroxide and iron promoted a corresponding increase in hexadecane mineralization. A number of oxidative products, such as β-keto acids, are oxidized slowly by hydroxyl radicals; therefore, other non-hydroxyl radical oxidations may be required to mineralize reaction intermediates (Dorfman and Adams, 1973). The data of Figure 8.3.4-5 suggest that iron species are essential for the oxidation of these intermediate products. The response surface describing the interaction of slurry volume and iron (II) amendment at a hydrogen peroxide concentration of 15,000 mM is shown in Figure 8.3.4-6. Similar to Figs 8.3.4-4 and 8.3.4-5, the data of Figure 8.3.4-6 show a trend toward increased mineralization as both slurry volume and iron concentration were increased. These data also document that hexadecane mineralization was enhanced by excess iron.

The results of this research show that >70% hexadecane mineralization can be achieved under a number of CHP reaction conditions. Numerous studies have been conducted on the microbial mineralization of organic compounds. For example, Schmidt and Gier (1989) documented the mineralization of 2,4-dinitrophenol (DNP) in soils over a range of DNP concentrations. The maximum DNP mineralization documented was 50% in a 100 ng kg^{-1} DNP system over 150 h. Furthermore, Hess et al. (1990), in enhancing the biodegradation of DNP in pure cultures and sequencing batch reactors (SBRs), found 37% recovery of ^{14}C-DNP as ^{14}C-

CO₂ in the SBRs. In a silt loam soil, Scow et al. (1989) found that, even with glucose and glutamate augmentation, only 30% mineralization of *p*-nitrophenol was achieved. The degradation and mineralization of a number of higher PCBs in soils were investigated with and without the addition of biphenyl (Focht and Brunner, 1985). The maximum mineralization found was 49% with the biphenyl augmentation.

Oxidative processes are considered ineffective in promoting the complete mineralization of organic compounds (Schwarzenbach et al., 1993), often because the dicarboxylic acids and b-keto acids that are common intermediates react slowly with hydroxyl radicals (Dorfman and Adams, 1973). Ronen et al. (1994) compared the mineralization of ^{14}C-labeled pyridine by an acclimated bacterial culture to Fenton's reagent. The bacterial culture was more effective than Fenton's reagent in mineralizing pyridine in deionized water, groundwater, and subsurface sediments. They found that the bacterial culture converted 54.4% of the labeled pyridine to ^{14}C-CO₂, but the Fenton's system promoted only 24.5% mineralization in the same system. Ronen et al. (1994) concluded that Fenton's reagent has limited applicability for the remediation of groundwater and subsurface solids due to the low degree of mineralization that was achieved. However, the authors did not optimize the Fenton's conditions; if properly optimized, greater mineralization of pyridine may have been achieved. The data provided in Figs 2–6 show that CHP reactions provide nearly complete mineralization of a hydrophobic hydrocarbon that is not irreversibly sorbed, just as biological methods do. The system stoichiometry for hexadecane mineralization superimposed on Figure 8.3.4-6 is shown in Figure 8.3.4-7. Similar to the results for parent compound oxidation (Figure 8.3.4-3), the most efficient conditions were found at slurry volumes <1.5 FC and hydrogen peroxide concentrations >10,000 mM; however, inefficient stoichiometric conditions were required to obtain >70% hexadecane mineralization. These data suggest that, like the oxidation of the parent compound, additional reagents reduce the reaction efficiency, which may be due to the physical characteristics of the system (i.e. sorbed and NAPL hexadecane). Sorption processes control the effectiveness of most remediation technologies including bioremediation and soil washing. The aggressive CHP conditions used in this study appear to promote a coupled mechanism of enhanced desorption and subsequent oxidization by hydroxyl radicals (Watts et al., 1994). These conditions, which have the potential to overcome sorption, provide a mechanism for the rapid remediation of soils, which may be applied under some situations, such as emergency response conditions.

Summary and Conclusions
The mineralization of sorbed and NAPL hexadecane was investigated using CHP reactions in silica sand slurries. Analysis of hexadecane-spiked silica sand showed that >99% of the hexadecane existed either in the sorbed or NAPL state due its high hydrophobicity. Results of gas-purge analysis documented that hexadecane did not dissolve or desorb over 72 h, which suggests that oxidation reactions occurring in <72 h occur through the oxidation or enhanced desorption/dissolution of sorbed and NAPL species. Effective hexadecane mineralization required aggressive reaction conditions, which consisted of H₂O₂ concentrations >10 M. Central composite rotatable experimental designs were used to develop response surfaces and evaluate the interaction of variables for hexadecane oxidation and mineralization. The results showed that parent compound degradation was independent of the iron (II) concentration in the range investigated (i.e. 5 to 25 mM), although the iron concentration was an important variable for hexadecane mineralization with increased iron concentrations resulting in additional hexadecane mineralization. These data suggest that mechanisms other than hydroxyl radicals may be

responsible for hexadecane mineralization. More importantly, this research showed that CHP reactions have the ability to mineralize hexadecane in a sorbed and/or nonaqueous phase state.

The results presented in Section 8.3 document that contaminants treated by CHP can be transformed through oxidative, reductive, and nucleophilic reactions. In most cases, contaminant mineralization is possible; however, promoting mineralization in the field is likely impractical because of the large masses of hydrogen peroxide required. CHP treatment in the field will likely be followed by monitored natural attenuation to reach site closure.
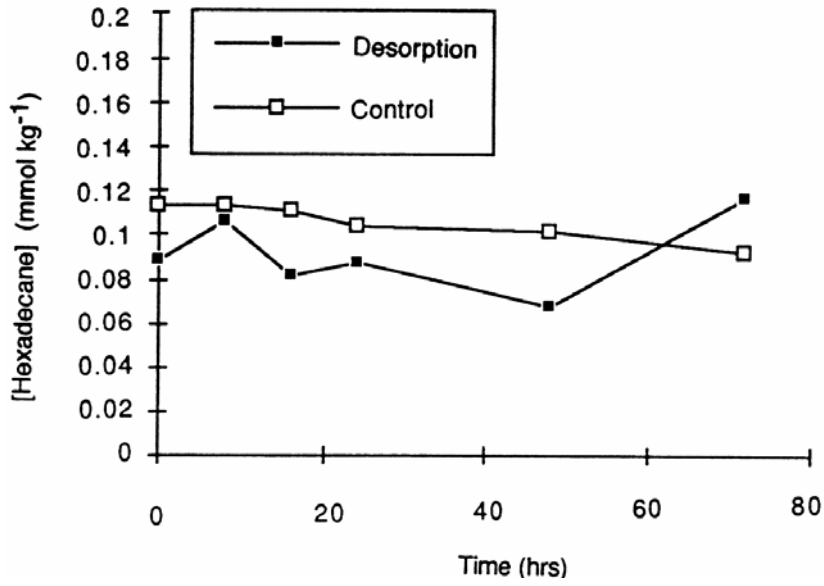
Figure 8.3.4-1. Desorption of 0.1 mmol kg^{-1} hexadecane from silica sand.
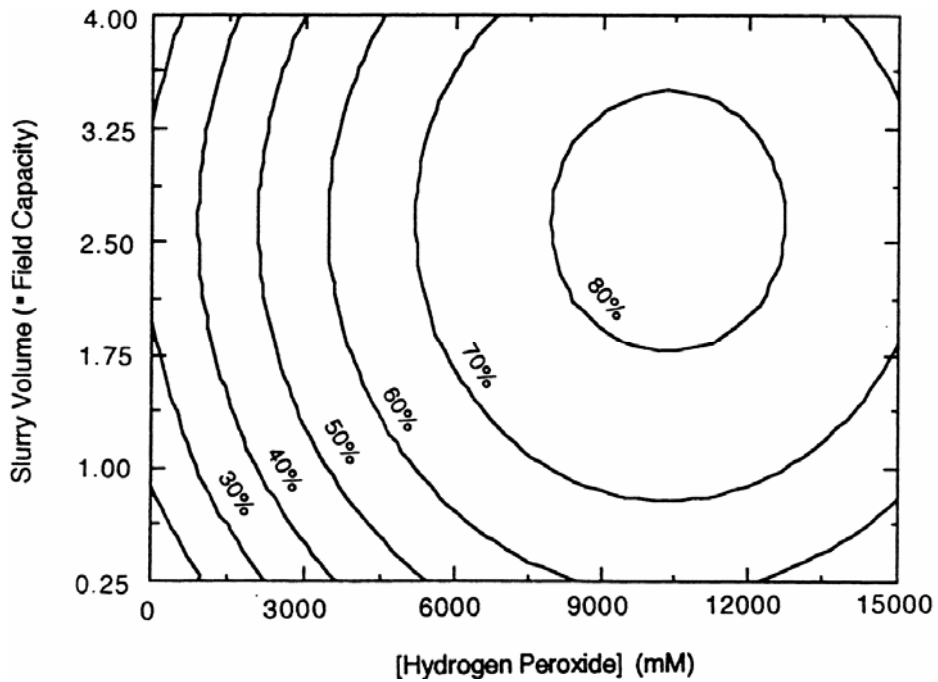
Figure 8.3.4-2. Response surface describing the interaction of hydrogen peroxide concentration and slurry volume for hexadecane oxidation. Contour lines represent percent hexadecane oxidation relative to controls.
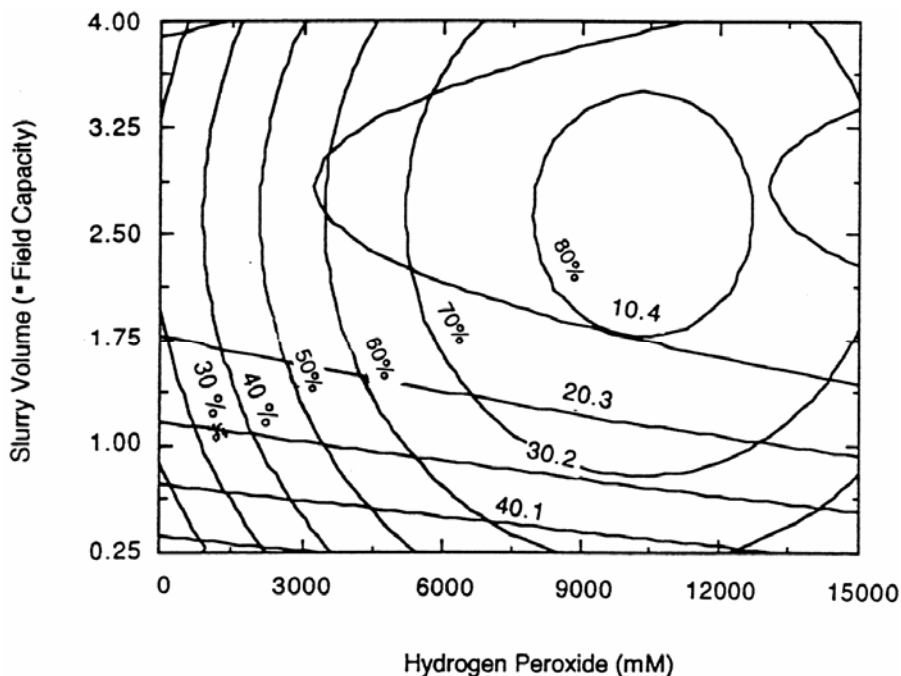
Figure 8.3.4-3. Response surface for hexadecane oxidation combined with oxidation stoichiometry for the interaction of hydrogen peroxide concentration and slurry volume. Contour lines represent percent hexadecane oxidation and mol H_2O_2 consumed (mmol hexadecane oxidized)$^{-1}$
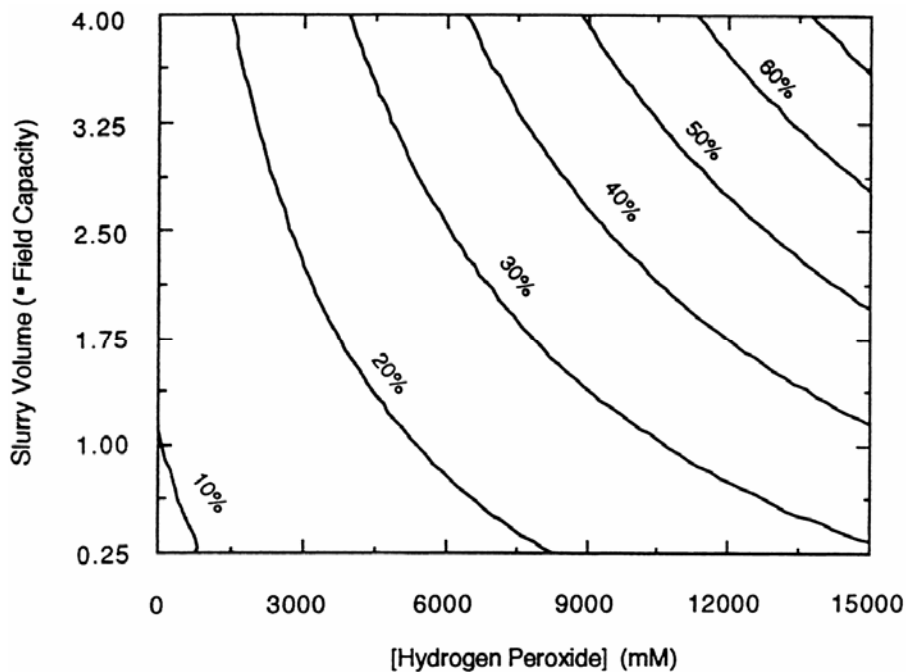
Figure 8.3.4-4. Response surface describing the interaction of hydrogen peroxide concentration and slurry volume at an iron (II) concentration of 25 mM for hexadecane mineralization. Contour lines represent percent ^{14}C-CO_2 evolved from 0.1 mmol kg^{-1} ^{14}C-hexadecane.

121
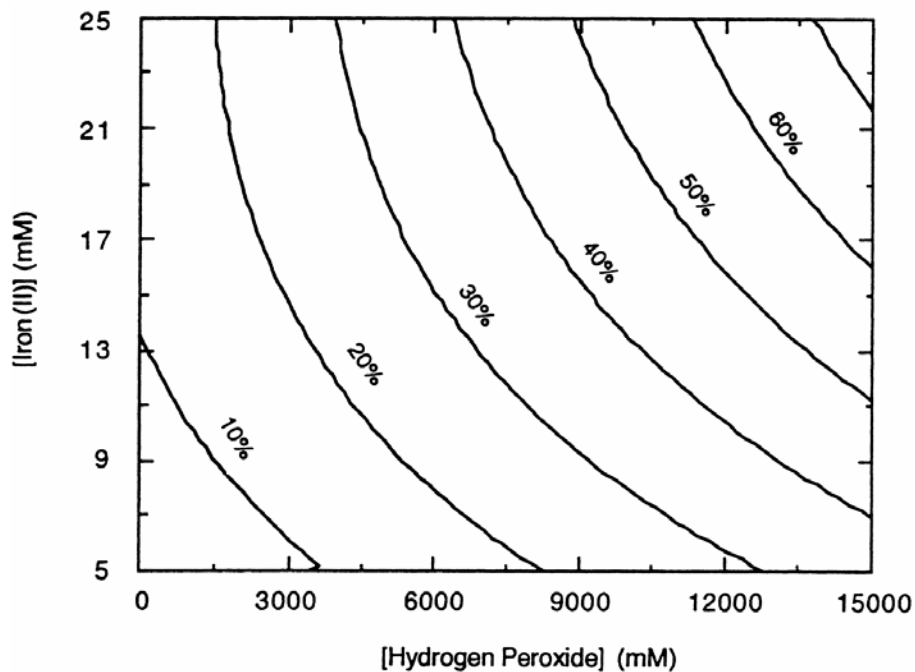
Figure 8.3.4-5. Response surface describing the interaction of hydrogen peroxide concentration and iron (II) concentration at a field capacity of 4°C for hexadecane mineralization. Contour lines represent percent ^{14}C -CO_2 evolved from 0.1 mmol kg^{-1} ^{14}C -hexadecane.
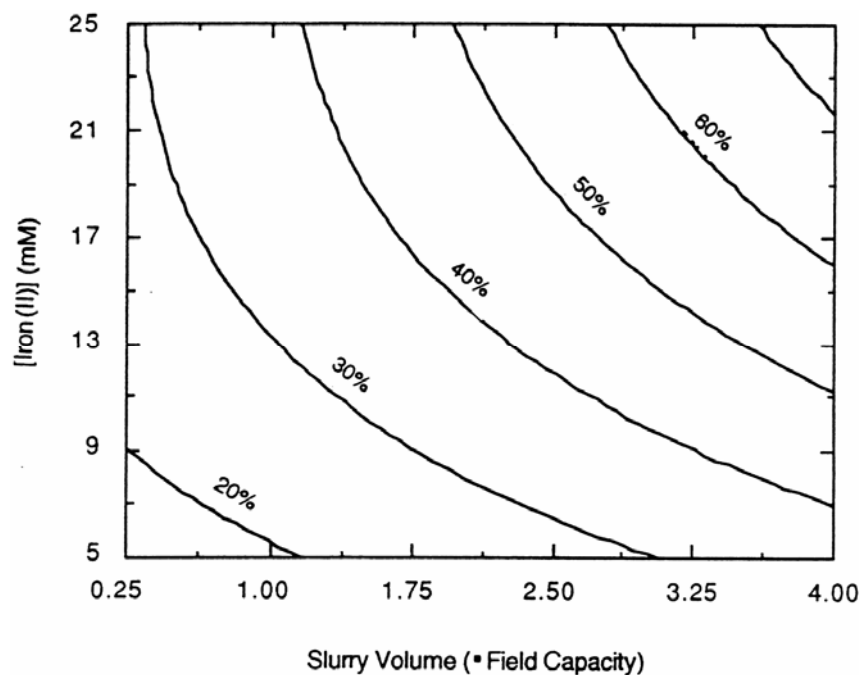
Figure 8.3.4-6. Response surface describing the interactions of slurry volume and iron (II) concentration at a hydrogen peroxide concentration of 15,000 mM for hexadecane mineralization. Contour lines represent percent ^{14}C -CO_2 evolved from 0.1 mmol kg^{-1} ^{14}C-hexadecane.

122
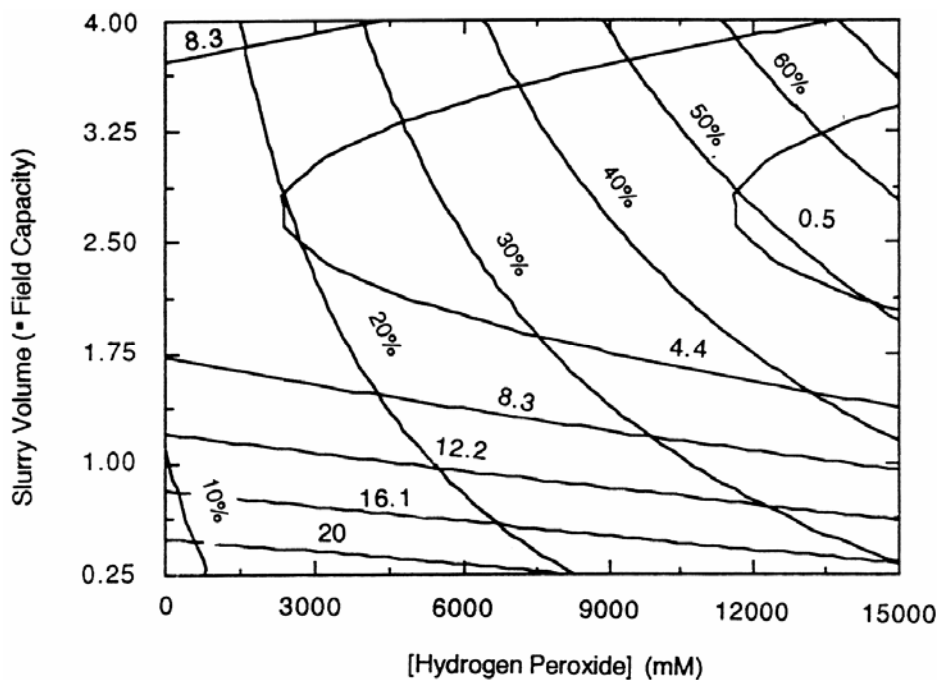
Figure 8.3.4-7. Response surfaces for hexadecane mineralization combined with oxidation stoichiometry for the interaction of slurry volume and iron (II) concentration with hydrogen peroxide concentration of 15 M. Contour lines represent percent ^{14}C -CO_2 evolved from 0.1 mmol kg^{-1} ^{14}C -hexadecane and mol H_2O_2 consumed (mmol ^{14}C -CO_2 evolved)$^{-1}$.

123

8.4 DNAPL Destruction

The presence of dense nonaqueous phase liquids (DNAPLs) at contaminated sites represents significant environmental and public health problems. Approximately 60% of the sites on the National Priorities List (NPL) are contaminated with DNAPLs in the form of large pools, smear zones, or ganglia (U.S. EPA, 1993). Dissolution of DNAPLs into ground water is slow, providing a continuous source of contamination emanating from contaminated sites. Dissolution is usually the rate-limiting step in DNAPL remediation; therefore, DNAPLs may persist for decades, even when actively treated (Johnson and Pankow, 1992; Lemke et al., 2004).

Although hydroxyl radical-mediated oxidations have been the degradation mechanism most commonly associated with CHP, hydroxyl radical reacts at diffusion-controlled rates and is not reactive with sorbed compounds (Sedlak and Andren, 1994; Watts et al., 1999), so it is not likely to react with nonaqueous phase contaminants (Sheldon and Kochi, 1981). However, rapid destruction of such DNAPLs has been demonstrated with CHP in the laboratory for a TCE DNAPL (Yeh et al., 2003). Such rapid destruction has also been observed in the field; for example, 94% of a 270 kg TCE DNAPL was destroyed at the Westinghouse Savannah River site using CHP (U.S. EPA, 1998). Reactive oxygen species other than hydroxyl radical generated through propagation reactions are important in CHP ISCO (Watts et al., 1999; Watts and Teel, 2004) and may be responsible for the rapid treatment of DNAPLs. However, the destruction of DNAPLs by CHP reactions is complex, and is affected not only by the rates of reaction of the contaminant with hydroxyl radical, superoxide, and other reactive oxygen species, but also by the rate of dissolution of the contaminant, the surface to volume ratio of the DNAPL, and many other factors (Stroo et al., 2004). The objectives of this segment of research were to demonstrate rapid destruction of a carbon tetrachloride DNAPL; determine the rates of DNAPL destruction in relation to the rates of DNAPL dissolution for six chlorinated aliphatic compounds; and to determine the reactive oxygen species responsible for the destruction of these DNAPLs.

8.4.1 Destruction of a Carbon Tetrachloride DNAPL by CHP: Proof of Concept

Soluble Iron-Catalyzed Reactions

Iron-catalyzed CHP reactions (5 mM Fe [III] and a steady-state concentration of 1470 mM H_2O_2 at pH 3) were used to treat CT DNAPLs of 3.0 g and 1.5 g (Figure 8.4.1-1). Treatment of CT DNAPLs with an initial mass of 3.0 g (19.5 mmol) and 1.5 g (9.75 mmol) for 3 h resulted in the destruction of 0.20 g (1.3 mmol) and 0.29 g (1.8 mmol) of CT, respectively, compared to control experiments using ORBO tubes that accounted for loss from volatilization. The similar masses lost in the 3.0 g and 1.5 g CT systems suggest that the destruction of the DNAPL is a function of the surface area exposed to the CHP reactions, which was equal in the two systems. In addition, dissolution in the fill-and-draw systems was not significantly different from that of control systems. Minimal CT dissolution was confirmed by analysis of the aqueous phase of the fill-and-draw reactors, which showed undetectable CT concentrations.   The stoichiometry in the iron (III)-catalyzed reactions was 49.7 mmol H_2O_2 consumed per mmol CT degraded in the 3.0 g CT reaction and 35.9 mmol H_2O_2 consumed per mmol CT degraded in the 1.5 g CT reaction.   These results demonstrate that soluble iron-catalyzed CHP reactions destroyed CT DNAPLs at rates significantly greater than the rate of CT dissolution into the

aqueous phase with stoichiometries comparable to the CHP treatment of sorbed contaminants (Gates and Siegrist, 1995; Watts and Stanton, 1999).

This segment of research provided proof-of-concept of DNAPL destruction by CHP, and provided hypotheses for their pathways of destruction. Because CT is unreactive with hydroxyl radicals (Haag and Yao, 1992), another reactive species must be responsible for CT destruction. Non-hydroxyl radical species that may be produced in CHP reactions include solvated electrons, hydroperoxide anion, perhydroxyl radical, and superoxide radical anion. Although CT is considered unreactive with low concentrations of superoxide (Hallewell and Gutteridge, 1985), the reactivity of CT with superoxide at high CT concentrations in vigorous CHP reactions is a possible pathway for CT destruction (Teel and Watts, 2002). The formation of superoxide in CHP reactions has been well-documented (Kitajima et al., 1978; Afanas'ev, 1989). In the presence of excess H_2O_2, a common CHP initiation reaction is the iron (III)-catalyzed decomposition of H_2O_2 to form perhydroxyl radical, the conjugate acid of superoxide (Walling and Weil, 1974):

$$Fe^{3+} + H_2O_2 \rightarrow Fe^{2+} + HO_2\bullet + H^+ \tag{1}$$

With the production of iron (II) in the system, the standard Fenton's initiation reaction can then proceed:

$$Fe^{2+} + H_2O_2 \rightarrow Fe^{3+} + OH\bullet + OH^- \tag{2}$$

Perhydroxyl radical is also formed by the reaction of the hydroxyl radicals generated in Equation 2 with excess H_2O_2:

$$OH\bullet + H_2O_2 \rightarrow H_2O + HO_2\bullet \tag{3}$$

Perhydroxyl radical then dissociates to superoxide:

$$HO_2\bullet \leftrightarrow O_2\bullet^- + H^+ \qquad pK_a = 4.8 \tag{4}$$

In addition, perhydroxyl radical can proceed through one more electron transfer mediated by the iron (II) generated in Equation 1 to form hydroperoxide anion:

$$HO_2\bullet + Fe^{2+} \rightarrow HO_2^- + Fe^{3+} \tag{5}$$

Reactions 3–5, which predominate at H_2O_2 concentrations > 0.3 M (1%), are likely integral to DNAPL destruction by CHP.

Manganese Oxide-Catalyzed Reactions

Metal oxide and oxyhydroxide minerals are ubiquitous in the subsurface and have been proposed as natural catalysts for ISCO using CHP (Tyre et al., 1991; Ravikumar and Gurol, 1994). Recent results have shown that manganese oxide-catalyzed CHP reactions generate non-hydroxyl radical species that destroy aqueous phase CT (Watts et al., 2003). Therefore, manganese oxide-catalyzed CHP reactions (1.0 g MnO_2 [pyrolusite] and a steady state concentration of 294 mM H_2O_2 at pH 7) were investigated for their ability to destroy CT

125

DNAPLs. Treatment of CT DNAPLs with an initial mass of 3.0 g (19.5 mmol) and 1.5 g (9.75 mmol) for 3 h resulted in the destruction of 0.56 g (3.6 mmol) (Figure 8.4.1-2) and 0.63 g (4.1 mmol) of CT (Figure 8.4.1-3), respectively, compared to control experiments that accounted for loss from volatilization. As in the soluble iron-catalyzed CHP systems, DNAPL mass destruction was similar in the two pyrolusite systems, suggesting that destruction is related to the surface area exposed to the transient oxygen species in the aqueous phase. Dissolution in the fill-and-draw systems was not significantly different from that of control reactions. Similar to soluble iron-catalyzed CHP reactions, MnO_2-catalyzed CHP reactions destroyed CT DNAPLs at rates much greater than the rate of CT dissolution; however, DNAPL destruction was more extensive and proceeded at neutral pH. Furthermore, the stoichiometry was even more efficient for the MnO_2-catalyzed reactions than for the iron (III)-catalyzed reactions, with 14.2 mmol H_2O_2 consumed per mmol CT degraded in the 3.0 g CT reaction and 12.5 mmol H_2O_2 consumed per mmol CT degraded in the 1.5 g CT reaction.

A mechanism for the catalytic heterogeneous decomposition of H_2O_2 on manganese oxides has been proposed by Hasan et al. (1999). Manganese oxides were hypothesized to decompose hydrogen peroxide to a proton and hydroperoxide anion:

$$H_2O_2 \rightarrow H^+ + HO_2^- \qquad\qquad\qquad [6]$$

Hasan et al. (1999) proposed that the hydroperoxide anion then decomposes to perhydroxyl radical and an electron, which is transferred to the proton via manganese ions:

$$HO_2^- \rightarrow HO_2\bullet + e^- \qquad\qquad\qquad [7]$$

$$e^- + Mn^{4+} \rightarrow Mn^{3+} \qquad\qquad\qquad [8]$$

$$H^+ + Mn^{3+} \rightarrow Mn^{4+} + H\bullet \qquad\qquad\qquad [9]$$

Perhydroxyl radical dissociates to superoxide and a proton as a function of the pH:

$$HO_2\bullet \leftrightarrow O_2\bullet^- + H^+ \qquad pK_a = 4.8 \qquad\qquad [4]$$

The mechanism proposed by Hasan et al. (1999) indicates that one of several transient oxygen species, as well as solvated electrons, could be involved in DNAPL destruction through manganese oxide-catalyzed CHP reactions. However, Kitajima et al. (1978) documented only the presence of superoxide in metal oxide-catalyzed CHP systems, which was confirmed by ESR spectra. Watts et al. (1993) and Teel et al. (2001) proposed the use of naturally-occurring metal oxides in soils and the subsurface as the most effective CHP catalysts. The results of this research support the use of metal oxide catalysts. Watts et al. (1999) found that a reductant or nucleophile that is scavenged by chloroform is responsible for the enhanced desorption and treatment of sorbed contaminants in CHP reactions; the same species may be responsible for the destruction of CT DNAPLs that was demonstrated in this work. The identity of the reactant responsible for DNAPL destruction in CHP reactions is currently under investigation.

Conclusions

   The results of this research provide proof-of-concept that DNAPLs consisting of CT, a compound not reactive with hydroxyl radicals, are rapidly destroyed in CHP reactions catalyzed by iron (III) at pH 3 and pyrolusite at pH 7. The hydroxyl radicals generated in Fenton's systems are highly reactive oxidants but they are not reactive with sorbed contaminants (Sedlak and Andren, 1994), and are likely too short-lived to destroy DNAPLs (Sheldon and Kochi, 1979). Although a significant amount of research has been conducted on DNAPL remediation, a process that can consistently destroy DNAPLs in the field has not been established. CHP ISCO, using the most effective catalyst and conditions to generate the DNAPL-destroying reactant, may provide an effective system for DNAPL remediation. The results of this segment of research provided the basis for evaluating pathways and the reactive oxygen species responsible for the destruction of six different DNAPL contaminants by CHP.
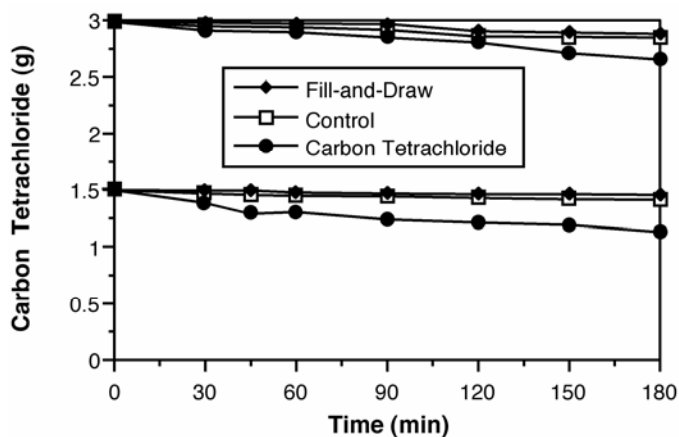
Figure 8.4.1-1. CHP destruction of 3.0 g and 1.5 g CT DNAPLs.
(Reaction conditions: 5 mM $Fe_2(SO_4)_3$, 1470 mM steady state H_2O_2, pH 3; T = 20 ± 2 ˚C)
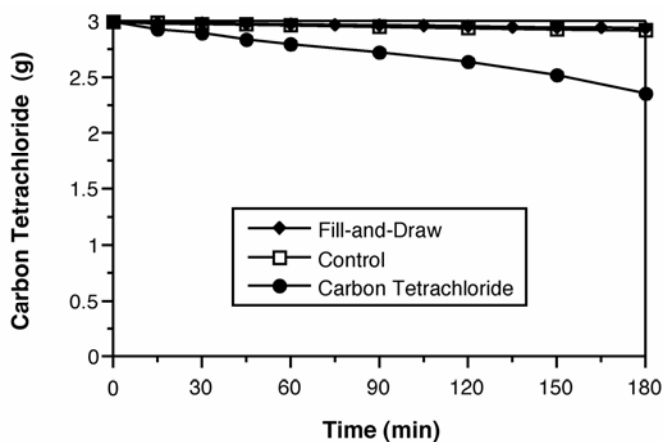
Figure 8.4.1-2. MnO_2-catalyzed CHP destruction of 3.0 g CT DNAPL.
(Reaction conditions: 1 g MnO_2, 294 mM steady state H_2O_2, pH 7; T = 20 ± 2 ˚C).
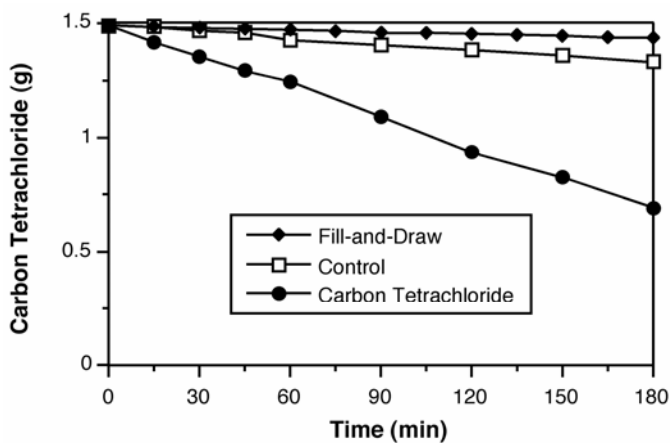
Figure 8.4.1-3. MnO_2-catalyzed CHP destruction of a 1.5 g CT DNAPL.
(Reaction conditions: 1 g MnO2, 294 mM steady state H2O2, pH 7; T = 20 ± 2 ˚C).

128

8.4.2 Pathways for the Destruction of Carbon Tetrachloride and Chloroform DNAPLs by CHP

Carbon tetrachloride and chloroform DNAPL destruction by CHP.

The destruction of a carbon tetrachloride DNAPL and a chloroform DNAPL by CHP is shown in Figure 8.4.2-1a–b. The total mass lost from the carbon tetrachloride DNAPL was 84% and from the chloroform DNAPL was 62% over 24 hr. After subtracting the masses of carbon tetrachloride and chloroform captured in the ORBO tubes and dissolved into the aqueous phase, the net destruction of the carbon tetrachloride DNAPL was 74% and the net destruction of the chloroform DNAPL was 44%. In parallel gas purge reactors, 18% of the carbon tetrachloride DNAPL mass and 97% of the chloroform DNAPL mass were lost through dissolution over the same time period. The mass lost from carbon tetrachloride and chloroform DNAPLs in control reactors containing deionized water in place of hydrogen peroxide was 4% and <1%, respectively. These results demonstrate that carbon tetrachloride and chloroform DNAPLs are rapidly destroyed by CHP, and that carbon tetrachloride DNAPLs are destroyed at a rate significantly greater than their maximum rate of dissolution.

Oxidation by hydroxyl radical is the mechanism usually associated with contaminant degradation in CHP systems; however, the reactive oxygen species superoxide radical anion and hydroperoxide anion are also generated by CHP reactions. Although hydroxyl radical reacts at near diffusion-controlled rates with such biorefractory compounds as trichloroethylene (TCE) ($k_{OH\bullet} = 4.0 \times 10^9$ M^{-1} s^{-1}; Buxton et al., 1988) and perchloroethylene (PCE) ($k_{OH\bullet} = 2.8 \times 10^9$ M^{-1} s^{-1}; Buxton et al., 1988), it is unreactive with carbon tetrachloride in deionized water ($k_{OH\bullet} < 2 \times 10^6$ M^{-1} s^{-1}; Haag and Yao, 1992) and minimally reactive with chloroform ($k_{OH\bullet} = 5.4 \times 10^7$ M^{-1} s^{-1}; Haag and Yao, 1992). Furthermore, hydroxyl radical is not likely to react directly with pools of DNAPLs because of its short-lived nature and corresponding inability to cross phase boundaries (Sheldon and Kochi, 1981).

Phosgene was detected by GC-MS analysis of the off-gas trapped during the CHP treatment of the carbon tetrachloride DNAPL. The formation of phosgene is consistent with the nucleophilic attack on carbon tetrachloride by superoxide in aprotic media (Roberts and Sawyer, 1981; Roberts et al., 1983; Stark and Rabani, 1999), and was recently observed in the degradation of aqueous carbon tetrachloride by CHP (Smith et al., 2004). To elucidate the reactive oxygen species responsible for carbon tetrachloride and chloroform DNAPL destruction, a series of DNAPL treatments was conducted in systems in which only one oxygen species was generated.

DNAPL destruction by hydroxyl radical.

The treatment of a carbon tetrachloride DNAPL and a chloroform DNAPL in a Fenton's system designed to generate only hydroxyl radical are presented in Figure 8.4.2-2a–b. In this hydroxyl radical-generating system, the total carbon tetrachloride DNAPL mass lost was 3% with a net destruction of 2% over 24 hr. The mass of carbon tetrachloride DNAPL lost in the control system over the same time period was 4%; therefore, the destruction of the carbon tetrachloride DNAPL observed in Figure 8.4.2-2 was not due to reactions with hydroxyl radical. The total chloroform DNAPL mass lost in the hydroxyl radical system was 22%; after

subtracting the mass of chloroform captured in the ORBO tubes and dissolved in the aqueous phase, the net destruction of the chloroform DNAPL was 12%, while no measurable loss of chloroform DNAPL mass was observed in the control reactors. The oxidation of chloroform in the hydroxyl radical generating system was greater than the undetectable oxidation of carbon tetrachloride demonstrated in Figure 8.4.2-3a, which is consistent with the second order rate constants. The $k_{OH\bullet}$ for carbon tetrachloride is $<2 \times 10^6$ M^{-1} s^{-1} (Haag and Yao, 1992), indicating that hydroxyl radical is unreactive with carbon tetrachloride; in contrast, the $k_{OH\bullet}$ for chloroform is 5.4×10^7 M^{-1} s^{-1} (Haag and Yao, 1992), which is consistent with the small amount of degradation shown in Figure 8.4.2-3b. These results indicate that all of the carbon tetrachloride and a large proportion of the chloroform destruction were promoted by a reactive species other than hydroxyl radical.

DNAPL destruction by hydroperoxide.

The treatment of a carbon tetrachloride DNAPL and a chloroform DNAPL in a system containing only hydroperoxide anion is shown in Figure 8.4.2-3a–b. No measurable loss of either carbon tetrachloride or chloroform was found in the controls or the experimental reactions. These results demonstrate that hydroperoxide is not the reactive species responsible for the destruction of carbon tetrachloride and chloroform DNAPLs by CHP systems. Although hydroperoxide is a strong nucleophile that readily attacks carbonyl groups and other electron-deficient carbon atoms (David and Seiber, 1999) it was not reactive with the carbon tetrachloride DNAPL or the chloroform DNAPL over the time evaluated. In addition to reacting as a nucleophile, hydroperoxide recombines with a proton to form hydrogen peroxide. This reaction, which proceeds at $\sim10^{10}$ M^{-1} s^{-1}, would also limit the reactivity of hydroperoxide in CHP systems.

DNAPL destruction by superoxide.

Two systems were used to evaluate the reactivity of superoxide with carbon tetrachloride and chloroform DNAPLs. The destruction of a carbon tetrachloride DNAPL and a chloroform DNAPL by a hydroxyl radical-scavenged CHP system (1 M hydrogen peroxide, 5 mM Fe-EDTA chelate, and 3 M ethanol at pH 9–9.5) is shown in Figure 8.4.2-4a–b. The total carbon tetrachloride DNAPL mass lost was 64% and the total chloroform DNAPL mass lost was 83% over 16 hr. After subtracting the masses of carbon tetrachloride and chloroform captured in the ORBO tubes and dissolved into the aqueous phase, the net destruction of the carbon tetrachloride DNAPL was 43% and the net destruction of the chloroform DNAPL was 54%. Approximately 11% of the carbon tetrachloride DNAPL and 87% of the chloroform DNAPL masses were lost through dissolution in gas purge reactors over 16 hr.

Superoxide was also generated using a 2 M potassium superoxide system containing 1 M of a cosolvent (acetone or hydroperoxide) to increase the reactivity of superoxide (Smith et al., 2004). The destruction of a carbon tetrachloride DNAPL and a chloroform DNAPL in the presence of 2 M potassium superoxide and 1 M acetone is shown in Figure 8.4.2-5a–b; the total masses lost over 8 hr were 33% from the carbon tetrachloride DNAPL and 71% from the chloroform DNAPL. After subtracting the masses of carbon tetrachloride and chloroform captured in the ORBO tubes and dissolved into the aqueous phase, the net destruction of the carbon tetrachloride DNAPL was 18% and the net destruction of the chloroform DNAPL was 45%. The destruction of a carbon tetrachloride DNAPL and a chloroform DNAPL in the presence of 2 M potassium superoxide and 1 M hydroperoxide is shown in Figure 8.4.2-6a–b;

130

the total masses lost over 8 hr were 32% from the carbon tetrachloride DNAPL and 57% from the chloroform DNAPL, while net destruction of the carbon tetrachloride DNAPL was 25% and net destruction of the chloroform DNAPL was 45%. In parallel gas purge reactors, 6% of the carbon tetrachloride DNAPL and 68% of the chloroform DNAPL masses were lost over 8 hr.

The data of Figures 8.4.2-1 and 8.4.2-4–6 show that carbon tetrachloride and chloroform DNAPLs are destroyed in both CHP systems and superoxide systems, indicating that superoxide plays a significant role in the destruction of the DNAPLs. The results from the reactions in which only hydroxyl radical (Figure 8.4.2-3) and only hydroperoxide (Figure 8.4.2-4) were generated demonstrate that superoxide is the sole reactive oxygen species in CHP responsible for carbon tetrachloride DNAPL destruction, and that the combined effects of superoxide and hydroxyl radical are responsible for destruction of the chloroform DNAPL.

To further evaluate the destruction of the DNAPLs by CHP, the relative rates of DNAPL dissolution and DNAPL destruction were compared. The experimental data of Figures 8.4.2-1–6 were fit to zero, first, and second order kinetic functions. Based on curve fits of these data, first order loss of the probe compounds was selected as the best fit model; the first order rates are listed in Table 8.4.2-1. The R^2 values for the calculated first order rate constants in the gas purge, CHP, and superoxide systems ranged from 0.83 to 0.98. In the hydroxyl radical and hydroperoxide systems the R^2 values were lower, ranging from 0.11 to 0.48 in the systems in which negligible destruction of the DNAPLs was found, up to 0.72 for the small amount of chloroform DNAPL destruction by hydroxyl radical. The k_{obs} for the net destruction of the carbon tetrachloride DNAPL by CHP was 5.0×10^{-2} hr^{-1}, which was 6.5 times greater than the corresponding rate of gas-purge dissolution of the DNAPL ($k_{obs} = 7.7 \times 10^{-3}$). These results are similar to those of Yeh et al. (2003), who found that a TCE DNAPL was destroyed by CHP at a rate greater than the rate of TCE dissolution. The k_{obs} values for the superoxide generating systems were 3.3–4.4 times greater than the gas purge dissolution rate. The destruction of carbon tetrachloride by CHP reactions and superoxide-generating reactions at rates significantly greater than gas-purge dissolution suggests that superoxide has the potential to overcome mass transfer limitations, possibly diffusion of superoxide into the DNAPL. Potassium superoxide is highly soluble in organic solvents and is often added to aprotic solvents, such as toluene and acetonitrile, in the presence of a crown ether to bind the potassium (Afanas'ev, 1989). When dissolved in such aprotic solvents, superoxide reacts rapidly with carbon tetrachloride and other halogenated compounds (Robert and Sawyer, 1981). The high reactivity of superoxide with carbon tetrachloride in aprotic solvents may be the basis for the enhanced destruction of carbon tetrachloride DNAPLs treated with CHP.

The dynamics of destruction of the chloroform DNAPL are different from those of the carbon tetrachloride DNAPL. The k_{obs} for the net destruction of chloroform DNAPL in CHP reactions was 2.4×10^{-2} hr^{-1}, which is slower than the k_{obs} for its maximum dissolution rate in gas purge reactors ($k_{obs} = 1.3 \times 10^{-1}$ hr^{-1}). The k_{obs} values for the superoxide generating systems were also lower than the gas purge dissolution rate. Chloroform is more soluble in water than carbon tetrachloride and, unlike carbon tetrachloride, is characterized by a measurable rate of reactivity with OH• ($k_{OH•} = 5.4 \times 10^7$ M^{-1} s^{-1}; Haag and Yao, 1992). As a result, the chloroform DNAPL was likely lost in part by dissolution followed by hydroxyl radical-mediated destruction in the aqueous phase, and in part by superoxide-mediated DNAPL disruption. The results shown in Figures 8.4.2-1–6 demonstrate that process conditions for the destruction of carbon tetrachloride

DNAPLs and chloroform DNAPLs are quite different; destruction of a carbon tetrachloride DNAPL requires only superoxide while chloroform DNAPL destruction is promoted by reactions with both hydroxyl radical and superoxide.

The relative rates of carbon tetrachloride (CT) and chloroform (CF) destruction were not consistent between the systems that generate superoxide (CHP, Fe-EDTA, and potassium superoxide with solvents). The value for k_{obs-CT}/k_{obs-CF} was 2.1 for the CHP system, 0.67 for the Fe-EDTA/hydrogen peroxide system, and 0.40 and 0.45 for the potassium superoxide systems with acetone and hydroperoxide addition, respectively. These differences in relative rates may be due to the varying proportions of superoxide and its conjugate acid, perhydroxyl radical, that were present at the different pH regimes of the three systems; the CHP reactions were conducted at pH 3, the Fe-EDTA-hydrogen peroxide reactions were conducted at pH 9–9.5, and the potassium superoxide reactions were conducted at pH 14. The dynamics and reactivity of perhydroxyl radical in CHP systems have not been investigated. As with superoxide, the reactivity of perhydroxyl radical has been considered insignificant in aqueous systems (Larson and Weber, 1994), but it may be more reactive in the presence of cosolvents or DNAPLs. Therefore, the differing proportions of superoxide and perhydroxyl radical in the three systems may have affected the relative rates of destruction of carbon tetrachloride and chloroform DNAPLs.

CHP has not received as much attention as other processes for DNAPL destruction. Bioremediation and permangangate ISCO are often recognized more for their potential for DNAPL destruction. Although DNAPL losses do occur during treatment with permanganate and bioremediation, the time requirements are likely significantly greater than with CHP. For example, a time frame of months is usually required to destroy DNAPLs using permanganate (Schnarr et al., 1998), and bioremediation is even slower (Yang and McCarty, 2002) In contrast, TCE and PCE DNAPLs are destroyed by superoxide and hydoxyl radical in CHP reactions at a rate significantly greater than such increased dissolution, which is probably related to the mass transfer of superoxide into the DNAPL and its resulting increased reactivity; this rapid treatment may be classified as enhanced destruction. The results of this research demonstrate that CHP has the potential to provide an effective technology for rapidly destroying DNAPLs in the field.

Summary and Conclusions

The destruction of carbon tetrachloride and chloroform DNAPLs by CHP was investigated, and the reactive oxygen species responsible for their destruction was evaluated using systems that generate only 1) hydroxyl radical, 2) hydroperoxide, and 3) superoxide. A carbon tetrachloride DNAPL was effectively destroyed by CHP at a rate 6.5 times that of gas purge dissolution. The carbon tetrachloride DNAPL was not destroyed by hydroxyl radical or hydroperoxide but was destroyed by superoxide, indicating that superoxide is the reactive oxygen species responsible for carbon tetrachloride DNAPL destruction in CHP reactions. Chloroform DNAPLs were also rapidly destroyed by CHP, but at a rate slower than that of gas purge dissolution. Hydroperoxide was not responsible for chloroform destruction; however, both hydroxyl radical and superoxide were involved in chloroform DNAPL destruction. Because of the rapid rates at which carbon tetrachloride and chloroform DNAPLs are destroyed, CHP may provide an effective process for destroying DNAPLs in situ.

Table 8.4.2-1. First Order Rate Constants for the Net Destruction of Carbon Tetrachloride and Chloroform DNAPLs

System	Carbon Tetrachloride		Chloroform	
	k_{obs} (hr^{-1})	R^2	k_{obs} (hr^{-1})	R^2
Gas Purge	7.7×10^{-3}	0.98	1.3×10^{-1}	0.96
CHP	5.0×10^{-2}	0.91	2.4×10^{-2}	0.97
Hydroxyl Radical	9.0×10^{-4}	0.11	6.3×10^{-3}	0.72
Hydroperoxide	3.7×10^{-3}	0.48	7.0×10^{-3}	0.42
Fe:EDTA	3.4×10^{-2}	0.94	5.0×10^{-2}	0.96
KO$_2$-Acetone	2.6×10^{-2}	0.83	6.5×10^{-2}	0.95
KO$_2$-HO$_2^-$	3.3×10^{-2}	0.85	7.3×10^{-2}	0.83
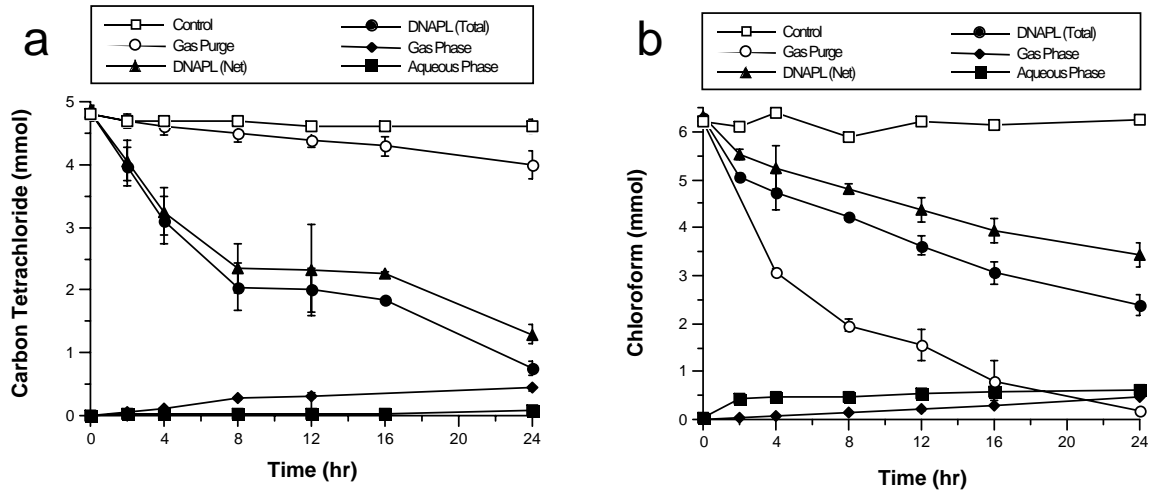
Figure 8.4.2-1. Destruction of (a) carbon tetrachloride and (b) chloroform DNAPLs in CHP systems (5 mM iron (III):HKCH chelate and 2 M hydrogen peroxide at pH 3).
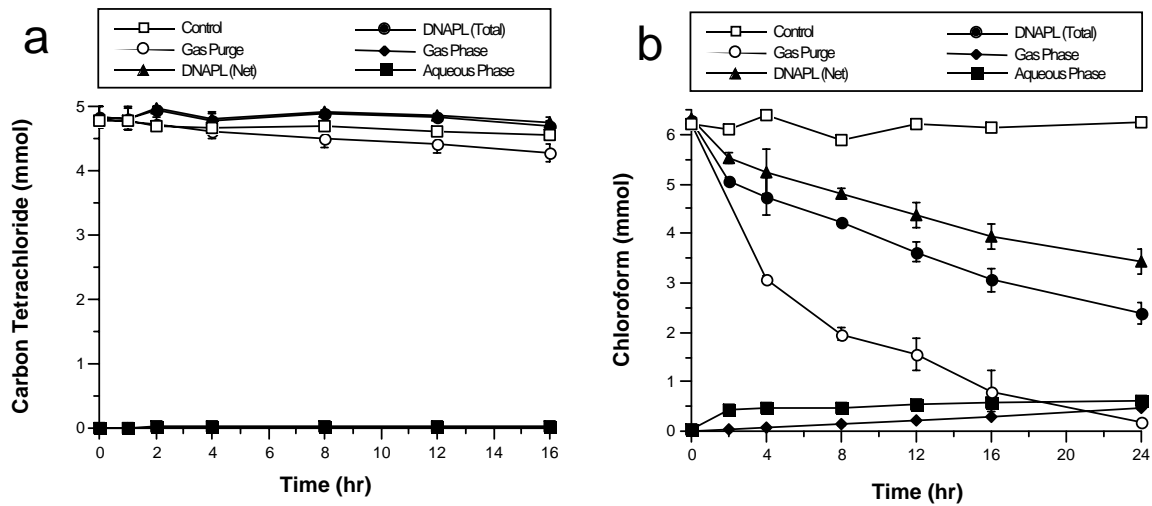
Figure 8.4.2-2. Destruction of (a) carbon tetrachloride and (b) chloroform DNAPLs by hydroxyl radical in standard Fenton's reagent (twenty-four 0.21 mL additions of 1 M hydrogen peroxide and 1 M iron (II)-citrate at pH 1.8 over 48 hr to 7 mL water and 0.5 mL of DNAPL).

134
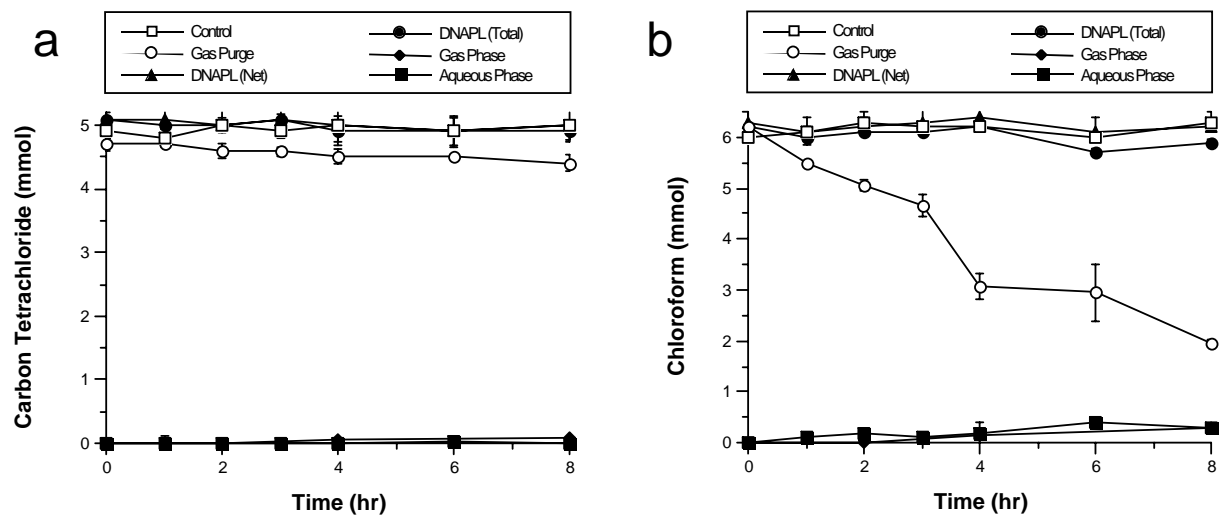
Figure 8.4.2-3. Destruction of (a) carbon tetrachloride and (b) chloroform DNAPLs in a hydroperoxide system (2 M hydrogen peroxide at pH 11.7).
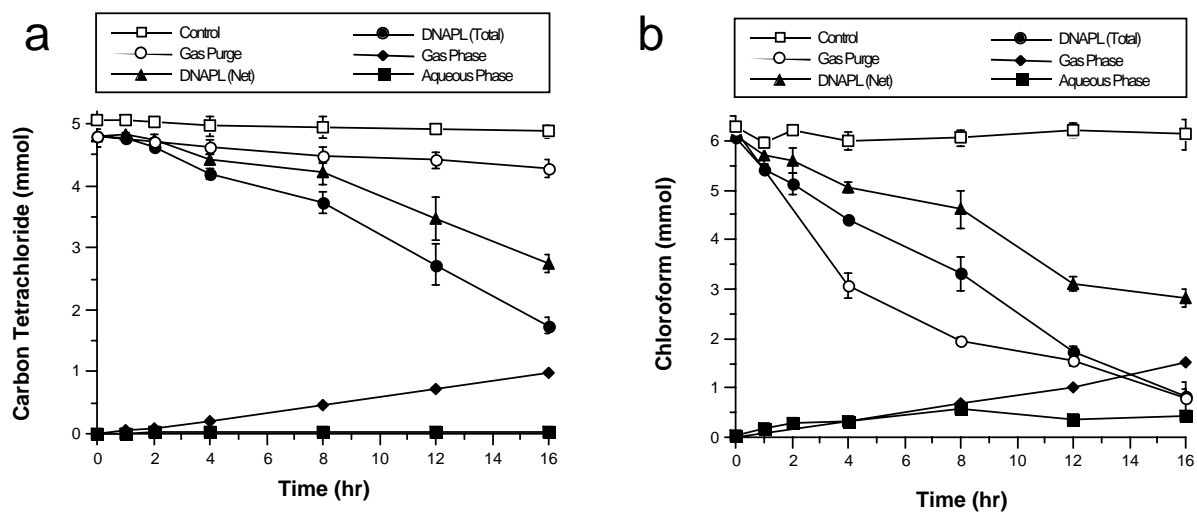
Figure 8.4.2-4. Destruction of (a) carbon tetrachloride and (b) chloroform DNAPLs in a soluble iron-based superoxide system (5 mM iron (III):EDTA complex and 1 M hydrogen peroxide at pH 9.0-9.5).

135
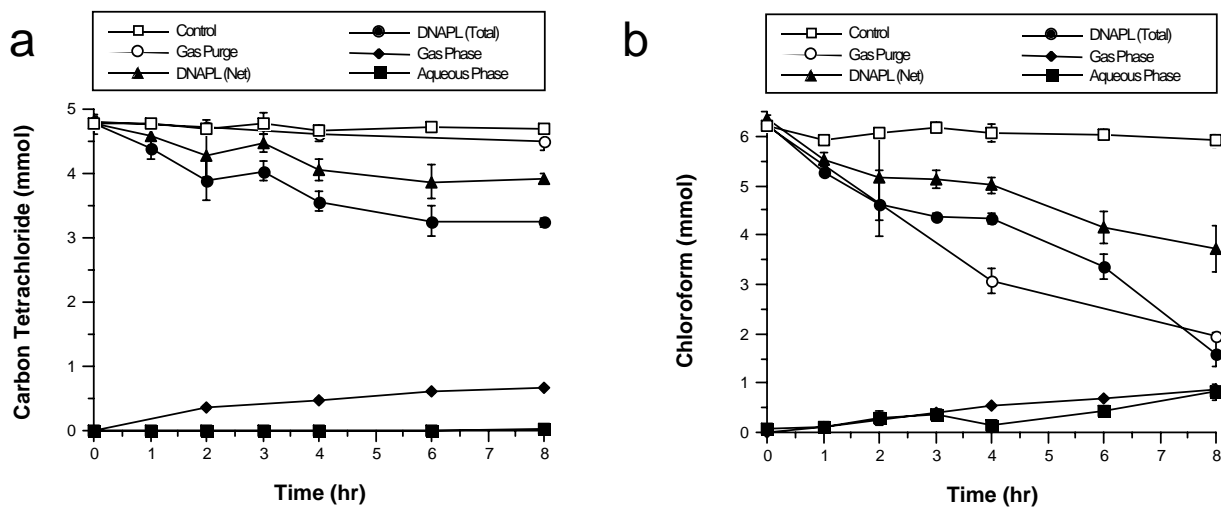
Figure 8.4.2-5. Destruction of (a) carbon tetrachloride and (b) chloroform DNAPLs in a potassium superoxide-based superoxide system with the cosolvent acetone (2 M potassium superoxide and 1 M acetone at pH 14.0).
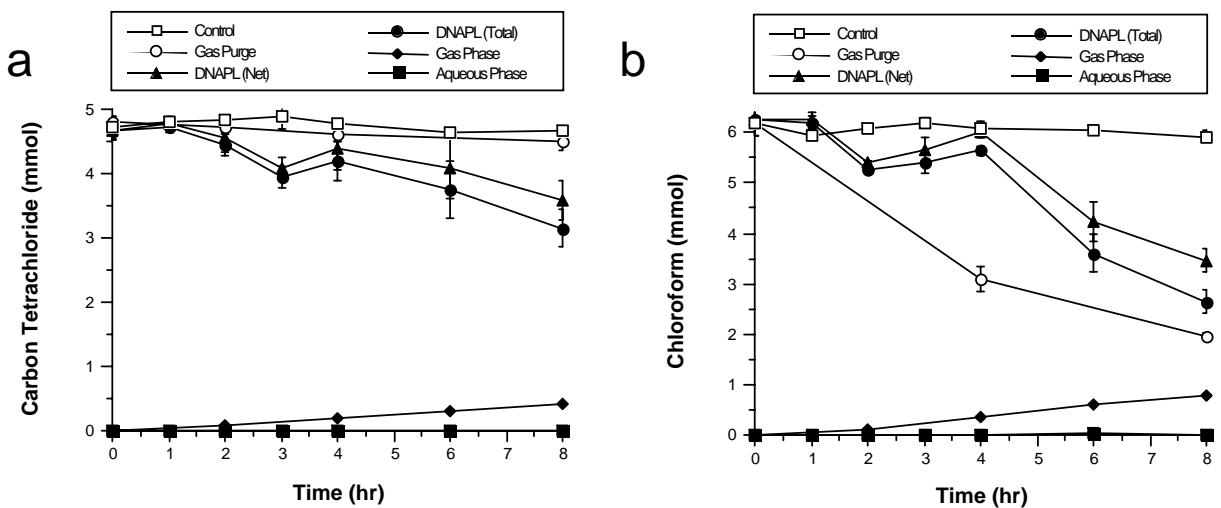
Figure 8.4.2-6. Destruction of (a) carbon tetrachloride and (b) chloroform DNAPLs in a potassium superoxide-based superoxide system with the cosolvent hydroperoxide (2 M potassium superoxide and 1 M hydrogen peroxide at pH 14.0).

8.4.3 Destruction of 1,1,1-Trichloroethane and 1,2-Dichloroethane DNAPLs by CHP

TCA and DCA DNAPL destruction by CHP.
      The destruction of a TCA DNAPL and a DCA DNAPL by CHP (2 M hydrogen peroxide and 10 mM iron (III)-citrate, pH 2.8) is shown in Figure 8.4.3-1a–b. The total mass lost from the TCA DNAPL (Figure 8.4.3-1a) was 85% over 24 hr; after subtracting the mass of TCA captured in the ORBO tubes and dissolved into the aqueous phase during the reactions, the net destruction of the TCA DNAPL was 70%. Over the same time period, only 29% of the TCA DNAPL mass was lost through dissolution in parallel gas purge reactors, which provides a model of the maximum dissolution rate of the DNAPL. The total mass lost from the DCA DNAPL (Figure 8.4.3-1b) was 56.5% over 24 hr, with a net destruction of 44.1%. In parallel gas purge reactors, 92.7% of the DCA DNAPL mass was lost through dissolution after 24 hr. In control reactors containing deionized water in place of hydrogen peroxide, approximately 4% of the DNAPL mass was lost for both TCA and DCA. These results demonstrate that TCA and DCA DNAPLs are rapidly destroyed by CHP, and that TCA DNAPLs are destroyed at a rate significantly greater than their maximum rate of dissolution.

      The traditional conceptual model of CHP is of organic contaminant transformation occurring through the activity of hydroxyl radical. However, the rapid destruction of the TCA DNAPL relative to the DCA DNAPL is not consistent with hydroxyl radical as the sole reactive species, because the reactivity of TCA with hydroxyl radical ($k_{OH•} = 1.0 \times 10^8$ M^{-1} s^{-1}; Getoff, 1989) is lower than that of DCA ($k_{OH•} = 7.9 \times 10^8$ M^{-1} s^{-1}; Getoff, 1990). TCA is also less soluble in water (657 mg/L) than DCA (8310 mg/L), while hydroxyl radical reacts only in the aqueous phase (Sedlak and Andren, 1994; Smith et al., 2006), further supporting the concept that hydroxyl radical is not the species responsible for TCA DNAPL destruction in CHP reactions. The reactive oxygen species superoxide radical anion and hydroperoxide anion are also generated by CHP reactions. To elucidate the reactive oxygen species responsible for TCA and DCA DNAPL destruction, a series of DNAPL treatments was conducted in systems that generate only one reactive oxygen species.

DNAPL destruction by hydroxyl radical.
      The treatment of a TCA DNAPL and a DCA DNAPL in a Fenton's system designed to generate only hydroxyl radical are presented in Figure 8.4.3-2a–b. In this system (dilute hydrogen peroxide and iron (II) added gradually over 24 hr, for a total of 10 mmol added of each), the total TCA DNAPL mass lost was 20% with a net destruction of 15% over 24 hr (Figure 8.4.3-2a). The mass of the TCA DNAPL lost in the control system over the same time period was less than 4%. The total DCA DNAPL mass lost was 50% with a net destruction of 42% over 24 hr (Figure 8.4.2-3b), with 4% of the DCA DNAPL lost in the control. The net destruction of the TCA DNAPL was 5 times slower in the hydroxyl radical generating system (Figure 8.4.3-2a) than in the CHP reaction (Figure 8.4.3-1a) despite the consumption of similar quantities of hydrogen peroxide, suggesting that hydroxyl radical is not likely the radical species responsible for the majority of TCA DNAPL destruction in the CHP reaction. The 15% of the TCA DNAPL that was destroyed by hydroxyl radical likely reflects the amount of the DNAPL that dissolved into the aqueous phase during the reactions. In contrast, the net destruction of the DCA DNAPL was nearly identical in the two systems, indicating that hydroxyl radical is responsible for the majority of DCA DNAPL destruction. This pathway for the destruction of the

DCA DNAPL is consistent with the relatively high water solubility of DCA and the rapid dissolution of the DCA DNAPL into the aqueous phase.

DNAPL destruction by hydroperoxide.

When a TCA DNAPL and a DCA DNAPL were treated in a system containing only hydroperoxide anion, no measurable loss of either TCA or DCA was found in the controls or the experimental reactions (data not shown). These results demonstrate that hydroperoxide is not the reactive species responsible for the destruction of TCA and DCA DNAPLs by CHP systems. In addition to reacting as a nucleophile, hydroperoxide recombines with a proton to form hydrogen peroxide. This reaction, which proceeds at $\sim 10^{10}$ M^{-1} s^{-1}, would also limit the reactivity of hydroperoxide in CHP systems.

DNAPL destruction by superoxide.

To investigate the role of superoxide in TCA and DCA DNAPL destruction, a CHP system was modified to generate only superoxide (Smith et al., 2004). The destruction of a TCA DNAPL and a DCA DNAPL by a hydroxyl radical-scavenged CHP system (1 M hydrogen peroxide, 5 mM Fe-EDTA chelate, and 3 M ethanol at pH 9–9.5) is shown in Figure 8.4.3-3a–b. The total TCA DNAPL mass lost was >99% after 24 hr with a net destruction of 70% (Figure 8.4.3-3a), while less than 1% was lost in the control. The total DCA DNAPL mass lost was 74% after 24 hr with a net destruction of 42% (Figure 8.4.3-3b), with 1% lost in the control. The data of Figs. 8.4.2-1 and 8.4.2-3 show that TCA and DCA DNAPLs are destroyed in both CHP systems and superoxide systems, indicating that superoxide plays a significant role in their destruction. Furthermore, the net destruction of both DNAPLs in the superoxide system was similar to that in the CHP system. As in the CHP system, the TCA DNAPL was destroyed at a rate greater than natural dissolution, and the DCA DNAPL was destroyed at rates less than its maximum dissolution rate. The results from the reactions in which only hydroxyl radical (Figure 8.4.3-2) and only hydroperoxide (Figure 8.4.3-3) were generated demonstrate that superoxide is the primary reactive oxygen species in CHP systems responsible for TCA DNAPL destruction, and that the combined effects of superoxide and hydroxyl radical are responsible for destruction of the DCA DNAPL. These results are analogous to those found by Smith et al. (2006) in the destruction of carbon tetrachloride and chloroform DNAPLs by CHP. Carbon tetrachloride destruction was mediated solely by superoxide, and chloroform was destroyed by both hydroxyl radical and superoxide.

To further evaluate the destruction of the DNAPLs by CHP, the relative rates of DNAPL dissolution and DNAPL destruction were compared by fitting the data of Figures 8.4.3-1–3 to first order kinetics; these values are listed in Table 8.4.3-1. The k_{obs} values for the net destruction of the TCA DNAPL by CHP and by superoxide were both 5.2×10^{-2} hr^{-1}, which was 3.5 times greater than the corresponding rate of gas-purge dissolution of the DNAPL and 10 times greater than the rate of destruction by hydroxyl radical. These results are similar to those of Yeh et al. (2003), who found that a TCE DNAPL was destroyed by CHP at a rate greater than the rate of TCE dissolution. Similar results were obtained by Smith et al. (2006), who found that a carbon tetrachloride DNAPL was destroyed at a rate significantly greater than its rate of gas-purge dissolution. The destruction of TCA by CHP reactions and superoxide-generating reactions at a rate significantly greater than gas-purge dissolution suggests that superoxide has the potential to overcome mass transfer limitations, possibly by disruption of the DNAPL boundary layer or by diffusion of superoxide into the DNAPL. Superoxide reactivity is increased

in aprotic solvents (Robert and Sawyer, 1981); if it diffuses into the DNAPL is reactivity may be increased by the compounds in the DNAPL even as it destroys those compounds.

The dynamics of destruction of the DCA DNAPL are different from those of the TCA DNAPL. The k_{obs} values for the net destruction of the DCA DNAPL in CHP, hydroxyl radical, and superoxide reactions were 2.7×10^{-2} hr^{-1}, 2.1×10^{-2} hr^{-1}, and 2.5×10^{-2} hr^{-1}, respectively. These rates are similar and were 4–5 times slower than the k_{obs} for its maximum dissolution rate in gas purge systems. Because DCA is more soluble in water than TCA and has a greater rate of reactivity with hydroxyl radical, the DCA DNAPL was likely lost in part by dissolution followed by hydroxyl radical-mediated destruction in the aqueous phase, and in part by superoxide-mediated DNAPL disruption. The results shown in Figures 8.4.3-1–3 demonstrate that process conditions for the destruction of TCA DNAPLs and DCA DNAPLs are quite different; destruction of a TCA DNAPL requires only superoxide while DCA DNAPL destruction is promoted by reactions with both hydroxyl radical and superoxide.

Mixed TCA-DCA DNAPL destruction by CHP.
DNAPLs found at contaminated sites are often composed of several different contaminants. DNAPLs consisting of individual compounds, such as DCA or TCA, each have very different destruction dynamics by CHP (Figures 8.4.3-1–3). Destruction of mixed DNAPLs by CHP is shown in Figures 8.4.3-4. The destruction of 5 mmol TCA and 5 mmol DCA in a single mixed DNAPL by CHP is presented in Figure 8.4.3-4a–b. The total mass of TCA and DCA in the mixed DNAPL decreased by >99% and 95%, respectively, with 82% and 81% of the TCA and DCA destroyed, and the difference lost through volatilization. The TCA and DCA masses dissolved into the aqueous phase in gas purge was were >99% and 68%, respectively; in control experiments, TCA loss was not observed and 10% of the DCA was lost. Despite different rates of dissolution, TCA and DCA masses decreased in the mixed DNAPL by CHP at near-equal rates.

The data of Figure 8.4.3-4 were fit to first order kinetics (Table 8.4.3-1). The mixed TCA-DCA DNAPL demonstrated different destruction dynamics in the presence of CHP than DNAPLs consisting entirely of TCA or DCA. In the gas purge reactors, TCA in the mixed DNAPL was lost at a rate 50% greater than in the pure TCA DNAPL, while DCA in the mixed DNAPL was lost at a rate nearly identical to that of the pure DCA DNAPL. The net destruction rate of TCA by CHP in the mixed DNAPL was 40% lower than in the pure TCA DNAPL, while the net destruction rate of DCA from the mixed DNAPL was 30% higher than in the pure DCA DNAPL. The comparison of net destruction rates between TCA and DCA in a mixed DNAPL and pure DNAPLs suggests that the destruction dynamics of TCA and DCA in a mixed DNAPL are different than in a single compound DNAPL.

The rates of the dual compound DNAPL treatments shown in Figure 8.4.3-4 demonstrate that the DNAPL destruction rates are controlled by a mechanism other than the rate of superoxide attack on the two compounds. A likely mechanism controlling the destruction rate of the two compounds in the mixed DNAPL is the rate of superoxide diffusion. The reaction rates of many short-lived species in liquids are controlled by their rates of diffusion. For example, hydroxyl radical reaction rates are diffusion controlled in water, with its reactivity with most organic compounds grouped in a cluster (e.g. 10^9–10^{10} M^{-1} s^{-1}). However, hydroxyl radical reaction rates in air, which are not diffusion controlled, are controlled more by reactivity of

139

hydroxyl radical with the specific compound than by its diffusion in air. The phenomenon of near-equal reaction rates of superoxide with TCA and DCA in a mixed DNAPL suggests that the rates of destruction for both compounds in completely limited by the rate of superoxide diffusion. Differences in DCA and TCA reaction rates are not observed in the aqueous phase; therefore, the diffusion controlled reaction rate is not likely occurring in the aqueous phase. The results suggest that the diffusion controlled mechanism occurs at the DNAPL double layer or within the DNAPL itself.

Reductive degradation pathway.

The traditional mechanism of contaminant destruction by CHP is via hydroxyl radical, a powerful oxidant. However, recent results (Watts et al., 1999; Smith et al., 2004; Smith et al., 2006 (chloromethane paper)) and the data shown in Figures 8.4.3-1–3 are consistent with a superoxide mechanism for contaminant destruction in CHP systems. In order to investigate the transformation pathways for TCA and DCA DNAPLs by CHP reactions, off gas trapped in ORBO tubes from TCA and DCA DNAPL reactors was analyzed by GC-MS to identify degradation products. The products of TCA DNAPL destruction were identified as 1,1-dichloroethene, 1,1-dichloroethane, chloroethene and chloroethyne, all with matching scores >93. The sole product found for DCA DNAPL destruction was identified as chloroethene, with a matching score of 97. The products identified are more reduced than TCA and DCA, and are consistent with the transformation of TCA and DCA under reducing conditions in both biotic and abiotic systems (Castro and Kray, 1966; Vogel et al, 1987; Fennelly and Roberts, 1998; Cervini-Silva et al, 2003) and with the reductive pathway in CHP systems described by Smith et al. (2004) and Smith et al. (2006). Proposed degradation pathways for TCA and DCA are shown in Figure 8.4.3-5. The pathways involve dehydrochlorination steps, which result in no net change in the oxidation state of compounds, and hydrogenolysis steps, which reduce the compounds via a two-electron transfer promoted by the reduction of superoxide.

Stroo et al. (2003) recently reviewed and summarized DNAPL destruction technologies, and they recommended bioremediation and permanganate as the most promising processes for DNAPL destruction at ambient temperatures. Although DNAPL losses do occur during treatment with permanganate and bioremediation, the time requirements may be significantly greater than with CHP. For example, 120 days were required to destroy a PCE DNAPL using permanganate (Schnarr et al., 1998). The slow DNAPL dissolution rates found in aquifers have been increased through bioremediation (Yang and McCarty, 2002) and by flushing the DNAPL with clean water (Rivett et al., 2001); however, the increased dissolution noted in these studies results from a deficit induced in the concentration in the aqueous phase resulting in an increased concentration gradient, and does not exceed the maximum gas-purge dissolution rate. In contrast, carbon tetrachloride DNAPLs are destroyed by superoxide in CHP reactions at a rate significantly greater than such increased dissolution, which is probably related to the mass transfer of superoxide into the DNAPL and its resulting increased reactivity; this rapid treatment may be classified as enhanced destruction. The results of this research demonstrate that CHP has the potential to provide an effective technology for rapidly destroying DNAPLs in the field.

Summary and Conclusions

The destruction of DNAPLs composed of TCA and DCA by CHP was investigated, and rates of DNAPL destruction were compared to rates of DNAPL dissolution. In addition, the reactive oxygen species responsible for destruction of the DNAPLs was elucidated and the

140

degradation products were identified. Both TCA and DCA DNAPLs were effectively destroyed by CHP. TCA DNAPLs were destroyed more rapidly than rates of gas purge dissolution, while the DCA DNAPL destruction rate was nearly equal to its dissolution rate. The reactive oxygen species responsible for TCA dissolution was superoxide, while both hydroxyl radical and superoxide were responsible for destruction of the DCA DNAPL. Degradation products included reduced species, such as dichloroethylenes and vinyl chloride. A DNAPL containing equimolar masses of TCA and DCA was treated with CHP; the two contaminants were destroyed at near-equal rates, suggesting that the rate of treatment was controlled by the rate of superoxide diffusion rather that its reactivity with each of the contaminants. The results of this research demonstrate that TCA and DCA DNAPLs are effectively destroyed by CHP, and that the most effective treatment conditions, which are dictated by the reactive oxygen species required, is contaminant specific.

Table 8.4.3-1. First Order Rate of Transformation of 1,1,1-Trichloroethane and 1,2-Dichloroethane DNAPL and Total Degradation (h^{-1})

System	1,1,1-TCA		1,2-DCA	
	DNAPL (R^2)	Total (R^2)	DNAPL (R^2)	Total (R^2)
Gas Purge	0.0146 (0.993)		0.113 (0.997)	
CHP	0.079 (0.990)	0.052 (0.993)	0.051 (0.967)	0.0271 (0.971)
Hydroxyl Radical	0.0078 (0.831)	0.0055 (0.804)	0.0254 (0.949)	0.021 (0.957)
Fe:EDTA	0.151 (0.960)	0.052 (0.804)	0.056 (0.974)	0.0246 (0.979)
MFR pH 4.8	0.033 (0.888)	0.02 (0.941)	0.0084 (0.961)	0.0034 (0.837)
MFR pH 6.8	0.184 (0.930)	0.041 (0.926)	0.0493 (0.953)	0.0241 (0.963)
Mixed DNAPL				
Gas Purge	0.0226 (0.976)		0.118 (0.993)	
CHP	0.0625 (0.859)	0.0381 (0.952)	0.0553 (0.935)	0.034 (0.943)
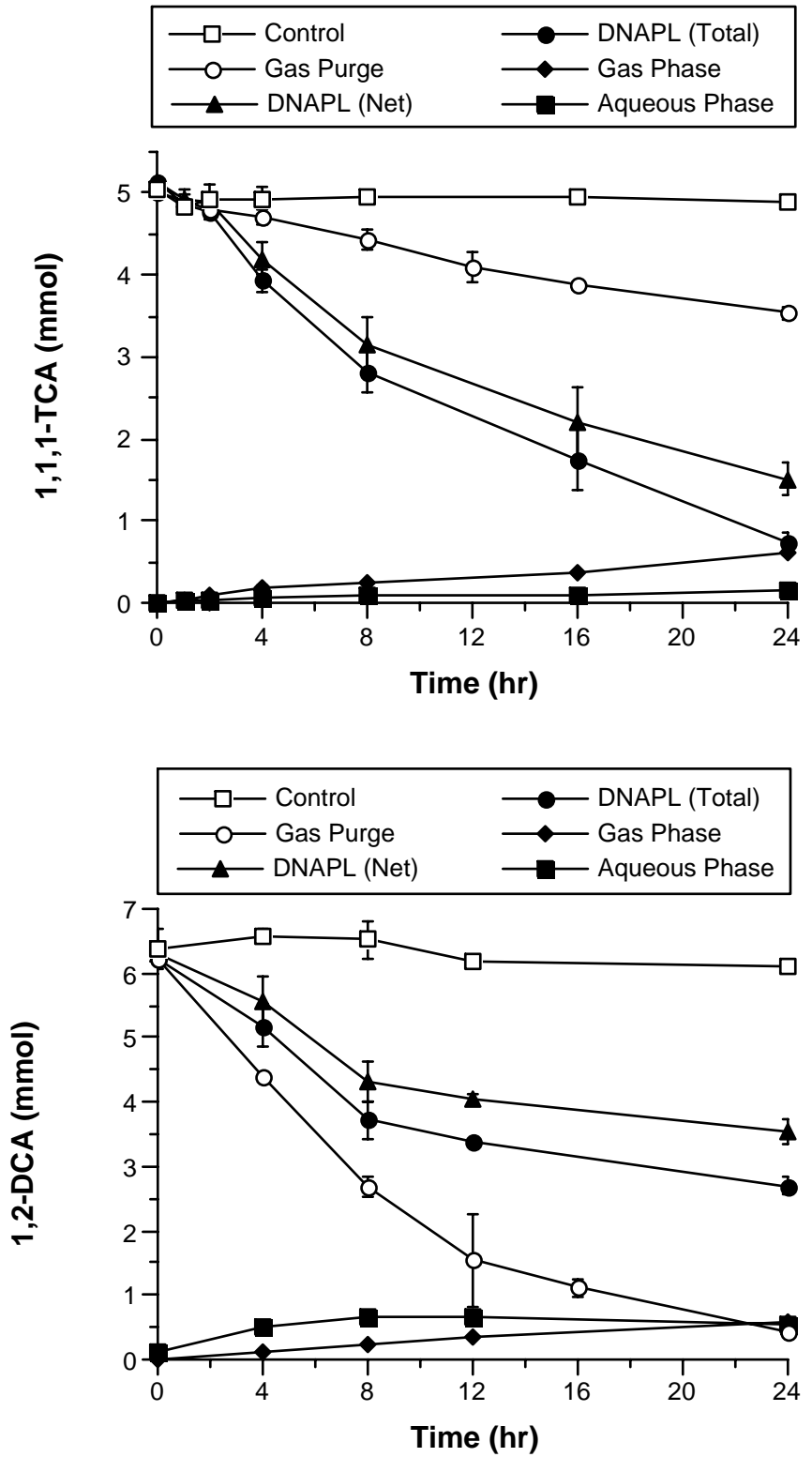
Figure 8.4.3-1. Degradation of 1,1,1-TCA (a) and 1,2-DCA (b) by CHP with 10 mM Fe (III):Citrate and 2 M Hydrogen Peroxide at pH 2.8
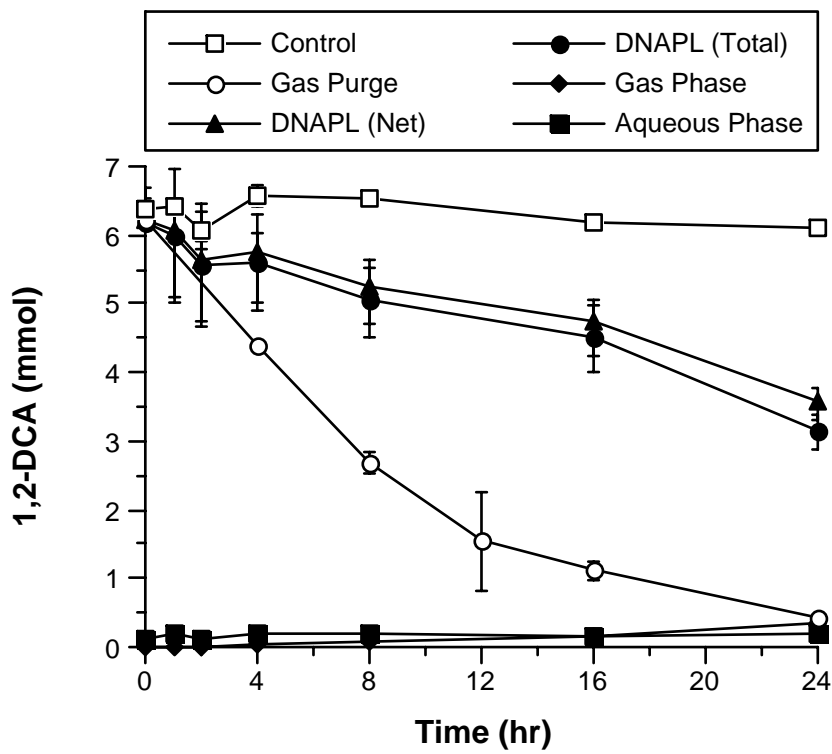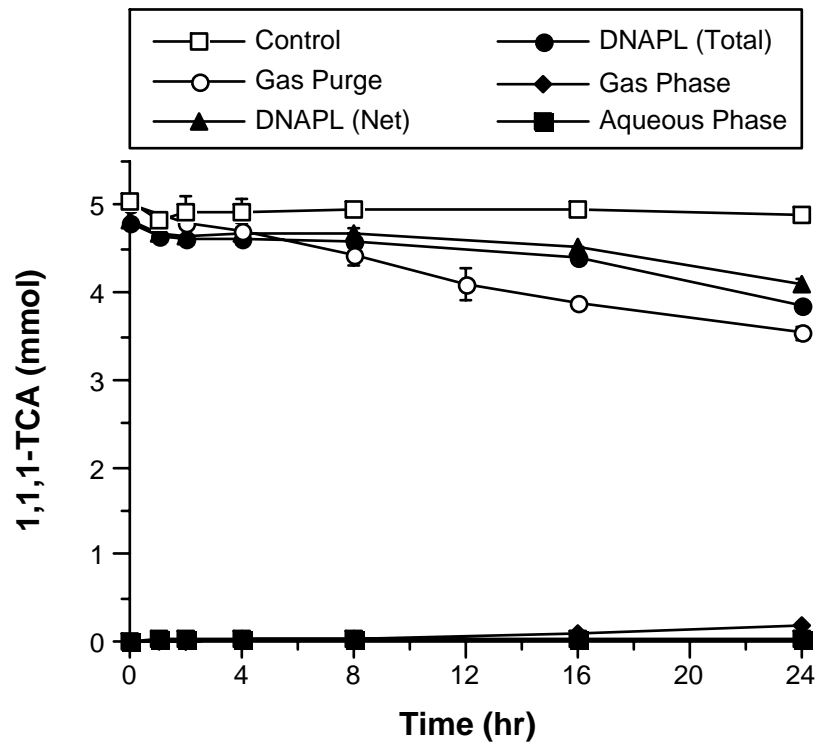
Figure 8.4.3-2. Degradation of 1,1,1-TCA (a) and 1,2-DCA (b) in Hydroxyl Radical System
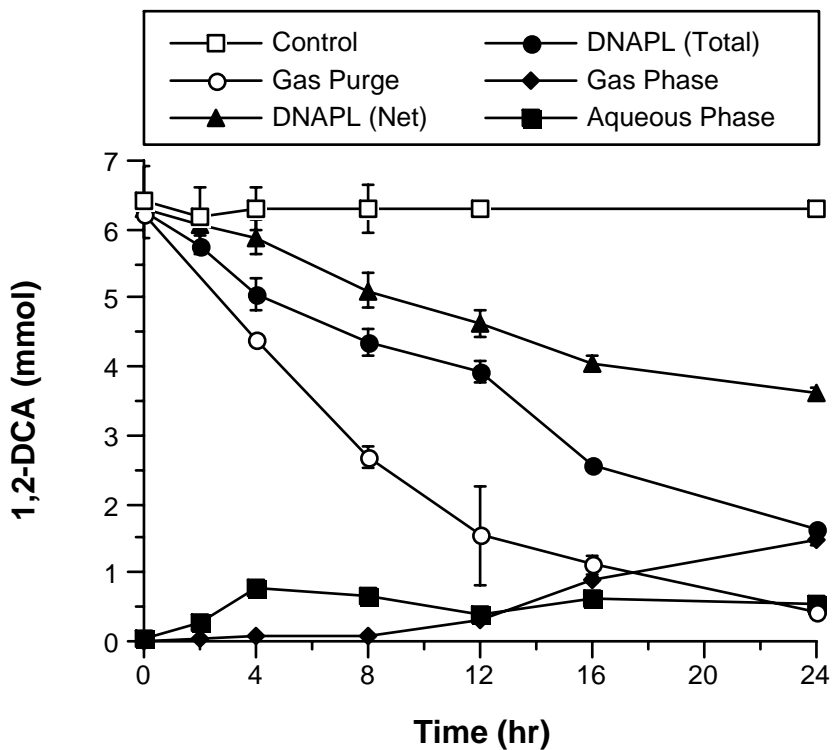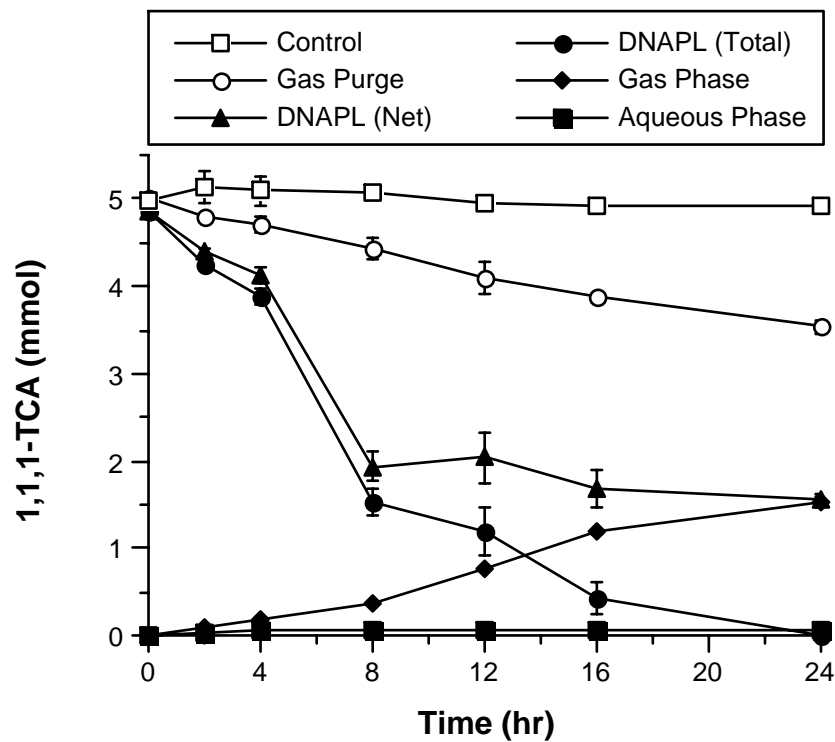
Figure 8.4.3-3. Degradation of 1,1,1-TCA (a) and 1,2-DCA (b) in Superoxide Generating System with 3 mM Fe:EDTA and 1 M Hydrogen Peroxide at pH 9.0-9.5
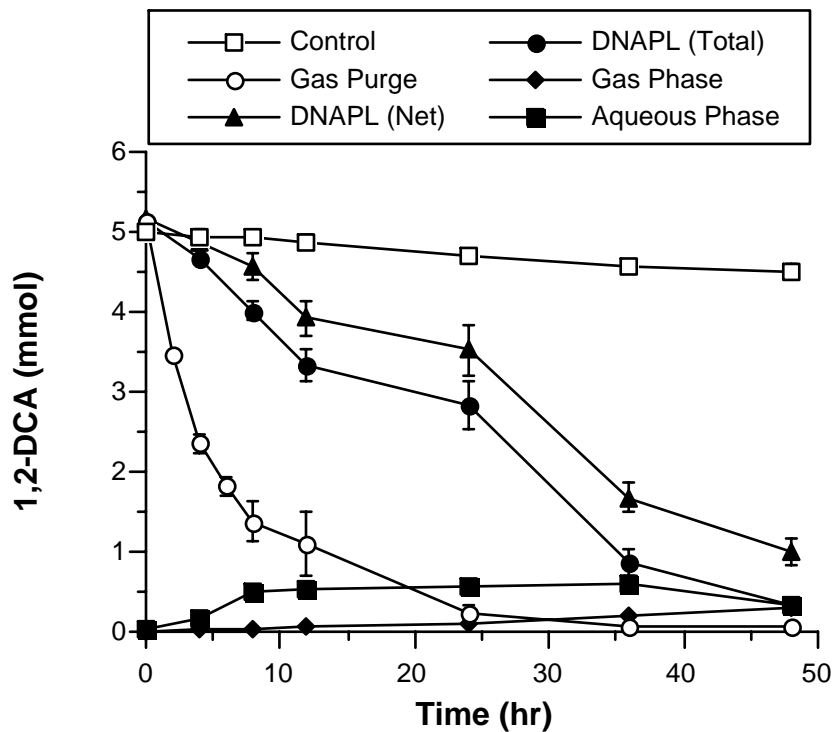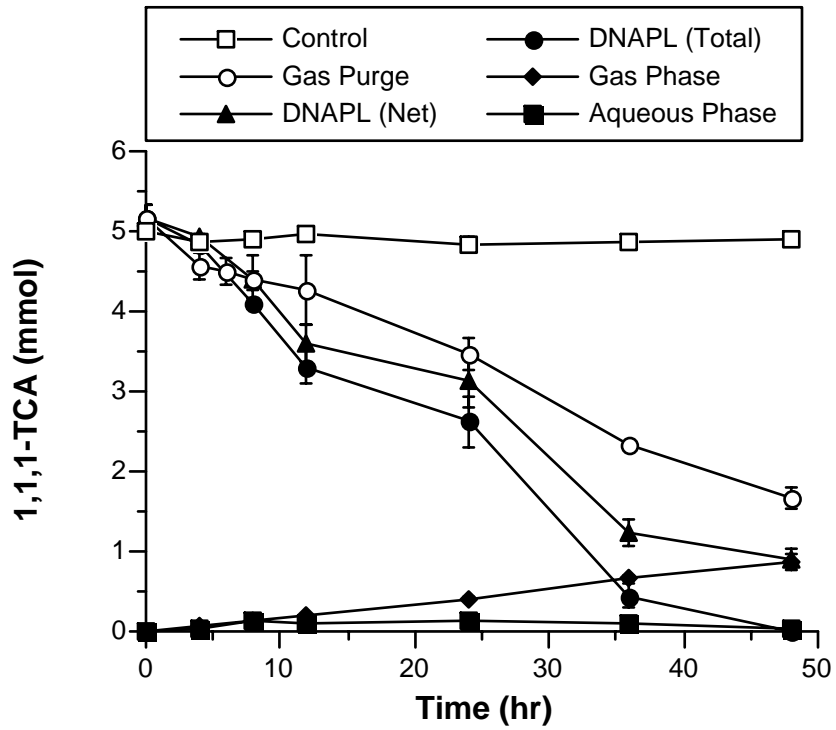
Figure 8.4.3-4. Degradation of Mixed DNAPL containing 1,1,1-TCA (a) and 1,2-DCA (b) by CHP with 10 mM Fe(III):Citrate and 2 M Hydrogen Peroxide at pH 2.8

TCA Non-Oxidative Decomposition Pathway

H$^+$ + Cl$^-$ 2e$^-$ + H$^+$ Cl$^-$

H$_3$C-CCl$_3$

2e$^-$ + H$^+$

H$_2$C=CCl$_2$ H$_3$C-CHCl$_2$

Cl$^-$ H$^+$ + Cl$^-$

H$_2$C=CHCl

H$^+$ + Cl$^-$

HC≡CCl

Legend

Dehydrochlorination ⟶

Hydrogenolysis ⟶

DCA Non-Oxidative Decomposition Pathway

H$^+$ + Cl$^-$

ClH$_2$C-CH$_2$Cl ⟶ H$_2$C=CHCl
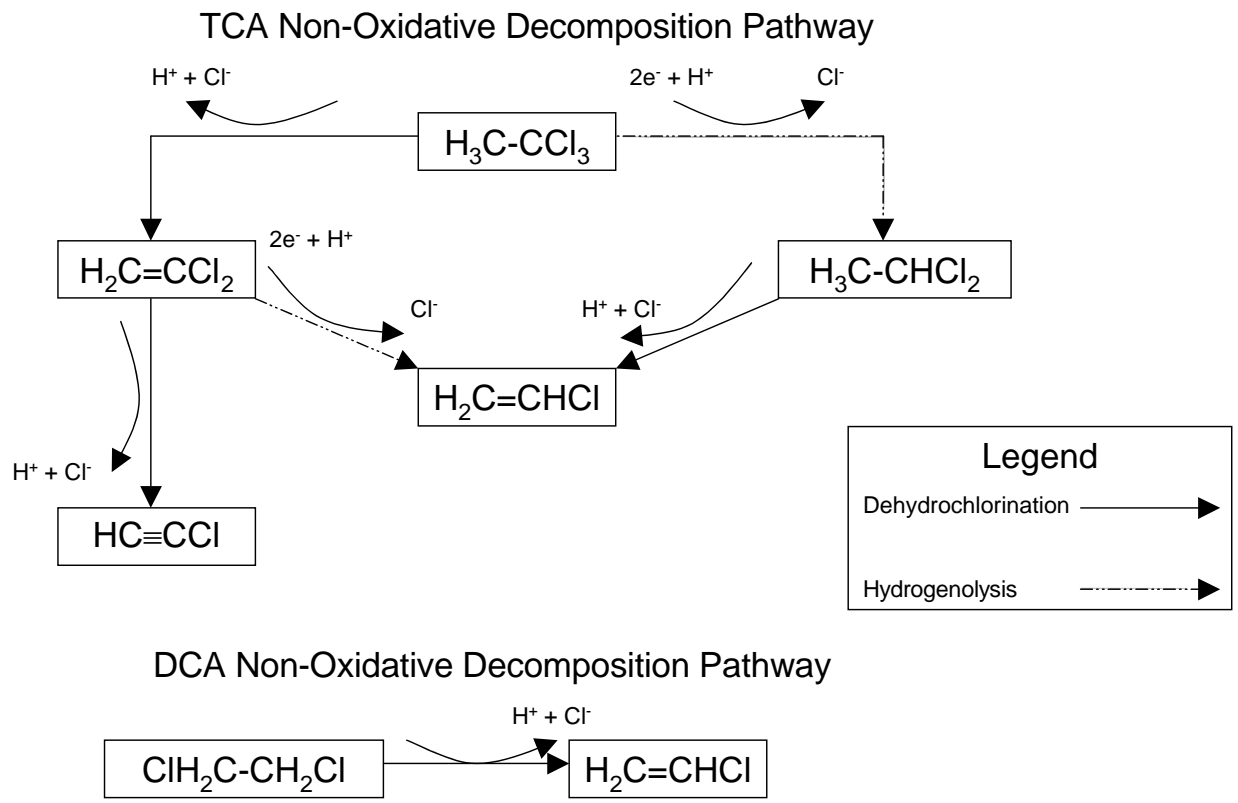
Figure 8.4.3-5. Proposed pathways for TCA and DCA decomposition

8.4.4 Destruction of Trichloroethylene and Perchloroethylene DNAPLs by CHP

TCE and PCE DNAPL destruction by CHP.
　　　　The destruction of a TCE DNAPL and a PCE DNAPL by CHP is shown in Figure 8.4.4-1a–b. The total mass lost from the TCE DNAPL was 82.0% and from the PCE DNAPL was 49.5% over 96 hr. After subtracting the masses of TCE and PCE captured in the ORBO tubes and dissolved in the aqueous phase, the net destruction of the TCE DNAPL was 75.0% and the net destruction of the PCE DNAPL was 47.4%. In parallel gas purge reactors, 78.6% of the TCE DNAPL mass and 20.8% of the PCE DNAPL mass were lost through dissolution over the same time period. The mass lost from TCE and PCE DNAPLs in control reactors containing deionized water in place of hydrogen peroxide was 0% and 2.1%, respectively. These results demonstrate that TCE and PCE DNAPLs are rapidly destroyed by CHP, and that PCE DNAPLs are destroyed at a rate significantly greater than their maximum rate of dissolution.

　　　　Oxidation by hydroxyl radical is the mechanism usually associated with contaminant degradation in CHP systems; however, the reactive oxygen species superoxide radical anion and hydroperoxide anion are also generated by CHP reactions. Hydroxyl radical reacts at near diffusion-controlled rates with TCE ($k_{OH\bullet}$ = 4.0 × 10^9 M^{-1} s^{-1}; Buxton et al., 1988) and PCE ($k_{OH\bullet}$ = 2.8 × 10^9 M^{-1} s^{-1}; Buxton et al., 1988). However, hydroxyl radical is not likely to react directly with pools of DNAPLs because of its short-lived nature and corresponding inability to cross phase boundaries (Sheldon and Kochi, 1981).   To elucidate the reactive oxygen species responsible for TCE and PCE DNAPL destruction, a series of DNAPL treatments was conducted in systems in which only one oxygen species was generated.

DNAPL destruction by hydroxyl radical.
　　　　The treatment of a TCE DNAPL and a PCE DNAPL in a Fenton's system designed to generate only hydroxyl radical are shown in Figure 8.4.4-2a–b. In this system, the total TCE DNAPL mass lost was 17.9% with a net destruction of 10.7% over 48 hr. The mass of TCE DNAPL lost in the control system over the same time period was 5.3%; therefore, only a small portion of the destruction of the TCE DNAPL observed in Figure 8.4.4-2 was due to reactions with hydroxyl radical. The total PCE DNAPL mass lost in the hydroxyl radical system was 9.1%; after subtracting the mass of PCE captured in the ORBO tubes and dissolved in the aqueous phase, the net destruction of the PCE DNAPL was 7.9%, while 5.1% of the PCE DNAPL mass was lost in the control reactors. The mass of TCE and PCE oxidized by hydroxyl radical was significantly less than the total TCE and PCE destroyed by CHP; these data suggest that hydroxyl radical oxidation accounted for only a small portion of the destruction of the TCE and PCE DNAPLs and that a large proportion of the TCE and PCE DNAPL destruction in CHP reactions was promoted by a reactive species other than hydroxyl radical.

DNAPL destruction by hydroperoxide.
　　　　The treatment of a TCE DNAPL and a PCE DNAPL in a system containing only hydroperoxide anion showed that no measurable loss of either TCE or PCE was found in the controls or the experimental reactions (data not shown). These results demonstrate that hydroperoxide is not the reactive species responsible for the destruction of TCE and PCE DNAPLs by CHP systems. Although hydroperoxide is a strong nucleophile that readily attacks carbonyl groups and other electron-deficient carbon atoms (David and Seiber, 1999) it was not reactive with the TCE DNAPL or the PCE DNAPL over the time evaluated. In addition to

reacting as a nucleophile, hydroperoxide recombines with a proton to form hydrogen peroxide. This reaction, which proceeds at ~10^{10} M^{-1} s^{-1}, would also limit the reactivity of hydroperoxide in CHP systems.

DNAPL destruction by superoxide.

Two systems were used to evaluate the reactivity of superoxide with TCE and PCE DNAPLs. The destruction of a TCE DNAPL and a PCE DNAPL by a hydroxyl radical-scavenged CHP system (1 M hydrogen peroxide, 5 mM Fe-EDTA chelate, and 3 M ethanol at pH 9–9.5) is shown in Figure 8.4.4-3a–b. The total TCE DNAPL mass lost was 84.9% and the total PCE DNAPL mass lost was 26.3% over 48 hr. After subtracting the masses of TCE and PCE captured in the ORBO tubes and dissolved into the aqueous phase, the net destruction of the TCE DNAPL was 62.6% and the net destruction of the PCE DNAPL was 20.0%. Approximately 46.4% of the TCE DNAPL and 10.8% of the PCE DNAPL masses were lost through dissolution in gas purge reactors over 48 hr. The mass lost from TCE and PCE DNAPLs in control reactors containing deionized water in place of hydrogen peroxide was 7.0% and 3.2%, respectively.

Superoxide was also generated using a 2 M potassium superoxide system containing 1 M of a cosolvent (acetone or hydroperoxide) to increase the reactivity of superoxide (Smith et al., 2004). The destruction of a TCE DNAPL and a PCE DNAPL in the presence of 2 M potassium superoxide and 1 M acetone is shown in Figure 8.4.4-4a–b; the total masses lost over 24 hr were 70.5% from the TCE DNAPL and 21.5% from the PCE DNAPL. After subtracting the masses of TCE and PCE captured in the ORBO tubes and dissolved into the aqueous phase, the net destruction of the TCE DNAPL was 57.1% and the net destruction of the PCE DNAPL was 19.4%. The DNAPL masses lost in parallel gas purge reactors were 28.6% for TCE and 7.3% for PCE. The destruction of a TCE DNAPL and a PCE DNAPL in the presence of 2 M potassium superoxide and 1 M hydroperoxide is shown in Figure 8.4.4-5a–b; the total masses lost over 24 hr were 56.6% from the TCE DNAPL and 25.9% from the PCE DNAPL, while net destruction of the TCE DNAPL was 45.9% and net destruction of the PCE DNAPL was 24.2%. In parallel gas purge reactors, 29.2% of the TCE DNAPL and 6.5% of the PCE DNAPL masses were lost over 24 hr. There was no measurable loss of TCE or PCE DNAPLs in control reactors for either of the potassium superoxide–cosolvent systems.

The results of the CHP reactions and reactions with individual reactive oxygen species are summarized in Table 8.4.4-1.

The data of Figures 8.4.4-1 and 8.4.4-3–5 show that TCE and PCE DNAPLs are destroyed in both CHP systems and superoxide systems, indicating that superoxide plays a significant role in the destruction of the DNAPLs. The results from the reactions in which only hydroxyl radical (Figure 8.4.4-3) was generated suggest that TCE and PCE are oxidized by hydroxyl radical in the aqueous phase after TCE and PCE have dissolved from the DNAPL. This concept is in agreement with the known behavior of hydroxyl radical; i.e., it is an extremely short lived species that does not diffuse and does not cross phase boundaries (Sheldon and Kochi, 1981). The k_{obs} values for TCE DNAPL destruction in the superoxide generating systems were 3.3–4.4 times greater than the gas purge dissolution rate. The destruction of TCE in superoxide-generating reactions at rates significantly greater than gas-purge dissolution suggests that superoxide has the potential to overcome mass transfer limitations, possibly by disruption of

the DNAPL boundary layer or by diffusion of superoxide into the DNAPL. Potassium superoxide is highly soluble in organic solvents and is often added to aprotic solvents, such as toluene and acetonitrile, in the presence of a crown ether to bind the potassium (Afanas'ev, 1989). When dissolved in such aprotic solvents, superoxide reacts rapidly with TCE and other halogenated compounds (Robert and Sawyer, 1981). The high reactivity of superoxide with TCE in aprotic solvents may be the basis for the enhanced destruction of TCE DNAPLs treated with CHP.

The dynamics of destruction of the PCE DNAPL are different from those of the TCE DNAPL. Over 96 hr, the net destruction of the PCE DNAPL in CHP reactions was 47%, which is less than the 20.8% loss of PCE by its maximum dissolution rate in gas purge reactors. The masses of PCE destroyed in the superoxide generating systems were also greater than in the gas purge systems. PCE is less soluble in water than TCE, and is characterized by a slower rate of dissolution. Based on the results of Figures 8.4.4-2b, 8.4.4-4b, 8.4.4-5b, and 8.4.4-6b, the PCE DNAPL was likely destroyed in CHP systems in part by dissolution followed by hydroxyl radical-mediated destruction in the aqueous phase, and in part by superoxide-mediated DNAPL disruption and destruction. The results shown in Figures 8.4.4-1–5 demonstrate that process conditions for the destruction of TCE DNAPLs and PCE DNAPLs are quite different; destruction of a TCE DNAPL requires only hydroxyl radical while PCE DNAPL destruction is likely promoted by reactions with both hydroxyl radical and superoxide.

The relative rates of TCE and PCE destruction were not consistent between CHP systems and the systems that generate superoxide (Fe-EDTA and potassium superoxide with cosolvents). These differences in relative rates may be due to the varying proportions of superoxide and its conjugate acid, perhydroxyl radical, that were present at the different pH regimes of the three systems; the CHP reactions were conducted at pH 3, the Fe-EDTA-hydrogen peroxide reactions were conducted at pH 9–9.5, and the potassium superoxide reactions were conducted at pH 14. Perhydroxyl radical is a weak oxidant, and is likely not involved in DNAPL destruction. Therefore, the differing proportions of superoxide and perhydroxyl radical in the CHP systems relative to the superoxide systems likely provided substantially higher TCE and PCE DNAPL destruction rates in the superoxide systems.

Summary and Conclusions

The destruction of TCE and PCE DNAPLs by CHP was investigated, and the reactive oxygen species responsible for their destruction was evaluated using systems that generate only 1) hydroxyl radical, 2) hydroperoxide, and 3) superoxide. Although hydroxyl radical oxidation is likely involved in CHP reactions when TCE and PCE DNAPLs dissolve into the aqueous phase, superoxide is also responsible for their destruction, particularly for PCE, with a rate of DNAPL destruction that exceeds its maximum rate of dissolution. Because of the rapid rates at which TCE and PCE DNAPLs are destroyed, CHP may provide an effective process for the in situ destruction of DNAPLs.

The results of Section 8.4 demonstrate that DNAPLs are effectively destroyed by CHP, often at rates more rapid than their rates of dissolution. In addition, attack by at least two reactive oxygen species provides multiple pathways of destruction. Future field applications of CHP ISCO will be able to rely on knowledge of potential oxidative and reductive pathways for the most efficient process conditions for DNAPL destruction.

Table 8.4.4-1. Percent destruction of TCE and PCE DNAPLs in five experimental systems.

Experimental System	Reaction Time	Percent Destruction			
		DNAPL (Total)	DNAPL (Net)	Gas Purge	Control
CHP	96 hr				
TCE		82.0	75.0	78.6	0
PCE		49.5	47.4	20.8	2.1
Hydroxyl Radical	48 hr				
TCE		17.9	10.7	46.4	5.3
PCE		9.1	7.9	10.8	5.1
Superoxide (EDTA System)	48 hr				
TCE		84.9	62.6	46.4	7.0
PCE		26.3	20.0	10.8	3.2
Superoxide (KO_2–Acetone)	24 hr				
TCE		70.5	57.1	28.6	0
PCE		21.5	19.4	7.3	0
Superoxide (KO_2–$HO_2\bullet^-$)	24 hr				
TCE		56.6	45.9	29.2	0
PCE		25.9	24.2	6.5	0
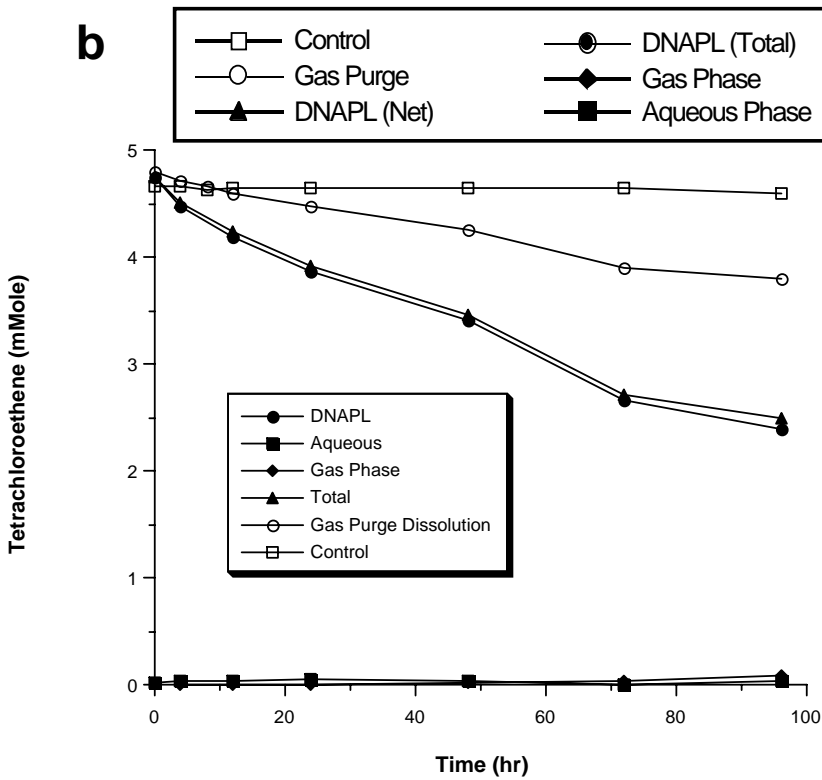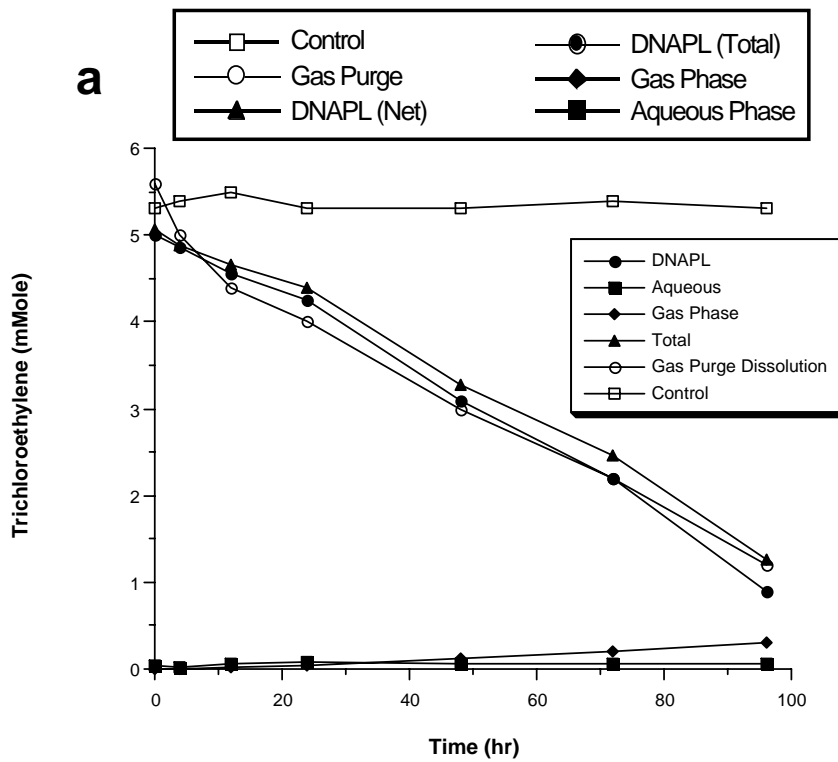
Figure 8.4.4-1. Destruction of (a) TCE and (b) PCE DNAPLs by CHP (5 mM iron (III):HKCH chelate and 2 M hydrogen peroxide at pH 3).

151
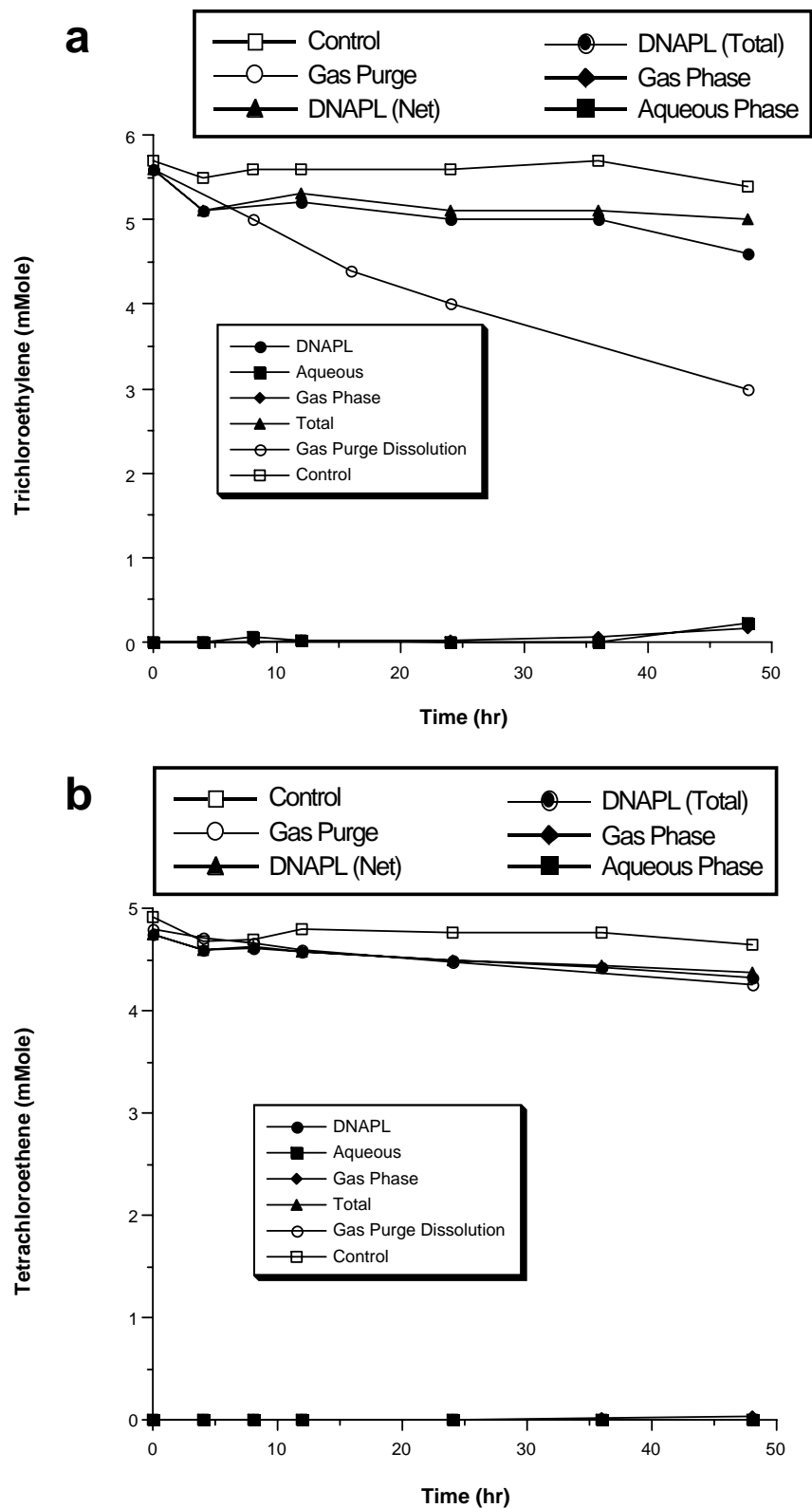
Figure 8.4.4-2. Destruction of (a) TCE and (b) PCE DNAPLs by hydroxyl radical in standard Fenton's reagent (twenty-four 0.21 mL additions of 1 M hydrogen peroxide and 1 M iron (II)-citrate at pH 1.8 over 48 hr to 7 mL water and 0.5 mL of DNAPL).
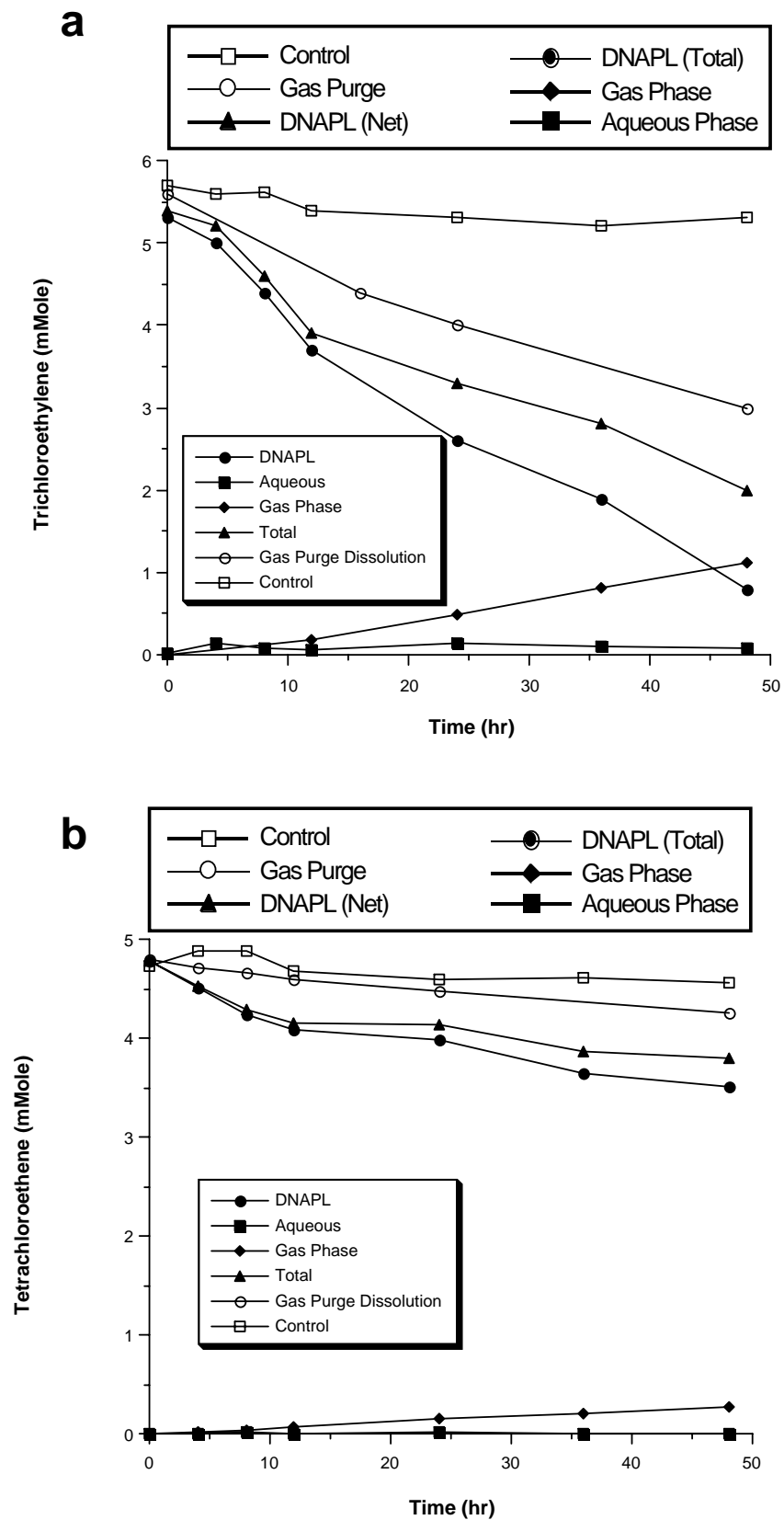
Figure 8.4.4-3. Destruction of (a) TCE and (b) PCE DNAPLs in a soluble iron-based superoxide system (5 mM iron (III):EDTA complex and 1 M hydrogen peroxide at pH 9.0-9.5).
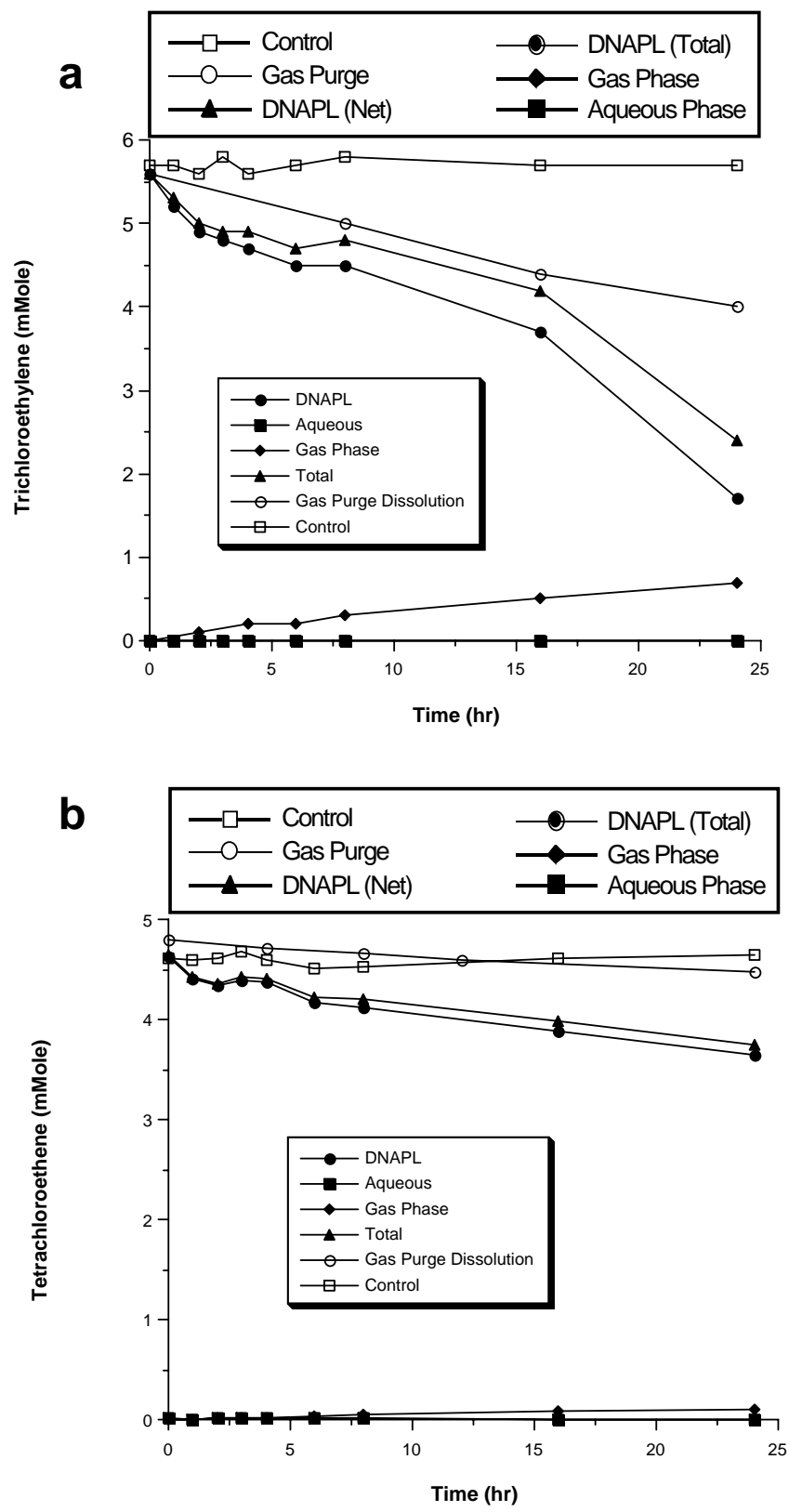
Figure 8.4.4-4. Destruction of (a) TCE and (b) PCE DNAPLs in a potassium superoxide-based superoxide system with the cosolvent acetone (2 M potassium superoxide and 1 M acetone at pH 14.0).

154
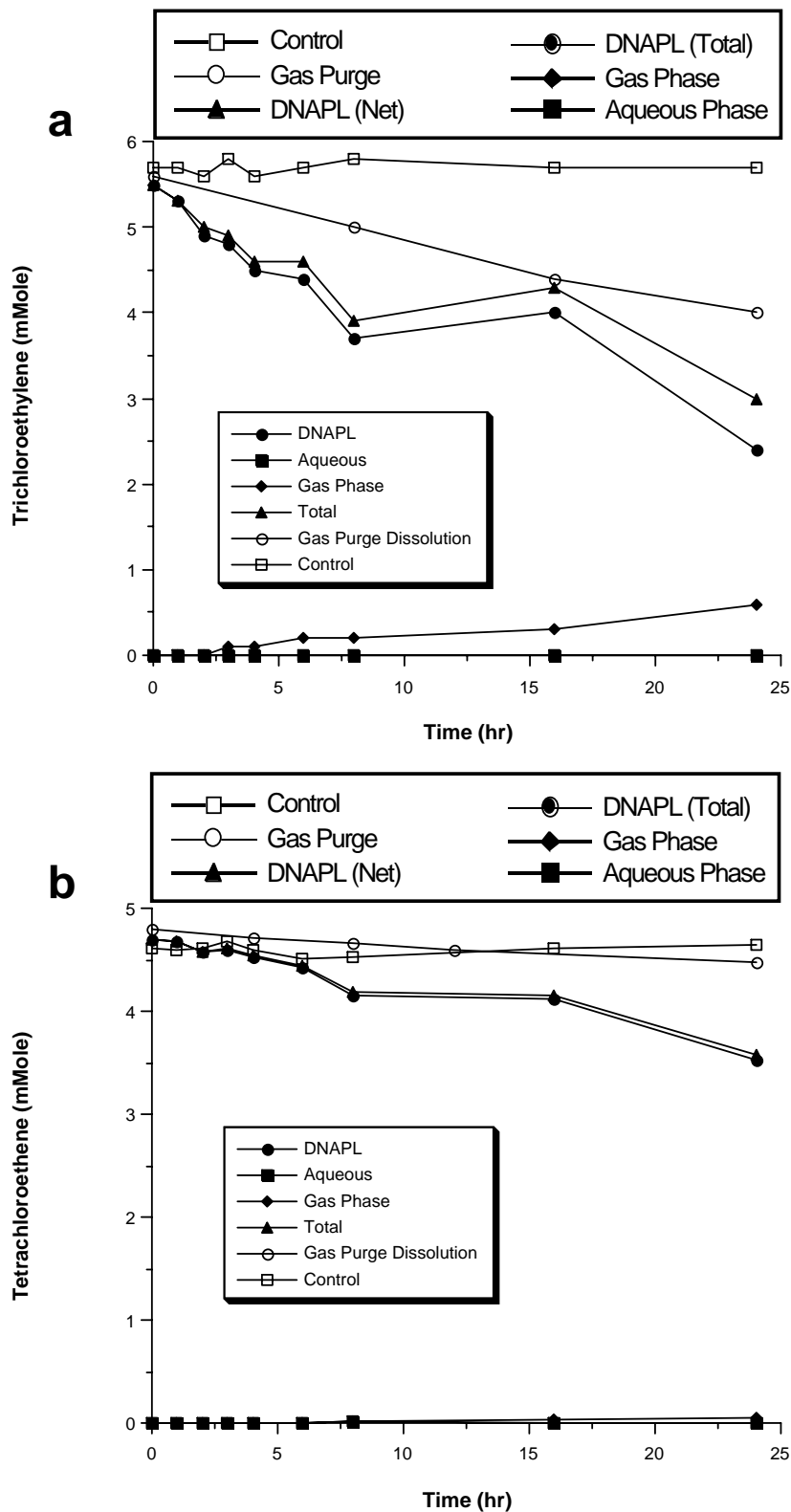
Figure 8.4.4-5. Destruction of (a) TCE and (b) PCE DNAPLs in a potassium superoxide-based superoxide system with the cosolvent hydroperoxide (2 M potassium superoxide and 1 M hydrogen peroxide at pH 14.0).

8.5 Enhanced Destruction of Sorbed Contaminants

Many soil and groundwater contaminants are characterized by high hydrophobicity, with log octanol-water partition coefficients (log K_{ow}s) in the range of 4 to 9. As a result, nearly all of the contaminant is present in the sorbed phase and desorption rates are often negligible. Most soil and groundwater treatment processes are effective only for aqueous phase contaminants because the reactive species (e.g., enzymes, hydroxyl radicals [OH•], solvated electrons) are generated and reactive only in the aqueous phase. Desorption rates of hydrophobic contaminants are often much slower than their transformation rates, and therefore limit their rates of treatment (Ogram et al., 1985; Watts, 1998).

Modifications of Fenton's reagent have been effective in degrading contaminants significantly more rapidly than their corresponding rate of gas-purge or fill-and-draw desorption. For example, Watts et al. (1994) demonstrated that hexachlorobenzene sorbed to silica sand was degraded more rapidly than it was lost by gas-purge desorption. Similar results were documented for trichloroethylene (TCE) (Gates and Siegrist, 1995), A common theme in these studies has been the high hydrogen peroxide concentrations used. Watts et al. (1999) found that in CHP reactions using hydrogen peroxide concentrations > 300 mM, a non-hydroxyl radical species, such as superoxide radical anion ($O_2^{•-}$) or hydroperoxide anion (HO_2^{-}), was generated that was responsible for the rapid degradation of sorbed hexachloroethane and hexachlorocyclopentadiene. The potential to rapidly treat sorbed contaminants has made CHP an important emerging remediation technology.

Effect of hydrophobicity on hydrogen peroxide dose required for desorption. High hydrogen peroxide concentrations in modified Fenton's reactions promote propagation reactions that result in non-hydroxyl radical transient oxygen species, including perhydroxyl radical ($HO_2^{•}$), superoxide radical anion ($O_2^{•-}$), and hydroperoxide anion (HO_2^{-}). Because these non-hydroxyl radical species are produced in greater amounts as the hydrogen peroxide concentration is increased, the degree of treatment of sorbed hydrophobic contaminants in CHP reactions may be a function of the hydrogen peroxide concentration. Based on this hypothesis, one objective of this section of research was to use a suite of probe compounds with equal rates of reaction with hydroxyl radicals to investigate the relationship between contaminant hydrophobicity and hydrogen peroxide dosage in the CHP treatment of contaminated soils.

Reactive oxygen species responsible for desorption. Although the enhanced treatment of sorbed contaminants has been documented in CHP reactions containing > 0.3 M H_2O_2, the species responsible for the enhanced treatment has not yet been identified (Watts and Stanton, 1999). While hydroxyl radical, generated in Fenton's reactions through equation (1), reacts rapidly with most soil and groundwater contaminants in the aqueous phase (Dorfman and Adams, 1973; Buxton et al., 1988; Haag and Yao, 1992), it is not reactive with sorbed contaminants (Sedlak and Andren, 1991). Watts et al. (1999) proposed that the enhanced desorption in CHP reactions is mediated by a reductant or nucleophile such as superoxide radical anion ($O_2^{•-}$) or hydroperoxide anion (HO_2^{-}); however, the reactive species responsible for enhanced desorption in CHP systems had not been identified prior to the completion of this research. Therefore, the other purpose of this segment of the research was to determine the reactive oxygen species responsible for the enhanced desorption of contaminants in CHP systems.

8.5.1 Effect of Contaminant Hydrophobicity on H_2O_2 Dosage Requirements in the CHP Treatment of Soils

Reactivity of hydroxyl radicals with probe compounds

In order to isolate the effect of contaminant hydrophobicity on hydrogen peroxide dosage requirements in the CHP treatment of sorbed compounds, probe compounds must be used that have varying hydrophobicities but equal or near-equal rates of reaction with hydroxyl radicals. The *n*-alcohols 1-hexanol, 1-heptanol, 1-octanol, 1-nonanol, and 1-decanol should have near-equal reactivity with hydroxyl radicals; however, available second-order rate constants for the alcohols were obtained under varying conditions, and could not be compared directly. Therefore, the standard Fenton's reaction was used to verify that the five *n*-alcohols are oxidized at near-equal rates. The oxidation of the probe compounds in a standard Fenton's system is shown in Figure 8.5.1-1; the results of analysis of variance (ANOVA) performed on the slopes of the treatment reactions as well as the control reactions are summarized in Table 8.5.1-1. Based on the ANOVA, no significant difference ($\alpha = 0.05$) was found between rates of oxidation of the five probe compounds by hydroxyl radicals. Therefore, any differences found in hydrogen peroxide requirements for the treatment of sorbed *n*-alcohols may be attributed to hydrophobicity rather than reactivity with hydroxyl radicals.

Evaluation of optimum hydrogen peroxide dosages for probe oxidation

Experiments with two-level central composite rotatable designs were used to determine the hydrogen peroxide and iron requirements for degradation of the five probe compounds. These designs are multivariable, multilevel experimental procedures that are used to produce regression equations describing the interactive effects between variables, which are then illustrated graphically using three-dimensional response Cochran and Cox, 1992). In central composite designs, the range of each variable is chosen to achieve complete rotatability around the central point of a two-level matrix. Using such matrix designs, all of the vertices within the experimental boundaries are tested, and interpolation anywhere within the two-dimensional space is valid (Diamond, 1989). The regression equations developed from the experimental data and their coefficients of correlation (R^2) with the experimental data are listed in Table 8.5.1-2, and the corresponding response surfaces for the oxidation of the five *n*-alcohols are shown in Figures 8.5.1-2–6. The concentric response lines in each of the response surfaces indicate that hydrogen peroxide and iron concentrations both had a significant effect on contaminant treatment. Furthermore, inspection of Figures 8.5.1-2–6 shows that the hydrogen peroxide dosage required for > 99% degradation increased with increasing size and corresponding hydrophobicity of the *n*-alcohol used.

The enhanced treatment of sorbed contaminants by CHP requires high concentrations of hydrogen peroxide relative to those required for aqueous contaminants. Watts et al. (1994) demonstrated that hexachlorobenzene sorbed on silica sand degraded significantly more rapidly than it was desorbed in CHP reactions using ≥ 100 mM hydrogen peroxide. Gates and Siegrist (1995) found enhanced TCE treatment in the vadose zone using CHP with 600 mM hydrogen peroxide. Furthermore, treatment and mineralization of ^{14}C-hexadecane required > 10 M hydrogen peroxide (Watts and Stanton, 1999). These results have suggested that the hydrogen peroxide dosages required for treatment may increase with increasing contaminant

hydrophobicity. The data shown in Figures 8.5.1-2–6 confirm that the destruction of sorbed *n*-alcohols of equal reactivity with hydroxyl radicals requires higher dosages of hydrogen peroxide for compounds of higher hydrophobicity.

A quantitative relationship that describes hydrogen peroxide concentrations required to treat contaminants of varying hydrophobicities would be valuable for the design of CHP treatment systems. The minimum hydrogen peroxide concentrations required to achieve 99% degradation for each probe compound were obtained by iteration using the regression equations, and are listed in Table 8.5.1-3. Numerous physical parameters have been used as predictors of hydrophobicity, including the octanol-water partition coefficient (K_{ow}) and water solubility (S). Because hydrophobicity appears to be the variable that controls the rate at which sorbed contaminants are treated by CHP reactions, the hydrogen peroxide concentrations required for 99% destruction of the *n*-alcohols were correlated with K_{OW}, log K_{OW}, $1/S$, and log $1/S$. The best correlation was obtained with log K_{OW}; the data of Figure 8.5.1-7 show a strong correlation ($R^2 = 0.97$) between compound hydrophobicity as measured by log K_{OW} (Verschueren, 2001) and the concentration of hydrogen peroxide required to achieve 99% destruction of the probe compound. The same quantitative relationship is not likely to be identical for other contaminants; however, based on recent studies (Watts and Stanton, 1999, Watts et al., 2002) hydrogen peroxide dosages will likely increase as a function of contaminant hydrophobicity. In addition, the soil organic carbon content may affect hydrogen peroxide requirements for a given soil; the soil organic carbon content of the Carson Valley soil was low at 0.36% and higher hydrogen peroxide dosages may be required for soils with more organic carbon.

Propagation reactions become dominant when hydrogen peroxide concentrations are increased in CHP reactions. For example, the reaction of hydroxyl radicals with hydrogen peroxide to generate perhydroxyl radical is favored at higher hydrogen peroxide concentrations. Perhydroxyl radical is a weak oxidant in CHP systems, while superoxide anion is a weak reductant and nucleophile, and hydroperoxide anion is a strong nucleophile (Halliwell and Gutteridge, 1989, Burkitt and Gilbert, 1990). One or more of these species have been implicated in enhanced desorption during CHP reactions and their generation likely resulted in lower total oxidation of the nonane above 300 mM H_2O_2 (Figure 8.5.1-5) (Watts et al., 1999). The correlation between increased hydrogen peroxide requirements and hydrophobicity of sorbed contaminants is likely related to the increased generation of the species (e.g., superoxide or hydroperoxide) required to desorb the increasingly hydrophobic probe compounds.

Although CHP has seen increased use for ISCO over the past decade, no design criteria have been established, and no starting points for bench-scale treatability studies of full-scale application of CHP have been developed. Hydrogen peroxide requirements vary substantially at full-scale CHP ISCO applications, often with no basis in process chemistry. Decomposition rates of hydrogen peroxide and generation rates of hydroxyl radicals and other transient oxygen species are a function of the soil mineralogy, soil organic matter content, and the dosage of catalyst added. Many contaminants of concern react with hydroxyl radicals at near diffusion-controlled rates ($> 3 \times 10^9$ $M^{-1}sec^{-1}$); however, K_{OW}s for these contaminants range from 500 to over 10^7, making hydrophobicity a significant variable in the CHP treatment of contaminated soils and groundwater. The results of this research demonstrate a strong correlation between log K_{OW} and the hydrogen peroxide dose required to treat *n*-alcohols sorbed to the Carson Valley soil and, although an identical quantitative relationship may not be found for other classes of

compounds and soils, hydrogen peroxide dosages will likely be proportional to log K_{OW}. These results will provide a basis for developing structure-treatability relationships and design criteria for soil and groundwater remediation systems using CHP reactions.

Conclusions

A homologous series of five *n*-alcohols was used as model contaminants to evaluate the relationship between contaminant hydrophobicity and dose of hydrogen peroxide required to treat contaminated soils using CHP. Treatment with a standard Fenton's system confirmed that there were no significant differences ($\alpha < 0.05$) among the five probe compounds in their second-order rate constants for reaction with hydroxyl radicals. When sorbed probe compounds were treated with varying concentrations of catalyst and hydrogen peroxide, the minimum hydrogen peroxide concentration required to treat > 99% of each of the *n*-alcohols increased as a function of the size of the compounds and correlated well ($R^2 = 0.97$) with their log K_{OWS}. The increased hydrogen peroxide concentration necessary for treatment of the more hydrophobic *n*-alcohols was likely due to the formation of transient oxygen species other than hydroxyl radicals, such as superoxide or hydroperoxide anion, which may be responsible for enhanced contaminant desorption. The results of this study show that a direct relationship exists between log K_{OW} and the concentration of hydrogen peroxide required in CHP reactions to treat contaminated soils and groundwater and serves as the basis for predicting hydrogen peroxide requirements.

Table 8.5.1-1. Analysis of variance from the standard Fenton's system

	df	Sum of Squares	Mean Square	f^*
Experiments				
Source of variation				
Treatments	4	2.574×10^{-4}	6.435×10^{-5}	1.046
Error	10	6.150×10^{-4}	6.154×10^{-5}	
Totals	14	8.728×10^{-4}		
Controls				
Source of variation				
Treatments	4	1.307×10^{-3}	3.267×10^{-4}	0.199
Error	10	1.640×10^{-2}	1.640×10^{-3}	
Totals	14	1.771×10^{-2}		

*values are valid because f of 2.61 using $\dfrac{df_1}{df_2}$ of $\dfrac{4}{10}$ was not exceeded

Table 8.5.1-2. Regression equations

Probe	Regression Equation[a]	R^{2b}
1-Hexanol	$87.5 + 12.6(\text{Iron}) + 9.21(\text{H}_2\text{O}_2) - 1.96(\text{Iron})(\text{H}_2\text{O}_2) - 2.80(\text{Iron})^2 - 3.33(\text{H}_2\text{O}_2)^2$	0.90
1-Heptanol	$90.3 + 7.03(\text{Iron}) + 14.0(\text{H}_2\text{O}_2) - 2.58(\text{Iron})(\text{H}_2\text{O}_2) - 1.93(\text{Iron})^2 - 7.22(\text{H}_2\text{O}_2)^2$	0.92
1-Octanol	$96.8 + 7.60(\text{Iron}) + 8.97(\text{H}_2\text{O}_2) - 5.23(\text{Iron})(\text{H}_2\text{O}_2) - 4.0(\text{Iron})^2 - 6.63(\text{H}_2\text{O}_2)^2$	0.95
1-Nonanol	$88.9 + 8.19(\text{Iron}) + 13.6(\text{H}_2\text{O}_2) - 5.24(\text{Iron})(\text{H}_2\text{O}_2) - 1.01(\text{Iron})^2 - 6.36(\text{H}_2\text{O}_2)^2$	0.88
1-Decanol	$87.4 + 10.5(\text{Iron}) + 12.5(\text{H}_2\text{O}_2) - 5.6(\text{Iron})(\text{H}_2\text{O}_2) - 7.1(\text{Iron})^2 + 2.61(\text{H}_2\text{O}_2)^2$	0.87

[a] where Iron and H_2O_2 are coded terms [16] for ferric sulfate concentration and hydrogen peroxide concentration, respectively

[b] derived with 12 degrees of freedom

Table 8.5.1-3. Probe characteristics and minimum H_2O_2 concentrations required for > 99% degradation

Probe	log K_{ow}	S (mg/L)	min. H_2O_2 (mM)
1-Hexanol	2.03	5900	51.9
1-Heptanol	2.41	2000	95.2
1-Octanol	2.80	300	149
1-Nonanol	3.67	100	222
1-Decanol	4.11	37	398

log K_{ow} = log octanol water coefficient

S = water solubility

Source: Verschueren, 2001
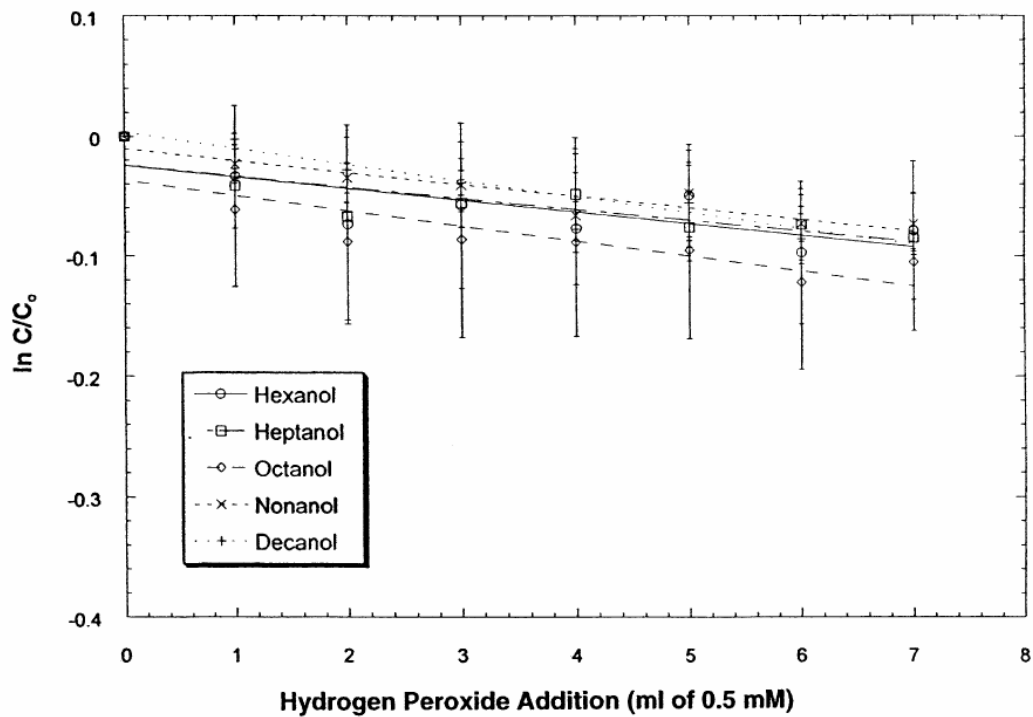
Figure 8.5.1-1. Oxidation of n-alcohols in a standard Fenton's system.
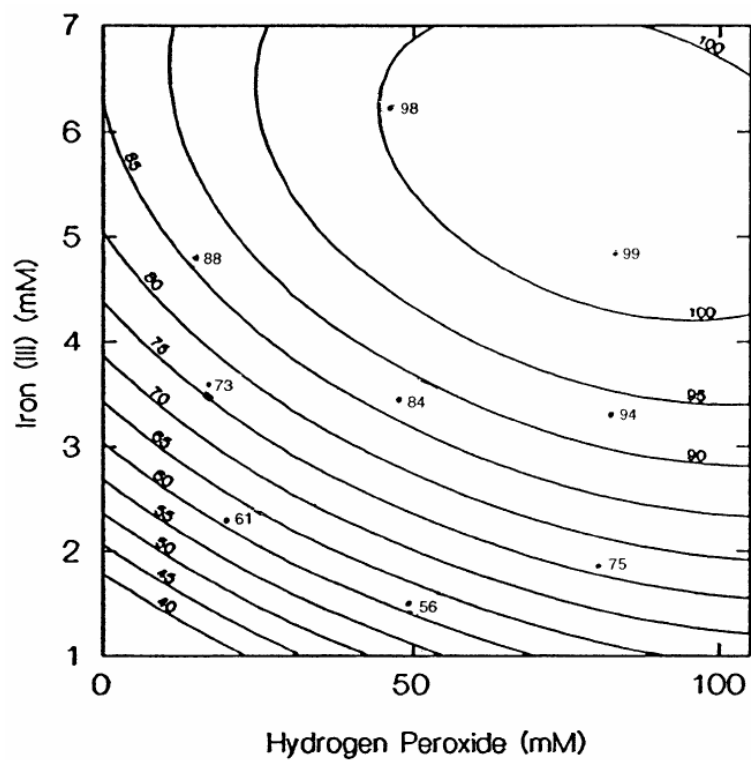
Figure 8.5.1-2. Response surface for the degradation of 1-hexanol sorbed to Carson Valley soil as a function of hydrogen peroxide and iron (III) sulfate concentrations. Isoresponse lines represent percent degradation.
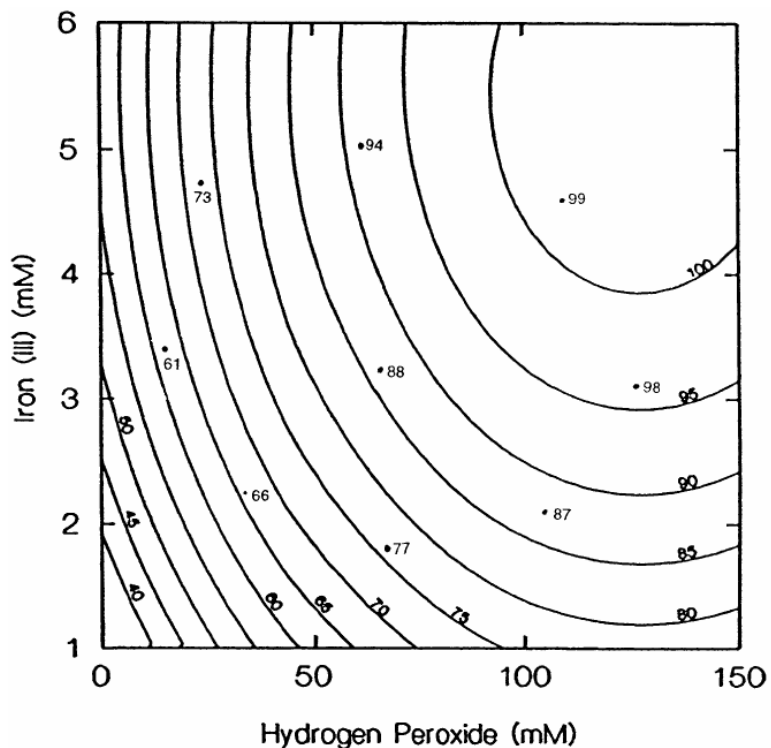
Figure 8.5.1-3. Response surface for the degradation of 1-heptanol sorbed to Carson Valley soil as a function of hydrogen peroxide and iron (III) sulfate concentrations. Isoresponse lines represent percent degradation.
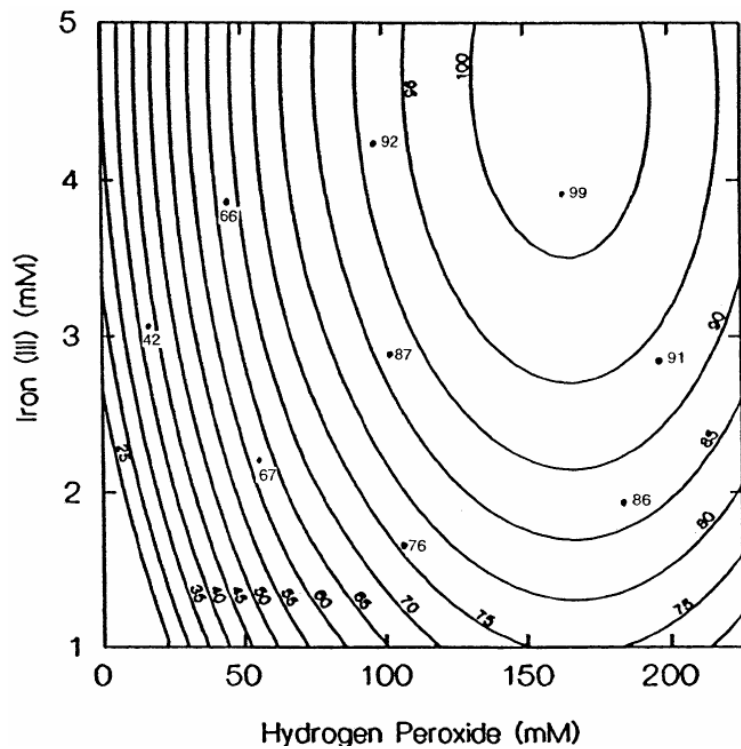
Figure 8.5.1-4. Response surface for the degradation of 1-octanol sorbed to Carson Valley soil as a function of hydrogen peroxide and iron (III) sulfate concentrations. Isoresponse lines represent percent degradation.

162
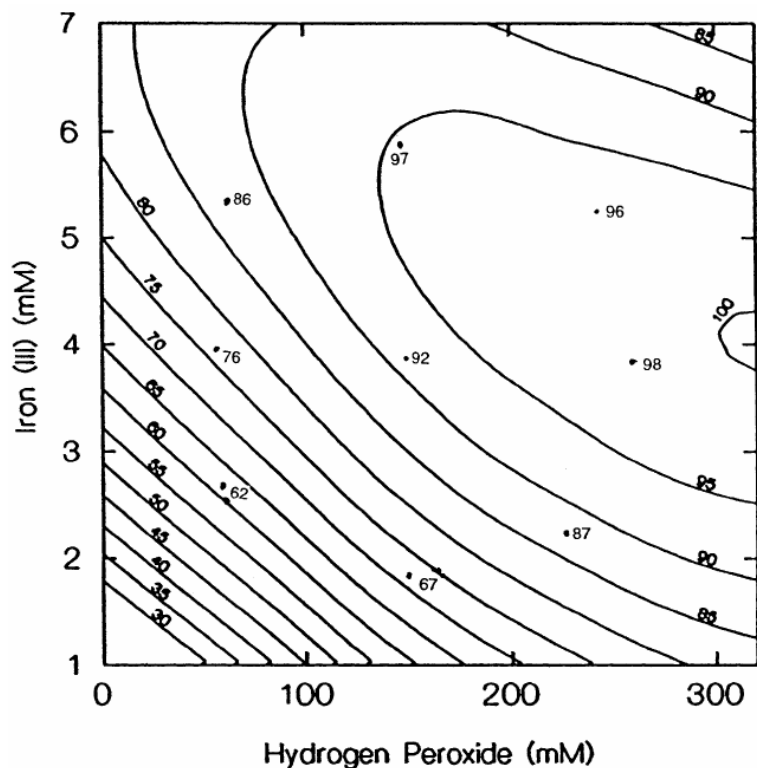
Figure 8.5.1-5. Response surface for the degradation of 1-nonanol sorbed to Carson Valley soil as a function of hydrogen peroxide and iron (III) sulfate concentrations. Isoresponse lines represent percent degradation.
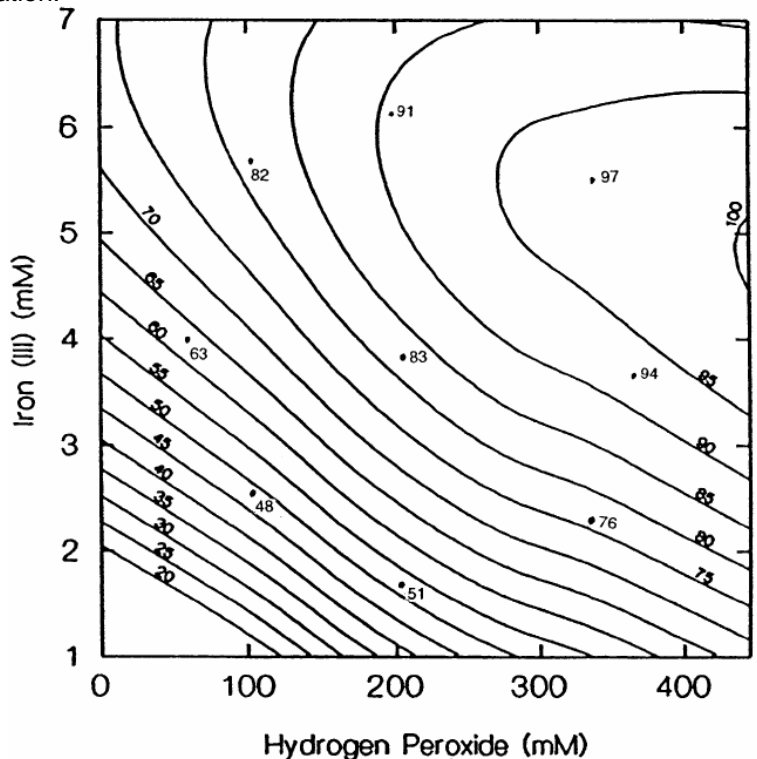
Figure 8.5.1-6. Response surface for the degradation of 1-decanol sorbed to Carson Valley soil as a function of hydrogen peroxide and iron (III) sulfate concentrations. Isoresponse lines represent percent degradation.

163
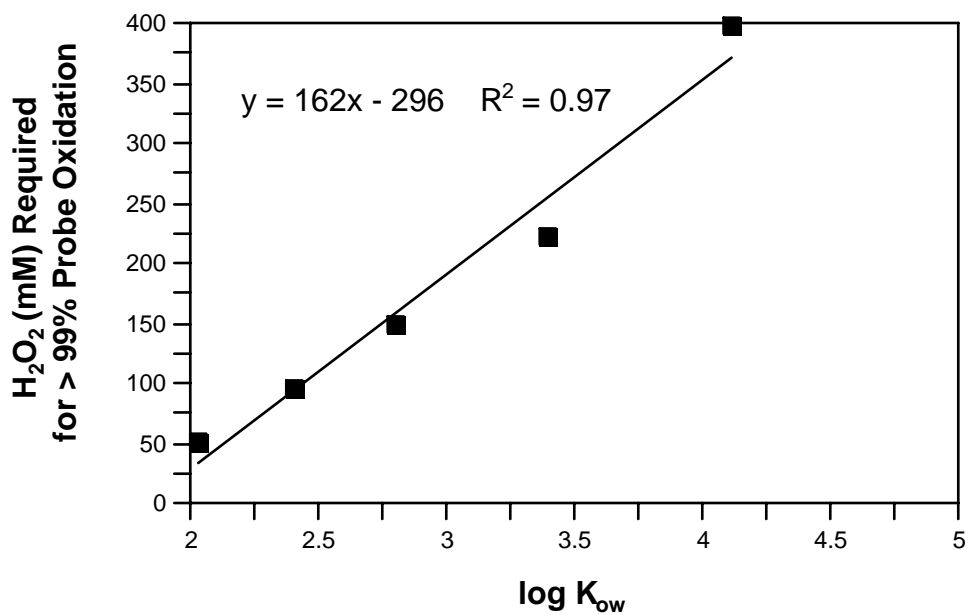
Figure 8.5.1-7. Relationship between log KOWs and the minimum hydrogen peroxide concentrations required for > 99% degradation of sorbed n-alcohols.

164

8.5.2 Reactive Oxygen Species Responsible for the Enhanced Desorption of Dodecane in CHP Systems

Desorption in a gas-purge system.

Desorption of dodecane in the gas-purge system containing no reactants is shown in Figure 8.5.2-1. Over 95% of the dodecane remained sorbed to the silica sand over 180 min, which is expected due to the high hydrophobicity and sorptivity of dodecane (log K_{ow} = 6.44) (Pavlostathis and Jaglal, 1991). Watts et al. (Watts et al., 2000) previously found minimal gas-purge desorption of dodecane from a surface soil over 50 h.

Enhanced desorption by CHP reactions.

The enhanced desorption of dodecane by CHP systems containing 5 mM Fe (III) and 0.5 M or 3 M H_2O_2 is shown in Figure 8.5.2-2. In the 0.5 M H_2O_2 CHP system, 45% of the dodecane was desorbed over 180 min (Figure 8.5.2-2a). A mass balance accounted for 72% of the dodecane; the remainder was likely degraded by hydroxyl radicals in the system. A chromatographic peak with retention time equal to that of dodecyl aldehyde, the expected oxidation product, was not seen on chromatograms, although other unidentified peaks were found. In the 3 M H_2O_2 system, 61% of the dodecane was desorbed over 180 min (Figure 8.5.2-2b). A mass balance for the 3 M CHP system demonstrated total dodecane recovery of 64%. These results show that the desorption of dodecane is enhanced significantly in CHP reactions relative to its gas-purge desorption rate, and that enhanced desorption and dodecane destruction increase with increasing H_2O_2 concentration. Such increasing destruction of an alkane is expected; Watts and Stanton (1999) found that increased mineralization of hexadecane occurred with increasing H_2O_2 concentration in a CHP system.

The data of Figures 8.5.2-2a–b demonstrate increased desorption as a function of H_2O_2 concentration, consistent with the results of Watts et al. (1994), Gates and Siegrist (1995), and Watts and Stanton (1999). The increased desorption at higher H_2O_2 concentrations is likely due to the increased generation of one or more of the major reactive species in CHP reactions: hydroxyl radicals, superoxide, or hydroperoxide anion. To determine the reactant responsible for the enhanced desorption in CHP systems, a series of reactions was conducted, each generating only one reactive oxygen species.

Desorption by hydroxyl radical.

The standard Fenton's reaction was used to generate hydroxyl radicals as the sole reactive oxygen species in the dodecane-silica sand system. The reaction conditions were based on the stoichiometrically efficient conditions developed by Babbs and Griffin (1989). No significant desorption was observed in the Fenton's system over 180 min compared to gas-purge controls (Figure 8.5.2-3). The results of Figure 8.5.2-3 are consistent with the characteristics of hydroxyl radical, which is short-lived and reacts at diffusion-controlled rates (Dorfman and Adams, 1973; Hagg and Yao, 1992); the findings are also consistent with those of Sedlak and Andren (1991) that this short-lived species is not reactive with sorbed organic contaminants.

Desorption by hydroperoxide.

In reactions using a 150 mM solution of sodium perborate to generate hydroperoxide in the dodecane-silica sand system, no significant desorption of dodecane occurred over 180 min compared to gas-purge controls (Figure 8.5.2-4). These data confirm that hydroperoxide is not

the desorbing agent in CHP systems. The results are logical because, although hydroperoxide is a strong nucleophile, it recombines with protons at a diffusion-controlled rate, minimizing its reactivity in Fenton's systems.

Desorption by superoxide.

The addition of 1 M KO_2 to the dodecane-spiked sand gas-purge system resulted in 22% dodecane desorption (Figure 8.5.2-5a), while the addition of 3 M KO_2 provided 82% dodecane desorption (Figure 8.5.2-5b). These results demonstrate that superoxide promotes enhanced dodecane desorption, and suggest that superoxide is the reactive species responsible for the enhanced desorption of other contaminants in CHP reactions.

To confirm the role of superoxide in enhanced dodecane desorption, ascorbate was used as a superoxide scavenger ($k_{O_2\bullet-} = 2.7 \times 10^5$ M^{-1} s^{-1}) (Cabelli and Belski, 1983). The ability of ascorbate to scavenge superoxide was confirmed by evaluating the transformation of 0.1 mM 1,4-benzoquinone ($k_{O_2\bullet-} = 9.0 \times 10^8$ M^{-1} s^{-1}) (Bielski, et al., 1985) in 3 M KO_2 with and without the addition of ascorbate. Without ascorbate, the benzonquinone was transformed to an undetectable concentration in 8 min; however, no measurable benzoquinone degradation occurred in the presence of 3 M ascorbate. Dodecane desorption in superoxide systems (3 M KO_2) and in CHP reactions (1 M H_2O_2 and 5 mM iron [III]) was then evaluated with the addition of 3 M ascorbate. In controls without scavenging, approximately 25% of the sorbed dodecane was trapped in ORBO tubes in both systems; however, no measurable dodecane desorption occurred in either system in the presence of excess ascorbate (Figure 8.5.2-6). The low desorption rate in the ascorbate-containing systems compared to the gas-purge controls in the other systems (Figures 8.5.2-2–6) may be due to a lower Henry's law constant for dodecane in the less polar KO_2–ascorbate system. The presence of ascorbate also lowered the efficiency of the hexane extractions, preventing quantification of the sorbed dodecane residuals.

The results shown in Figure 8.5.2-6 confirm that superoxide generated in a KO_2 system desorbs dodecane, and that superoxide is the desorbing species in CHP systems. Therefore, the enhanced treatment of sorbed contaminants previously reported (Watts et al., 1994; Gates and Siegrist, 1995; Watts et al., 1999) was likely due to the action of superoxide on sorbed species. Sorption of apolar compounds, such as dodecane, to mineral surfaces is driven primarily by van der Waals forces (Schwartzenbach et al., 2003). The vapor deposition method used for preparing the sorbed dodecane was conducted under dry, heated conditions, which ensures that the dodecane was adsorbed to the mineral surface with little hydration prior to the initiation of the desorption experiments. The adsorbed dodecane concentration constituted approximately two molecular layers of surface coverage, based on the assumption that dodecane and the mineral surface were not hydrated, an average sand diameter of 0.25 mm, and a dodecane total surface area (TSA) determined from the liquid density (0.75 g/cm^3) and molecular weight (170.3 g/mol) with a spherical shape. As a result, the experiments began with sand grains that were oil-wet, a condition which inhibits water from adsorbing to the surface when the treated sand is transferred into the water-filled reactors. Superoxide has been shown to be solvated by apolar solvents (Bielski et al., 1985; Afanas'ev, 1989) and therefore likely partitions into the dodecane layers at the mineral surface. Because superoxide can participate in hydrogen bonding on the mineral surface, it may displace dodecane from the surface adsorption sites, thus facilitating dodecane desorption into the aqueous phase. Superoxide-mediated desorption from TiO_2 surfaces to aqueous solution has been documented by Konaka et al. (1999), and such desorption has been

implied as important step in photocatalytic transformation of organic compounds in solution (Feitz and Waite, 2003). Once the dodecane is desorbed it would proceed through oxidation reactions with hydroxyl radical in the aqueous phase.

The results of this research provide evidence that CHP transforms contaminants through multiple pathways for the remediation of soils and groundwater. In addition to its ability to oxidize contaminants reactive with hydroxyl radical, CHP treatment can transform contaminants not reactive with hydroxyl radical (Teel and Watts, 2002; Smith et al., 2004), rapidly destroy dense nonaqueous phase liquids (DNAPLs) (Yeh et al., 2003; Watts et al., 2005), and desorb hydrophobic contaminants. The use of surfactants has been proposed to enhance the CHP treatment of hydrophobic contaminants in soils and groundwater. Although some success has been seen with the use of surfactants in the treatment of sorbed contaminants (Li et al., 1997), their addition, which results in a demand on H_2O_2, is not necessary because superoxide effectively desorbs contaminants.

The generation of superoxide at effective concentrations will improve CHP remediation systems for the treatment of sorbed contaminants found in soil and groundwater systems. Based on the results showing that superoxide is the desorbing species in CHP reactions, the process chemistry can be modified to generate more or less superoxide, depending on contaminant sorptivity, resulting in more efficient use of H_2O_2 and minimizing treatment costs. By optimizing CHP reactions to promote enhanced desorption, the contaminant rebound that is common in the remediation of contaminated sites may be minimized. The use of such a rational basis for system design will improve the stoichiometry of CHP ISCO processes, which are reagent-intensive relative to bioremediation and monitored natural attenuation, and will ultimately lead to more effective full-scale treatment.
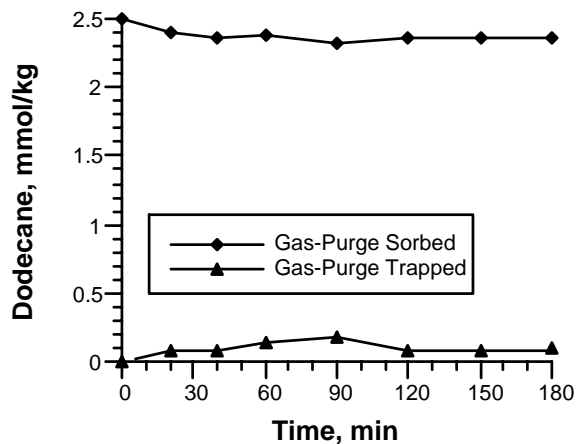
Figure 8.5.2-1. Desorption of dodecane in water in a gas-purge system (experimental reactors: 50 g of silica sand spiked with dodecane at 2.5 mmol/kg sand; 50 ml deionized water at pH 6.8; T = 20 ± 2°C).
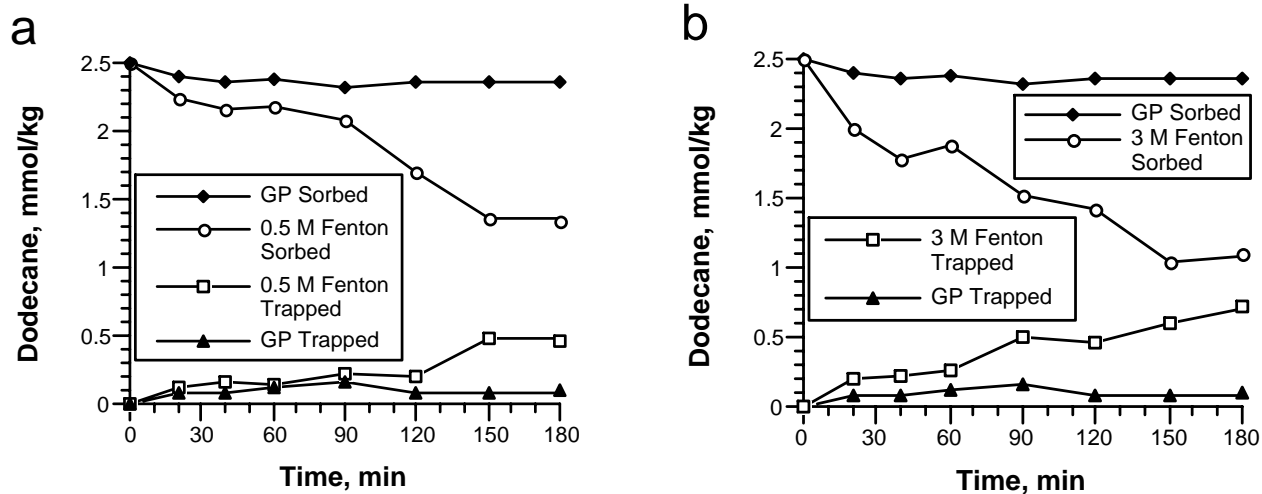
Figure 8.5.2-2. Desorption of dodecane by a CHP reaction: a) 0.5 M H_2O_2; b) 3 M H_2O_2 (experimental reactors: 50 g of silica sand spiked with dodecane at 2.5 mmol/kg sand; 5 mM Fe(III) and 0.5 M or 3 M H_2O_2; 50 ml total volume at pH 3.0; control reactors: H_2O_2 substituted by deionized water; T = 20 ± 2°C).
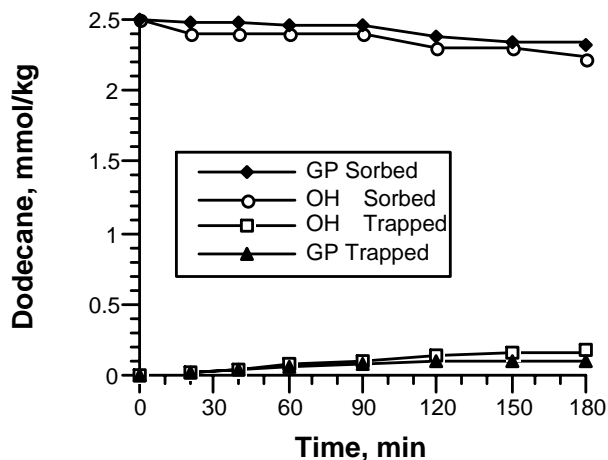
Figure 8.5.2-3. Desorption of dodecane using the standard Fenton's reaction optimized for the generation of hydroxyl radicals (experimental reactors: 50 g of silica sand spiked with dodecane at 2.5 mmol/kg sand; 5 mM Fe(III) with 0.1 ml of 100 mM H_2O_2 added every 10 min over 180 min; 50 ml initial volume at pH 3.0; control reactors: H_2O_2 substituted by deionized water; T = 20 ± 2°C).
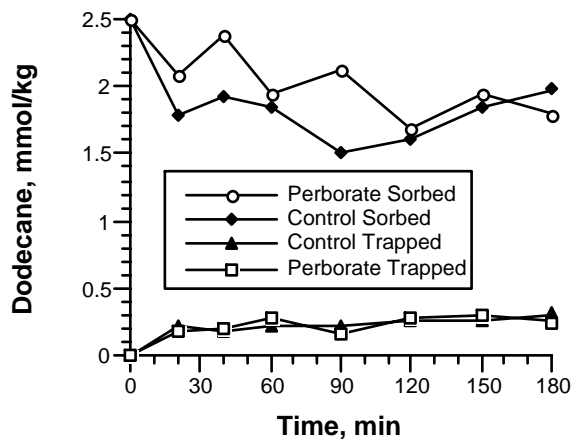
Figure 8.5.2-4. Linear regression of desorption of dodecane using sodium perborate to generate hydroperoxide anion (experimental reactors: 50 g of silica sand spiked with dodecane at 2.5 mmol/kg sand; 150 mM sodium perborate; 50 ml total volume at pH 10.0; control reactors: sodium perborate substituted by deionized water; T = 20 ± 2°C).

169
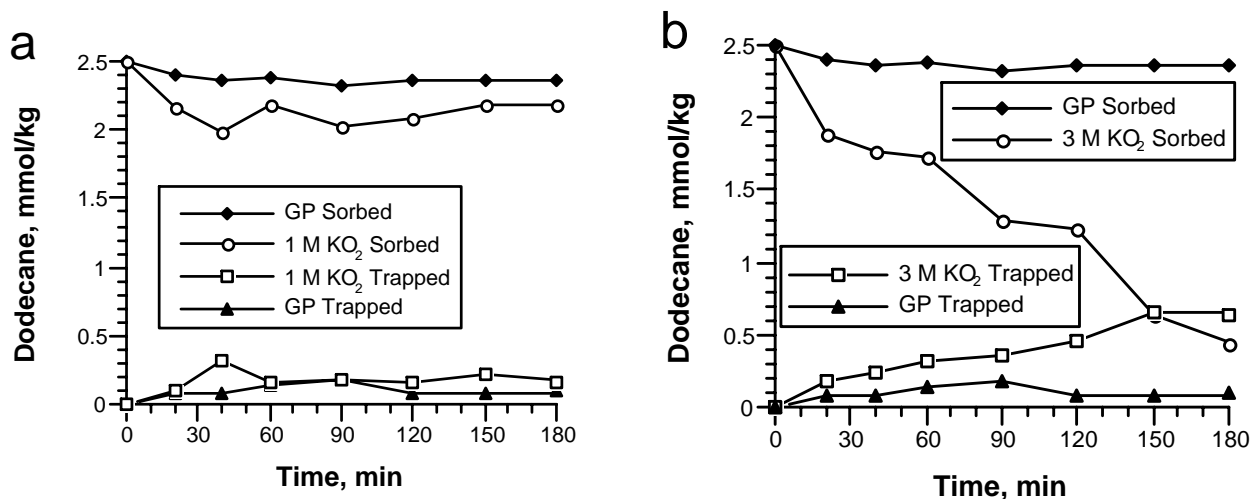
Figure 8.5.2-5. Desorption of dodecane using 1 M potassium superoxide to generate superoxide anion: a) 1 M KO_2; b) 3 M KO_2 (experimental reactors: 50 g of silica sand spiked with dodecane at 2.5 mmol/kg sand; 0.1 M NaOH, 1 mM DTPA, and 1 M or 3 M KO_2; 50 ml total volume at pH 14.0; control reactors: KO_2 substituted by deionized water; T = 4 ± 1°C).
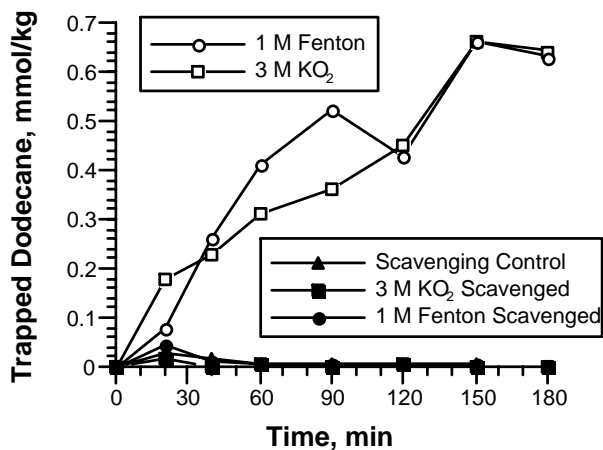
Figure 8.5.2-6. Scavenging of superoxide by ascorbate in KO_2 and CHP systems (all experimental reactors: 50 g of silica sand spiked with dodecane at 2.5 mmol/kg sand; superoxide reactors: 0.1 M NaOH, 1 mM DTPA, and 3 M KO_2, with or without 3 M ascorbate; 50 ml total volume at pH 14.0; scavenging control reactors: KO_2 substituted by deionized water; T = 4 ± 1°C; CHP reactors: 5 mM Fe(III) and 1 M H_2O_2, with or without 3 M ascorbate; 50 ml total volume at pH 3.0; T = 20 ± 2°C).

170

8.6 Delivery of Peroxide

The results provided in Sections 8.1-8.5 demonstrate that CHP is characterized by fundamental chemistry that provides mechanisms for degrading contaminants by oxidation, reduction, and nucleophilic attack on biorefractory contaminants, as well as destroying sorbed and DNAPL contaminants more rapidly than their rates of desorption and dissolution. CHP remediation has been implemented at hundreds of sites throughout the world over the past decade, and the results have been highly varied. Contaminants have been treated to undetectable concentrations at some sites, while minimal cleanup has been accomplished at other sites. Among the possible reasons for the mixed results of CHP are the inhibitory effects of soil organic matter (SOM) and the rapid decomposition of hydrogen peroxide near the injection site. CHP reagents must be delivered to the subsurface with minimal interference by organic matter and with hydrogen peroxide lifetimes sufficiently long to allow contact with contaminants. In addition, the potential for displacement of heavy metals that may be present at the site requires investigation.

Interactions between hydrogen peroxide and soil organic matter. The most common conceptual model for the role of naturally occurring SOM in ISCO processes is that its oxidation by ISCO reagents is rapid and occurs preferentially to contaminant oxidation. Oxidation of SOM by permanganate has been studied most extensively. A parameter developed for use in permanganate ISCO is natural oxidant demand (NOD), which is defined as the mass of permanganate consumed through the oxidation of a mass of SOM, reduced inorganic compounds, and reduced metals (Siegrist et al., 2001). The concept of NOD has not been applied to CHP because, unlike permanganate, numerous other pathways of hydrogen peroxide decomposition exist (e.g., its catalytic decomposition by iron and manganese oxides), and many reactive species are generated. Therefore, the complicated relationships between SOM and CHP are not well understood, and many studies have demonstrated conflicting results. For example, some studies have concluded that the effectiveness of CHP treatment of polycyclic aromatic hydrocarbons (PAHs) decreases with increasing SOM (Bogan and Trbovic, 2003). In contrast, Huling et al. (2001) documented that an increase in the demand of hydroxyl radical by peat is insignificant compared to the scavenging of hydroxyl radical by hydrogen peroxide. Concentrations of hydrogen peroxide similar to those used in CHP ISCO are commonly used in laboratory procedures to oxidize SOM prior to mineralogical analysis (Kunze and Dixon, 1986). Griffith and Schnitzer (1977) documented the formation of hundreds of degradation products from SOM treated with hydrogen peroxide, most of which were organic acids, aldehydes, and ketones. However, the nature of SOM is inherently variable and complex, and its dynamics in various fate and remediation processes remain in question. The purpose of this segment of research was to determine the effects of a range of CHP conditions on different pools of SOM, and to evaluate the effects of SOM on hydrogen peroxide stability and hydroxyl radical activity in CHP reactions in a well-characterized surface soil.

Mobility of metals in CHP treatment. Many soil and groundwater systems are contaminated with both organic compounds and metals. In the United States, 738 of the over 1,235 sites found on the National Priority List (NPL) are characterized by contamination with heavy metals and organic contaminants such as benzene, trichloroethylene (TCE), and perchloroethylene (PCE) (Watts, 1998). The co-occurrence of organic compounds and heavy metals is a significant factor complicating the cleanup of contaminated soils and groundwater

because treatment technologies used for the remediation of organic contaminants may have an effect on metal mobility. Most soil and groundwater remediation research has focused on either organic contaminants or metals, but not both simultaneously, as they occur *in situ*.

Advantages of ISCO include elimination of the need to excavate contaminated soils and pump groundwater, the rapid treatment of biorefractory contaminants compared to bioremediation and natural attenuation, and the potential for rapid site closure. However, ISCO technologies are currently in early stages of development and are challenged by site complexities, such as the risk of releasing contaminants, including metals. The enhanced desorption of organic contaminants by CHP processes has been investigated extensively (Watts et al., 1994; Gates and Siegrist, 1995; Kakarla and Watts, 1997; Watts et al., 1999); however, little attention has been given to the displacement of metals exchanged on soils and groundwater solids in these treatment systems. Therefore, the objective of this segment of research was to investigate the potential of CHP to displace sorbed metals, using gadolinite as a model sorbent, and to provide a more detailed investigation of the effect of CHP ISCO on lead and cadmium mobility in natural soils.

Stabilization of hydrogen peroxide. Although CHP is a near universal treatment matrix, it is also highly unstable in the subsurface, with the half-life of hydrogen peroxide in these systems ranging from a few hours to a few days at most. As a result, CHP ISCO is ineffective at many contaminated sites because hydrogen peroxide decomposes before it can contact contaminants. Some attempts have been made to stabilize hydrogen peroxide in the subsurface, primarily through the addition of phosphates to bind transition metals; however, hydrogen peroxide stabilization has not been effective to date. Sun and Pignatello (1992) screened over 30 organic acid–iron (III) complexes as CHP catalysts, and found a wide range of catalytic activity. Because some organic acid–iron complexes are inactive CHP catalysts, the sodium salts of these acids may serve as effective hydrogen peroxide stabilizers when added along with hydrogen peroxide to the subsurface. Therefore, the purpose of this segment of research was to investigate the potential for increased hydrogen peroxide stability in mineral slurries and soils and subsurface solids using sodium salts of a number of low molecular weight organic acids, and to investigate their ability to stabilize hydrogen peroxide in flow-through columns representative of subsurface conditions.

8.6.1 Soil Organic Matter–Hydrogen Peroxide Dynamics in the Treatment of Contaminated Soils and Groundwater using CHP

To aid in elucidating SOM dynamics in environmental processes, size fractionation has been developed for investigating the fate of labile and recalcitrant carbon in soils (Cambardella and Elliott, 1992; Cambardella and Elliott, 1993; Kelly et al., 1996; Gill et al., 1999). Organic matter > 53 μm is classified as particulate organic matter (POM), and organic matter smaller < 53 μm is classified as non-particulate organic matter (NPOM). The POM fraction is composed predominantly of biologically labile carbon fragments in various stages of decomposition; the NPOM fraction consists of biologically recalcitrant carbon usually sorbed to minerals (Cambardella and Elliott, 1992). Such fractionation techniques provide an effective method for evaluating 1) the effect of CHP on SOM pools and 2) the effect of SOM on CHP dynamics.

Destruction of SOM by CHP reactions.

Reactions were conducted in systems containing soil depth A and six different CHP process conditions; when the reactions were complete, the remaining SOM was fractionated to evaluate the effect of CHP reactions on the different pools of organic carbon. Destruction of organic carbon associated with the total SOM, the POM fraction, and the NPOM fraction of soil depth A by CHP treatment using 0.5-3 M hydrogen peroxide catalyzed by 5 mM and 10 mM soluble iron (III) at pH 3 is shown in Figure 8.6.1-1a-b. Destruction of all organic carbon fractions was directly proportional to the hydrogen peroxide dosage for both iron (III) catalyst concentrations. Results from linear regression analyses of carbon destruction as a function of hydrogen peroxide dosages are listed in Table 8.6.1-1. Reactions conducted at pH 3 resulted in a significant destruction of organic carbon mass (30-60%) as the hydrogen peroxide dosage increased. Statistical analysis of the data using completely randomized design analysis of variance (ANOVA) showed no significant difference ($\alpha = 0.05$) for the destruction of each organic carbon fraction between the 5 mM and 10 mM soluble iron (III) CHP catalysts at pH 3. Approximately 90% of the organic carbon in soil depths A, B, and C exists in the NPOM fraction therefore, on a mass basis, the loss of carbon in the NPOM fraction was greater than the loss of carbon in the POM fraction. A greater loss of organic carbon in the NPOM fraction is expected because 1) this pool of organic carbon is more abundant, and 2) water soluble organic carbon is included in the NPOM fraction and therefore more available for oxidant attack.

To evaluate potential differences in SOM destruction between the use of added soluble iron and natural soil minerals as catalysts, subsequent reactions were conducted using soil minerals as the only CHP catalyst. Destruction of organic carbon associated with the total SOM, the POM fraction, and the NPOM fraction by CHP reactions using 0.5-3 M hydrogen peroxide catalyzed by naturally occurring soil minerals at pH 3 and at neutral pH is shown in Figure 8.6.1-2a-b. The loss of organic carbon in each fraction using naturally occurring mineral catalysts at pH 3 was not significantly different ($\alpha = 0.05$) from that in reactions catalyzed by soluble iron (III) at pH 3 (Figure 8.6.1-1a–b). In contrast, no measurable organic carbon loss occurred when naturally-occurring minerals catalyzed CHP reactions at the neutral soil pH. These results suggest that SOM destruction in CHP reactions is pH-dependant.

To further investigate the role of pH in organic carbon destruction, CHP reactions were conducted using an iron (III)-EDTA catalyst at pH 7. Destruction of organic carbon associated with the total SOM, the POM fraction, and the NPOM fraction by CHP reactions using 0.5-3 M hydrogen peroxide catalyzed by 5 mM and 10 mM iron (III)-EDTA at pH 7 is shown in Figure 8.6.1-3a–b. Similar to the reactions catalyzed by naturally-occurring minerals at neutral pH, minimal destruction of the SOM and NPOM fractions was found in CHP reactions catalyzed by 5 mM EDTA-iron (III) at pH 7, and no measurable organic carbon destruction occurred in the reactions catalyzed by 10 mM iron (III)-EDTA. Statistical analysis of the data of Figures 8.6.1-3a–b using completely randomized design ANOVA demonstrated no significant difference ($\alpha = 0.05$) between the loss of organic carbon using 5 mM iron (III)-EDTA and 10 mM iron (III)-EDTA as catalysts. These results are consistent with the data shown in Figures 8.6.1-1 and 8.6.1-2 that neither SOM nor its fractions were destroyed by any CHP conditions at pH 7. Using hexanol ($k_{OH\bullet} = 3 \times 10^9$ M^{-1} s^{-1}) as a hydroxyl radical probe, hydroxyl radical activity was confirmed in the iron (III)-EDTA catalyzed reactions at neutral pH (Figure 8.6.1-4). The results shown in Figures 8.6.1-3a–b and 8.6.1-4 confirm that neither hydroxyl radical nor any other reactive oxygen species destroy SOM in the soil at neutral pH regimes.

173

Soluble iron (III)-catalyzed CHP reactions at pH 3 (Figure 8.6.1-1a–b) and EDTA-iron (III)-catalyzed CHP reactions at pH 7 (Figure 8.6.1-3) were conducted with equal concentrations of iron (III) and hydrogen peroxide. The reactions conducted at pH 7 resulted in minimal SOM loss compared to those conducted at pH 3, suggesting that organic carbon destruction through CHP reactions is greater at acidic pH regimes. Cationic organic matter is bound to negatively charged clay minerals by hydrogen bonds in soil systems (Mortland, 1986). Furthermore, the SOM can occlude iron and manganese oxides, decreasing the available surface area and corresponding catalytic activity (Tate, 1987). The disruption of hydrogen bonds between SOM and soil minerals at acidic pH regimes and the corresponding release of SOM has been well documented (Troech and Thompson, 1993); this release of SOM at acidic pH regimes likely makes it more accessible for oxidation by CHP reactions. The data of Figures 8.6.1-1–4 demonstrate that system pH of CHP reactions has a significant effect on the destruction of SOM, and may also influence other aspects of CHP dynamics.

Effect of SOM on hydrogen peroxide stability.

Hydrogen peroxide stability is the primary limitation of the use of CHP for ISCO (Kakarla and Watts, 1996; Watts and Teel, 2005b). In order to investigate the effect of SOM on hydrogen peroxide consumption rates, hydrogen peroxide concentrations were measured over time in two soil horizons of varied organic carbon contents under acidic conditions at the natural pH of the soil. Hydrogen peroxide decomposition as a function of time using natural soil mineral catalysts and 3 M hydrogen peroxide at pH 3 or at the neutral soil pH in two soils of similar mineralogical content, but different organic carbon content, is shown in Figure 8.6.1-5a–b. Hydrogen peroxide decomposed at equal rates in both soil depth B (organic carbon content = 1.6%) and soil depth C (organic carbon content = 0.2%) at pH 3. These results are in agreement with the results of Tyre et al. (1991), who also found no significant difference (α =0.05) in hydrogen peroxide decomposition rates as a function of soil organic carbon content at pH 3 when CHP reactions were catalyzed by naturally occurring minerals. Huling et al. (2001) proposed that the minimal influence of SOM on hydrogen peroxide decomposition results from the predominant catalytic decomposition of hydrogen peroxide by iron and manganese oxides, rather than SOM.

Under neutral pH conditions, hydrogen peroxide decomposed more slowly in soil depth B (organic carbon = 1.6%) than in soil depth C (organic carbon = 0.2%), which may be due to SOM coating the iron and manganese minerals and inhibiting their catalytic decomposition of hydrogen peroxide. The data of Figure 8.6.1-5a–b are in agreement with the dynamics of SOM destruction at neutral vs. acidic pH regimes (Figures 8.6.1-1–3); at neutral pH regimes, SOM may occlude iron and manganese oxides, which are the primary catalysts for hydrogen peroxide decomposition and SOM destruction.

Effect of SOM on hydroxyl radical activity.

If SOM competes with hydroxyl radical in a manner similar to NOD in permanganate ISCO, then SOM would represent a significant limitation to contaminant treatment in CHP ISCO systems containing high SOM. In order to investigate the effect of SOM on the ability of CHP reactions to generate hydroxyl radical, hexanol ($k_{OH\bullet}$ = 3 x 10^9 M^{-1} s^{-1}) was used as a hydroxyl radical probe in CHP reactions in two soil horizons of different organic carbon contents, but similar mineralogical characteristics (Soils B and C). The oxidation of hexanol during CHP reactions using naturally occurring soil mineral catalysts with the addition of 3 M hydrogen

peroxide at pH 3 and at neutral pH is shown in Figure 8.6.1-6a–b. In the reactions conducted at pH 3 (Figure 8.6.1-6a), hexanol was oxidized to undetectable concentrations at the same rate in both soil horizons. In reactions conducted at neutral pH, approximately 60% of the hexanol was oxidized in soil depth B (1.6% soil organic carbon) while approximately 40% of the hexanol was oxidized in soil depth C (0.2% organic carbon). Minimal hexanol loss was observed in control reactions conducted in parallel to each of the CHP treatments.

The results shown in Figure 8.6.1-6a-b demonstrate that hydroxyl radical activity was not affected by the SOM content when CHP reactions were conducted at pH 3. In contrast, at neutral pH, hydroxyl radical activity was higher in soil depth B with higher SOM than in soil depth C with lower SOM. These data are similar to the results described by Huling et al. (2001), in which hydroxyl radical activity was enhanced in the presence of peat, possibly by the enhanced catalytic activity of metals chelated by the peat. The results shown in Figures 8.6.1-4 and 8.6.1-5 suggest that when CHP reactions are conducted at neutral pH regimes, some SOM may enhance CHP reaction effectiveness by providing a decreased hydrogen peroxide decomposition rate as well as an increase in hydroxyl radical generation compared to lower SOM concentrations. The results of this research are in agreement with previous studies by Tyre et al. (1991) and Huling et al. (2001) showing that contaminant destruction by CHP is not affected by the SOM content of the soil. However, the data shown in Figures 8.6.1-1–4 differ from the most common conceptual model for the destruction of SOM by chemical oxidant; although permanganate rapidly oxidizes SOM, CHP systems do not. Larson and Weber (1994) reported a rapid second-order rate constant of 5×10^4 mg/L·sec for the oxidation of dissolved organic matter (DOM) by hydroxyl radical. However, the slower oxidation of SOM shown in this study suggests that the sorbed and colloidal nature of SOM likely lowers its reactivity with oxidants,

Conclusions

Three horizons of a well characterized surface soil were evaluated for the effects of different CHP formulations on SOM destruction and for the effect of SOM on CHP dynamics. The CHP process conditions included catalysis by iron (III) at pH 3, catalysis by naturally occurring soil minerals at pH 3 and neutral pH, and catalysis by an iron (III)-EDTA chelate at neutral pH. The destruction of SOM in CHP systems was directly proportional to the hydrogen peroxide dosage, and was significantly greater at pH 3 than at neutral pH regimes; furthermore, SOM destruction occurred predominantly in the NPOM fraction. SOM destruction at pH 3 was likely due to disruption of hydrogen bonds in these acidic systems, resulting in the release of exchanged SOM and its resulting increased reactivity in the aqueous phase. At pH 3, SOM did not affect hydrogen peroxide decomposition rates or hydroxyl radical activity. However, at neutral pH, larger masses of SOM decreased the hydrogen peroxide decomposition rate and increased the rate of hydroxyl radical generation in CHP systems.

The results of this research demonstrate that SOM does not significantly affect the remediation of contaminated soils and groundwater when CHP ISCO reactions are conducted at pH 3 because SOM does not affect hydroxyl radical activity nor prevents its generation. However, when CHP reactions are conducted at neutral pH regimes, some SOM may enhance CHP reaction effectiveness by providing a decreased hydrogen peroxide decomposition rate as well as an increase in hydroxyl radical generation compared lower SOM concentrations.

Table 8.6.1-1. Slopes of the lines created by the change in carbon (y-axis) with increasing hydrogen peroxide concentrations using various CHP conditions.

CHP Conditions	Total Carbon			POM			NPOM		
	Slope	Intercept	R^2	Slope	Intercept	R^2	Slope	Intercept	R^2
5 mM Iron (III) pH 3	-2.35	16.2	0.97	-0.236	2.04	0.55	-2.13	14.2	0.947
10 mM Iron (III) pH 3	-1.55	15.6	0.967	-0.359	2.22	0.695	-1.19	13.1	0.878
Naturally-Occurring Mineral Catalyst pH 3	-2.31	16.5	0.99	-0.485	2.31	0.921	-1.83	14.2	0.969
Naturally-Occurring Mineral Catalyst pH 7	-0.0905	15.7	0.017	-0.0903	2.54	0.0982	-0.000217	13.2	6.7E-08
5 mM EDTA-Iron (III) pH 7	-0.847	18.1	0.32	-0.125	2.23	0.715	-0.723	15.9	0.252
10 mM EDTA-Iron (III) pH 7	0.0662	19.2	0.014	-0.124	2.15	0.464	0.186	17.1	0.081
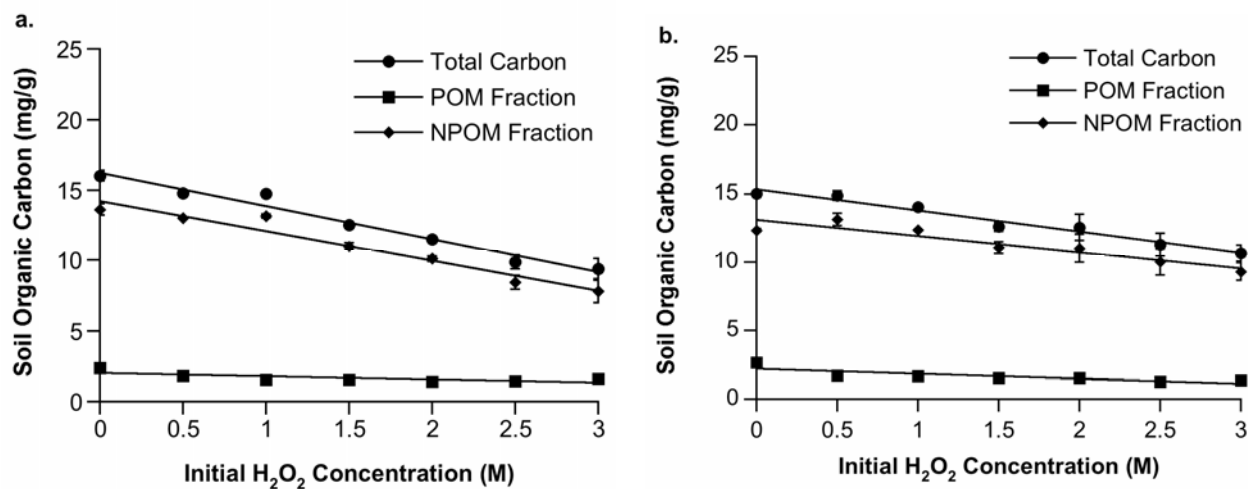
Figure 8.6.1-1. Mass of carbon remaining in soil depth A fractions after reaction completion with a) 5 mM soluble iron (III) catalyst at pH 3 and b) with 10 mM soluble iron (III) catalyst at pH 3
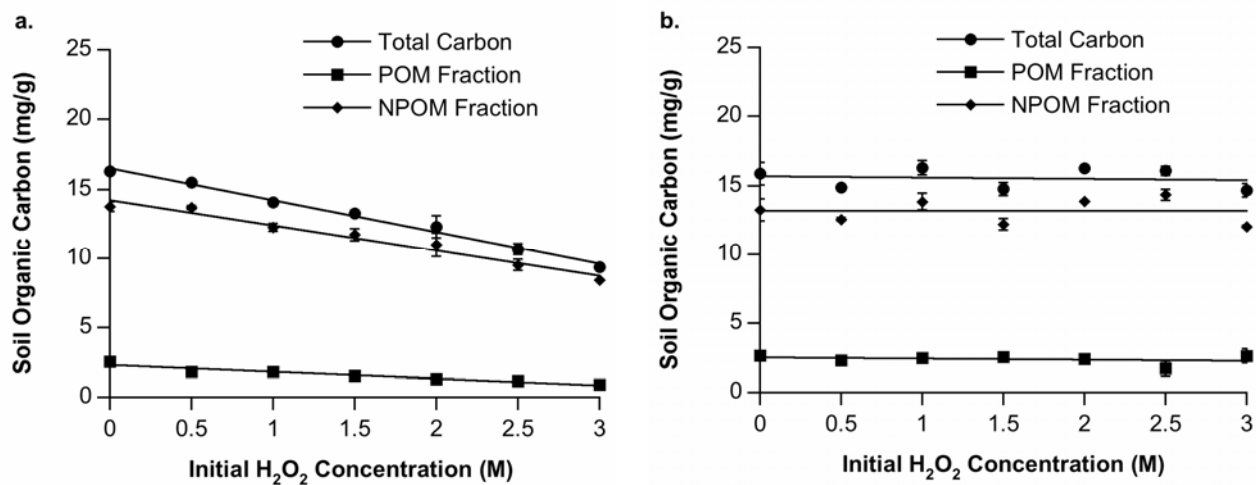
Figure 8.6.1-2. Mass of carbon remaining in soil depth A fractions after reaction completion with a) naturally-occuring soil minerals as the catalyst at pH 3 and b) with naturally-occurring soil minerals as the catalyst at neutral pH
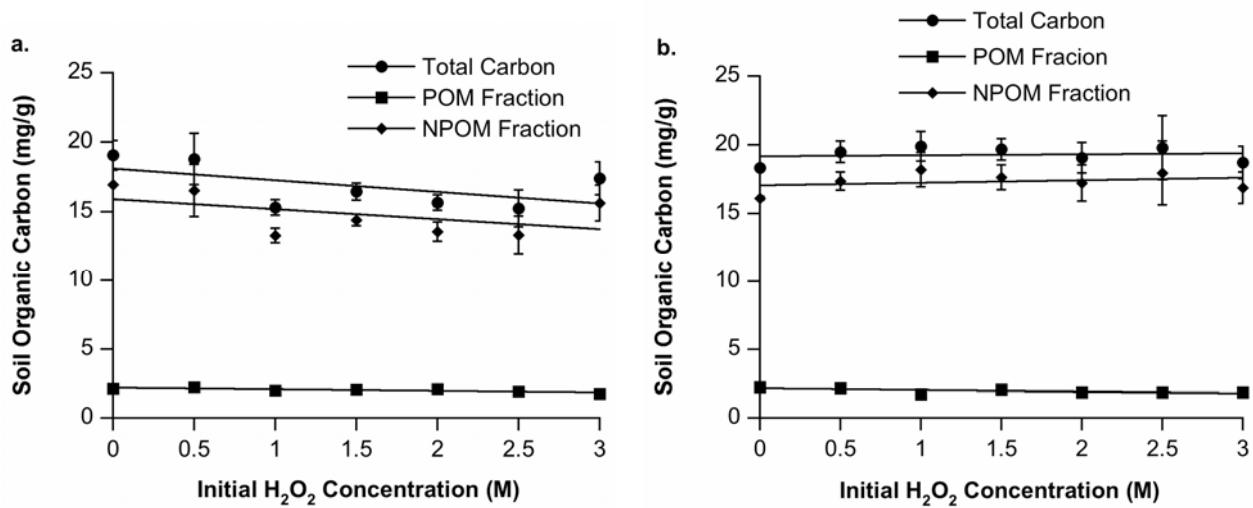
Figure 8.6.1-3. Mass of carbon remaining in soil depth A fractions after reaction completion with a) 5 mM EDTA-iron(III) as the catalyst at pH 7 and b) with 10 mM EDTA-iron (III) as the catalyst at pH 7
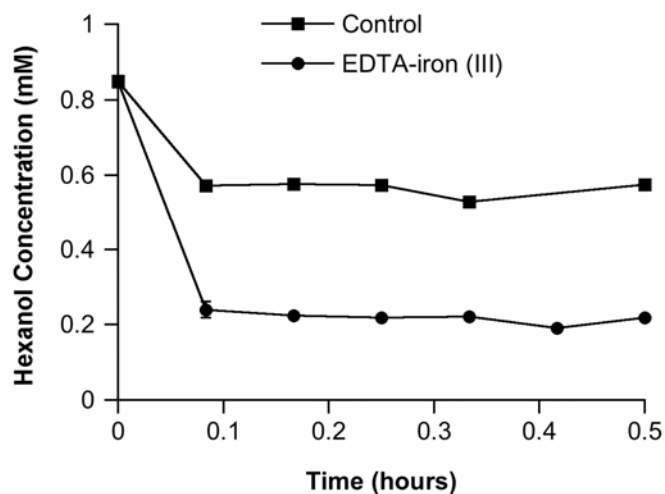
Figure 8.6.1-4. Confirmation of hydroxyl radical generation in iron(III)-EDTA-chelated CHP systems using hexanol as a probe molecule using soil depth B (1.6 % C) and soil depth C (0.2% C).
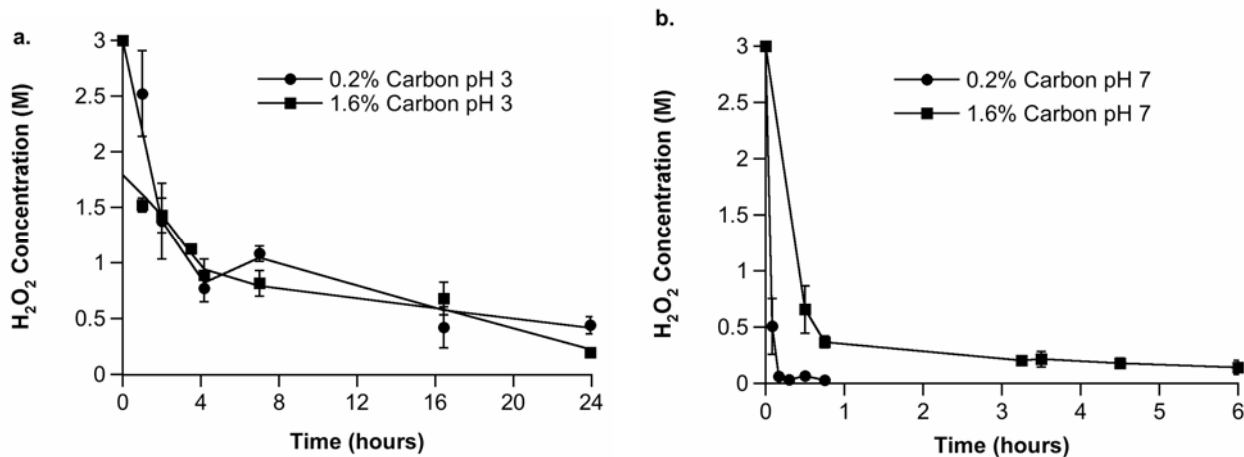
Figure 8.6.1-5. Hydrogen peroxide decomposition over time in soils of similar mineralogical content and different carbon content (soil depth B (1.6 % C) and soil depth C (0.2% C))for CHP reactions using a) 3 M hydrogen peroxide and naturally occurring mineral catalysts at pH 3 and b) 3 M hydrogen peroxide and naturally occurring mineral catalysts at neutral pH.
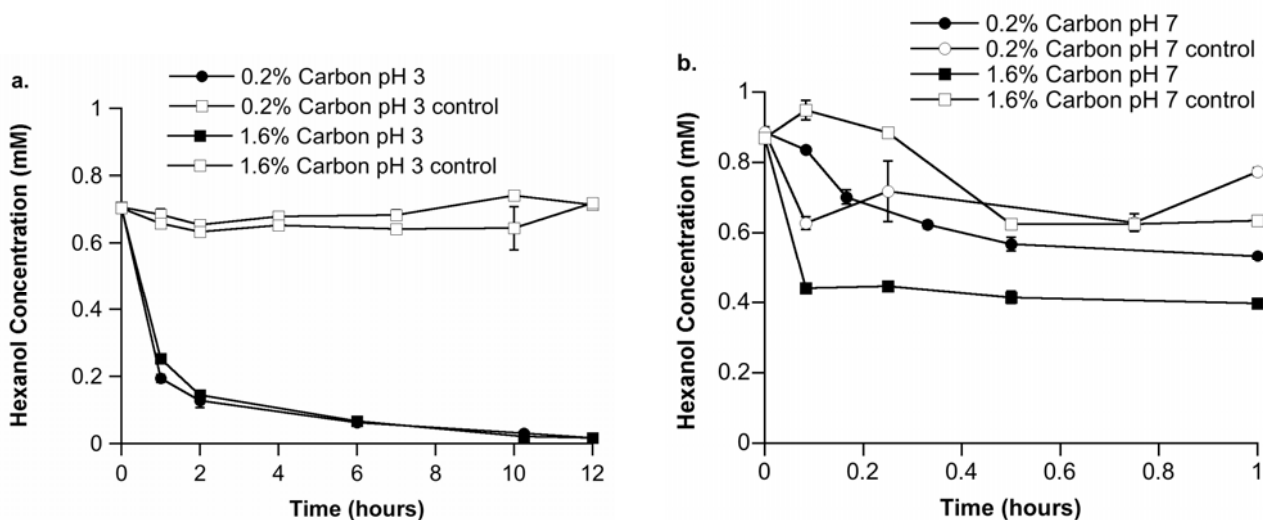
Figure 8.6.1-6. Hexanol degradation over time in soils of similar mineralogical content but different SOM contents (soil depth B (1.6 % C) and soil depth C (0.2% C)). CHP reactions consisted of a) 3 M hydrogen peroxide with naturally-occurring minerals as the catalyst at pH 3 and b) naturally-occurring minerals as the catalyst at neutral pH

179

8.6.2 Displacement of Five Metals Sorbed on Kaolinite During Treatment by CHP

Metal displacement by iron (III)-catalyzed CHP reactions.

        Displacement of metals from kaolinite by CHP reactions using 0.9 M, 1.8 M and 2.7 M H_2O_2 catalyzed by 1 mM iron (III) at pH 3 is shown in Figure 8.6.2-1a–e. The average release of each metal over time in the reactions is shown in Table 1; values that are significantly different according to Fisher's least significant difference (LSD) procedure using $\alpha < 0.05$ are noted in the table. For cadmium (Figure 8.6.2-1a), the aqueous concentration for the pH 3 control was greater than the pH 6 control, which is expected because most metals are more soluble at acidic pH regimes. The mean cadmium amount released in the CHP reactions was greater than in either of the pH 3 and pH 6 control reactions ($\alpha \leq 0.05$), and was statistically the same for all three H_2O_2 concentrations. The displacement of copper from kaolinite under the same experimental conditions is illustrated in Figure 8.6.2-1b. Copper was released at all three H_2O_2 concentrations, with more released at 2.7 M H_2O_2 than at 0.9 M or 1.8 M H_2O_2. In contrast, lead was not released from the kaolinite in any of the reactions (Figure 8.6.2-1c). Results for nickel were similar to those for lead (Figure 8.6.2-1d); furthermore, the aqueous phase concentrations of nickel in the samples treated with CHP were lower than those in the pH 6 control. Zinc was also released from kaolinite in the reactions (Figure 8.6.2-1e), and the release was similar at all three H_2O_2 concentrations.

        In general, more metals were released into the aqueous phase in the pH 3 controls relative to the pH 6 controls. The most important property affecting metals mobility in soils is pH (Lee et al., 1998). The natural pH of soils and groundwater is generally in the range of 4 to 8.5 (Sposito, 1989), but some highly contaminated soils may be found at pH regimes as low as 3 (EPA, 1997). In general, the capacity of a soil to sorb cationic metals, such as cadmium, copper, lead, nickel, and zinc, decreases under acidic conditions (Deutsch, 1997).

        Results for metals release during iron (III)-catalyzed CHP reactions at pH 3 are summarized in Table 8.6.2-1. An additional level of metals release was evident in the CHP treatment compared to the pH 3 controls for three of the metals. For the three metals that were released in the reactions, cadmium, copper, and zinc, the amount of each metal released was similar for all three H_2O_2 concentrations, with the exception of copper, which showed greater release at the highest H_2O_2 concentration. The exchange and aqueous solubility of metals is influenced by their oxidation states; lower oxidation states may change the potential for ion exchange by orders of magnitude (Lee et al., 1998). All three H_2O_2 concentrations used in these experiments are high enough to promote formation of transient oxygen species other than hydroxyl radical, such as superoxide radical anion ($O_2\bullet^-$) and hydroperoxide anion (HO_2^-), which are generated by propagation reactions that predominate at higher H_2O_2 concentrations (Walling, 1975):

$$OH\bullet + H_2O_2 \rightarrow H_2O + HO_2\bullet \qquad\qquad\qquad\qquad\qquad\qquad [1]$$

$$HO_2\bullet \leftrightarrow O_2\bullet^- + H^+ \qquad pK_a = 4.8 \qquad\qquad\qquad\qquad\qquad [2]$$

$$HO_2\bullet + Fe^{2+} \rightarrow HO_2^- + Fe^{3+} \qquad\qquad\qquad\qquad\qquad\qquad [3]$$

Superoxide may reduce metals through the following reaction:

$$M^{2+} + O_2 \bullet^- \rightarrow M^+ + O_2 \qquad\qquad\qquad [4]$$

where M is a transition metal. Therefore, a potential mechanism for metals mobility in CHP reactions may be a reduction of the sorbed metals that promotes their release into the aqueous solution. The second-order rate constant for the reduction of iron (III) by superoxide is $(1.5 \pm 0.2) \times 10^8$ M^{-1} s^{-1} (Rush and Bielski, 1985), and the rate constant for the reduction of copper (II) is $(6.63 \pm 0.07) \times 10^9$ M^{-1} s^{-1} (Zafiriou et al, 1998), indicating that superoxide has the potential to rapidly reduce metals, though superoxide reduction rates for other metals have not yet been determined. Nonetheless, the superoxide reduction rates of the metals investigated in this research are likely to vary (Afanas'ev, 1989); such differences would result in different rates at which the metals are reduced, which may explain the differences in metals release demonstrated in the iron (III)-catalyzed CHP reactions at pH 3. Rate constants for the reduction of metals by superoxide may aid in predicting metals release and mobility as data become available.

Metal displacement by iron (III)–NTA-catalyzed CHP reactions.
The displacement of metals from kaolinite using 0.9 M, 1.8 M and 2.7 M H_2O_2 catalyzed by iron (III)–NTA at pH 6 is shown in Figure 8.6.2-2a–e. The average release of each metal over time in the reactions is shown in Table 2; values that are significantly different according to Fisher's least significant difference (LSD) procedure using $\alpha < 0.05$ are noted in the table. Cadmium was released from kaolinite at all three concentrations of H_2O_2 (Figure 8.6.2-2a) with more released at 0.9 M and 1.8 M H_2O_2 than at 2.7 M H_2O_2 ($\alpha \leq 0.05$). Copper was also displaced at all three concentrations of H_2O_2 (Figure 8.6.2-2b), with more released at 0.9 M than at 1.8 M or 2.7 M H_2O_2 ($\alpha \leq 0.05$). Lead was displaced at all concentrations of H_2O_2 ($\alpha \leq 0.05$) (Figure 8.6.2-2c), in contrast to its lack of displacement in iron (III)-catalyzed reactions at pH 3; as with copper, more lead was released at 0.9 M H_2O_2 than at 1.8 M or 2.7 M H_2O_2 in the iron (III)–NTA-catalyzed reactions. Lead displacement in the Fe-NTA-catalyzed CHP system was unexpected because lead is usually strongly sorbed in most soil systems. However, these CHP conditions could provide an effective process for removing lead from soils and other solids. Nickel showed no significant ($\alpha \leq 0.05$) release at any H_2O_2 concentration (Figure 8.6.2-2d), similar to results for nickel in the iron (III)-catalyzed reactions at pH 3. Zinc exhibited the highest degree of release from kaolinite in iron (III)–NTA-catalyzed reactions (Figure 8.6.2-2e), and more zinc was released in the 0.9 M and 1.8 M H_2O_2 than in the 2.7 M H_2O_2 treatments ($\alpha \leq 0.05$).

Percentages and concentrations of metals released from kaolinite after 120 min in the pH 6 iron (III)–NTA-catalyzed CHP reactions are listed in Table 8.6.2-2. As in the pH 3 iron (III)-catalyzed reactions, the variation in release among the metals may be due in part to different rates of reduction by superoxide. Four of the five metals were released in the iron (III)–NTA-catalyzed reactions at pH 6, compared to only three of the metals in the iron (III)-catalyzed reactions at pH 3. Nickel was not displaced under either of the two CHP process conditions, which may be due to a low rate of reduction by superoxide. Furthermore, with the exception of zinc, the concentrations of metals released from the kaolinite in CHP reactions were greater in the iron (III)–NTA-catalyzed reactions at pH 6. A possible reason for this increase in metals release is the difference in pH regimes for the iron (III)-catalyzed reaction (pH 3) vs. the iron (III)–NTA-catalyzed reactions (pH 6). If superoxide is the displacing species, its relationship to its conjugate acid, perhydroxyl radical (pK_a = 4.8), may provide an explanation for the data of

Tables 8.6.2-1 and 8.6.2-2. Perhydroxyl radical is a weaker reductant than superoxide, and may not be effective in displacing metals; it predominates over the presence of superoxide at pH 3, while the reverse is true at pH 6.

For the four metals that were released in the iron (III)–NTA-catalyzed reactions, displacement decreased with increasing H_2O_2 concentration, in contrast to the pH 3 iron (III)-catalyzed reactions in which varying the H_2O_2 concentration had little or no effect. Sun and Pignatello (1992) tested iron (III) chelates as CHP catalysts and found that NTA was a very effective ligand but was also rapidly oxidized in the reactions. They found that at hydrogen peroxide concentrations as low as 10 mM, NTA was oxidized and iron (III) precipitated within 2–3 hr. At the higher hydrogen peroxide concentrations used in this study NTA destruction was likely more rapid. Destruction of NTA at the highest H_2O_2 concentrations may have been so rapid that NTA was completely destroyed after catalyzing only minimal superoxide generation in the system, resulting in less metals release at the highest H_2O_2 concentrations. If the NTA chelate was not destroyed, lower metals release may have been because the higher concentrations of reducing species formed at higher H_2O_2 concentrations may have been negated by the higher oxidation potential due to the higher concentration of H_2O_2 in the system.

Based on the hypothesis that propagation reactions driven by the relatively high H_2O_2 concentrations used in the experiments may generate the metal-releasing species, CHP reactions were repeated using 1 mM iron (III) at pH 3 and 0.2 M H_2O_2, a concentration that promotes minimal generation of non-hydroxyl radical species (Haag and Yao, 1993). The reactions were conducted with zinc, which was released in the greatest amount of the five metals tested in both pH 3 iron (III)-catalyzed reactions and pH 6 iron (III)–NTA-catalyzed reactions, and with nickel, which was not released under either condition and which was used as a negative control. These reaction conditions resulted in no significant displacement of nickel and zinc ($\alpha \leq 0.05$) (Figures 8.6.2-3a–b). These results support the concept that a non-hydroxyl radical species generated by propagation reactions at high H_2O_2 concentrations results in metals displacement. The data of Figure 8.6.2-3 suggest that, if H_2O_2 concentrations are maintained at a lower concentration (0.2 M), metals displacement will likely not occur.

The comparison of pH 3 iron (III)- vs. pH 6 iron (III)–NTA-catalyzed CHP systems demonstrates that metals displacement in the reactions is not governed solely by acidic pH, which is a predominant mechanism for the leaching of metals from soils (Mulligan et al., 2001). Rather, the release of metals in CHP systems is high at the neutral pH used in the iron (III)–NTA-catalyzed CHP systems, in which a transient oxygen species generated with high H_2O_2 concentrations may mediate the displacement of metals from kaolinite. CHP reactions conducted in the kaolinite slurries may be considered simple physical systems compared to soils and subsurface solids, which contain a wide range of exchange sites on manganese oxides, iron oxides, and organic matter. Although the results of this research show that metals may be released from soils and subsurface solids due to treatment with CHP, the metals release in natural soils and surface regimes may not be as extensive because of the quantity and range of cation exchange sites. Furthermore, metals release may potentially be prevented if H_2O_2 concentrations are maintained below 0.2 M.

Increased metal mobility associated with ISCO processes has recently become a concern among regulators.   Use of permanganate ISCO can result in increased soluble metals

concentrations downgradient from the point of injection because 1) potassium permanganate contains metal impurities, and 2) permanganate impacts metal behavior by altering the system pH, oxidation-reduction potential, and organic carbon structure (Crimi and Siegrist, 2004). The results of this research demonstrate that CHP reactions also displace metals from contaminated soils, and that leaching of metals may be significant when CHP is used to remediate soil and groundwater systems contaminated with both heavy metals and organic contaminants. However, the displacement of metals can be minimized by using dilute H_2O_2 during CHP ISCO. Furthermore, the displacement of metals from solids using an iron (III)–NTA chelate at neutral pH may have positive environmental applications such as treating metal-laden biosolids, tank-bottom residuals containing metals, and metal-contaminated construction materials and debris. Subsequent research is focusing on confirming the transient oxygen species in CHP systems responsible for metals displacement from soils.

Conclusions

Five transition metals (cadmium, copper, lead, nickel and zinc) sorbed on kaolinite were used to study the effect of CHP on metal displacement. Iron (III) at pH 3 and iron (III)–NTA chelate at pH 6 were used to catalyze CHP reactions using 0.9 M, 1.8 M, and 2.7 M H_2O_2, and to evaluate the potential for releasing metals from the model sorbent kaolinite. In CHP reactions at pH 3 using soluble iron (III) as the catalyst, zinc, cadmium, and copper were released into the aqueous phase significantly more than in control systems at pH 3 and pH 6, while lead and nickel were not displaced. In CHP reactions at pH 6 using iron (III)-NTA as the catalyst, zinc, cadmium, copper, and lead were released compared to control samples, while there was no significant release of nickel. The concentrations of the metals released into the aqueous phase were higher in the iron (III)–NTA catalyzed systems than in the iron (III)-catalyzed systems.

Both systems contained concentrations of H_2O_2 high enough to generate non-hydroxyl radical reactive species such as superoxide, which may reduce sorbed metals and facilitate their release. Variations in the release of the metals tested may be due to differences in reduction rates by superoxide. The generally greater release of metals in the pH 6 iron (III)–NTA-catalyzed reactions may be due to higher concentrations of superoxide existing at the higher pH, where its presence is favored over its conjugate acid, perhydroxyl radical. Reactions conducted with iron (III) at pH 3 using 0.2 M H_2O_2, a concentration that promotes minimal generation of non-hydroxyl radical species, showed no release of zinc, further confirming the involvement of a non-hydroxyl radical species in metals release in CHP reactions.

Although the results of this study demonstrate that, like permanganate ISCO, CHP has he potential to mobilize metals in the subsurface, proper control of CHP process conditions (e.g. <0.2 M H_2O_2) can potentially minimize downgradient metals contamination. Use of site characterization data, treatability studies, and effective application of CHP process chemistry will also help in minimizing metals release during ISCO. In addition, further elucidation of transient oxygen species generated by the use of higher H_2O_2 concentrations in CHP reactions and their relationship to metals release will aid in minimizing metal releases during CHP ISCO remediation, and may lead to new methods for *ex situ* treatment of metals contaminated solids.

Table 8.6.2-1.   Release of metals sorbed to kaolinite after treatment with iron (III)-catalyzed CHP reactions at pH 3 with 0.9 M, 1.8 M or 2.7 M H_2O_2. Controls: deionized water used in place of H_2O_2.

Metals Released

H_2O_2 Concentration	Cd		Cu		Pb		Ni		Zn	
	%[§]	meq/L	%[§]	meq/L	%[§]	meq/L	%[§]	meq/L	%[§]	meq/L
Control	0a	0	0a	0	0	0	0	0	0a	0
0.9 M	20.0b	0.20	7.8b	0.04	n.d.[*]	0.00	n.d.	0.03	39.2b	0.40
1.8 M	27.1b	0.30	10.9b	0.06	n.d.	0.00	n.d.	0.01	43.2b	0.47
2.7 M	19.9b	0.20	20.8a	0.13	n.d.	0.00	n.d.	0.00	45.8b	0.52

[§] Means within a column followed by the same letter are not different at $P < 0.05$ on the basis of LSD

[*] not detectable

Table 8.6.2-2.   Release of metals sorbed to kaolinite after treatment with NTA–iron (III)-catalyzed CHP reactions at pH 6 with 0.9 M, 1.8 M or 2.7 M H_2O_2. Controls: deionized water used in place of H_2O_2.

Metals Released

H_2O_2 Concentration	Cd		Cu		Pb		Ni		Zn	
	%[§]	meq/L	%[§]	meq/L	%[§]	meq/L	%[§]	meq/L	%[§]	meq/L
Control	0a	0	0a	0	0a	0	0a	0	0a	0
0.9 M	24.6b	0.22	29.5b	0.16	29.4b	0.41	14.6a	0.05	28.7b	0.11
1.8 M	23.6b	0.21	19.9c	0.09	24.1c	0.31	7.8a	0.03	31.6b	0.12
2.7 M	13.2c	0.10	19.6c	0.09	23.0c	0.29	6.2a	0.02	24.8c	0.09

[§] Means within a column followed by the same letter are not different at $P < 0.05$ on the basis of LSD
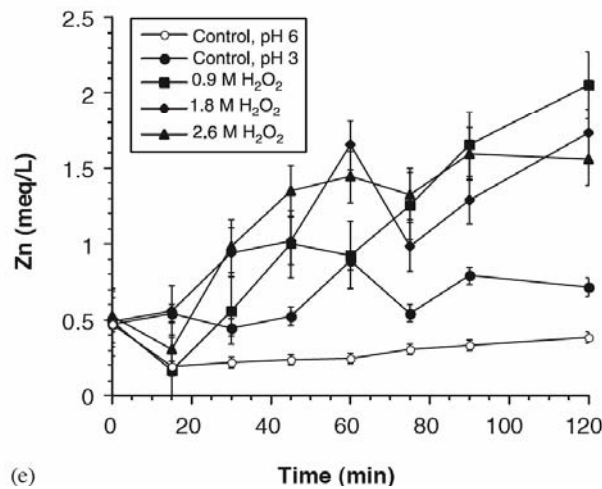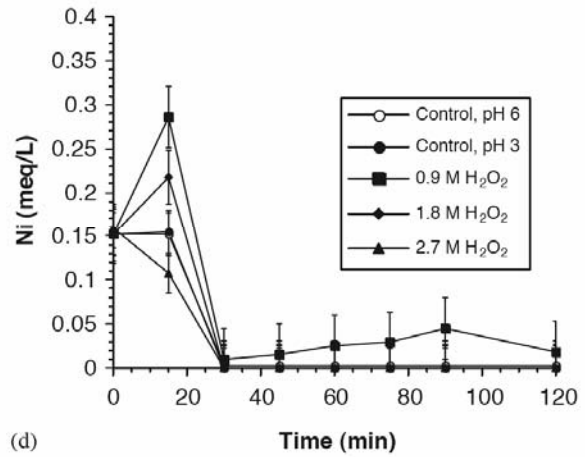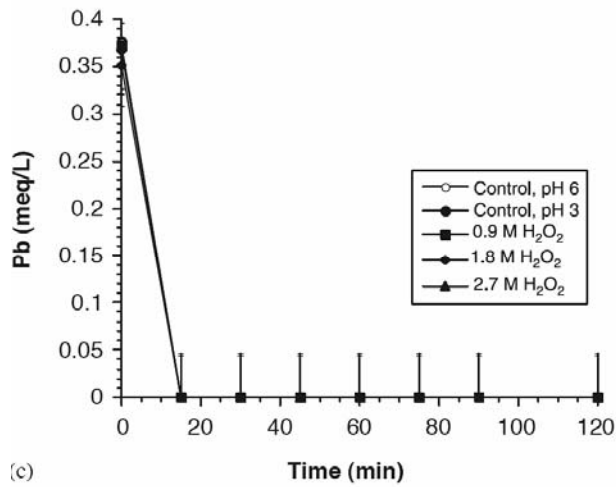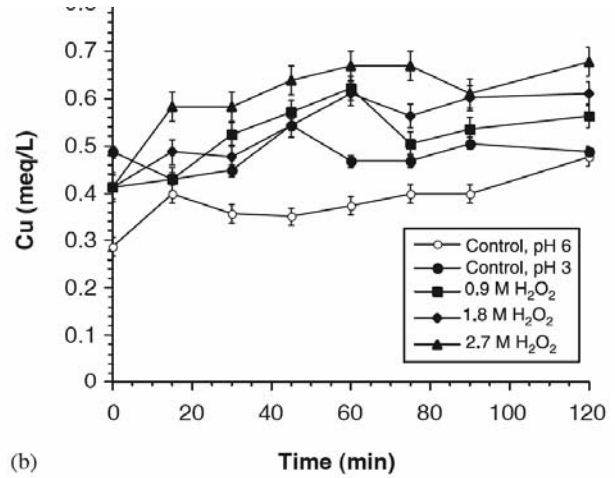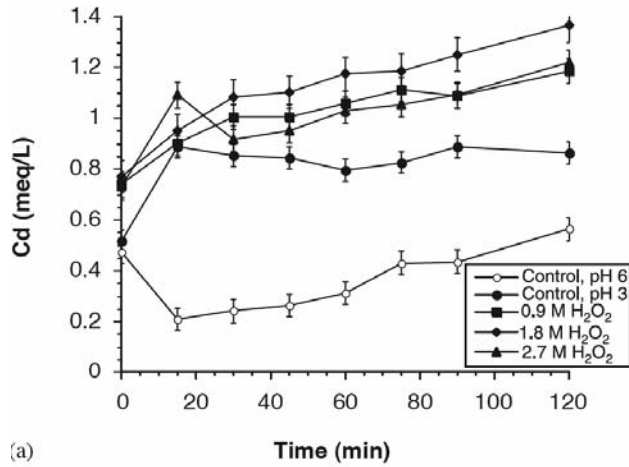
Figure 8.6.2-1. Change in metals mobility after treatment with iron (III) mediated CHP (pH 3) with varying H_2O_2 concentrations (0 M, 0.9 M, 1.8 M, 2.7 M); a) cadmium; b) copper; c) lead; d) nickel; e) zinc
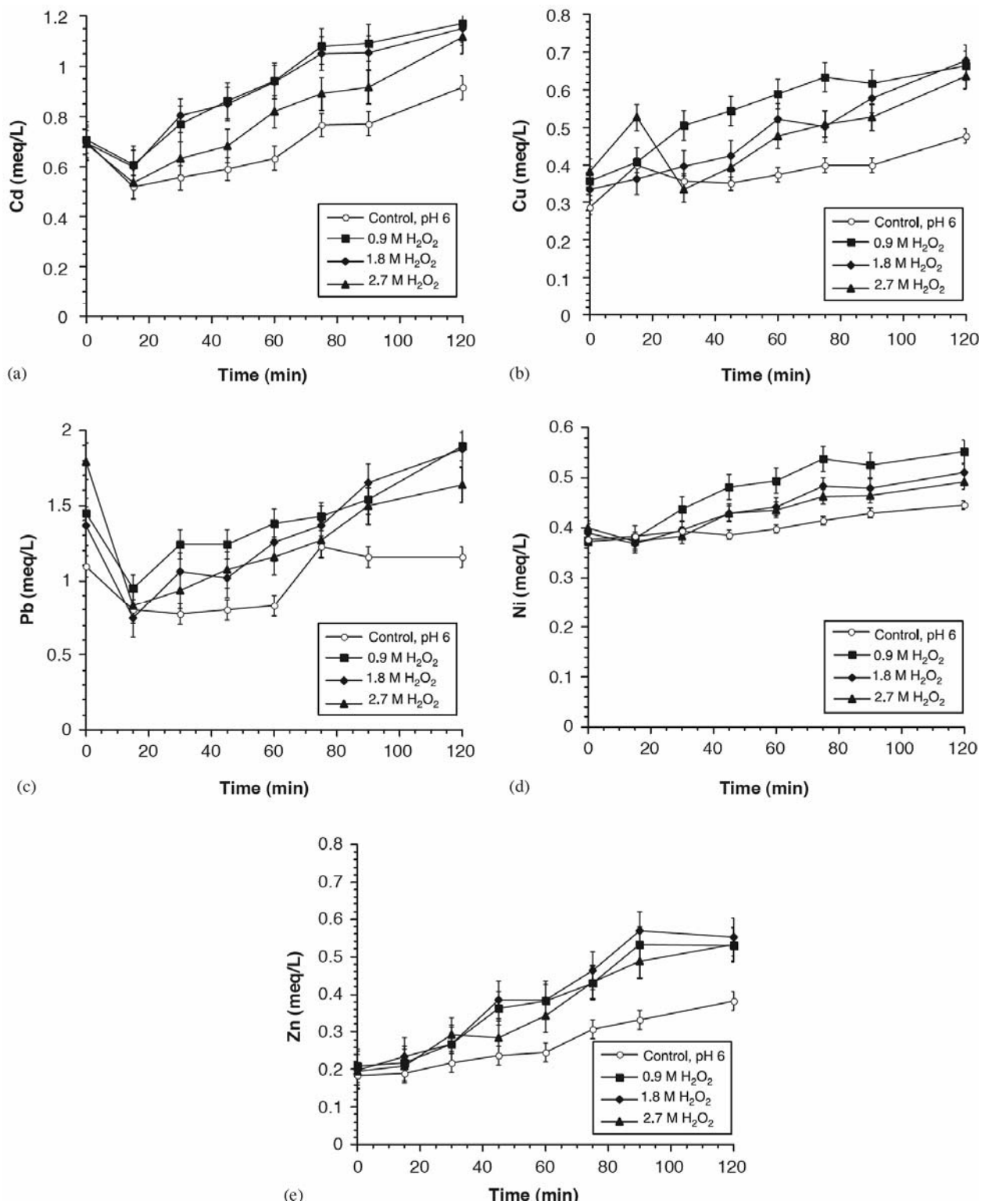
Figure 8.6.2-2. Change in metals mobility after treatment with NTA chelated iron (III) mediated CHP (pH 6) with varying H_2O_2 concentrations (0 M, 0.9 M, 1.8 M, 2.7 M); a) cadmium; b) copper; c) lead; d) nickel; e) zinc

186
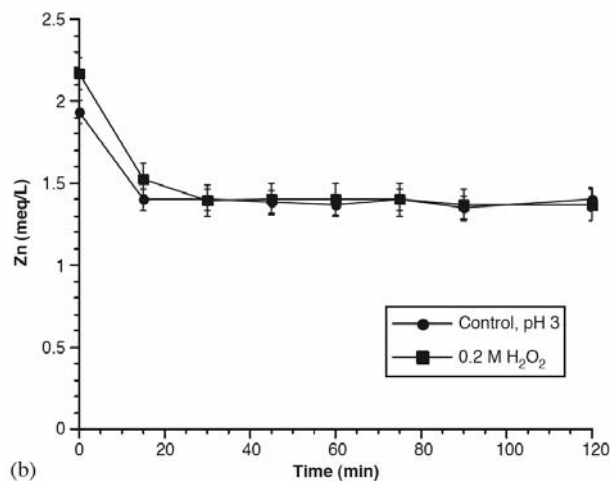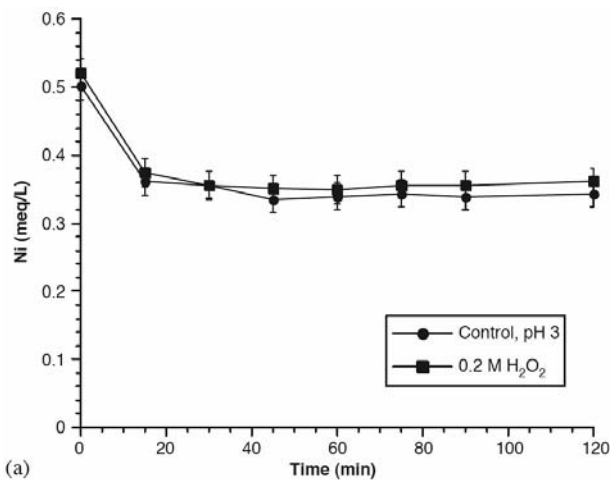
Figure 8.6.2-3. Change in metals mobility after treatment with iron (III) mediated CHP (pH 3) using 0.2 M H_2O_2; a) nickel; b) zinc

8.6.3 Fate of Sorbed Lead During Treatment of Contaminated Soils by CHP

Most soil and groundwater treatment processes target either organic contaminants or metals, but not both. Only one study has been conducted on the effect of CHP ISCO on metals release: Monahan et al. (2005) found that copper, cadmium, and zinc sorbed on kaolinite were released by CHP conducted at neutral pH, while nickel and lead releases were minimal. The purpose of this research was to provide a more detailed investigation of the effect of CHP ISCO on lead mobility in soils using natural soils rather than the simple sorbent kaolinite.

Lead desorption by CHP at pH 3.

The concentration of lead in the aqueous phase of Hanford soil slurries during CHP treatment at pH 3 is shown in Figure 8.6.3-1. The net increase in soluble lead in the treated system was approximately 0.5 mM after 120 min; however, a similar increase was found in the aqueous phase of the control system. Therefore, no significant net increase of aqueous lead concentrations was found for Hanford soil treated with CHP at pH 3. In contrast, aqueous lead concentrations in the Kamiak Butte soil and the Colorado soil increased during CHP treatment. CHP treatment of the Kamiak Butte soil resulted in increased aqueous lead concentrations of 1.5 mM while control levels increased by 1 mM, for a net increase of 0.5 mM (Figure 8.6.3-2). Similarly, CHP treatment of the Colorado soil increased the lead concentration in the aqueous phase by approximately 1 mM, while the controls increased by 0.5 mM, resulting in the same net increase of 0.5 mM (Figure 8.6.3-3). These results demonstrate that CHP reactions at pH 3 had little effect on lead desorption from the Hanford soil, but increased lead desorption from the two other soils. Organic matter is usually the primary sorbent in soil systems (Sposito, 1994). Based on the soil characteristics listed in Table 7.6.3-1, the Kamiak Butte and Colorado soils contain more soil organic matter than the Hanford soil, which may have been destroyed during CHP treatment, releasing lead into the aqueous phase.

Lead Desorption by CHP at pH 7.

CHP reactions conducted at neutral pH had a markedly different effect on lead sorption than those conducted at acidic pH. The effect of CHP on lead desorption from the Hanford soil at pH 7 is shown in Figure 8.6.3-4. Treatment of Hanford soil slurries with CHP resulted in no change in the aqueous lead concentration, while parallel control systems were characterized by a 0.5 mM increase in aqueous lead concentration. Overall, the aqueous lead concentrations in the control reactions were slightly lower at pH 7 than at pH 3. At pH 3, protons compete with lead for exchange sites on soil organic matter, which may result in increased concentrations of lead in the aqueous phase relative to pH 7. Unlike the pH 3 reactions, CHP treatment of Hanford soil at pH 7 resulted in greater sorption of lead compared to controls. The release of lead from the Kamiak Butte soil by CHP treatment at pH 7 is shown in Figure 8.6.3-5. Lead concentrations increased in the controls by 0.5 mM; however, CHP treatment resulted in a decrease in the aqueous lead concentration by approximately 1 mM. A similar trend was found in the CHP treatment of the Colorado soil at pH 7 (Figure 8.6.3-6). CHP treatment decreased the aqueous lead concentration by approximately 1.5 mM, although no changes in aqueous lead concentrations were found in the controls. These results demonstrate that for all three soils, CHP treatment at pH 7 decreased the extent of lead desorption compared to controls, and actually increased the sorption of lead relative to the initial amount of lead sorbed in two of the soils.

Possible reasons for the decreased aqueous concentrations of lead in CHP reactions at neutral pH are related to the higher oxidation-reduction potential and increased potential for precipitation at pH 7. A soil slurry containing 1.5 M hydrogen peroxide has a significantly higher oxidation reduction potential than the control systems, providing an environment favorable to lead precipitation. In addition, the iron chelates used in the pH 7 reactions are oxidized during CHP reactions (Sun and Pignatello, 1994), and the iron released would precipitate as ferrihydrite, which can then co-precipitate lead as it forms.

Scavenging of hydroxyl radical.
Hydroxyl radical is a major reactant in CHP systems, along with other reactive oxygen species. To investigate the role of hydroxyl radical in lead desorption by CHP, 1.3 M isopropanol was added as a hydroxyl radical scavenger (Watts et al., 1999). CHP treatment of the Hanford soil at pH 3 with and without the addition of isopropanol is shown in Figure 8.6.3-7. Although minimal release of lead occurred with CHP treatment, the aqueous lead concentration increased by approximately 0.5 mM compared to control reactions when hydroxyl radical was scavenged during the reactions. The effect of hydroxyl radical scavenging on CHP treatment of the Hanford soil at pH 7 is shown in Figure 8.6.3-8. Similar to the data of Figure 8.6.3-7, scavenging of hydroxyl radical increased the aqueous lead concentration by approximately 1 mM, which is in notable contrast to the net decrease in the reactions without the scavenger. These results show that hydroxyl radical is not responsible for lead release, and suggest that the activity of another reactive species responsible for lead desorption may be increased when isopropanol is added to scavenge hydroxyl radical. A possible mechanism for enhanced lead desorption is the superoxide-driven Fenton initiation reaction, which is independent of the formation of hydroxyl radical:

$$H_2O_2 + Fe^{3+} \rightarrow O_2 \bullet^- + H^+ + Fe^{2+} \tag{1}$$

The superoxide formed via equation 1 may be the species responsible for lead release when isopropanol is added to the system. Superoxide activity in water is enhanced by the presence of low molecular weight solvents, including alcohols (Smith et al., 2004); the isopropanol used to scavenge hydroxyl radical in these reactions likely enhanced the activity of superoxide. The increased activity of superoxide in the systems containing isopropanol likely lowered oxidation-reduction potential in the system, promoting the solubility of lead. Superoxide has been shown to desorb organic contaminants (Corbin et al., 2006), and may also be involved in the release of several metals sorbed on kaolinite (Monahan et al., 2005).

The release of heavy metals from soils and subsurface solids is a significant concern during ISCO treatment. Hazardous waste contamination problems are not solved if one group of contaminants (metals) is released while another group (organic contaminants) is destroyed. The results of this research demonstrate that lead release is minimal at pH 3 and the lead concentrations actually decrease at pH 7 relative to controls. These results indicate that lead mobility should not be a problem when soils and groundwater systems are treated with CHP.

Summary and Conclusions
The effect of catalyzed H_2O_2 propagations (CHP) on the release of lead sorbed to three soils was investigated at pH 3 and pH 7. At pH 3, CHP treatment resulted in increased lead concentrations in the aqueous phase with two of the soils (the Colorado and Kamiak Butte soils)

189

and the lead concentrations did not change in the other system (the Hanford soil) relative to the controls. At pH 7, the concentrations of lead decreased during the treatment of all three soils relative to the controls. Addition of the hydroxyl radical scavenger isopropanol increased lead desorption, showing that hydroxyl radical was not involved in lead desorption. However, the results of the scavenging reactions suggest that superoxide has a role in lead desorption from these three soils during CHP treatment. The results of this research show that under most CHP conditions, lead desorption from soils and solids is not a significant threat to soil and groundwater quality.
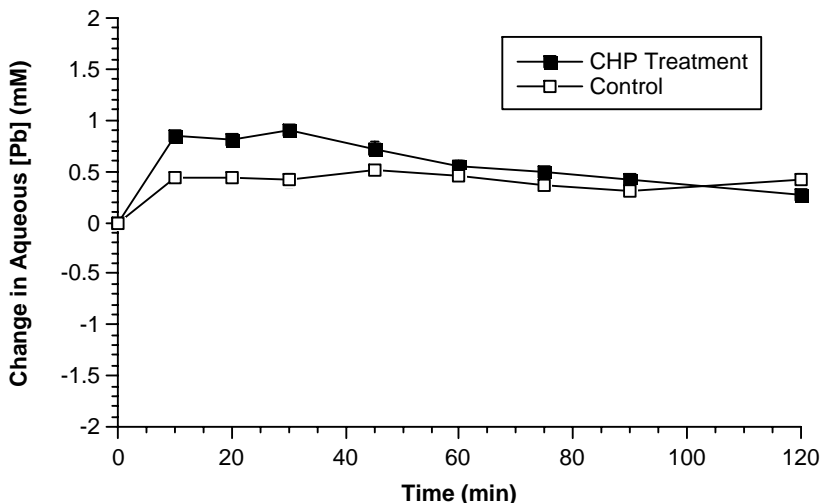
Figure 8.6.3-1. Effect of CHP at pH 3 on the mobility of lead sorbed to the Hanford soil. [Experimental conditions: 20 mL of 3 mM Pb exchanged onto 1 g Hanford soil; CHP reactions: 5 mM iron (III), and 1.5 M H_2O_2; 18 mL total reaction volume; T = 23±˚C]
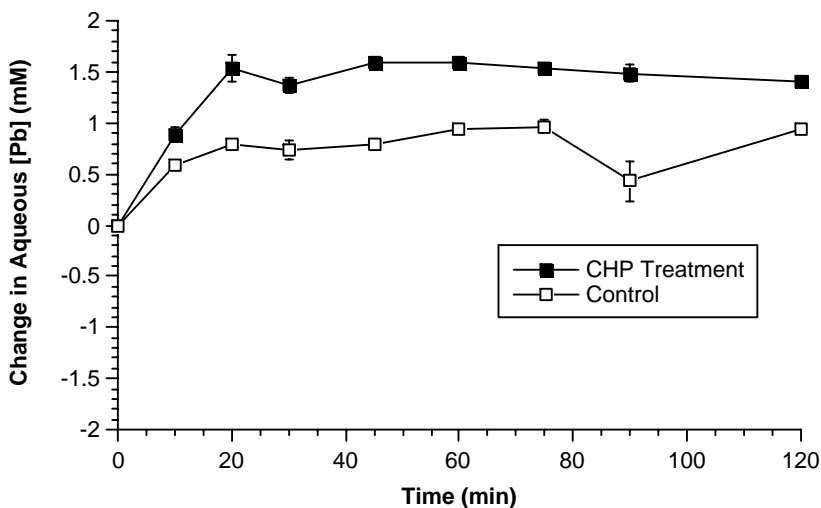
Figure 8.6.3-2. Effect of CHP at pH 3 on the mobility of lead sorbed to the Kamiak Butte soil. [Experimental conditions: 20 mL of 5 mM Pb exchanged onto 1 g Kamiak Butte soil; CHP reactions: 5 mM iron (III), and 1.5 M H_2O_2; 18 mL total reaction volume; T = 23±˚C]

190
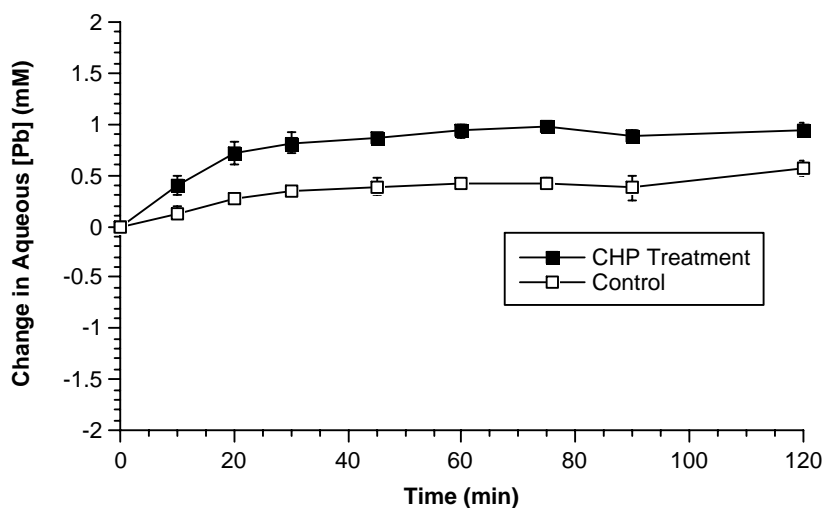
Figure 8.6.3-3. Effect of CHP at pH 3 on the mobility of lead sorbed to the Colorado soil. [Experimental conditions: 20 mL of 5 mM Pb exchanged onto 1 g Colorado soil; CHP reactions: 5 mM iron (III), and 1.5 M H_2O_2; 18 mL total reaction volume; T = 23±˚C]
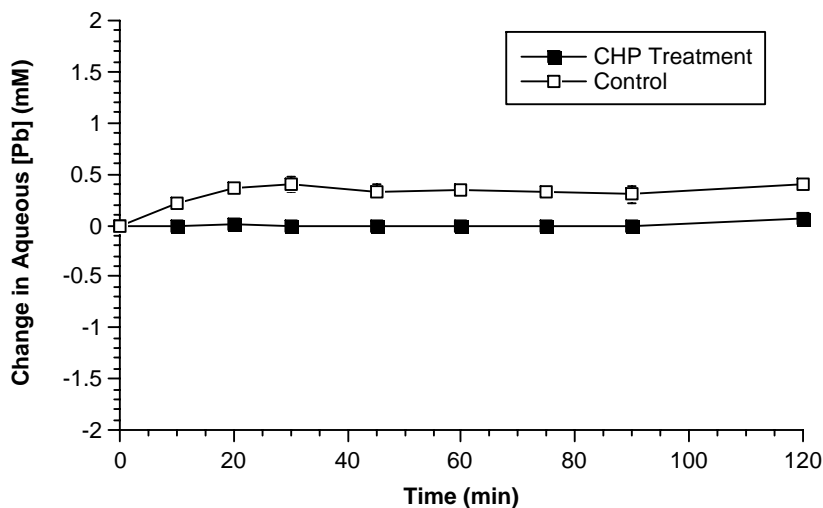
Figure 8.6.3-4. Effect of CHP at pH 7 on the mobility of lead sorbed to the Hanford soil. [Experimental conditions: 20 mL of 3 mM Pb exchanged onto 1 g Hanford soil; CHP reactions: 5 mM iron (III)-NTA chelate, and 1.5 M H_2O_2; 18 mL total reaction volume; T = 23±˚C]
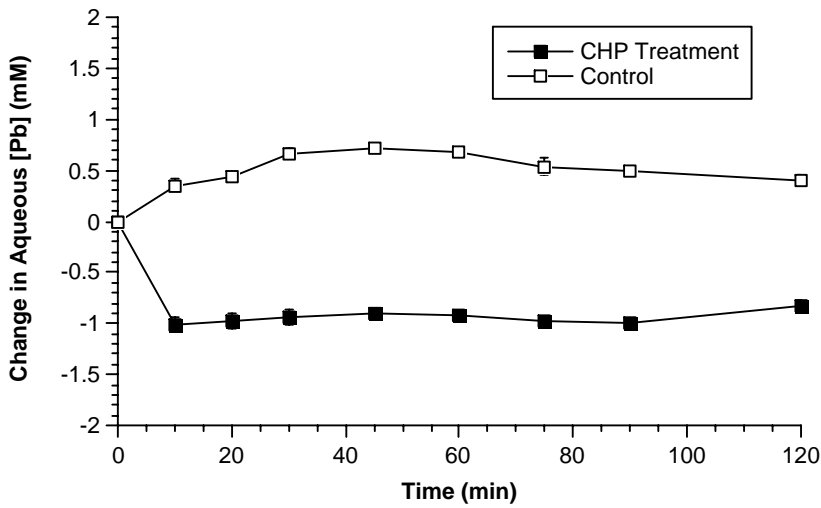
Figure 8.6.3-5. Effect of CHP at pH 7 on the mobility of lead sorbed to the Kamiak Butte soil. [Experimental conditions: 20 mL of 5 mM Pb exchanged onto 1 g Kamiak Butte soil; CHP reactions: 5 mM iron (III)-NTA chelate, and 1.5 M H_2O_2; 18 mL total reaction volume; T = 23$\pm$˚C]
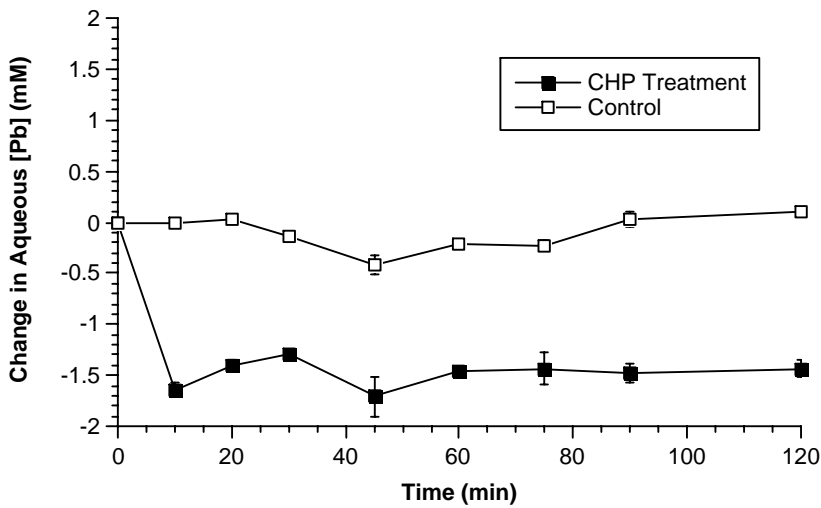
Figure 8.6.3-6. Effect of CHP at pH 7 on the mobility of lead sorbed to the Colorado soil. [Experimental conditions: 20 mL of 5 mM Pb exchanged onto 1 g Colorado soil; CHP reactions: 5 mM iron (III)-NTA chelate, and 1.5 M H_2O_2; 18 mL total reaction volume; T = 23$\pm$˚C]
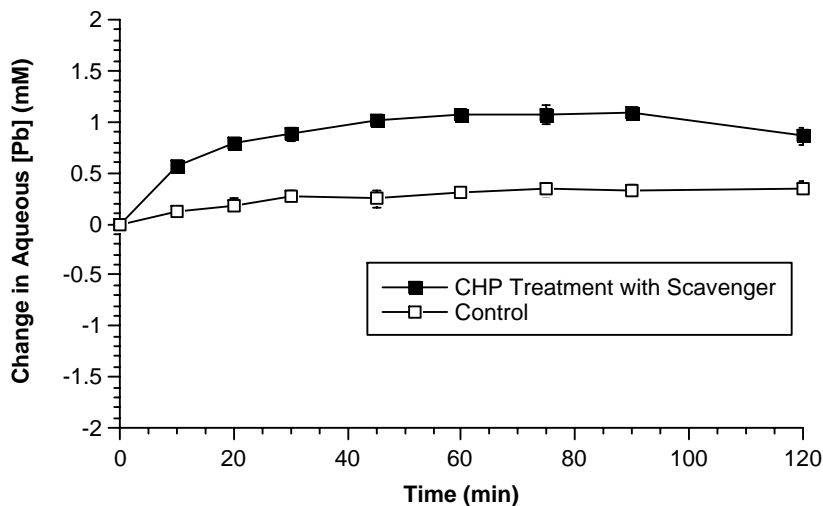
Figure 8.6.3-7. Effect of hydroxyl radical scavenging on the mobility of lead sorbed to Hanford soil during CHP treatment at pH 3. [Experimental conditions: 20 mL of 3 mM Pb exchanged onto 1 g Hanford soil; CHP reactions: 5 mM iron (III), 1.5 M H_2O_2 and 1.3 M isopropanol; 19.9 mL total reaction volume; T = $23\pm°C$]
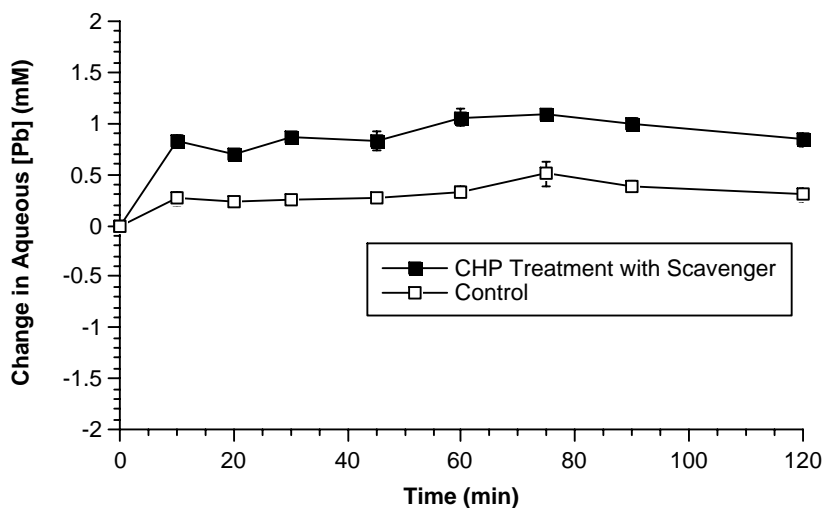
Figure 8.6.3-8. Effect of hydroxyl radical scavenging on the mobility of lead sorbed to Hanford soil during CHP treatment at pH 7. [Experimental conditions: 20 mL of 3 mM Pb exchanged onto 1 g Hanford soil; CHP reactions: 5 mM iron (III)-NTA chelate, 1.5 M H_2O_2 and 1.3 M isopropanol; 19.9 mL total reaction volume; T = $23\pm°C$]

8.6.4 Fate of Sorbed Cadmium During Treatment of Contaminated Soils by CHP

Cadmium desorption by CHP at pH 3 with and without hydroxyl radical scavenging.

The release of cadmium from the Colorado soil by CHP treatment at pH 3 is shown in Figure 8.6.4-1. Cadmium release was minimal in the control systems with an increase in the aqueous cadmium concentration of approximately 0.4 mM over 120 min. However, CHP treatment resulted in significantly higher cadmium release, with a 1.2 mM increase in the concentration of cadmium in the aqueous phase. Cadmium release was minimal when hydroxyl radical was scavenged from the system by the addition of excess isopropanol, with an increase of 0.7 mM in the scavenged system compared to an increase of 0.6 mM in the corresponding control. These results suggest that hydroxyl radical is involved in cadmium release from the Colorado soil.

The release of cadmium from the Kamiak Butte soil by CHP treatment at pH 3 is shown in Figure 8.6.4-2. Similar to the Colorado soil, the concentration of cadmium in the aqueous phase increased by 0.4 mM in the control and by 1.1 mM in reactors treated with CHP after 120 min. Scavenging of hydroxyl radical with isopropanol increased the amount of cadmium released, with a 0.7 mM increase in the aqueous cadmium concentration in the treated sample compared to a 0.4 mM increase in the control.

The release of cadmium from the Hanford soil by CHP treatment at pH 3 is shown in Figure 8.6.4-3. Net cadmium release from the Hanford soil was slightly less that that from the Colorado and Kamiak Butte soils, with a 1.0 mM increase in the aqueous phase concentration of cadmium in the CHP system and a 0.4 mM increase in the control. Scavenging of hydroxyl radical had a less pronounced effect on cadmium release from the Hanford soil than from the Colorado and Kamiak Butte soils. After 120 min, cadmium in the aqueous phase increased by 0.7 mM in the CHP treatment with scavenging, and a 0.3 mM increase in the corresponding control.

The release of cadmium from illite by CHP treatment at pH 3 is shown in Figure 8.6.4-4. The net release of cadmium was the lowest of the four solids evaluated, with an increase of 0.7 mM in the aqueous phase concentration of cadmium in the CHP treatment and an increase of 0.4 mM in the corresponding control. Scavenging of hydroxyl radical had a minimal effect on cadmium release, with a 0.3 mM increase in the scavenged system compared to a 0.1 mM increase in the corresponding control.

Cadmium desorption by CHP at pH 7 with and without hydroxyl radical scavenging.

The concentration of cadmium in the aqueous phase as a function of time in the Colorado soil by CHP reactions conducted at pH 7 is shown in Figure 8.6.4-5. In contrast to the reactions conducted at pH 3 in the Colorado soil, aqueous cadmium concentrations decreased by approximately 0.2 mM in the treated samples, while they increased by 0.3 mM in control reactions. In CHP systems at pH 7 with isopropanol added to scavenge hydroxyl radicals, 0.6 mM cadmium was released, while 0.4 mM cadmium was released in the corresponding scavenging control.

Cadmium release from the Kamiak Butte soil during CHP treatment at pH 7 is shown in Figure 8.6.4-6. No change in aqueous cadmium concentration was observed in the CHP-treated

194

samples: however, cadmium concentration increased by 0.2 mM in the parallel control reactions. Cadmium concentrations in CHP reactions with the addition of the hydroxyl radical scavenger isopropanol increased to 0.7 mM while cadmium concentrations in the corresponding control systems increased by 0.3 mM.

When CHP reactions were conducted with the Hanford soil, cadmium concentrations decreased by 0.2 mM; in contrast, cadmium concentrations in parallel control systems increased by 0.6 mM (Figure 8.6.4-7). Parallel reactions in which hydroxyl radical was scavenged resulted in an increase in soluble cadmium of 0.6 mM, while cadmium concentrations in control systems containing the scavenger increased by 0.2 mM.

Cadmium concentrations in the illite systems treated with CHP at pH 7 are shown in Figure 8.6.3-8. Concentrations of cadmium declined by 0.8 mM while the cadmium concentrations in parallel control systems decreased by only 0.2 mM. Cadmium concentrations in systems in which hydroxyl radical was scavenged showed quite different results; both the CHP system with scavenger addition and the control with the scavenger exhibited no measurable cadmium release.

The results shown in Figures 8.6.4-1–4 show that cadmium was released in all CHP reactions at pH 3. The data of Figure 8.6.4-1 show that cadmium release was highest in the Colorado soil, which has the highest SOM. In contrast, cadmium release from illite, which has no detectable OM, was minimal (Figure 8.6.4-4). The relationship of the amount of organic matter in the sorbent to its release of cadmium is shown in Figure 8.6.4-9; a strong correlation exists for net cadmium release over concentrations in the controls, as a percentage of the amount of cadmium originally sorbed to the solids, and the percentage of organic matter in the sorbents ($R^2 = 0.99$). At pH 3, SOM is protonated and is released from where it is sorbed onto organic solids. This release provides the potential for greater oxidation of the SOM, Bissey et al. (2006) found that CHP treatment of soils at pH 3 destroyed SOM more rapidly than at neutral pH. Such SOM destruction by CHP treatment can potentially release cadmium; therefore, CHP treatments should be conducted at neutral pH to minimize cadmium release.

In contrast to the results at pH 3, no cadmium was released from any of the four solids during CHP treatment at pH 7; furthermore, aqueous cadmium concentrations actually decreased at pH 7 in the Colorado soil, Hanford soil, and illite systems. Lower aqueous phase concentrations of most metals, including cadmium, are characteristic of neutral and higher pH regimes; the high oxidation potential provided by the hydrogen peroxide in the system combined with the neutral pH regime likely resulted in a decrease in soluble cadmium concentration, probably by precipitation (Sposito, 1989).

Although cadmium concentrations generally decreased in CHP systems at pH 7, the net aqueous cadmium concentrations increased compared to control reactions when hydroxyl radical was scavenged during the reactions in all four solid systems. These results suggest that the activity of another reactive species responsible for cadmium desorption may be increased when isopropanol is added to scavenge hydroxyl radical. A possible mechanism for enhanced cadmium desorption is the superoxide-driven Fenton initiation reaction, which is independent of the formation of hydroxyl radical:

$$H_2O_2 + Fe^{3+} \rightarrow O_2\bullet^- + H^+ + Fe^{2+} \qquad pK_a = 4.8 \qquad\qquad [1]$$
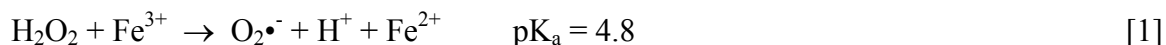
The superoxide formed via equation 1 may be the species responsible for cadmium release when isopropanol is added to the system. Superoxide activity in water is enhanced by the presence of low molecular weight solvents, including alcohols (Smith et al., 2004); the isopropanol used to scavenge hydroxyl radical in these reactions likely enhanced the activity of superoxide. The increased activity of superoxide in the systems containing isopropanol likely lowered the oxidation-reduction potential in the system, promoting the solubility of cadmium. Superoxide has been shown to desorb organic contaminants (Corbin et al., 2006) and may also be involved in the release of several metals sorbed on kaolinite (Monahan et al., 2005).

The release of heavy metals from soils and subsurface solids is a significant concern during ISCO treatment. Hazardous waste contamination problems are not solved if one group of contaminants (metals) is released while another group (organic contaminants) is destroyed. The results of this research demonstrate that cadmium release is directly proportional to the SOM content of the soil when reactions are conducted at pH 3 and the cadmium concentrations actually decrease at pH 7 relative to controls. These results indicate that cadmium mobility should not be a problem when soils and groundwater systems are treated with CHP at neutral pH.

Figure 8.6.4-1. Effect of CHP at pH 3 with and without hydroxyl radical scavenging on the mobility of Cadmium sorbed to the Colorado soil.
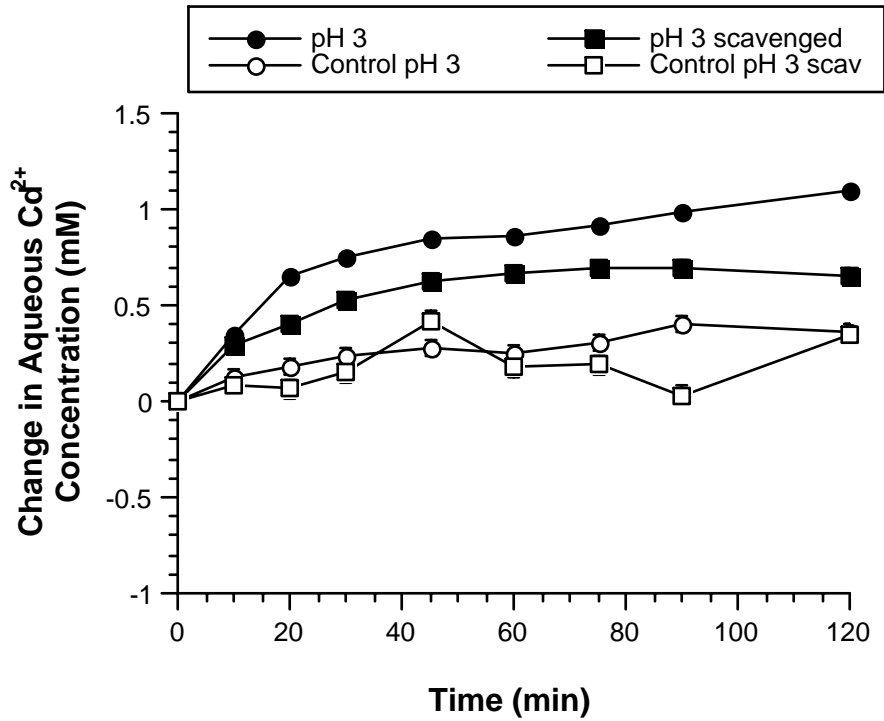
Figure 8.6.4-2. Effect of CHP at pH 3 with and without hydroxyl radical scavenging on the mobility of Cadmium sorbed to the Kamiak Butte soil.
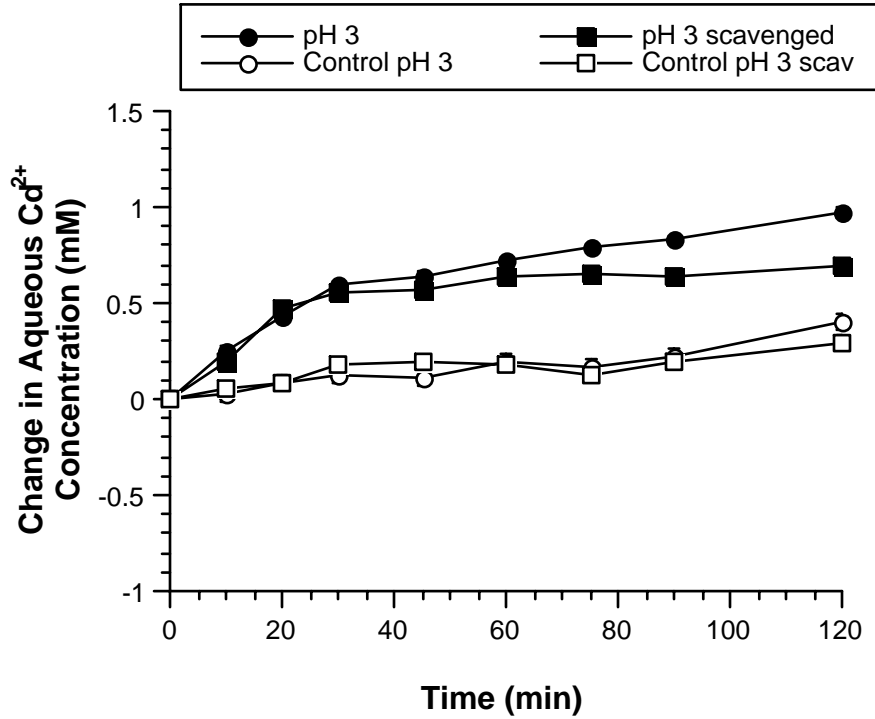
Figure 8.6.4-3. Effect of CHP at pH 3 with and without hydroxyl radical scavenging on the mobility of Cadmium sorbed to the Hanford soil.
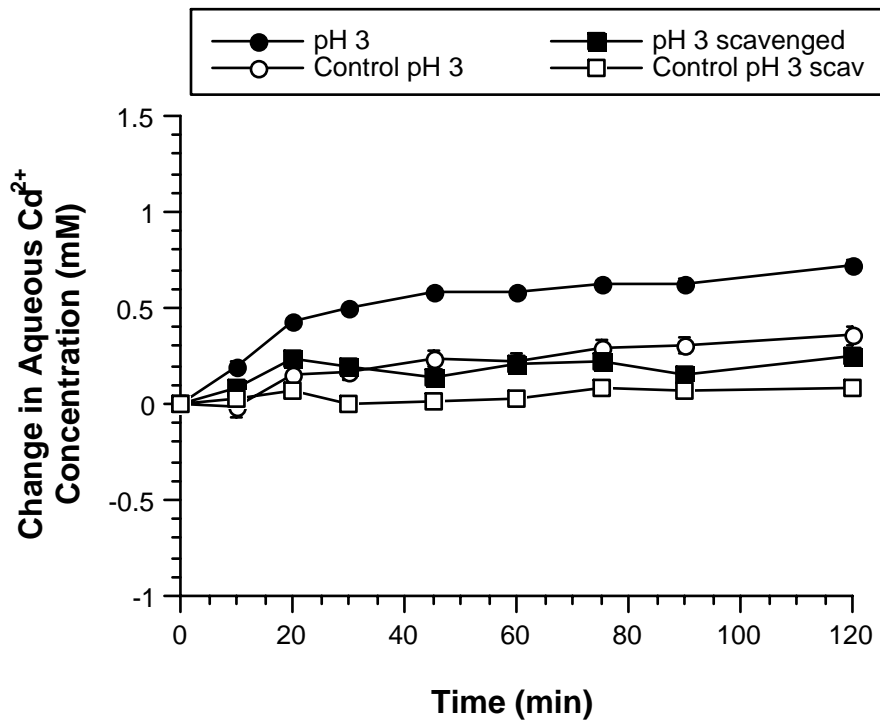
Figure 8.6.4-4. Effect of CHP at pH 3 with and without hydroxyl radical scavenging on the mobility of Cadmium sorbed to illite.
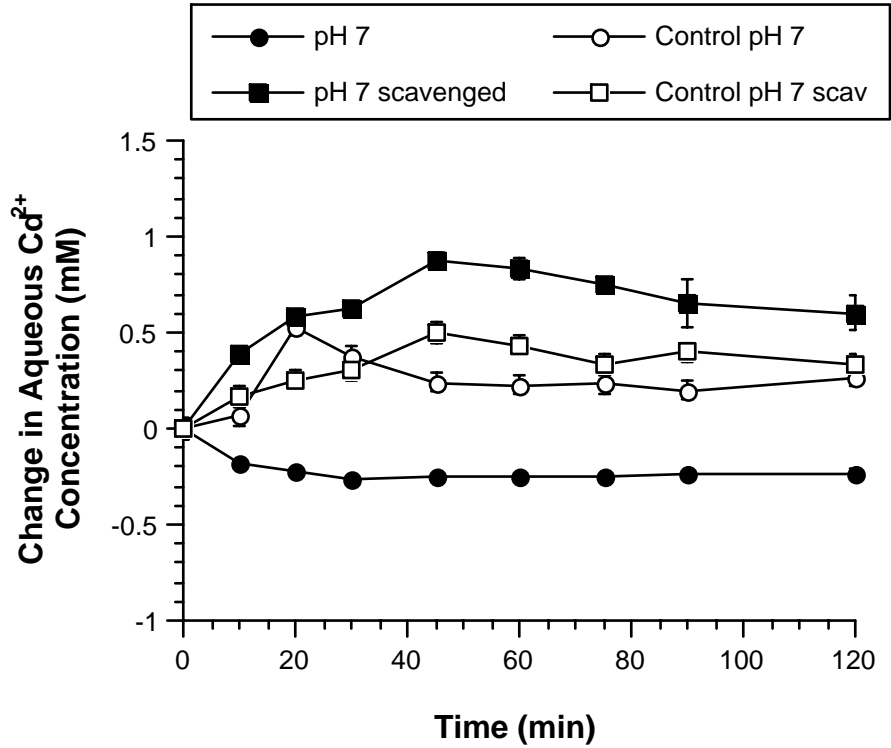
Figure 8.6.4-5. Effect of CHP at pH 7 with and without hydroxyl radical scavenging on the mobility of Cadmium sorbed to the Colorado soil.
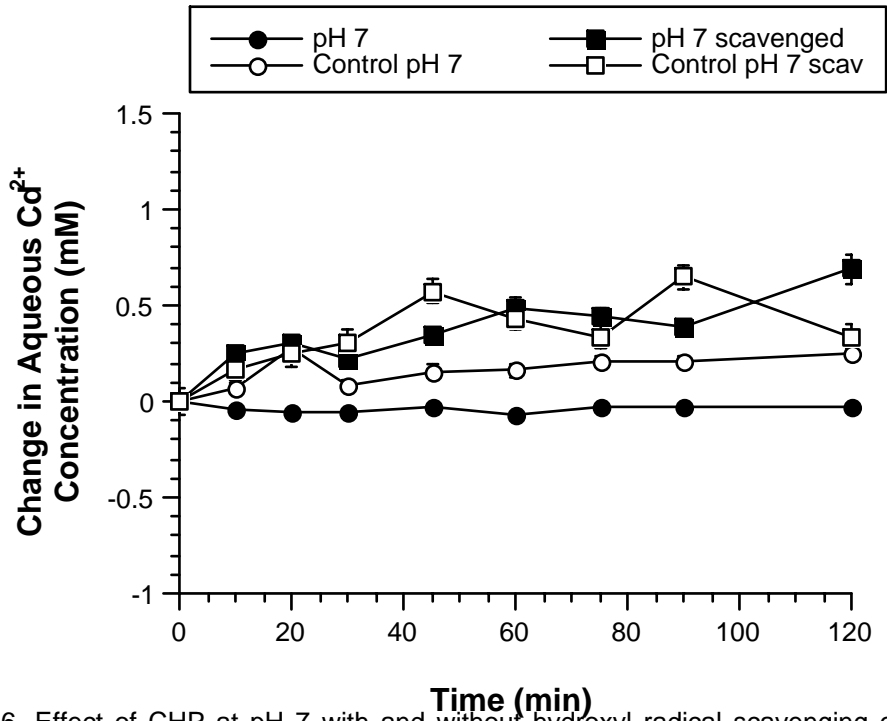
Figure 8.6.4-6. Effect of CHP at pH 7 with and without hydroxyl radical scavenging on the mobility of Cadmium sorbed to the Kamiak Butte soil.

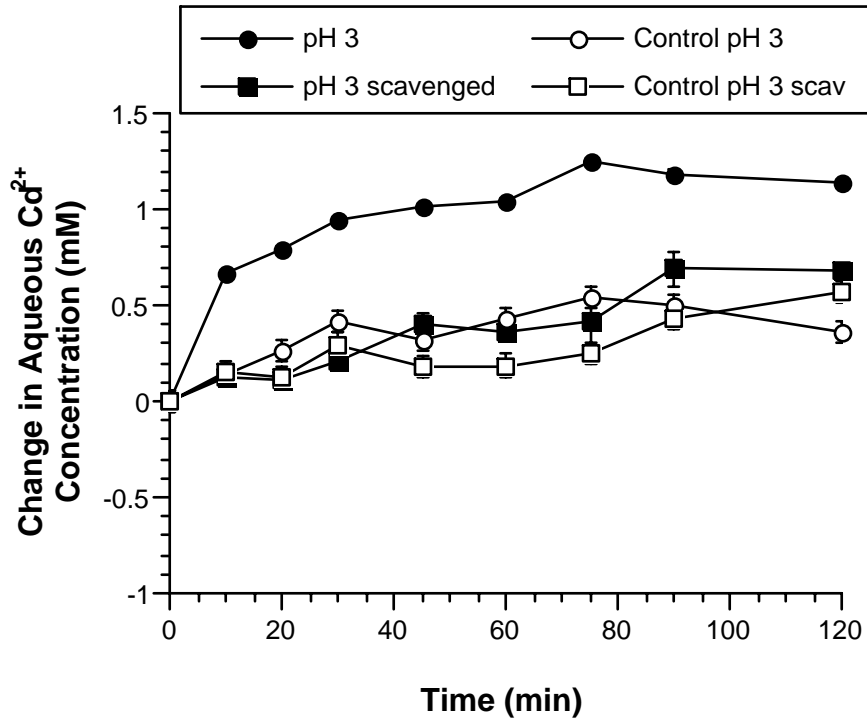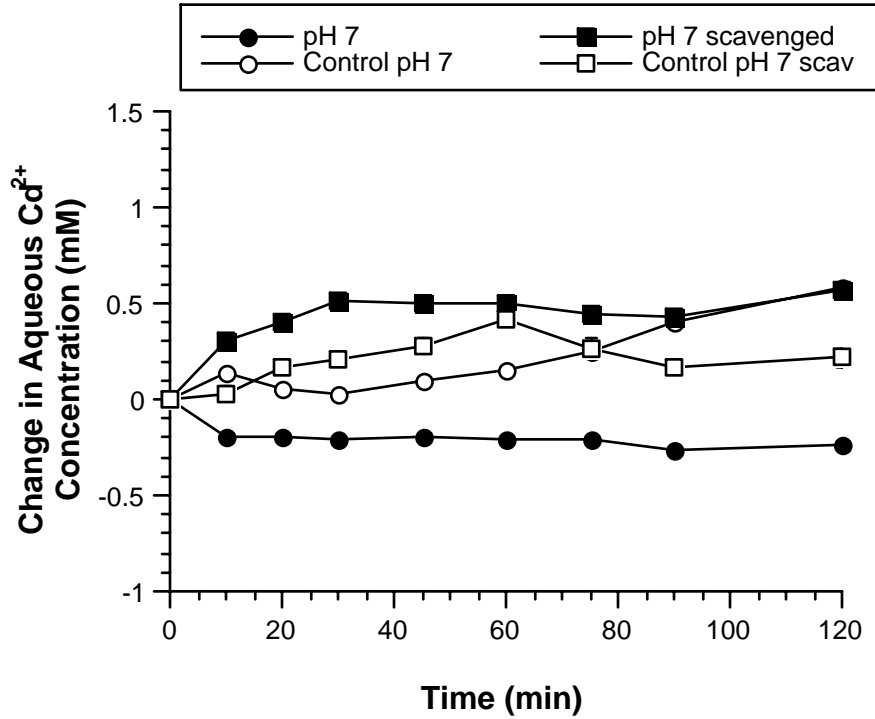Figure 8.6.4-7. Effect of CHP at pH 7 with and without hydroxyl radical scavenging on the mobility of Cadmium sorbed to the Hanford soil.
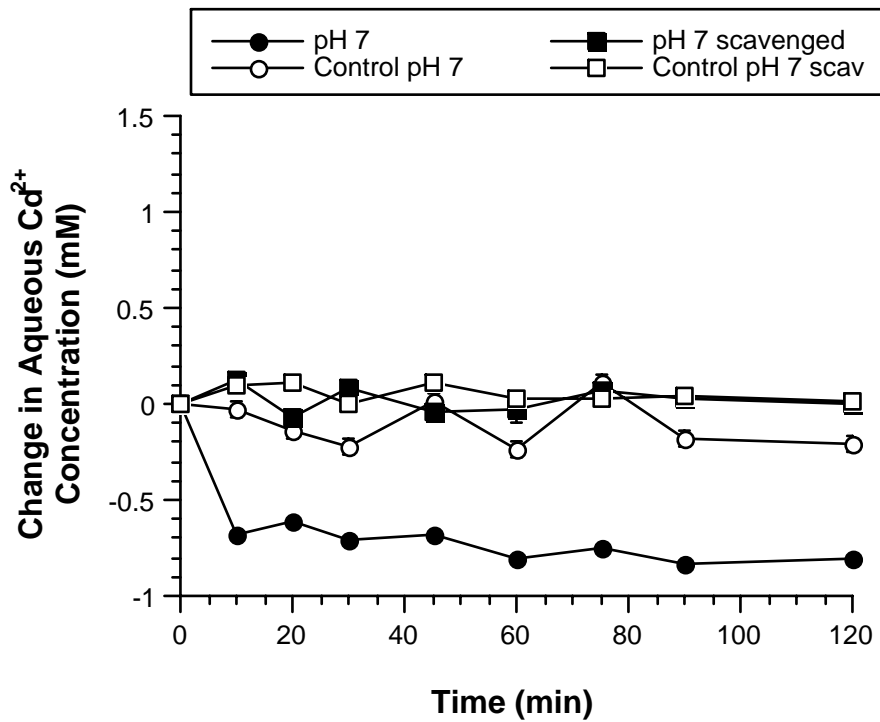
Figure 8.6.4-8. Effect of CHP at pH 7 with and without hydroxyl radical scavenging on the mobility of Cadmium sorbed to illite.
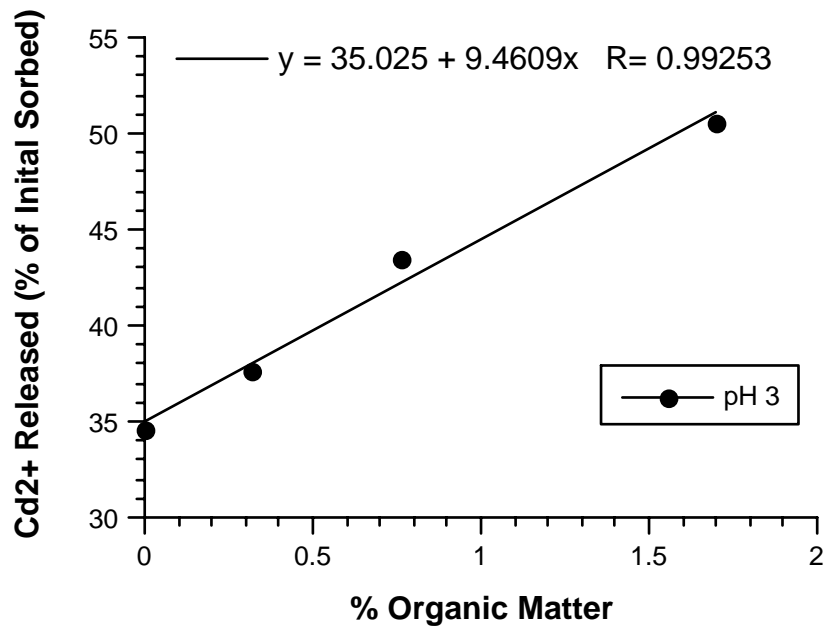
Figure 8.6.4-9. Correlation of cadmium release from sorbents in CHP reactions at pH 3 to the organic matter content of the sorbents.

8.6.5 Hydrogen Peroxide Stabilization in Minerals and Soils

Screening of potential hydrogen peroxide stabilizers.

Numerous organic acids were screened for their ability to deactivate the catalytic activity of iron and manganese oxides. The organic acids that were evaluated include:

DTPA (Diethylenetriamine pentaacetic acid)
Citric acid
Gallic acid
Malic acid
Malonic acid
Oxalacetic acid
Oxalic acid
Phytic acid
Pyruvic acid
Succinic acid

The potential stabilizers were screened by adding each stabilizer to a 2% solution of hydrogen peroxide, mixing the hydrogen peroxide-stabilizer solution containing 1 g of each of goethite, hematite, manganite, or pyrolusite; hydrogen peroxide residuals were then quantified over several days. The rates of hydrogen peroxide decomposition were then compared to rates in parallel systems with no stabilizers. The results of initial screening efforts showed that malonate, citrate, and phytate are the most effective stabilizers.

Hydrogen peroxide decomposition and stabilization in mineral slurries at pH 3.

The decomposition of hydrogen peroxide in goethite slurries at pH 3 with and without stabilizers is shown in Figure 8.6.5-1. The hydrogen peroxide half-life in the unstabilized goethite slurries was 3 hr. Stabilization of hydrogen peroxide with citrate, malonate, and phytate significantly increased hydrogen peroxide lifetimes; the hydrogen peroxide half-life in goethite slurries containing 1 M citrate was 60 hr, the hydrogen peroxide half-life in 1 M malonate studies was 120 hr, and the hydrogen peroxide half-life in 1 M phytate solutions was 15 hr.

The decomposition of hydrogen peroxide in unstabilized and stabilized hematite slurries at pH 3 is shown in Figure 8.6.5-2. The hydrogen peroxide half-life in the unstabilized systems was 7 hr. Citrate and malonate were the most effective stabilizers in hematite slurries, increasing the hydrogen peroxide half-life to well over 350 hr. Phytate, while not as effective as citrate or malonate, increased the hydrogen peroxide half-life to 55 hr. Hydrogen peroxide decomposition in manganite slurries at pH 3 is shown in Figure 8.6.5-3. The hydrogen peroxide half-life in unstabilized manganite slurries was 20 min. Both citrate and malonate increased the half-life to 25 hr, while phytate increased the half life to 10 hr.

Hydrogen peroxide decomposition in unstabilized pyrolusite slurries at pH 3 is shown in Figure 8.6.5-4. Pyrolusite was highly reactive in decomposing unstabilized hydrogen peroxide resulting in a half-life of approximately 1 min. Citrate was the most effective stabilizer, increasing the hydrogen peroxide half-life to 15 min. Both malonate and phytate increased the half-life to 10 min.

Hydrogen peroxide decomposition and stabilization in mineral slurries at pH 7.

The decomposition of hydrogen peroxide in goethite slurries at pH 7 with and without stabilizers is shown in Figure 8.6.5-5. The hydrogen peroxide half-life in the unstabilized goethite slurries was 18 min. Stabilization of hydrogen peroxide with citrate, malonate, and phytate significantly increased hydrogen peroxide lifetimes; the hydrogen peroxide half-life in goethite slurries containing 1 M citrate studies was 18 hr, the hydrogen peroxide half-life in 1 M malonate was 12 hr, and the hydrogen peroxide half-life in 1 M phytate solutions was 30 hr.

Similar results were found in hematite slurries (Figure 8.6.5-6). The half-life of hydrogen peroxide in unstabilized hematite slurries decomposed was 1 hr; stabilization significantly increased hydrogen peroxide stability. Addition of 1 M citrate increased the hydrogen peroxide lifetime to 18 hr. Malonate and phytate at 1 M also increased hydrogen peroxide lifetimes to 14 and 40 hr, respectively.

Hydrogen peroxide concentrations as a function of time in manganite slurries with and without the three stabilizers is shown in Figure 8.6.5-7. Unstabilized hydrogen peroxide decomposition was rapid with a hydrogen peroxide half-life of approximately 15 min. However, each of the three stabilizers increased the lifetime of hydrogen peroxide dramatically. Phytate and citrate were the most effective stabilizers, increasing the hydrogen peroxide half-life to approximately 2 hr. Malonate was nearly as effective, increasing the hydrogen peroxide half-life to approximately 1.5 hr.

Hydrogen peroxide decomposition rates as a function of time for unstabilized and stabilized pyrolusite slurries at pH 7 are shown in Figure 8.6.5-8. Unstabilized pyrolusite was highly reactive with a hydrogen peroxide half-life of <30 sec. Hydrogen peroxide stabilization significantly increased the half-life; the half-life for stabilized hydrogen peroxide was 5 min for citrate, 3 min for malonate, and 7 min for phytate.

Hydrogen peroxide is more stable at acidic pH regimes in the presence of most minerals and subsurface solids. A possible reason for such increased stability is the dissolution of some of the metal oxide minerals, particularly manganese oxides, which are potent mediators of hydrogen peroxide decomposition. Nonetheless, the stabilizers citrate, malonate, and phytate increased hydrogen peroxide stabilization to a significantly in both pH 7 and pH 3 mineral systems.

Hydrogen peroxide decomposition and stabilization in soils.

Hydrogen peroxide decomposition in slurries containing the Georgia soil at pH 7 is shown in Figure 8.6.5-9a–b. The hydrogen peroxide decomposition rate in this soil slurry was moderate, with a half-life of approximately 4 hr. Phytate addition at both 10 mM and 250 mM increased the hydrogen peroxide half-life; with 10 mM phytate addition, the hydrogen peroxide half-life increased to 9 hr (Figure 8.6.5-9a), and the addition of 250 mM increased the half-life to 15 hr (Figure 8.6.5-9b). Malonate and citrate were effective to the same degree in increasing the hydrogen peroxide half-life; 10 mM malonate or citrate increased the half-life to 6 hr, and 1 M citrate or malonate increased the half-life to 7 hr.

Hydrogen peroxide decomposition in the Maine soil under unstabilized conditions and stabilized by two concentrations of the stabilizers phytate, citrate, and malonate are shown in Figure 8.6.5-10a–b. Under conditions of no stabilization, the hydrogen peroxide half-life was 1.5

hr. Stabilization of the Maine soil with phytate was highly effective; 10 mM phytate addition increased the hydrogen peroxide half-life to 10 hr, and 250 mM phytate addition increased the half-life to 32 hr. Similar to the Georgia soil, the effectiveness of malonate and citrate stabilizers was similar. Addition of 10 mM citrate or 10 mM malonate increased the hydrogen peroxide half-life to 4 hr. Using 1 M citrate or malonate, the hydrogen peroxide half-life increased to 4 hr for citrate and 8 hr for malonate.

Hydrogen peroxide decomposition without stabilization in the California soil was very rapid with a half-life of <0.5 hr (Figure8.6.5-11a–b). However, stabilization with phytate was highly effective, increasing the half-life to 12 hr with 10 mM phytate addition and 26 hr with 250 mM phytate addition. Stabilization using citrate and malonate was strongly influenced by the stabilizer concentration. Using 10 mM citrate or malonate, the hydrogen peroxide half-life increased to 2hr; however, when 1 M citrate was added to the slurries the hydrogen peroxide half-life increased to 6 hr, and when 1 M malonate was added, the half-life increased to 12 hr.

Hydrogen peroxide concentrations as a function of time in slurries containing the Washington soil with and without stabilization are shown in Figure 8.6.5-12a–b. The unstabilized hydrogen peroxide half-life in the Washington soil was 4 hr. Hydrogen peroxide decomposition in the Washington soil was unique among the four soils studied in that all three stabilizers were equally effective, and the stabilizer concentration had minimal effect on the rate of hydrogen peroxide decomposition. The hydrogen peroxide half-life for all three stabilizers at 10 mM concentrations was approximately 12 hr and at high (250 mM or 1 M) stabilizer concentrations was 18–22 hr.

Effect of stabilizers on hydroxyl radical and superoxide generation.
The relative production of hydroxyl radicals in mineral-mediated CHP reactions with and without stabilization by 10 mM phytate is shown in Figure 8.6.5-13a–d. The relative production of hydroxyl radical as measured by oxidation of the probe molecule hexanol was different between each of the soils. In addition, detection of hydroxyl radical in some of the soils showed no difference between the stabilized and unstabilized systems, while others showed a small difference in hydroxyl radical production between stabilized and unstabilized systems. Hydroxyl radical production in the Georgia soil was greater without phytate than with phytate, with only 10% of the hexanol oxidized with phytate addition and 25% oxidized without phytate addition (Figure 8.6.5-13a). There was no difference in relative hydroxyl radical generation between unstabilized and stabilized systems in the Maine soil and the California soil, with 80% oxidation of the hexanol in the Maine soil and 85% oxidation in the California soil (Figures 8.6.4-13b and c). The relative rate of hydroxyl radical production was low in the Washington soil with 5% of the hexanol oxidized, and there was no difference in hexanol oxidation rates between the systems with and without phytate addition (Figure 8.6.5-13d).

Relative rates of hydroxyl radical generation in CHP slurries containing each of the four soils with and without citrate stabilization are shown in Figures 8.6.5-14a–d. In the Georgia soil, systems with no citrate addition provided a higher rate of hydroxyl radical generation than systems with citrate stabilization; nonetheless, oxidation of the hydroxyl radical probe hexanol was slow with 20% hexanol oxidation in the unstabilized systems and 10% oxidation in the citrate-stabilized systems (Figure 8.6.5-14a). There was minimal difference in oxidation in the unstabilized and citrate-stabilized systems in slurries containing the Maine soil, with

approximately 75% hexanol oxidation in each (Figure 8.6.5-14b). However, relative hydroxyl radical production in the California soil (Figure 8.6.5-14c) was quite different. Relative hydroxyl radical production was significantly greater with citrate stabilization, with 80% hexanol oxidation in the citrate-stabilized system, and 40% oxidation in the unstabilized system. Similar results were observed in the CHP systems with the Washington soil (Figure 8.6.4-14d). With citrate stabilization, 35% hexanol oxidation occurred, while 15% hexanol oxidation was observed in the stabilized systems.

The relative rates of hydroxyl radical generation in soil slurries with and without malonate stabilization are shown in Figure 8.6.5-15a–d. These data indicate that the presence of malonate has a significant effect on hydroxyl radical generation rates in some soil systems. Rates of hydroxyl radical generation in the Georgia soil were not significantly different with 35% of the hydroxyl radical probe hexanol oxidized in each (Figure 8.6.5-15a). In the Maine soil, however, hydroxyl radical generation rates were greater in the stabilized system, with 100% of the hydroxyl radical probe oxidized in the system with malonate, compared to 80% oxidation in the unstabilized system (Figure 8.6.5-15b). Relative hydroxyl radical generation rates were approximately ten times greater with malonate stabilization in the California soil compared to unstabilized systems (Figure 18.6.5-5c). A similar trend was observed in the Washington soil; the relative hydroxyl radical generation rate in the malonate-stabilized systems was approximately two times the rate in the unstabilized systems (Figure 8.6.5-15d).

The effect of phytate stabilization on superoxide generation in the four soils systems using the probe molecule hexachloroethane (HCA) is shown in Figures 8.6.5-16a–d. The relative rates of superoxide generation in the Georgia soil and the Maine soil were greater in the unstabilized systems relative to the phytate stabilized systems. The difference was small in the Georgia soil slurries with 80% HCA degradation without phytate addition and 70% degradation in the phytate-stabilized system (Figure 8.6.5-16a). Differences in relative superoxide generation were more pronounced in CHP reactions conducted with the Maine soil (Figure 8.6.5-16b). Under conditions of no stabilization, 80% of the HCA was degraded, while 50% of the HCA was degraded in the phytate-stabilized systems. Similar results were observed in the California soil, with 70% of the HCA degraded in the unstabilized system and 40% of the HCA degraded in the phytate-stabilized systems. Minimal difference in the relative rates of superoxide generation between the unstabilized and stabilized systems was observed with CHP reactions in the Washington soil, with 75% HCA degradation in unstabilized system and 70% HCA degradation in the presence of phytate (Figures 8.6.5-16c–d).

Relative rates of superoxide generation in unstabilized and citrate-stabilized soils during CHP reactions are shown in Figures 8.6.5-17a–d. Small to negligible differences in relative rates of superoxide generation were observed in CHP reactions in the four soils. There was a small difference in relative rates of superoxide generation between unstabilized and citrate-stabilized samples of the Georgia soil, with 65% degradation the unstabilized system and 75% degradation in the presence of citrate (Figure 8.6.5-17a). Similarly, in the Maine soil, unstabilized hydrogen peroxide provided slightly higher rates of superoxide generation (Figure 8.6.5-17b), while differences were minimal in the California soil (Figure 8.6.5-17c) and the Washington soil (Figure 8.6.5-17d).

Relative rates of superoxide generation for unstabilized and malonate-stabilized CHP reactions in the four soils are shown in Figures 8.6.5-18a–d. The degradation of HCA in the unstabilized samples was greater by approximately 10% than in the malonate-stabilized samples for CHP reactions conducted in the Georgia soil, and was greater by approximately 20% in the Maine soil (Figure 8.6.5-18a and b) and (Figures 8.6.5-18a–c). However, relative superoxide generation rates were not significantly different in the California soil and the Washington soil (Figures 8.6.5-18c and d).

The results shown in Figures 8.6.5-13–8.6.5-18 of relative rates of hydroxyl radical generation and relative rates of superoxide generation in unstabilized and stabilized hydrogen peroxide–soil slurries indicate that stabilization had a minimal effect on the generation of these reactive oxygen species. Relative hydroxyl radical and superoxide generation rates increased in some stabilized systems and decreased in other stabilized systems relative to their rates in unstabilized systems; however, most of the differences between the relative rates of generation of the reactive oxygen species were minimal. Therefore, effective contaminant treatment and DNAPL destruction will likely be as effective in full-scale stabilized applications as in unstabilized applications, but with the benefit of better transport and contaminant contact with stabilized hydrogen peroxide.
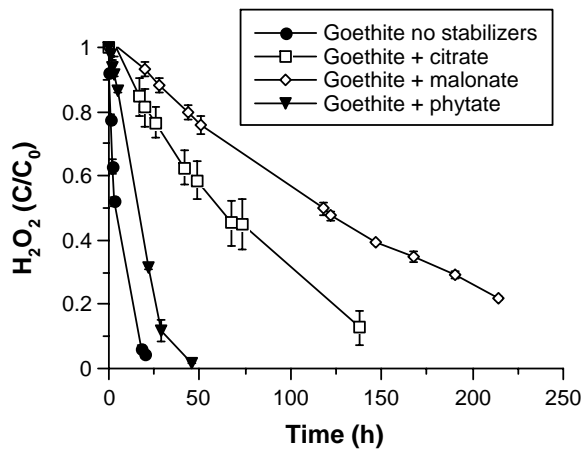
Figure 8.6.5-1. Decomposition of hydrogen peroxide in goethite slurries at pH 3 without stabilization or with addition of 10 mM citrate, malonate, or phytate
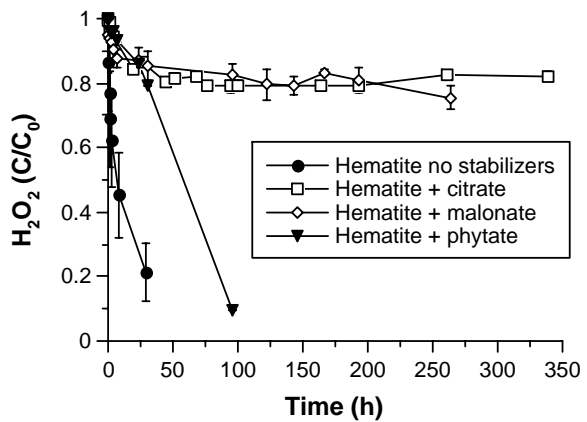
Figure 8.6.5-2. Decomposition of hydrogen peroxide in hematite slurries at pH 3 without stabilization or with addition of 10 mM citrate, malonate, or phytate
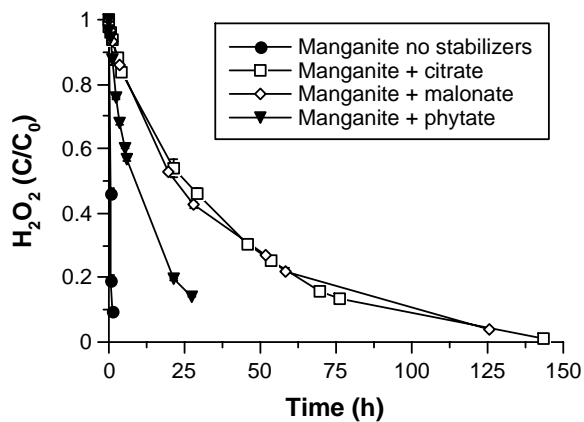
Figure 8.6.5-3. Decomposition of hydrogen peroxide in manganite slurries at pH 3 without stabilization or with addition of 10 mM citrate, malonate, or phytate
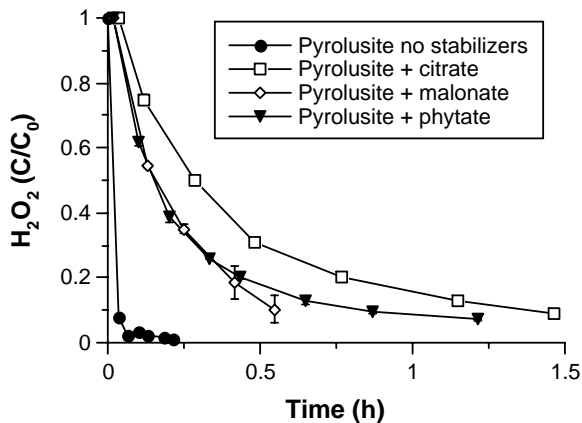
Figure 8.6.5-4. Decomposition of hydrogen peroxide in pyrolusite slurries at pH 3 without stabilization or with addition of 10 mM citrate, malonate, or phytate

207
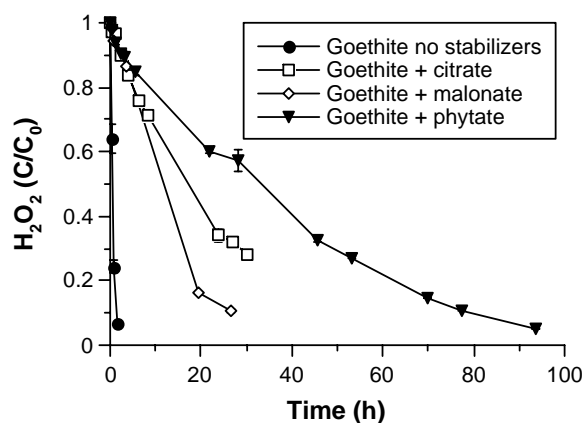
Figure 8.6.5-5. Decomposition of hydrogen peroxide in goethite slurries at pH 7 without stabilization or with addition of 10 mM citrate, malonate, or phytate
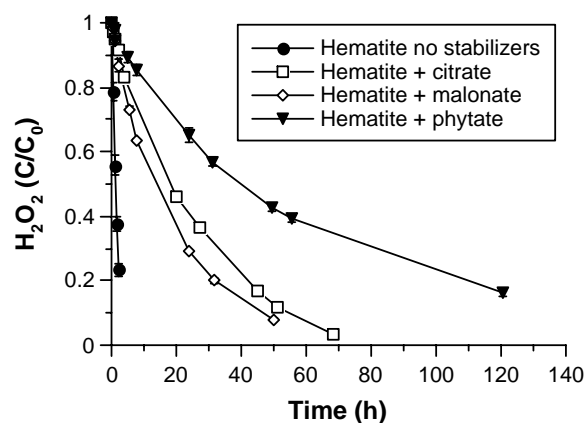
Figure 8.6.5-6. Decomposition of hydrogen peroxide in hematite slurries at pH 7 without stabilization or with addition of 10 mM citrate, malonate, or phytate
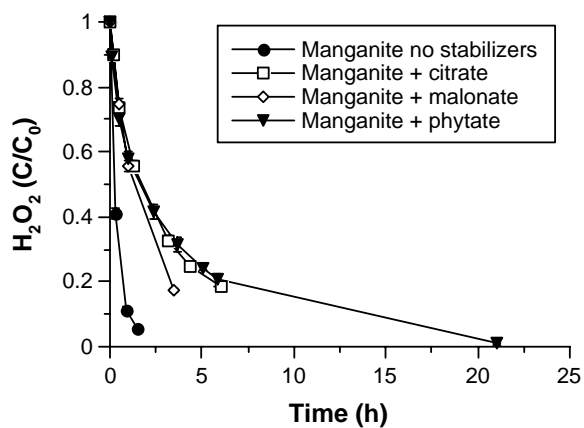
Figure 8.6.5-7. Decomposition of hydrogen peroxide in manganite slurries at pH 7 without stabilization or with addition of 10 mM citrate, malonate, or phytate
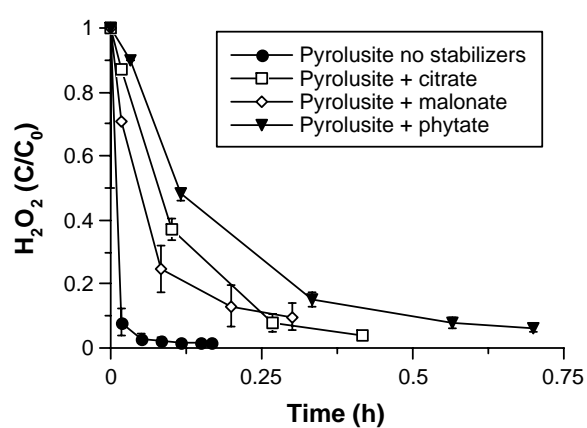
Figure 8.6.5-8. Decomposition of hydrogen peroxide in pyrolusite slurries at pH 7 without stabilization or with addition of 10 mM citrate, malonate, or phytate

208
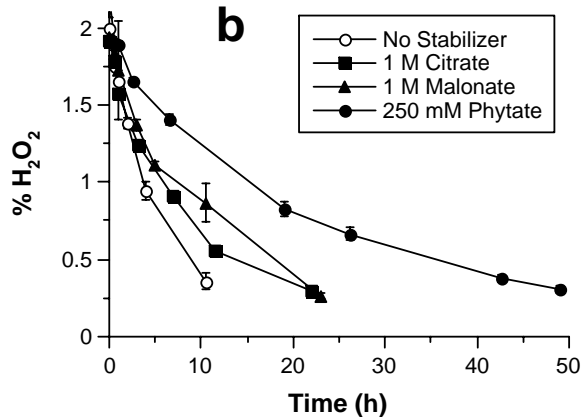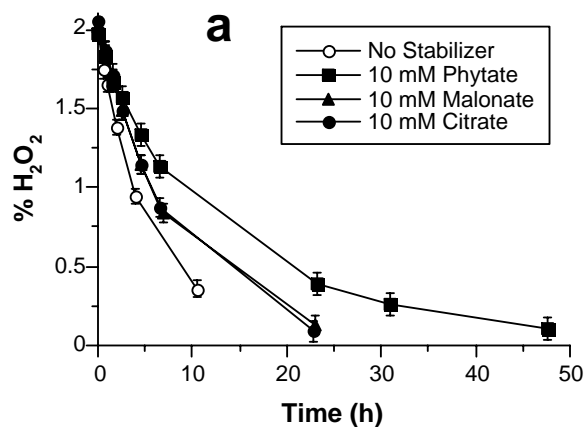
Figure 8.6.5-9. Decomposition of hydrogen peroxide in the Georgia soil without stabilization or with addition of citrate, malonate, or phytate. (a) 10 mM stabilizer; (b) 1 M or 250 mM stabilizer
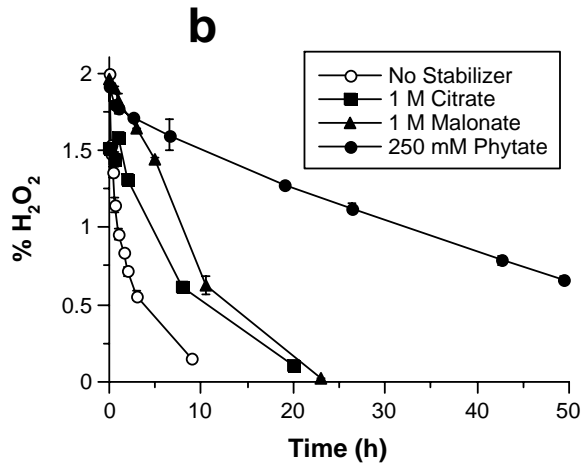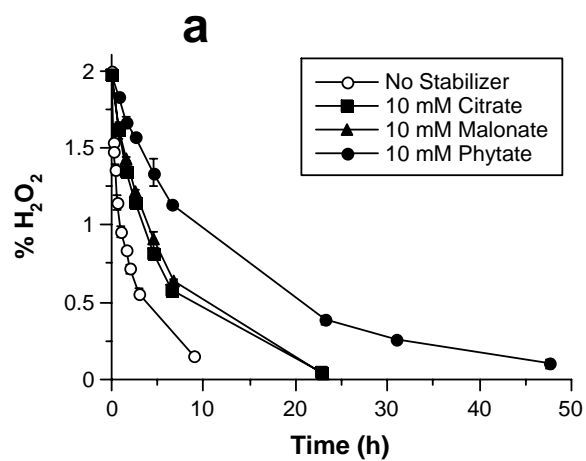
Figure 8.6.5-10. Decomposition of hydrogen peroxide in the Maine soil without stabilization or with addition of citrate, malonate, or phytate. (a) 10 mM stabilizer; (b) 1 M or 250 mM stabilizer
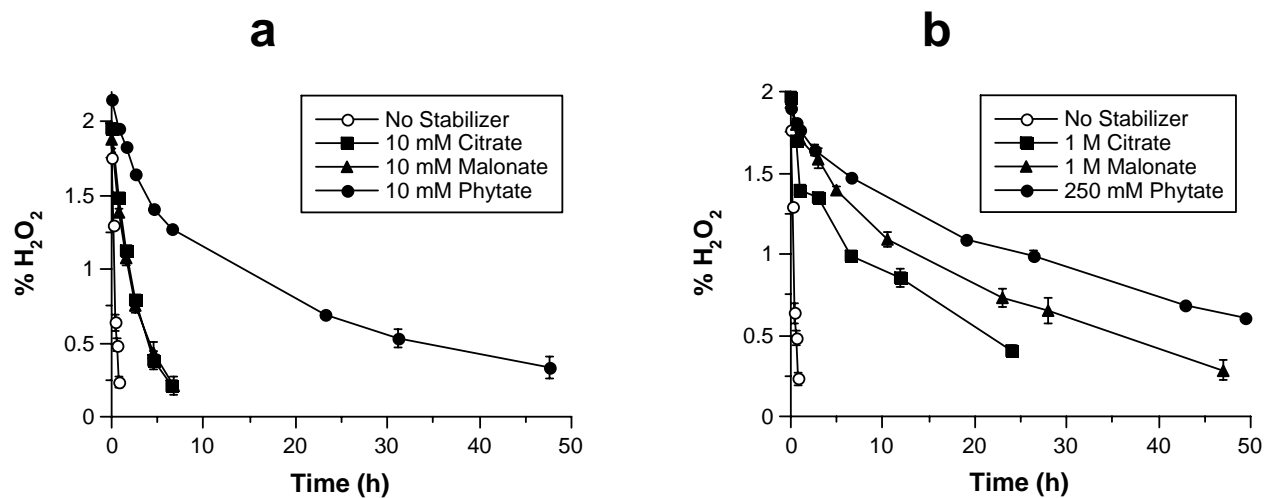
Figure 8.6.5-11. Decomposition of hydrogen peroxide in the California soil without stabilization or with addition of citrate, malonate, or phytate. (a) 10 mM stabilizer; (b) 1 M or 250 mM stabilizer
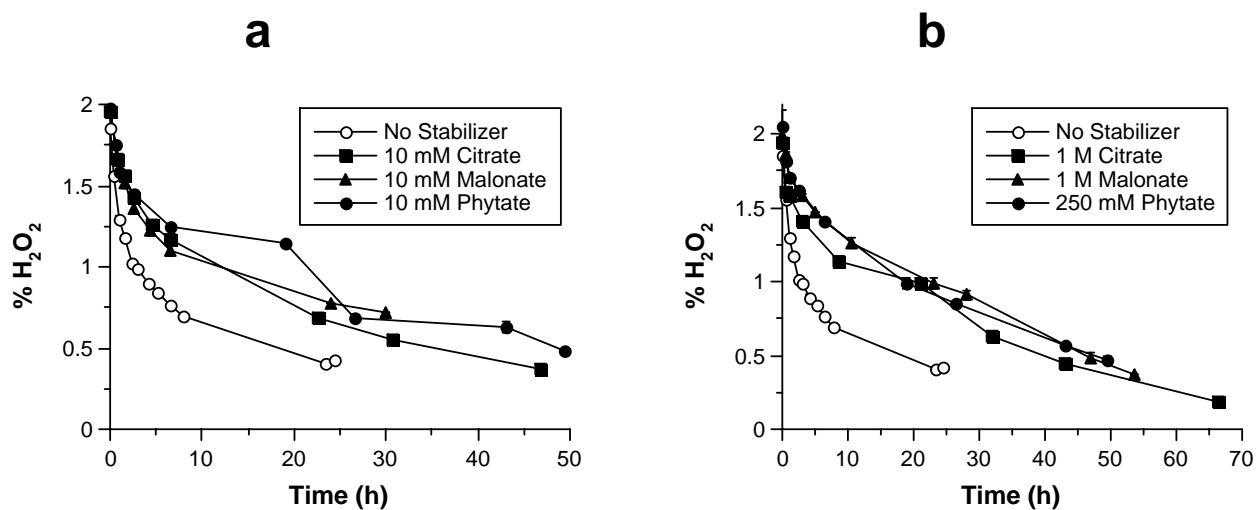
Figure 8.6.5-12. Decomposition of hydrogen peroxide in the Washington soil without stabilization or with addition of citrate, malonate, or phytate. (a) 10 mM stabilizer; (b) 1 M or 250 mM stabilizer
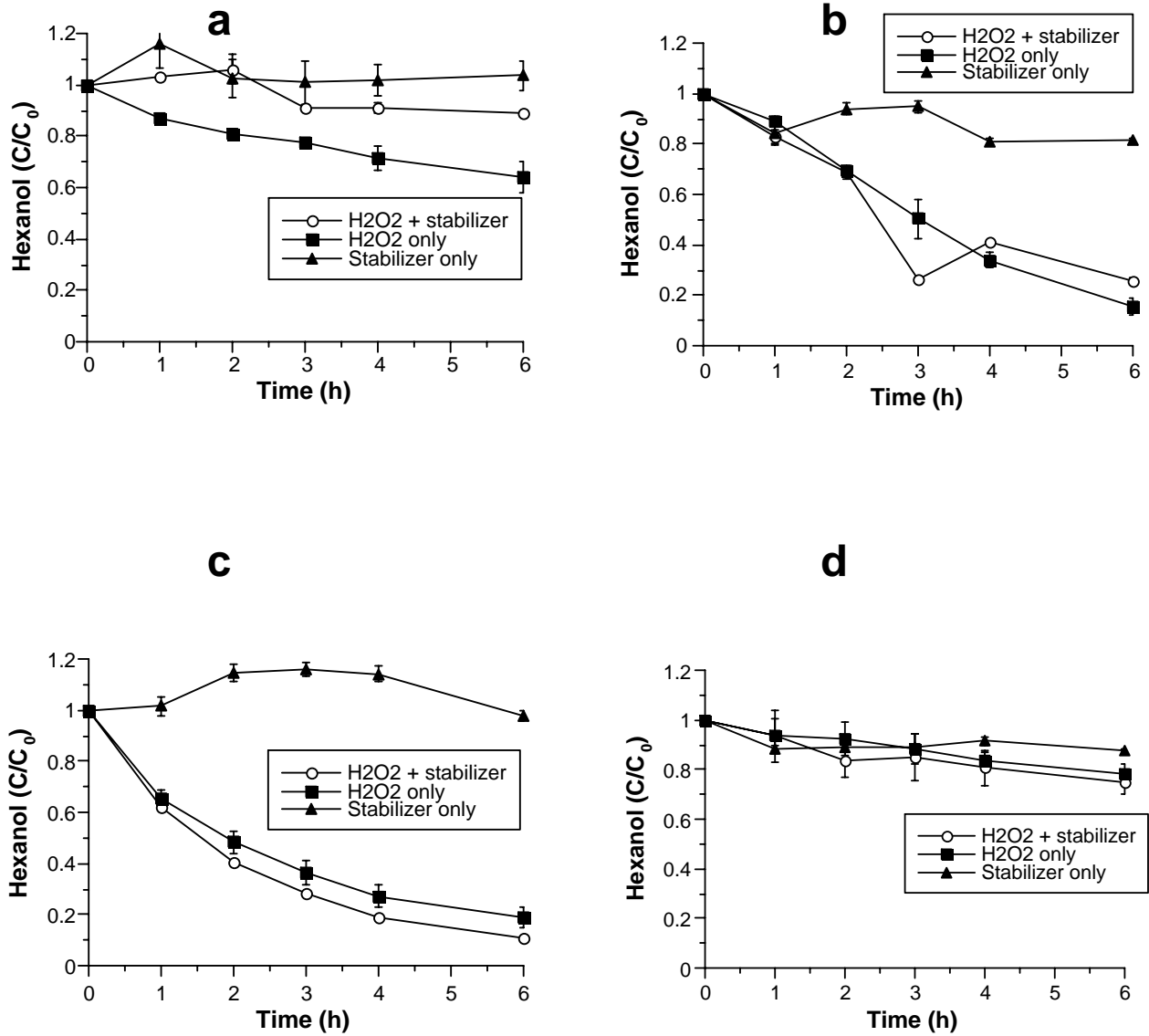
Figure 8.6.5-13. Relative activity of hydroxyl radical measured by hexanol oxidation in four soils with and without stabilization with 10 mM phytate. (a) Georgia soil; (b) Maine soil; (c) California soil; (d) Washington soil.
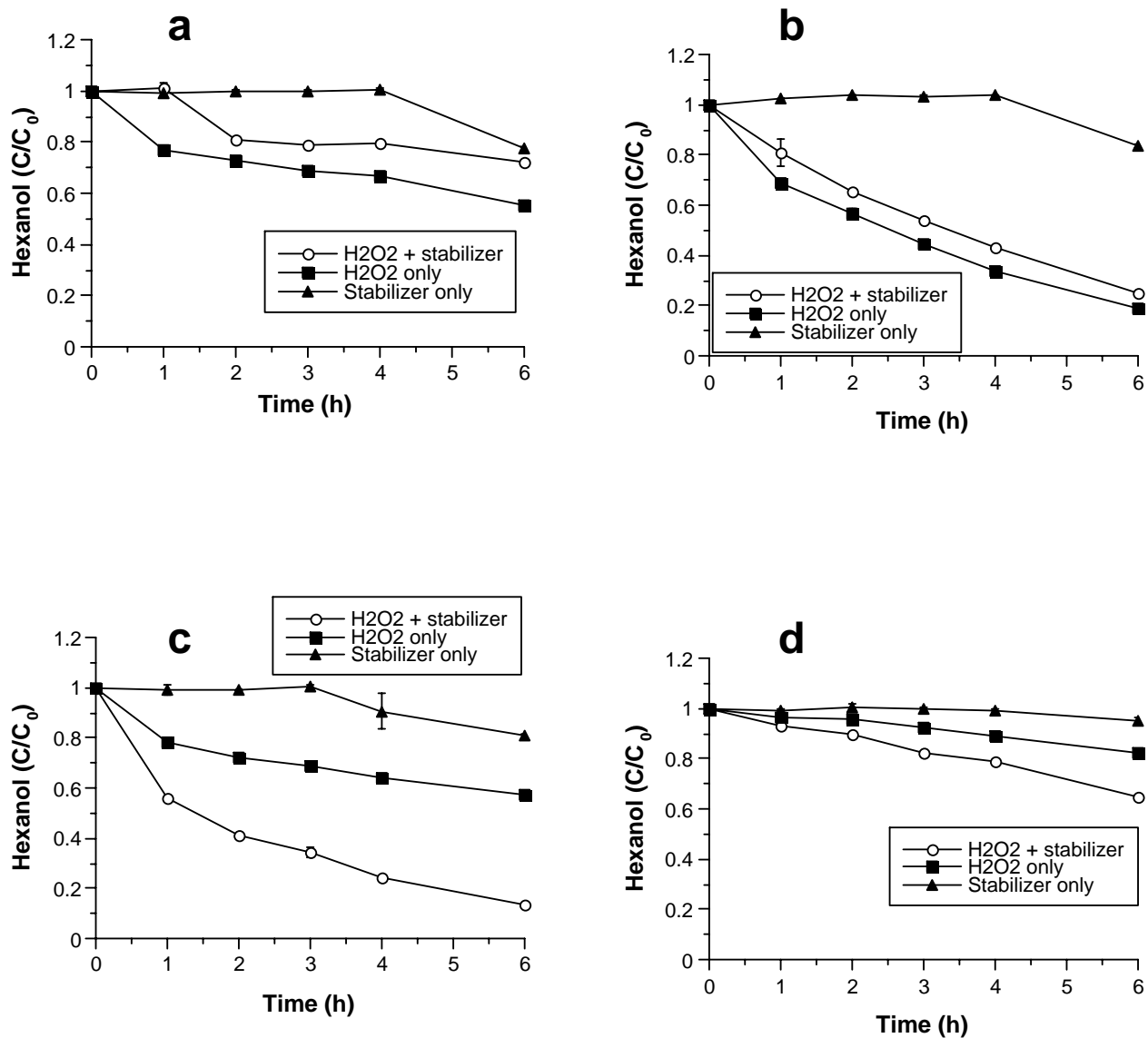
Figure 8.6.5-14. Relative activity of hydroxyl radical measured by hexanol oxidation in four soils with and without stabilization with 10 mM citrate. (a) Georgia soil; (b) Maine soil; (c) California soil; (d) Washington soil.
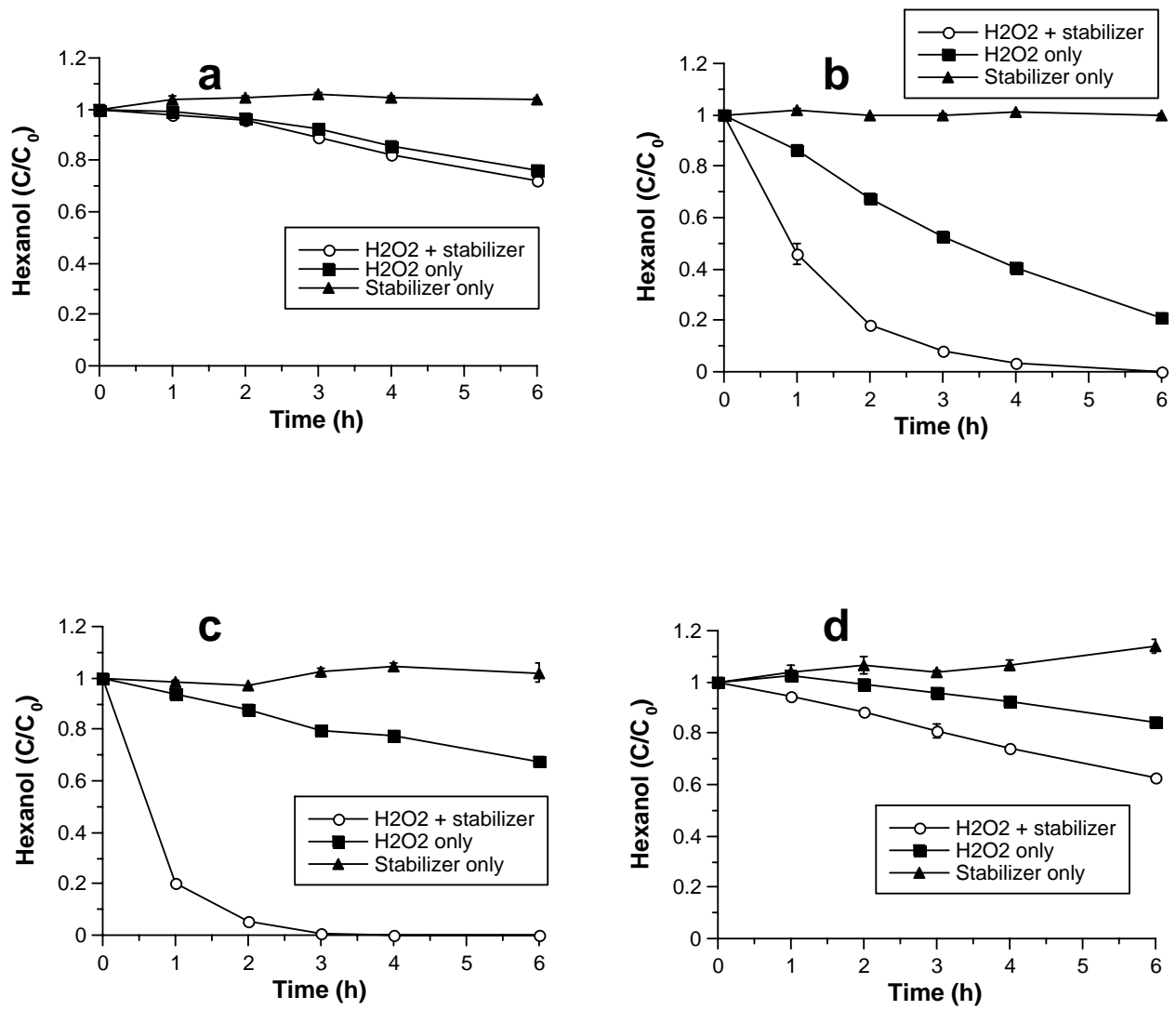
Figure 8.6.5-15. Relative activity of hydroxyl radical measured by hexanol oxidation in four soils with and without stabilization with 10 mM malonate. (a) Georgia soil; (b) Maine soil; (c) California soil; (d) Washington soil.
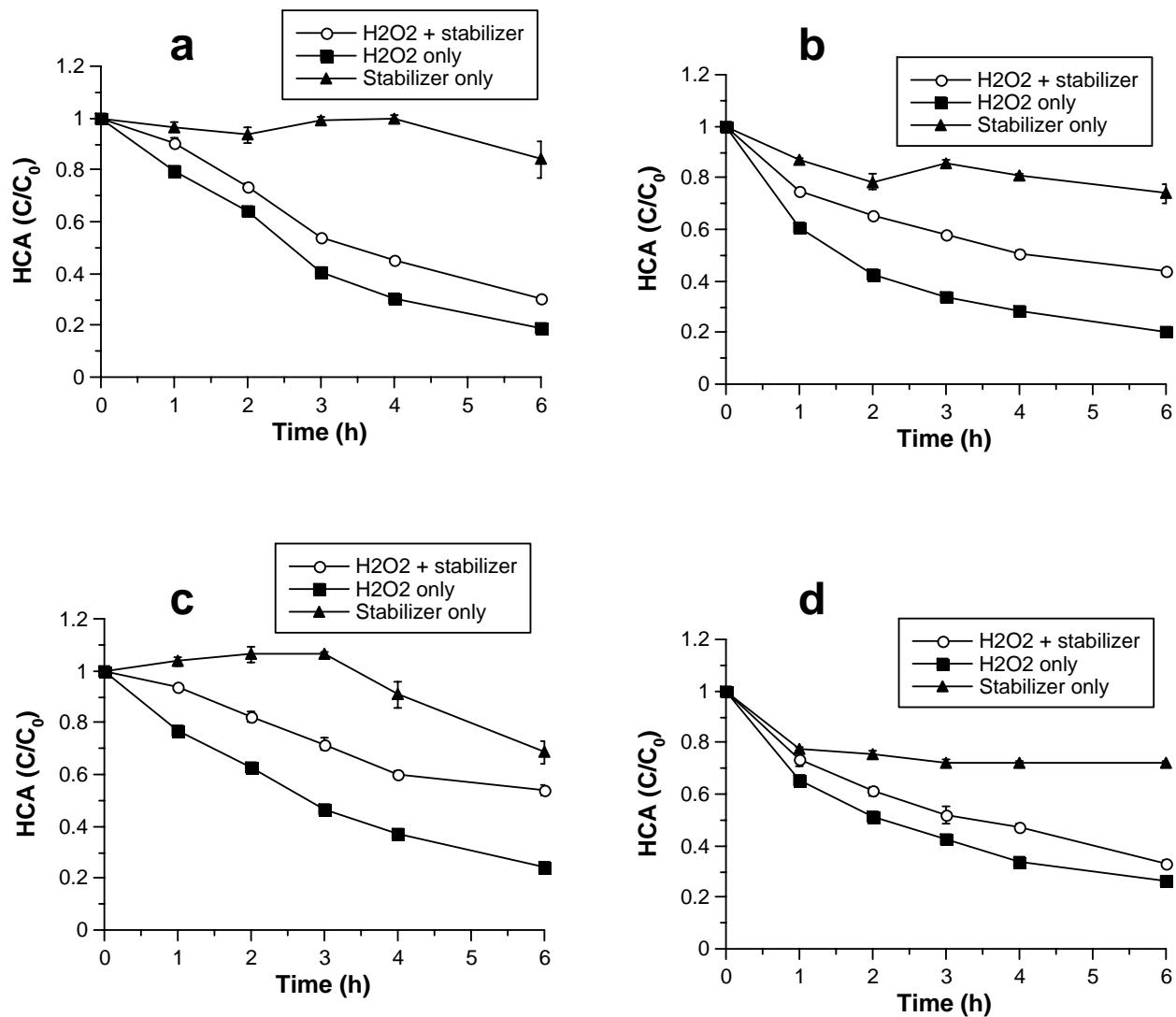
Figure 8.6.5-16. Relative activity of superoxide measured by hexachloroethane (HCA) destruction in four soils with and without stabilization with 10 mM phytate. (a) Georgia soil; (b) Maine soil; (c) California soil; (d) Washington soil.
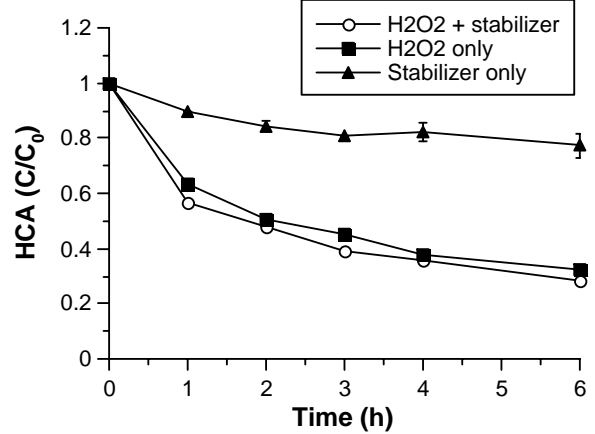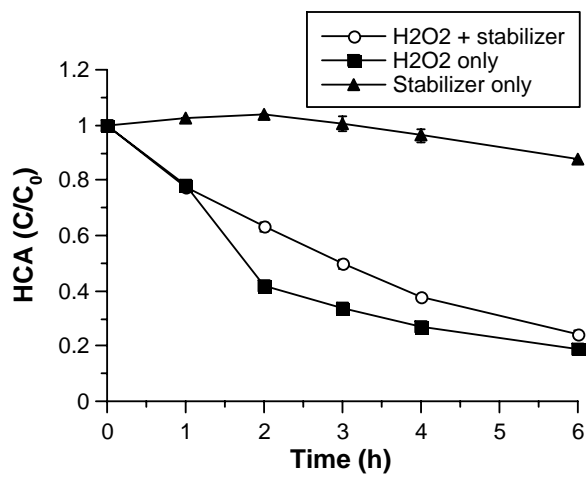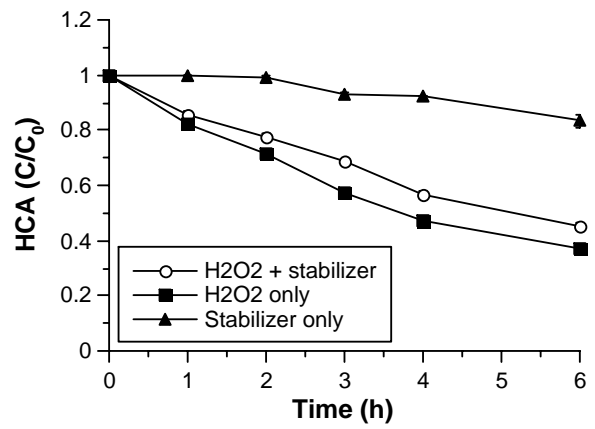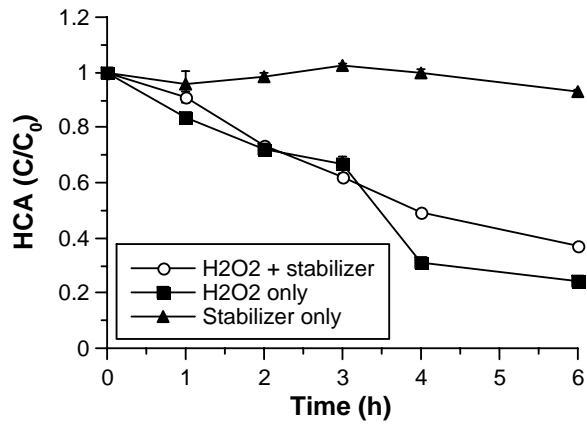
Figure 8.6.5-17. Relative activity of superoxide measured by hexachloroethane (HCA) destruction in four soils with and without stabilization with 10 mM citrate. (a) Georgia soil; (b) Maine soil; (c) California soil; (d) Washington soil.

215
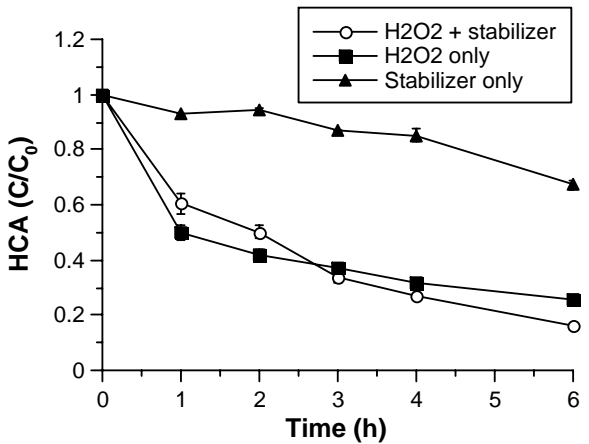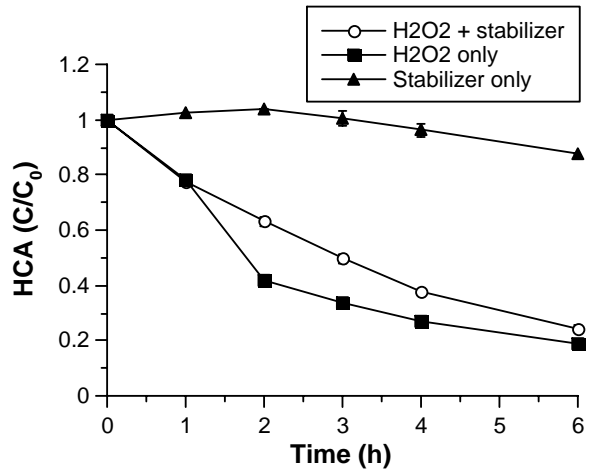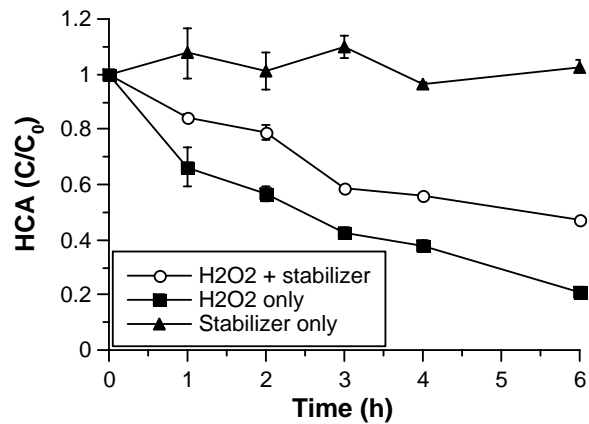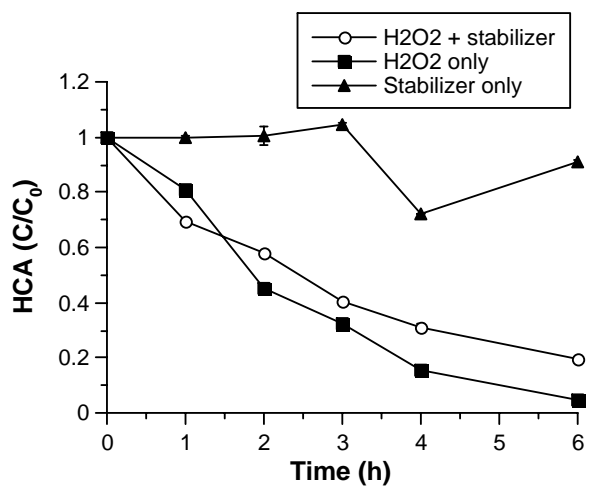
Figure 8.6.5-18. Relative activity of superoxide measured by hexachloroethane (HCA) destruction in four soils with and without stabilization with 10 mM malonate. (a) Georgia soil; (b) Maine soil; (c) California soil; (d) Washington soil.

8.6.6 Hydrogen Peroxide Stabilization in One-Dimensional Flow Columns

Batch studies.

CHP reactions were first conducted in batch systems at pH 7 to investigate the effectiveness of each stabilizer at a range of concentrations. The effect of different stabilizer concentrations on hydrogen peroxide decomposition in ICS systems is shown in Figure 8.6.6-1. The only effective stabilizer in ICS systems was sodium phytate; its lowest effective concentration in extending the lifetime of hydrogen peroxide in an ICS system was 25 mM. These results demonstrate that phytate can dramatically reduce the rate of hydrogen peroxide decomposition in ICS batch systems at a neutral pH. To be consistent, the citrate and phytate concentrations were maintained at 25 mM when applied to the one-dimensional columns. The effectiveness of different stabilizer concentrations in MCS systems are shown in Figure 8.6.6- 2. Phytate and citrate were both effective stabilizing hydrogen peroxide in MCS systems at concentrations < 100 mM. These results demonstrate that both 25mM sodium citrate and 25mM sodium phytate were effective in stabilizing hydrogen peroxide in MCS systems, and each of the stabilizers were applied to one-dimensional columns at concentrations of 25 mM.

Hydrogen peroxide stabilization in one-dimensional columns using combined stabilizer-hydrogen peroxide formulations .

To investigate the effectiveness of stabilizing reagents in lowering the rate of hydrogen peroxide decomposition in one-dimensional saturated columns, reactions were conducted at pH 7 in the ICS and MCS systems using 25 mM citrate or phytate. Hydrogen peroxide concentrations in each of the eight ports as a function of time for unstabilized hydrogen peroxide in the ICS column are shown in Figure 8.6.6-3. Hydrogen peroxide residuals were detected in Port 1, but decreased dramatically in Ports 2 and 3, with no detectable hydrogen peroxide concentration reaching Port 4. These results are similar to hydrogen peroxide decomposition rates found in the subsurface with high concentrations of iron or manganese oxides, which would result in a lifetime of hydrogen peroxide < 1 hr. The hydrogen peroxide concentrations at different column depths in a parallel system with the addition of 25 mM phytate are shown in Figure 8.6.6-4. The hydrogen peroxide concentration at Port 8 reached a maximum of 3.3% in the stabilized experiment, demonstrating a significant increase in stabilization relative to the unstabilized hydrogen peroxide. These results show that phytate is effective in stabilizing the decomposition rate of hydrogen peroxide in ICS. In addition, the columns with phytate addition showed minimal decrease in flow rates compared to the systems in which unstabilized hydrogen peroxide was applied.

Hydrogen peroxide concentrations in each of the eight ports as a function of time for unstabilized hydrogen peroxide applied to the column containing MCS are shown in Figure 8.6.6-5. The maximum hydrogen peroxide concentration at Port 1 was 4.75% and the hydrogen peroxide concentration decreased slightly in each of the ports, but maintained a concentration of 3.8% in Port 8. However, in the column stabilized with 25 mM phytate, the maximum hydrogen peroxide concentration showed no significant decrease from Port 1 to Port 8 (Figure 8.6.6-6). In the column stabilized with 25 mM citrate (Figure 8.6.6-7), the maximum hydrogen peroxide concentration decreased from 4.8% in Port 1 to 4.4% in Port 8. These results demonstrate that both citrate and phytate were effective in stabilizing hydrogen peroxide in MCS.

Hydrogen peroxide stabilization in one-dimensional columns using stabilizer-preconditioning followed by hydrogen peroxide dosing.

Parallel experiments were conducted in which pulses of citrate and phytate were added to the column before the column was dosed with hydrogen peroxide. The results obtained were identical to the data shown in Figures 8.6.6-4 through 8.6.6-7 and 8.6.6-15 through 8.6.6-18. Implementation of hydrogen peroxide stabilization in the field will be easier using the stabilizer combined with the hydrogen peroxide in order that only one injection is conducted; therefore, the combined application of stabilizer and hydrogen peroxide has been emphasized in this report.

Treatment of a sorbed contaminant.

To investigate the potential for phytate and citrate stabilized hydrogen peroxide to treat contaminants in the subsurface, HCB was sorbed to ICS and MCS before treatment in one-dimensional columns. The relative degradation of HCB in samples collected from each of the sampling ports after treatment with stabilized and unstabilized hydrogen peroxide is shown in Figures 8.6.5-8–14 . The results of Figure 8.6.5-8 demonstrate that 18.5% of the initial HCB was destroyed in an ICS column at pH 3 with unstabilized hydrogen peroxide. However, more contaminant destruction occurred with unstabilized hydrogen peroxide in the ICS column at pH 7 (Figure 8.6.6-9); in this experiment, 39% of the HCB was destroyed, with most of the destruction occurring in the middle of the column. The contaminant destruction is likely due to the generation of a high proportion of superoxide as wells as the generation of hydroxyl radicals. In contrast to the ICS column results, HCB destruction in the MCS column with unstabilized hydrogen peroxide at pH 3 was minimal (Figure 8.6.6-10). Unlike iron oxide CHP reactions, manganese oxide-mediated hydrogen peroxide decomposition generates superoxide but no hydroxyl radicals (Watts et al., 2005). However, at pH 3 superoxide is protonated, and the perhydroxyl radical from is predominant:

$$HO_2\bullet \leftrightarrow O_2\bullet^- + H^+ \qquad pKa = 4.8 \tag{1}$$

$HO_2^.$ is a weak oxidant and likely has minimal potential for HCB destruction, which is supported by the data of Figure 8.6.5-10. In this experiment, HCB destruction was conducted in the MCS system at pH 3, resulting in minimal HCB destruction. At pH 7, which is well above the pKa of 4.8 for Equation 2, MnO_2-mediated hydrogen peroxide decomposition generates superoxide, which likely desorbs and degrades HCB. This concept is supported by the results of Figure 8.6.6-11, where 45.7% of the HCB was destroyed in the MCS system at pH 7.

The destruction of HCB in the citrate-stabilized MCS column is shown in Figure 8.6.5-12. These results show that HCB was degraded even when the hydrogen peroxide was stabilized with citrate, providing more efficient stoichiometry than HCB degradation with unstabilized hydrogen peroxide. The concentration of citrate in each port as a function of time can be found in Figure 8.6.6-15, which shows that citrate is not degraded by the CHP reactions as the solution moves through the column. In an MCS column stabilized with phytate, no detectable HCB destruction occurred (Figure 8.6.6-13). Although the phytate was not retarded in the column and did not degrade (Figure 8.6.6-16), the phytate may have stabilized the hydrogen peroxide so effectively that superoxide and hydroxyl radicals were not being produced. However, in an ICS column stabilized with phytate, 18.5% of the HCB was destroyed (Figure 8.6.6-14). Similar to the data in Figure 8.6.5-16, the phytate moved readily through the column and did not degrade

218

(Figure 8.6.6-17). The flow rates of column experiments are shown in Figure 8.6.6-18. These results show that the flow rates in the stabilized column systems do not decline as much as in unstabilized column systems. Plugging can be a significant problem in the application of CHP in the field, often through the gases produced by CHP reactions. The results of this research demonstrate that stabilization of hydrogen peroxide using citrate and phytate lower the rate of hydrogen peroxide decomposition in model subsurface systems, provides contaminant destruction comparable to unstabilized systems, and potentially minimizes plugging of the subsurface.

Summary and Conclusions

The stabilization of hydrogen peroxide using citrate and phytate was studied in one-dimensional columns containing iron oxide and manganese oxide coated sand. Hydrogen peroxide at an initial concentration of 5% was applied to the columns without stabilization and with stabilization by sodium citrate and sodium phytate at neutral pH. Citrate and phytate were effective hydrogen peroxide stabilizers, increasing hydrogen peroxide residuals by 70% over unstabilized hydrogen peroxide. Although they provided much lower hydrogen peroxide decomposition rates, the stabilized CHP systems provided effective contaminant destruction. Because of the increased lifetime of stabilized hydrogen peroxide, the treatment efficiency and depth of treatment in the subsurface may potentially increase by at least an order of magnitude. Citrate and phytate stabilization appears to be mineral specific; therefore a matrix of treatability studies using native materials will need to be conducted to determine the most effective stabilizer and its concentration.

The results of Section 8.6 demonstrated that soil organic matter does not significantly affect contaminant destruction when CHP is conducted at acidic pH regimes, while soil organic matter enhances the effectiveness of CHP treatment at neutral pH regimes. Release of metals during CHP remediation is metal- and sorbent-specific. Cadmium and lead sorbed on the natural soils were not released by CHP reactions conducted at neutral pH, but were released in reactions at pH 3, due primarily to the destruction of organic matter. One of the most important findings of the this segment of research is that hydrogen peroxide half-lives in the presence of minerals and subsurface solids can be increased by one to three orders of magnitude by adding one of three stabilizers: citrate, malonate, or phytate. These results provide promise for increased effectiveness and decreased cost in the application of CHP ISCO.
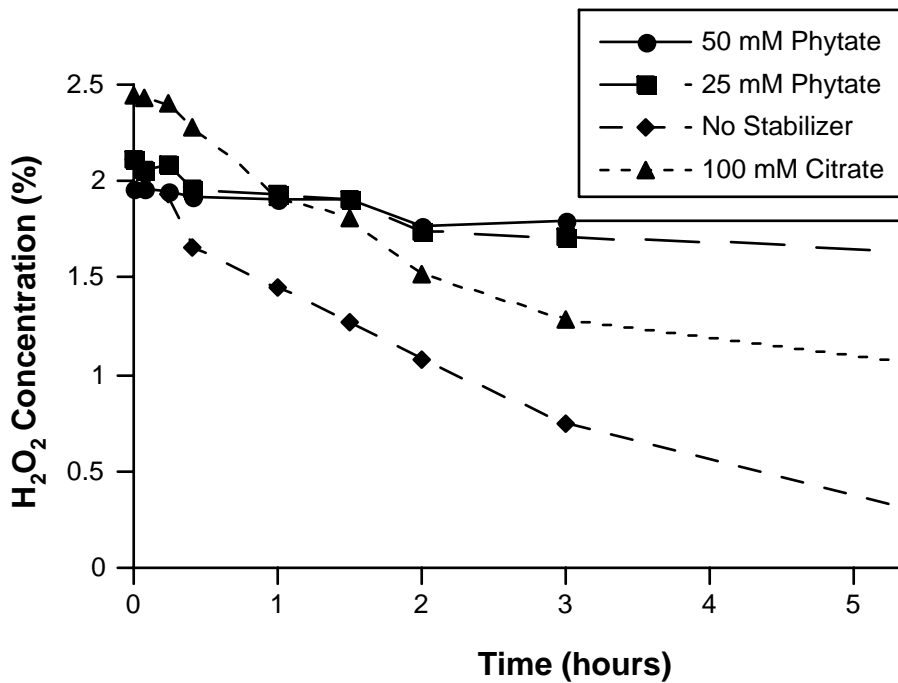
Figure 8.6.6-1. Rate of stabilized and unstabilized H_2O_2 decomposition in a column of iron coated sand (ICS).
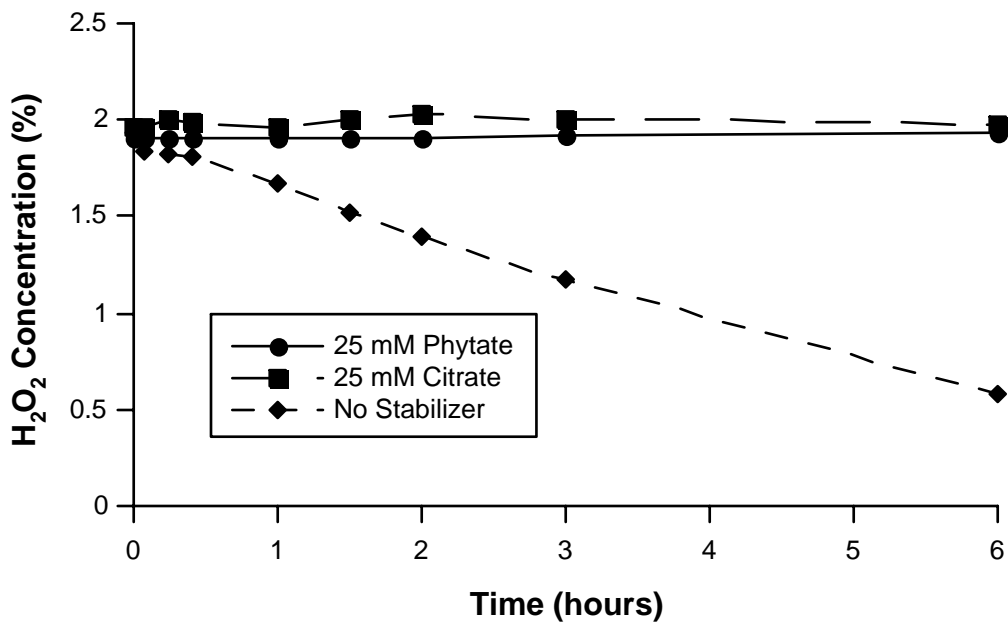
Figure 8.6.6-2. Rate of stabilized and unstabilized H_2O_2 decomposition in a column of manganese coated sand (MCS).
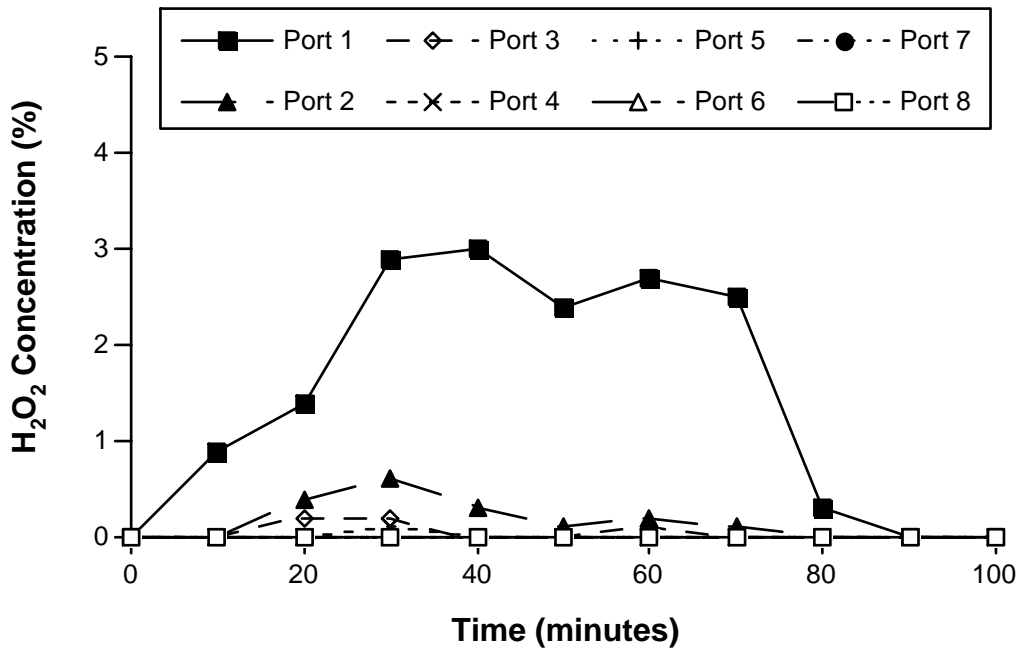
Figure 8.6.6-3. Decomposition of unstabilized H_2O_2 in a column of iron coated sand (ICS) at pH 7.
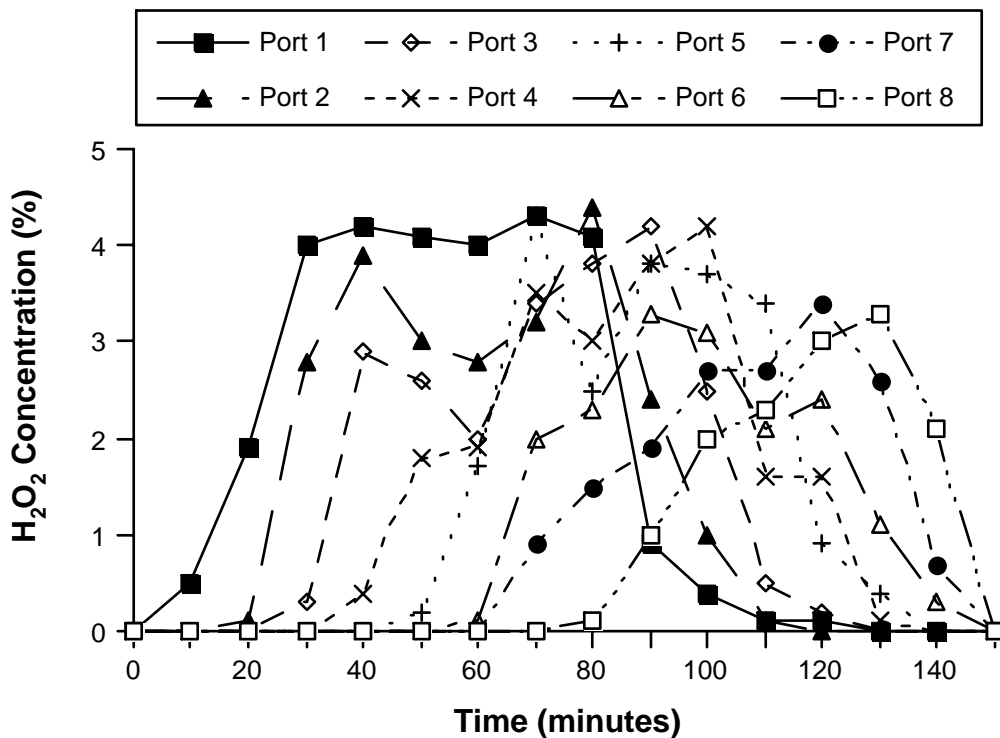
Figure 8.6.6-4. Decomposition of H_2O_2 stabilized by 25 mM phytate in a column of iron coated sand (ICS) at pH 7.

221
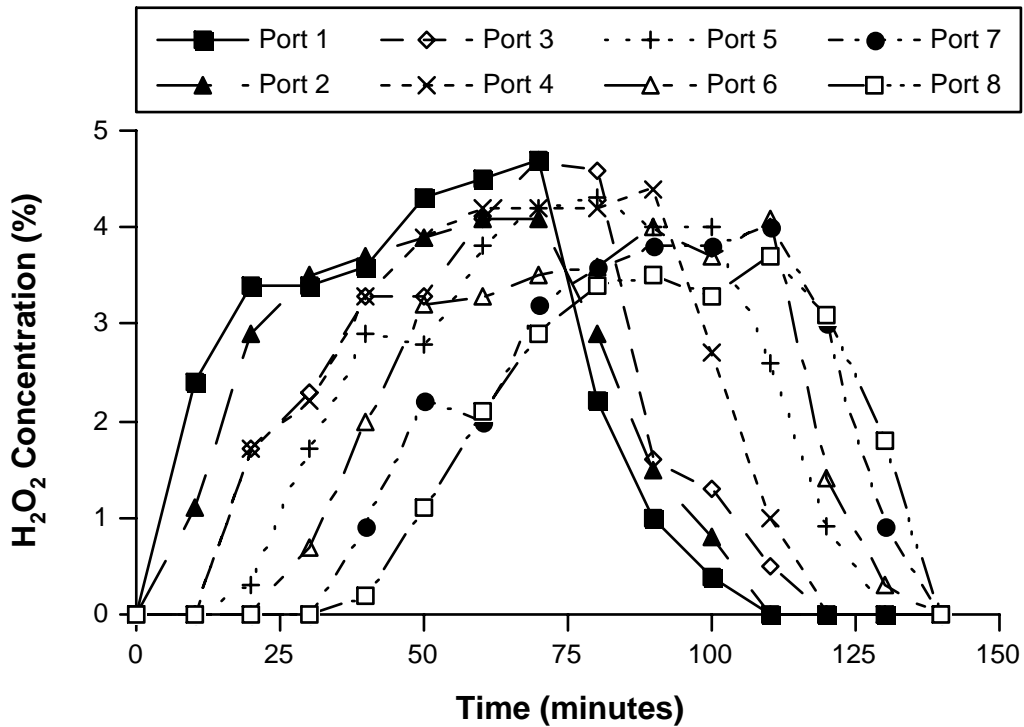
Figure 8.6.6-5, Decomposition of unstabilized H_2O_2 in a column of manganese coated sand (MCS) at pH 7.
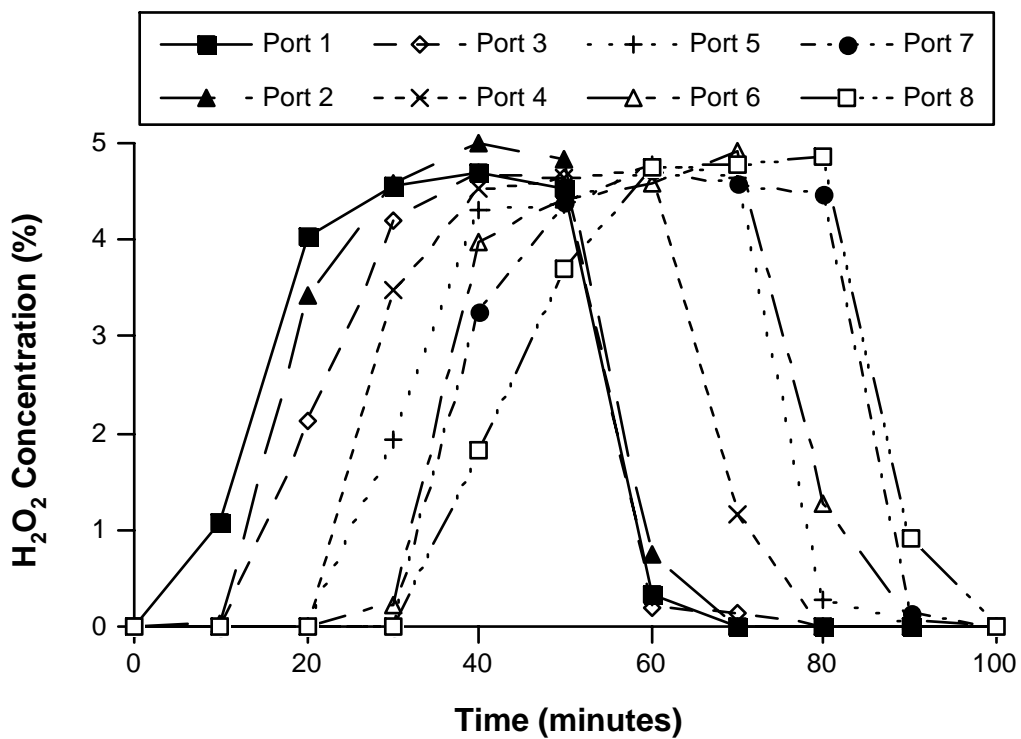
Figure 8.6.6-6. Decomposition of H_2O_2 stabilized by 25 mM phytate in a column of manganese coated sand (MCS) at pH 7.
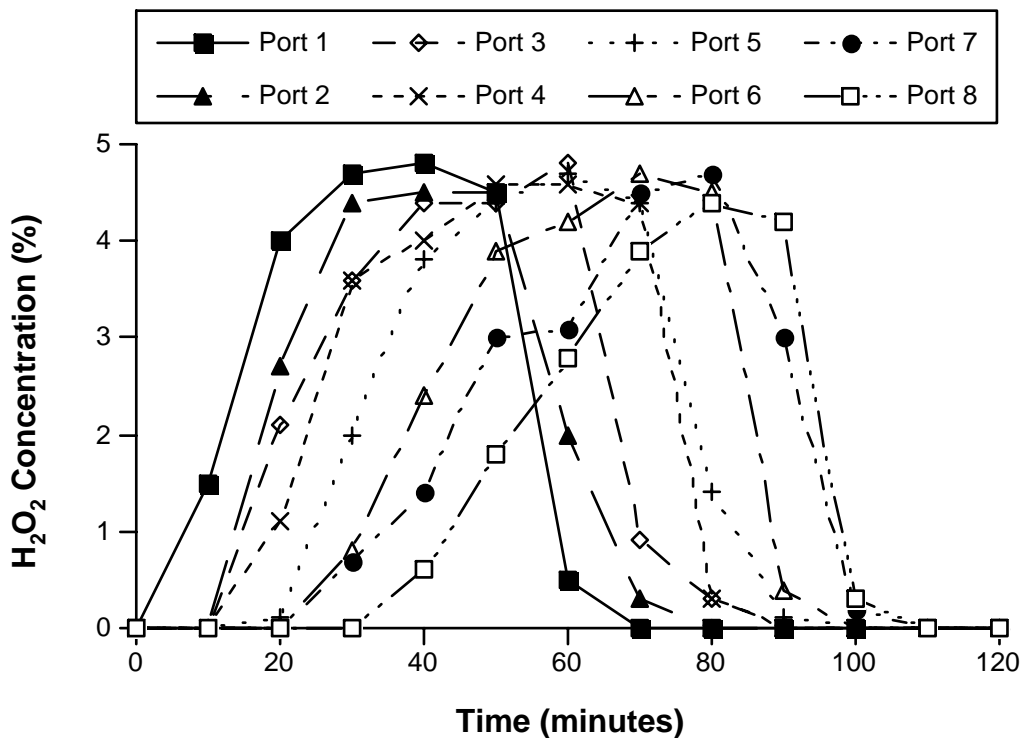
Figure 8.6.6-7. Decomposition of H_2O_2 stabilized by 25 mM citrate in a column of manganese coated sand (MCS) at pH 7.
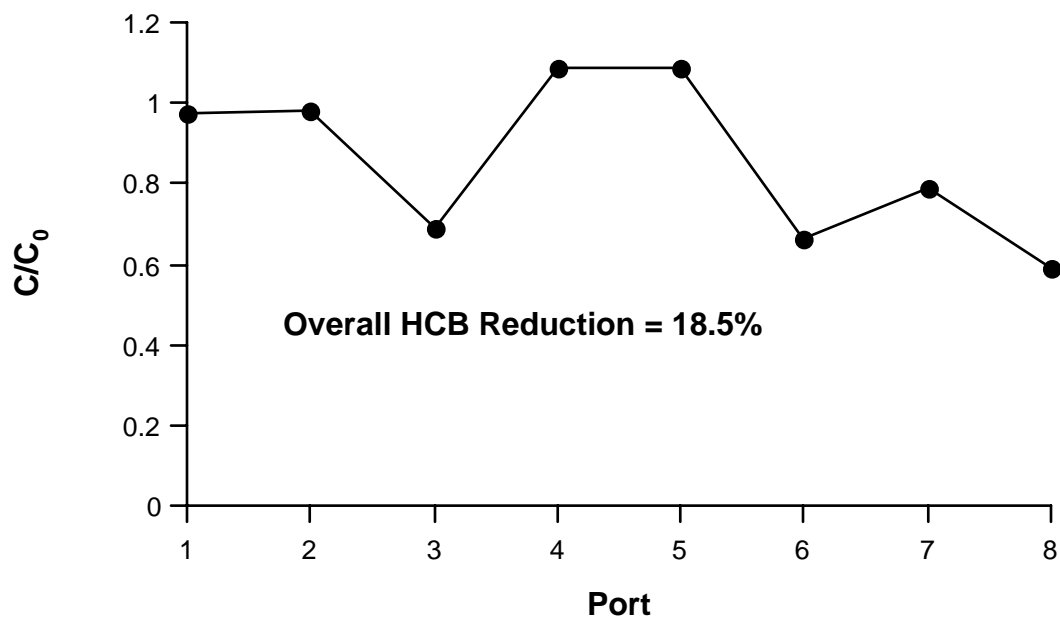
Figure 8.6.6-8. Relative concentration of hexachlorobenzene (HCB) in each of eight ports in a column of iron coated sand (ICS) treated with unstabilized H_2O_2 at pH 3.
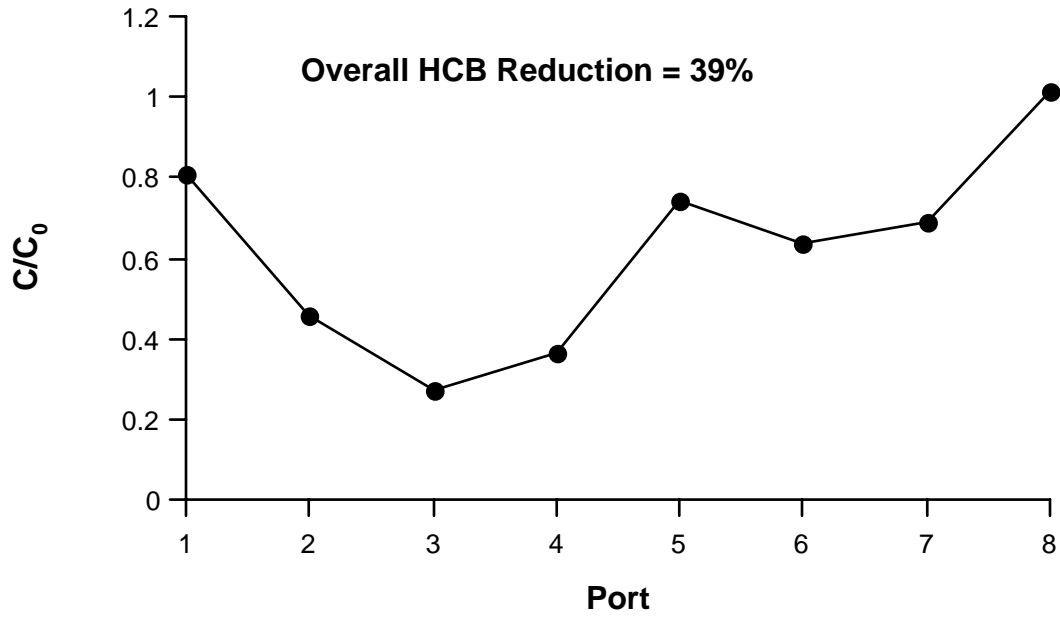
Figure 8.6.6-9. Relative concentration of hexachlorobenzene (HCB) in each of eight ports in a column of iron coated sand (ICS) treated with unstabilized H_2O_2 at pH 7.
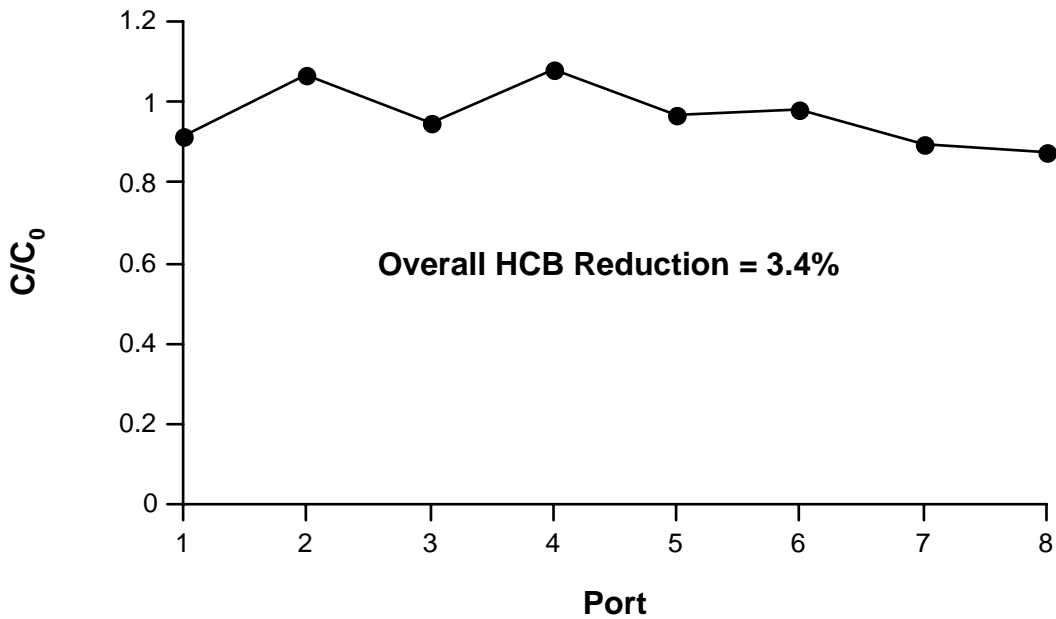
Figure 8.6.6-10. Relative concentration of hexachlorobenzene (HCB) in each of eight ports in a column of manganese coated sand (MCS) treated with unstabilized H_2O_2 at pH 3.
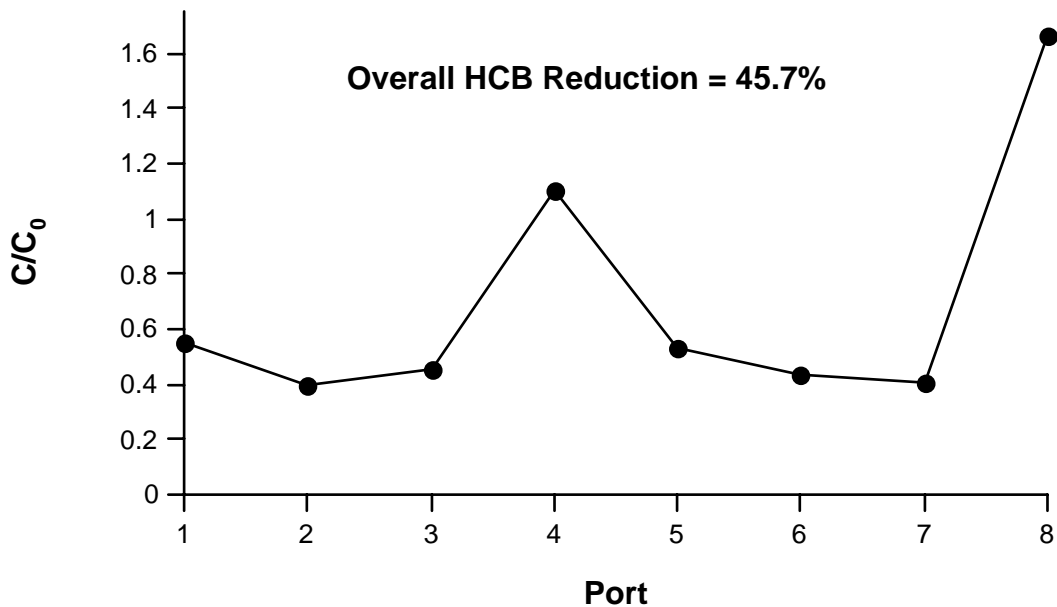
Figure 8.6.6-11. Relative concentration of hexachlorobenzene (HCB) in each of eight ports in a column of manganese coated sand (MCS) treated with unstabilized H_2O_2 at pH 7.
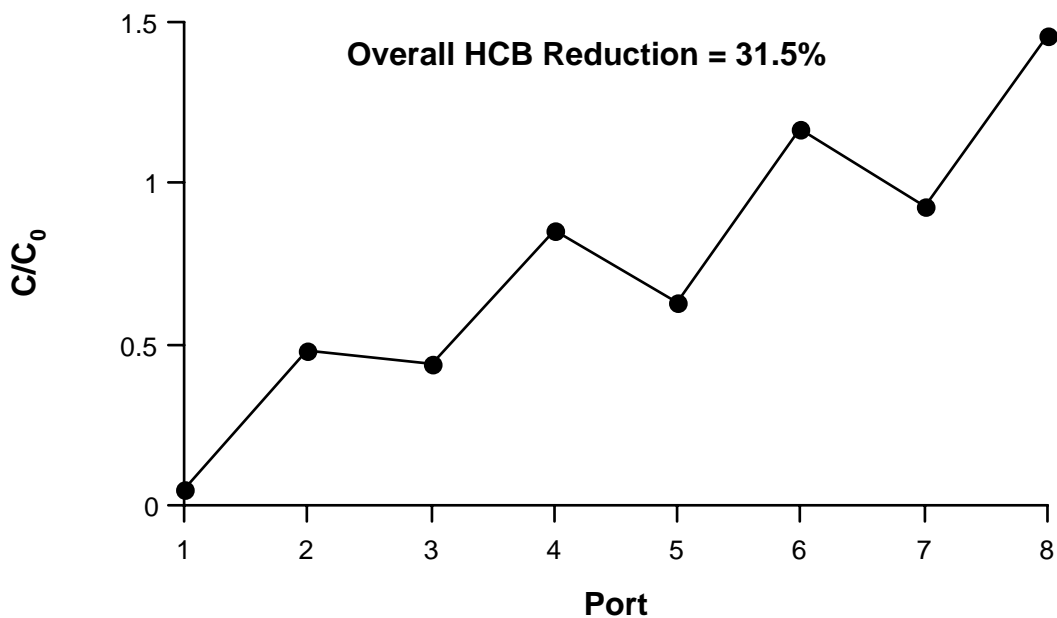
Figure 8.6.6-12. Relative concentration of hexachlorobenzene (HCB) in each of eight ports in a column of manganese coated sand (MCS) treated with H_2O_2 stabilized by 25 mM citrate at pH 7.
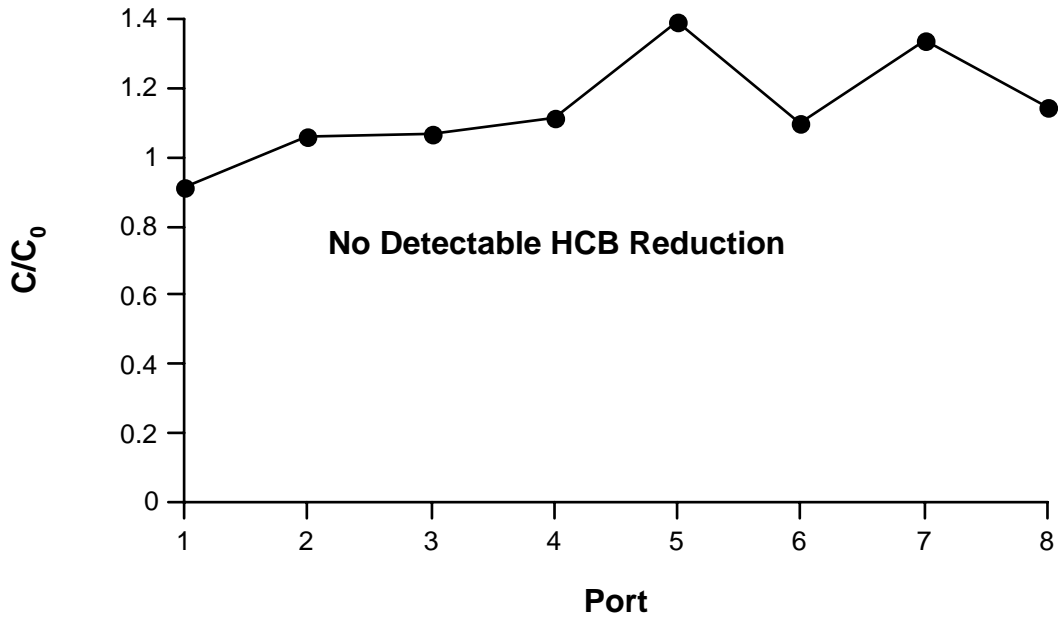
Figure 8.6.6-13. Relative concentration of hexachlorobenzene (HCB) in each of eight ports in a column of manganese coated sand (MCS) treated with H_2O_2 stabilized by 25 mM phytate at pH 7.
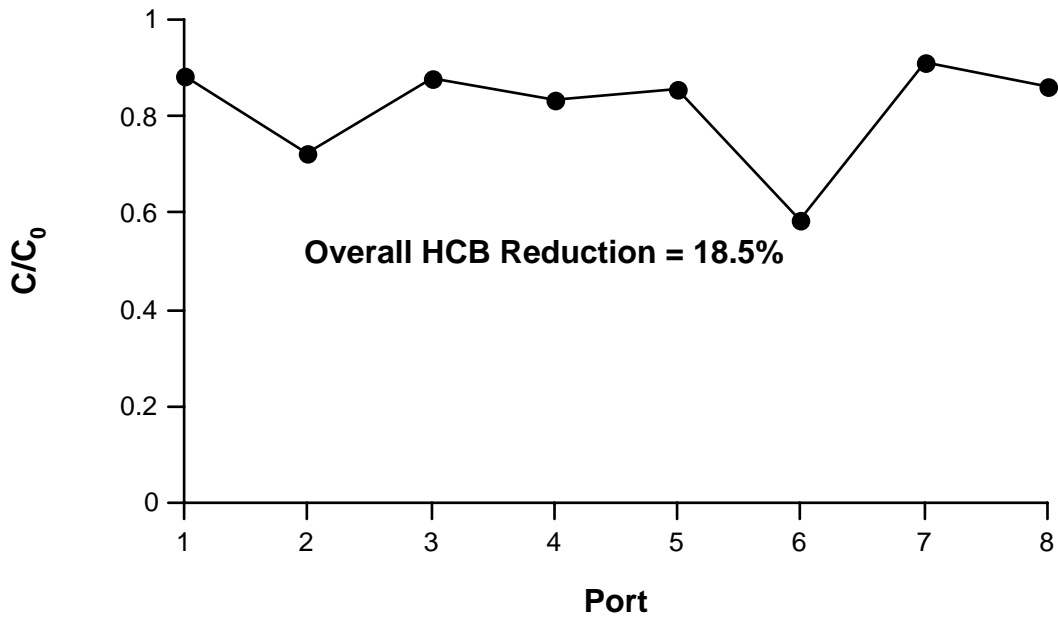
Figure 8.6.6-14. Relative concentration of hexachlorobenzene (HCB) in each of eight ports in a column of iron coated sand (ICS) treated with H_2O_2 stabilized by 25 mM phytate at pH 7.
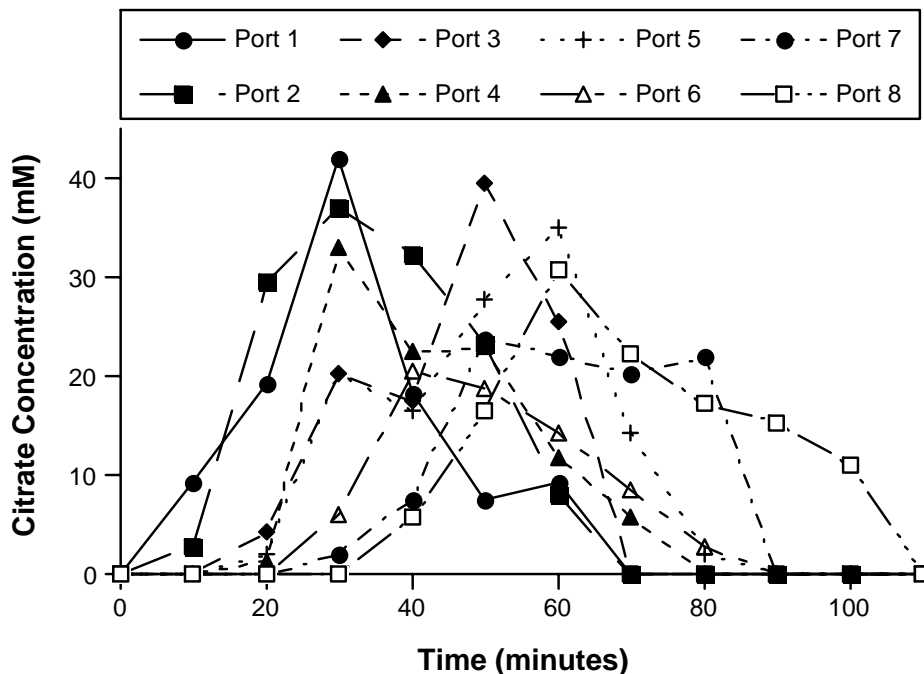
Figure 8.6.6-15. Concentration of citrate in each of eight ports over time in a column of manganese coated sand (MCS) containing hexachlorobenzene (HCB) treated with H_2O_2 stabilized by 25 mM citrate at pH 7.
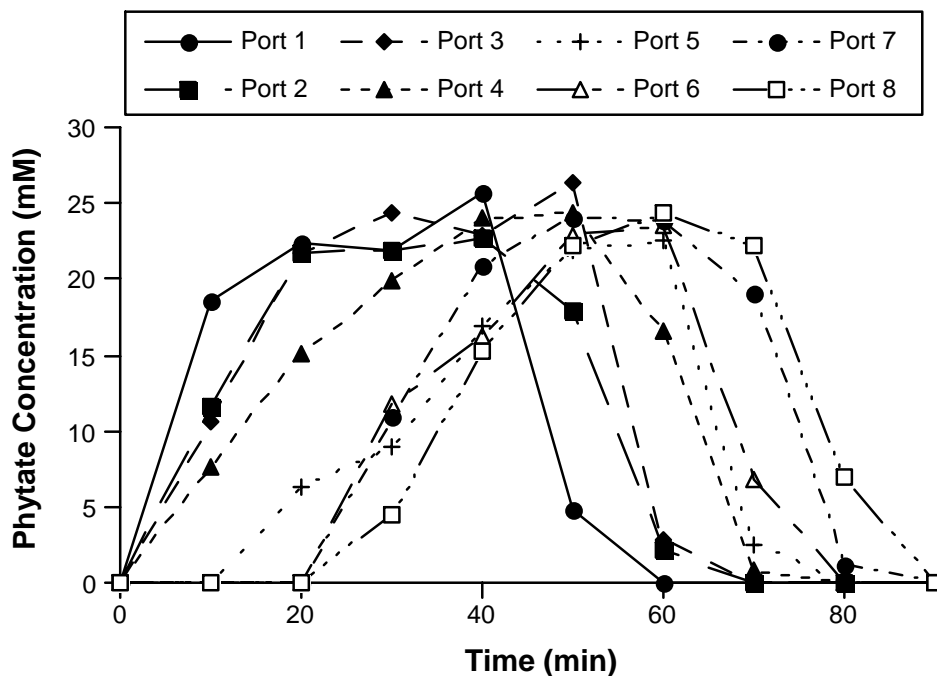
Figure 8.6.6-16. Concentration of phytate in each of eight ports over time in a column of manganese coated sand (MCS) containing hexachlorobenzene (HCB) treated with H_2O_2 stabilized by 25 mM phytate at pH 7.
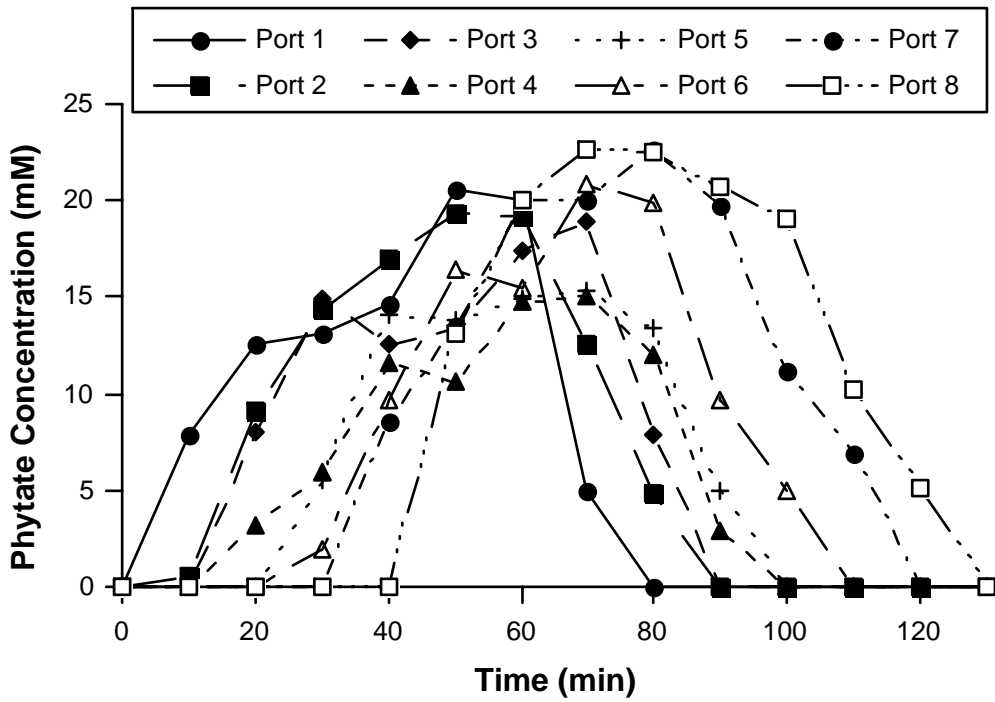
Figure 8.6.6-17. Concentration of phytate in each of eight ports over time in a column of iron coated sand (ICS) containing hexachlorobenzene (HCB) treated with H_2O_2 stabilized by 25 mM phytate at pH 7.
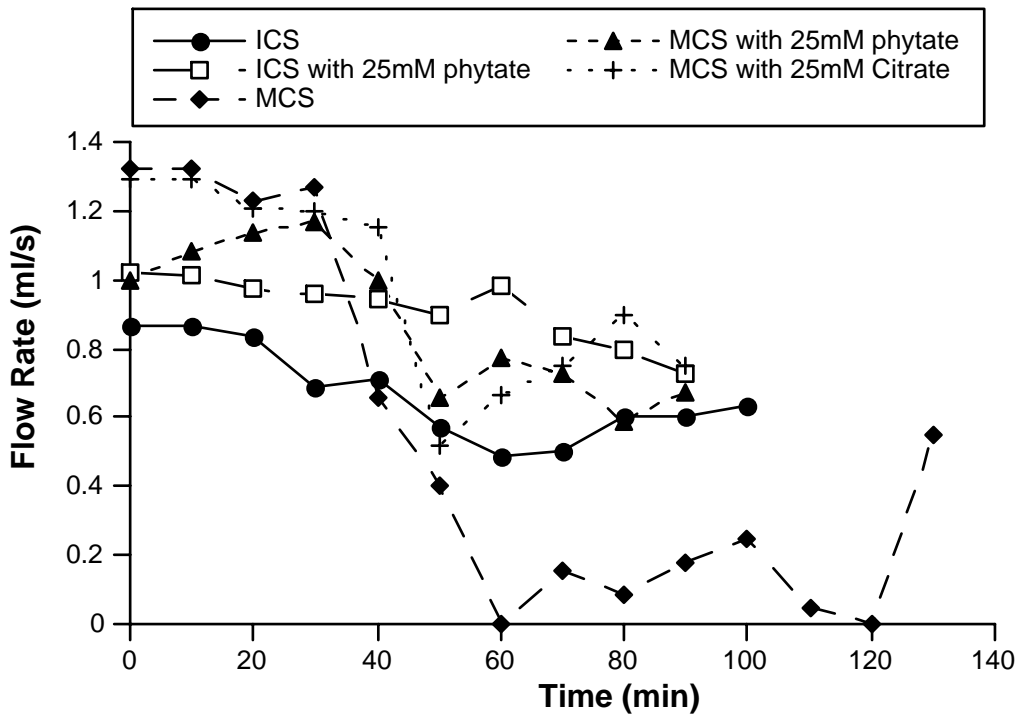
Figure 8.6.6-18. Flow rate with time in each type of column experiment.

9. CONCLUSIONS

A detailed study of catalyzed H_2O_2 propagations (CHP) was conducted to investigate mechanisms and pathways of contaminant destruction and to improve the delivery of CHP reagents to the subsurface. Results from the study provide the following specific conclusions:

- Hydrogen peroxide decomposition by soluble iron generates an increasing flux of superoxide anion as hydrogen peroxide concentrations are increased.

- On a per mass basis, manganese oxide minerals are the most active catalysts of the subsurface minerals for the decomposition of hydrogen peroxide. In natural soils and subsurface solids, both crystalline iron and manganese oxides are active catalysts for hydrogen peroxide decomposition; although iron oxides are less active on a per mass basis, they are found in significantly higher concentrations in soils and subsurface solids relative to manganese oxide minerals.

- Trace minerals, such as anatase, bauxite, and cuprite, decompose hydrogen peroxide at rates several orders of magnitude lower than do iron and manganese oxides.

- Soluble manganese (II) mediates the decomposition of hydrogen peroxide with the generation of hydroxyl radical at a relatively slow rate, but with efficient stoichiometry. Solid manganese dioxides decompose hydrogen peroxide rapidly to superoxide anion.

- Superoxide, which has traditionally been considered unreactive with carbon tetrachloride in water, does exhibit significant reactivity when hydrogen peroxide is present as a cosolvent in CHP systems.

- Degradation products for the reaction of carbon tetrachloride with superoxide include phosgene, which rapidly collapses to carbonate and chloride.

- Under oxidizing conditions, perchloroethylene is degraded to dichloroacetic acid and dichloroacetyl chloride. These products are oxidized further to a labile phosgene-like intermediate and then to carbon dioxide and water.

- Chlorinated alkenes and alkanes are reduced by superoxide in CHP systems through pathways similar to other reductive abiotic and biotic processes. Reaction products include dichlorotheylenes and vinyl chloride.

- Benzo[a]pyrene and hexadecane are rapidly oxidized in CHP systems with minimal detection of degradation products. Use of ^{14}C-labeled parent compounds confirmed that 85% of the benzo[a]pyrene and 73% of the hexadecane carbon is rapidly converted to CO_2, with the remaining ^{14}C persisting as sorbed and undegraded.

- Dense nonaqueous phase liquids (DNAPLs) are destroyed by several mechanisms in CHP reactions depending on the rate of dissolution of the contaminant and relative rates of reactivity with hydroxyl radical and superoxide. Slowly dissolving DNAPLs with higher degrees of chlorination (e.g., carbon tetrachloride, perchloroethylene) are destroyed by superoxide at rates more rapidly than their rates of gas purge dissolution. Compounds with moderate chlorination (e.g., chloroform, 1,1-dichloroethane) are destroyed by both hydroxyl radical and superoxide at rates slower than their rates of gas purge dissolution.

- CHP is capable of treating hydrophobic contaminants significantly more rapidly than their rates of desorption. The hydrogen peroxide dosage required for enhanced treatment of sorbed contaminants is directly proportional to the contaminant octanol-water partition coefficient. Superoxide is the reactive species responsible for the enhanced desorption of hydrophobic contaminants from soils and subsurface solids. The conceptual model for the enhanced treatment of sorbed contaminants is desorption promoted by superoxide, followed by destruction via hydroxyl radical or superoxide in the bulk solution.

- Soil organic matter does not significantly affect contaminant destruction when CHP is conducted at acidic pH regimes. At neutral pH regimes, soil organic matter enhances the effectiveness of CHP treatment.

- Release of metals during CHP remediation is metal- and sorbent-specific. Superoxide generated at neutral pH can promote the release of some metals sorbed on kaolinite. However, cadmium and lead sorbed on the natural soils are not released by CHP reactions conducted at neutral pH, but are released in reactions at pH 3, due primarily to the destruction of organic matter.

- Hydrogen peroxide half-lives in the presence of minerals and subsurface solids can be increased by one to three orders of magnitude by adding one of three stabilizers: citrate, malonate, or phytate. Studies in one-dimensional columns containing iron oxide coated sand or manganese oxide coated sand demonstrate that transport of citrate and phytate is not retarded by the solids and are not rapidly degraded by the CHP reactions catalyzed by mineral coated sand. In addition, dosing the one-dimensional columns with a combined stabilizer-hydrogen peroxide solution resulted in equally effective hydrogen peroxide stabilization compared to preconditioning the columns with the stabilizer followed by dosing with hydrogen peroxide.

The results of this research demonstrate that numerous mechanisms are found in CHP systems and that, in many cases, the generation and reactivity of superoxide is as important as that of hydroxyl radical. Prior to completion of this research, superoxide was considered to be an unimportant byproduct of CHP reactions. The results of this research have confirmed that superoxide is more reactive in water than previously thought due to the presence of cosolvents, and that its presence is critical to the destruction of DNAPLs and the enhanced treatment of sorbed contaminants. The suite of reactive oxygen species, including hydroxyl radical, superoxide, and the strong nucleophile hydroperoxide provide a near-universal treatment matrix. However, the rapid decomposition of hydrogen peroxide, promoted by natural iron and manganese oxides in the subsurface, has limited the utility of CHP for the remediation of contaminated sites. Advances attained through the completed research in the stabilization of

hydrogen peroxide by citrate, malonate, and phytate will increase the utility and economic viability of CHP treatment.

All of the tasks and issues proposed for the project have been completed and resolved. Other issues that remain unstudied in CHP remediation include 1) the reactivity of perhydroxyl radical in CHP systems, 2) the mechanism of enhanced contaminant desorption by superoxide, and 3) the mechanism of enhanced DNAPL destruction by superoxide. Superoxide appears to have a significant effect on solution interfacial tension, which may aid in explaining many of its beneficial properties. Transition of the results of this research is in progress through the start of ESTCP Project ER-0632.

10. APPENDIX

List of Technical Publications

Refereed Publications

Published

Watts, R. J., Teel, A. L., 2006. Treatment of contaminated soils and groundwater using *in situ* chemical oxidation. *Pract. Period. Haz. Waste Manag.,* 10(1), 2-9.

Monahan, M. J., Teel, A. L., Watts, R. J**.,** 2005. Displacement of five metals sorbed on kaolinite during and after treatment with modified Fenton's reagent. *Water Res.,* 39(13), 2955-2963

Watts, R. J., Howsawkeng, J., Teel, A. L., 2005. Destruction of a carbon tetrachloride DNAPL by modified Fenton's reagent. *J. Environ. Eng.,* 131(7), 1114-1119.

Watts, R. J., Teel, A. L., 2005. Chemistry of modified Fenton's reagent (catalyzed H_2O_2 propagations—CHP) for *in situ* soil and groundwater remediation., *J. Environ. Eng.,* 131(4), 612-622.

Watts, R. J., Sarasa, J., Loge, F. J., and Teel, A. L. 2005. Oxidative and reductive pathways in manganese-catalyzed Fenton's reactions. *J. Environ. Eng.*, 131(1), 158-164.

Smith, B. A., Teel, A. L., Watts, R. J., 2004. Identification of the reactive oxygen species responsible for carbon tetrachloride degradation in modified Fenton's systems. *Environ. Sci. Technol.,* 38(20), 5465–5469.

Quan, H. N., Teel, A. L., and Watts, R. J. 2003. Effect of contaminant hydrophobicity on H_2O_2 dosage requirements in the Fenton-like treatment of soils. *J. Hazard. Mater.,* 102(2-3), 277-289.

Teel, A. L., and Watts, R. J. 2002. Degradation of carbon tetrachloride by Fenton's reagent. *J. Hazard. Mater.* 94:179-189.

Watts, R. J., Stanton, P.C., Howsawkeng, J., and Teel, A. L. 2002. Mineralization of a sorbed polycyclic aromatic hydrocarbon in two soils using catalyzed hydrogen peroxide. *Water Res.* 36:4283-4292.

Accepted for Publication

Smith, B. A., Teel, A. L., Watts, R. J. 2006. Destruction of carbon tetrachloride and chloroform DNAPLs by modified Fenton's reagent. *J. Contam. Hydrol.* In Press.

Bissey, L.L., Smith, J.L., and R. J. Watts, R.J. 2006. Soil Organic Matter-Hydrogen Peroxide Dynamics in the Treatment of Contaminated Soils and Groundwater using Catalyzed H_2O_2 Propagations (Modified Fenton's Reagent). *Water Res*. In Press.

Submitted

Teel, A. L., Watts, R. J., 2006. Fate of Sorbed Lead During Treatment of Contaminated Soils by Catalyzed H$_2$O$_2$ Propagations (Modified Fenton's Reagent). *J. Hazard. Mater*. Under Review.

Corbin III, J. F., Teel, A. L., Allen-King, R. M., and Watts, R. J. 2006. Reactive Oxygen Species Responsible for the Enhanced Desorption of Dodecane in Modified Fenton's Systems. *Water Environ. Res*. Under Review.

Watts, R.J., Schmidt, J., Cutler, L.M., and Teel, A.L. 2006. Decomposition of Hydrogen Peroxide by Trace Minerals. *J. Environ. Engr*. Under Review.

Abstracts

Watts, R.J., and A.L. Teel. 2006. Hydrogen peroxide decompositon dynamics in the subsurface: Catalyst selection for maximum oxidant distribution. Reduction Technologies for the Remediation of Contaminated Soils and Groundwater. Chicago, IL October 22-25, 2006

Watts, R.J., and A.L. Teel. 2006. New Advances in the Stabilization of Hydrogen Peroxide for ISCO. SERDP/ESTCP Partners in Technology Conference. Washington, DC. November 29-December 2, 2006

Smith, B.A., and Watts, R.J. 2004. Mechanism of Carbon Tetrachloride Degradation in Modified Fenton's Systems. American Chemical Society Meetings. Philadelphia, Pennsylvania

Bissey, L.L., Smith, J.L., and R. J. Watts, R.J. 2004. Fate of Organic Matter During ISCO with Catalyzed Hydrogen Peroxide Propagations (CHP). Second International Conference on Oxidation and Reduction Technologies for the In Situ Treatment of Soil and Groundwater. October 24-21. San Diego, California

Smith, B.A., and Watts, R.J. 2004. Enhanced Destruction of Dense Nonaqueous Phase Liquids (DNAPLs) Using Catalyzed Hydrogen Peroxide. Second International Conference on Oxidation and Reduction Technologies for the In Situ Treatment of Soil and Groundwater. October 24-21. San Diego, California

Smith, B.A., and Watts, R.J. 2004. A Fundamental Approach to Minimizing Net Hydrogen Peroxide Decomposition in Modified Fenton's Reactions.. Tenth International Conference on Advanced Oxidation Technologies for Water and Air Remediation. October 24-21. San Diego, California

Smith, B.A., and Watts, R.J. 2004. Identification of the Reactive Species in the Degradation of Carbon Tetrachloride in Modified Fenton's Systems. The Fourth International Conference on Remediation of Chlorinated and Recalcitrant Compounds. May 18-22 Monterey, CA

Smith, B.A., and Watts, R.J. 2003. Mechanism of CT Degradation in DNAPL Destruction. Subsurface Science Symposium, Inland Northwest Research Alliance. October 21-24, Salt Lake City, Utah.

Monahan, M.J., and Watts, R.J. 2003. Displacement of Metals from Subsurface Solids by Modified Fenton's Reagent. Subsurface Science Symposium, Inland Northwest Research Alliance. October 21-24, Salt Lake City, Utah.

Corbin, J., and Watts, R.J. 2002. Mechanism of Enhanced Contaminant Desorption by Modified Fenton's Reactions. Second International Conference on Oxidation and Reduction Technologies for the In Situ Treatment of Soil and Groundwater. November 17-21. Toronto, Ontario, Canada.

Monahan, M.J., and Watts, R.J. 2002. Investigation of Metal Mobility and Transient Oxygen Species Generation with Modified Fenton's Reactions using Varying Catalysts. Second International Conference on Oxidation and Reduction Technologies for the In Situ Treatment of Soil and Groundwater. November 17-21. Toronto, Ontario, Canada

Smith, B.A., and Watts, R.J. 2002. Destruction of a Carbon Tetrachloride DNAPL by Modified Fenton's Reagent. Second International Conference on Oxidation and Reduction Technologies for the In Situ Treatment of Soil and Groundwater. November 17-21. Toronto, Ontario, Canada.

Smith, B.A., and Watts, R.J. 2002. Mechanism of Carbon Tetrachloride Degradation in DNAPL Destruction. 2002. Subsurface Science Symposium, Inland Northwest Research Alliance. October 15-16. Boise, Idaho.

Kohtz, S.A., and Watts, R.J. Reagent Delivery Effects Involving Modified Fentons's Reactions in Subsurface Systems. 2002. The Third International Conference on Remediation of Chlorinated and Recalcitrant Compounds. May 20-23. Monterey, CA (S.A. Khotz and R.J. Watts)

Corbin, J., and Watts, R.J. 2002. Enhanced Contaminant Desorption by Modified Fenton's Reactions. The Third International Conference on Remediation of Chlorinated and Recalcitrant Compounds. May 20-23. Monterey, CA

Monahan, M.J., and Watts, R.J. 2002. Investigation of Metal Mobility and Transient Oxygen Species Generation with Modified Fenton's Reactions using Varying Catalysts. The Third International Conference on Remediation of Chlorinated and Recalcitrant Compounds. May 20-23. Monterey, CA

Destruction of a Carbon Tetrachloride DNAPL by Modified Fenton's Reagent. 2002. The Third International Conference on Remediation of Chlorinated and Recalcitrant Compounds. May 20-23. Monterey, CA (B.A. Smith and R.J. Watts)

11. REFERENCES

Addink, R., and Olie, K., (1995) Mechanism of Formation and Destruction of Polychlorinated Dibenzo-p-dioxins and Dibenzonfurans in Heterogeneous Systems, *Environ. Sci. Technol.* 29(6), 1425-1435.

Afanas'ev, I. B., 1989. Superoxide Ion: Chemistry and Biological Implications Vol.1. CRC Press, Boca Raton, FL.

Al-Ekabi, H., Edwards, G., Holden, W., Safaazadeh-Amiri, A., and Story, J. (1992). Chemical Oxidation. W.W. Eckenfelder, A.R. Bowers and J.A. Roth, eds., Technomic, Lancanster, PA, 254-261.

Al-Hayek, N. and M. Dore. 1990. Oxidation of phenols in water by hydrogen peroxide on alumina supported iron. *Water Res.* 24:973-982.

Allen, D.T., and D.R. Shonnard. 2001. *Green Engineering: Environmentally Consciousness Design of Chemical Processes*. Prentice-Hall. Englewood Cliffs, NJ.

Amonett, J.E., Dixon, J.B., and Schulze, D.G., (2002) *Soil Mineralogy with Environmental Applications*, Soil Science Society of America, Madison, WI.

Anderson, M.R., R.L. Johnson, and J.F. Pankow. 1992. Dissolution of dense chlorinated solvents into groundwater. I. Dissolution from a well-defined residual source. Ground Water. 30: 250-256.

APHA. 1998. Standard Methods for the Examination of Water and Wastewater, 20th Edition. American Public Health Association, Water Environment Federation, American Water Works Association. New York.

Archibald, F.S., and Fridovich, I, 1982. The scavenging of superoxide radical by manganous complexes: in vitro. Arch. Biochem. Biophys. 214, 452-463.

Asmus, K. D., 1988. In: Reactive Oxygen Species in Chemistry, Biology, and Medicine, Quintanilha, A., Ed.. NATO ASI Series, Plenum Press, New York.

ASTDR Biannual Report to Congress: October 17, 1986–September 30, 1988 (1989) Agency for Toxic Substances and Disease Registry, U.S. Public Health Service, Atlanta, GA.

Auzerais, F.M., J. Dunsmuir, B.B. Ferreol, N. Martys, J. Olson, T.S. Ramakrishnan, D.H. Rothman, and L.M. Schwartz. 1996. Transport in sandstone: a study based on three dimensional microtomography. *Geophys. Res. Lett.* 23(7):705–708.

Babbs, C. F. and Griffin, D. W. 1989. Scatchard analysis of methane sulfinic acid production from dimethyl sulfoxide: A method to quantify hydroxyl radical formation in physiologic systems. Free Radical Biol. Med., 6(5), 493-503.

Barb, W. G., Baxendale, J. H., George, P., and Hargrave, K. R. (1950) Reactions of ferrous and ferric ions with hydrogen peroxide. *J. Amer. Chem. Soc.* 121, 462-499.

Barbeni, M., C. Minero, and E. Pelizzetti. 1987. Chemical degradation of chlorophenols with Fenton's reagent. *Chemosphere*. 16:2225-2237.

Bedient, P. B., Rifai, H. S., and Newell, C. J. (1994). *Ground Water Contamination: Transport and Remediation*. Prentice-Hall Publishing Co., Englewood Cliffs, NJ.

Beltran, F. J. (2003) *Ozone Reaction Kinetics for Water and Wastewater Systems*. CRC Press LLC. Boca Raton, Fl.

Bielski, B. H. J., Shiue, G. G., and Bajuk, S. (1980). "Reduction of nitro blue tetrazolium by CO_2^- and O_2^- radicals." *J. Phys. Chem.,* 84(8), 830-833.

Bielski, B.H.J., and R.L. Arudi, 1983. Preparation and stabilization of aqueous/ethanolic superoxide solutions. *Analytical Biochem.* 133(1):170-178.

Bielski, B.H.J., Cabelli, D.E., Arudi, R.L., Ross, A.B., 1985. Reactivity of HO_2/O_2^- radicals in aqueous solution. J. Phys. Chem Ref. Data 14, 1041-1102.

Bowers, A.R., P. Gaddipati, W.W. Eckenfelder, and R.M. Monsen. 1989. Treatment of toxic or refractory wastewater with hydrogen peroxide. *Water Sci. Technol.* 21:477-486.

Box, G.E.P., W.G. Hunter and J.S. Hunter. 1978. Statistics for experimenters. John Wiley & Sons. New York, NY.

Bruckner, J. V., Davis, B. D., and Blancato, J. N. (1989) Mechanisms, toxicity, and carcinogenicity of trichloroethylene. *Crit. Rev. Toxicol.* 20, 31-50.

Brusseau, M.L., Jessup, R.E., Rao, P.S.C., 1990. Sorption kinetics of organic chemicals: evaluation of gas-purge and miscible-displacement techniques. Environ. Sci. Technol. 24, 727-735.

Burcat A, Khachatryan L, Dellinger BL. 2003. Thermodynamics of chlorinated phenols, polychlorinated dibenzo-p-dioxins, polychlorinated dibenzofurans, derived radicals, and intermediate species. *J Phys Chem Ref Data* 32:443-518.

Butler E.C, Hayes K.F. Effects of solution composition and pH on the reductive dechlorination of hexachloroethane by iron sulfide. . *Environ. Sci. Technol.* 1998, *32(9)*: 1276-1284

Butler E.C, Hayes K.F. Kinetics of the transformation of trichloroethylene and tetrachloroethylene by iron sulfide. *Environ. Sci. Technol.* 1999, *33(12)*, 2021-2027.

Buxton, G. V., C. L. Greenstock, W. P. Helman, A. B. Ross. 1988. Critical review of rate constants for reactions of hydrated electrons, hydrogen atoms, and hydroxyl radicals in aqueous solution. *J. Phys. Chem.*, 17: 513-780.

Buyuksonmez, F., T.F. Hess, R.L. Crawford, A. Paszczynski, and R.J. Watts. 1999. Optimization of simultaneous chemical and biological mineralization of perch loroethylene (PCE). Appl. *Environ. Microbiol.* 65:2784-2788.

Buyuksonmez, F., T.F. Hess, R.L. Crawford, and R.J. Watts. 1998. Toxic effects of modified Fenton reactions on Xanthobacter flavus FB7 1. *Appl. Environ. Microbiol.* 64:3759-3764.

Cabelli, D. E.; Bielski, B. H. J. (1983) Kinetics and Mechanisms for the Oxidation of Ascorbic Acid/Ascorbate by HO_2/O_2^- Radicals. A Pulse Radiolysis and Stopped-Flow Photolysis Study. J. Phys. Chem., 87, 1809.

Carter, D.L., M.M. Mortland, and W. D. Kemper. Specific surface. *In*: A. Klute, Ed., *Methods of Soil Analysis.* Amer. Soc. of Agronomy, Madison, WI. pp. 413–422.

Chen, C.T. 1992. Assessment of the applicability of chemical oxidation technologies for the treatment of contaminants at leaking underground storage tank (LUST) sites. *in* Chemical Oxidation Technologies for the Ninties, J.A. Roth and A.R. Bowers (Eds.), Technomic Publishing Co., Inc.

Cherna, C.I., R. DiCosimo, R. De Jesus, and J. San Filippo, Jr. 1978. A study of superoxide reactivity. Reaction of potassium superoxide with alkyl halides and tosylates. *J. Am. Chem. Soc.* 100:7317–7326.

Chou, S. S. and Huang, C. P. (1999). "Application of a supported iron oxyhydroxide catalyst in oxidation of benzoic acid by hydrogen peroxide." *Chemosphere,* 38(12), 2719-2731.

Clesceri, L.S., Greenberg., L.E., and Eaton, A.E. (1998). Standard Methods for the Examination of Water and Wastewater, 20th Edition.. APHA, AWWA, and WEF.

Cochran, W.G. and G.M. Cox. 1992. Experimental designs. 2nd ed. John Wiley & Sons, Inc. New York, NY.

Corbin, J. F., R. J. Watts, and A. L. Teel. 2004. Reactive oxygen species responsible for the enhanced desorption of dodecane in modified Fenton's systems. *Environ. Sci. Technol.,* Under Review.

Csanyi, L. J., Nagy, L., Galbacs, Z. M., Horvath, I., 1983. Alkali-induced generation of superoxide and hydroxyl radicals from aqueous hydrogen peroxide solution. Z. Phys. Chem. 138, 107-116.

Curtis, G.P. and M. Reinhard. 1994. Reductive dehalogenation of hexachloroethane, carbon tetrachloride, and bromoform by anthrahydroquinone disulfonate and humic acid. *Environ. Sci. Technol.* 28: 2393-2401.

David, M. D., Seiber, J. N., 1999. Accelerated hydrolysis of industrial organophosphates in water and soil using sodium perborate. Environ. Pollut. 105(1), 121-128.

De Laat, J., Gallard, H., 1999. Catalytic decomposition of hydrogen peroxide by Fe(III) in homogeneous aqueous solution: Mechanism and kinetic modeling. Environ. Sci. Tech., 33(16), 2726-2732.

Dekker, T. J., and Abriola, L. M. (2000). "The influence of field-scale heterogeneity on the surfactant-enhanced remediation of entrapped nonaqueous phase liquids." *J. Contam. Hydrol.,* 42(2-4), 219-251.

Deutsch, W. J. Groundwater chemistry: fundamentals and applications to contamination. Lewis Publishers, Boca Raton, Fl., 1997.

Diamond, W.J. (1989) Practical Experiment Designs For Engineers and Scientists, 2nd Edition. Van Nostrand Reinhold, New York, 268-275.

DiStefano, T.D., J.M. Gossett, and S.H. Zinder. 1991. Reductive dechlorination of high concentrations of tetrachoroethene to ethene by an anaerobic enrichment culture in the absence of methanogenisis. *Applied and Environmental Microbiology.* 57:2287-2292.

Dixon, J.B., Weed, S.B. (1977) Mineral in Soil Environments. 186-190, Soil Science Society of America.

Dorfman, L. M., Adams, G. E., 1973. Reactivity of the Hydroxyl Radical in Aqueous Solutions. U.S. Department of Commerce, National Bureau of Standards NSRDS-NS, 46.

Dragun, J. and Chiasson, A. (1991). *Elements in North American Soils*. Hazardous Materials Control Resources Institute. Greenbelt, MD.

Droste, R.L. 1997. *Theory and Practice of Water and Wastewater Treatment.* John Wiley & Sons. New York. 800 p.

Dureja, P., S. Walia, and S.K. Mukerjee. 1984. Superoxide-mediated monodehalogenation of cyclodienes insecticides. *J. Agric. Food Chem.* 32:1217–1225.

Edwards, J.O., Pearson, R.G., 1962. The factors determining nucleophilic reactivities. J. Am. Chem. Soc. 84(1), 16-24.

Eickhoff, H., Jung, G., and Rieker, A., (2001) "Oxidative Phenol Coupling-Tyrosine Dimers and Libraries Containing Tyrosyl Peptide Dimers," *Tetrahedron* 57(2), 353-264.

ESTCP (1999) *Technology Status Review: In Situ Oxidation*. Environmental Security Technology Certification Program, Arlington, VA.

Farhataziz and A.B. Ross. 1977. Selected specific rates of reactions of transients from water aqueous solution. NSRDS-NBS 59. U.S. Department of Commerce.

Fedorak, P.M., J.M. Foght and W.S. Westlake. 1982. A method for monitoring mineralization of ^{14}C-labeled compounds in aqueous samples. *Water Res.* 16:1285-1290.

Fenton, H.J.H. 1894. Oxidation of tartaric acid in presence of iron. *J. Chem. Soc.* 65:899-910.

Feuerstein, W., E. Gilbert, and S.H. Eberle. 1981. Model experiments for the oxidation of aromatic compounds by hydrogen peroxide in wastewater treatment. *Vom Wasser.* 56:35-54.

Francis, K.C., Cummins, D., Oakes, J., 1985. Kinetic and structural investigations of [FeIII(edta)]–[edta = ethylenediaminetetra-acetate(4–)] catalysed decomposition of hydrogen peroxide. J. Chem. Soc. Dalton Trans. (3), 493-501.

Freeman, H.M. 1990. *Hazardous Waste Minimization.* McGraw-Hill, New York, NY.

Freeze, R.A. (2000). "The Environmental Pendulum: A Quest for Truth About Toxic Chemicals, Human Health, and Environmental Protection." University of California Press, Berkeley, CA.

Freund, J.E. Mathematical statistics; fifth edition. Prentice-Hall, Inc. Englewood Cliffs, N.J. 1992.

Frimer, A.A., I. Rosenthal, and S. Hoz. 1977. The reaction of superoxide radical anion with electron poor olefins. *Tetrahedron Lett.* 4631–4638.

Gambrell, R.P. In *Methods of Soil Analysis: Part 3. Chemical Methods*; Sparks, D.L., Ed.; Soil Science Society of America: Madison, WI, 1996.

Gates, D.D., and R.L. Siegrist. 1995. In situ chemical oxidation of trichloroethylene using hydrogen peroxide. *J. Environ. Engr.* 121:639-644.

Gee, B.W., Bauder, J.W. Particle size analysis in: A. Klute (Ed.), Methods of soil analysis; part 1. physical and mineralogical methods, American Society of Agronomy, Madison, WI, 1986; p. 399.

Glaze, W.H. and J.W. Kang. 1988. Advanced oxidation processes for treating groundwater contaminated with TCE and PCE: Laboratory studies. *J. Am. Water Works Assoc.* 80:57-63.

Glaze, W.H., J.F. Kenneke, and J.L. Ferry. 1993. Chlorinated by-products from the T102-mediated photodegradation of trichloroethylene and tetrachloroethylene in water. *Environ Sci. Technol.* 27:177-184.

Goldman, B.A. (1986). "Hazardous Waste Management: Reducing the Risk." Island Press, Washington, D.C.

Goss, K.-U. (1992) Effects of Temperature and Relative Humidity on the Sorption of Organic Vapors on Quartz Sand. Environ. Sci. Technol., 26, 2287.

Gousetis, C. and H-J. Opgenorth. 1991. Ullman's Encyclopedia of Industrial Chemistry. VCH. 5th Edition. A17: 377-381.

Graedel, T.E. and B.R. Allenby. 2002. *Industrial Ecology.* Prentice-Hall. Englewood Cliffs, NJ.

Griffith, S.M. and J. Schnitzer. 1977. Organic compounds formed by the hydrogen peroxide oxidation of soils. *Can. J. Soil Sci.* 57:223-231.

Haag, W.R. and C.D.D. Yao. 1992. Rate constants for reaction of hydroxyl radicals with several drinking water contaminants. *Environ. Sci. Technol.* 26:1005-1013.

Haber, F., and Weiss, J. 1934. The catalytic decomposition of hydrogen peroxide by iron salts. *Proc. Royal Soc. London Ser. A.* 147:332-351.

Haeri-McCaroll, T.M. 1994. The use of catalyzed hydrogen peroxide to oxidize chlorobenzenes in soil. Ph.D. Dissertation, Washington State University, Pullman, WA.

Hagiwara, K. 1984. Treatment of wastewater containing nondecomposable organic compounds. *JETI.* 32:79-82.

Hallewell, B., and Gutteridge, J. M. C. (1985). *Free Radicals in Biology and Medicine.* Clarendon Press, Oxford University Press, New York.

Hamilton, S.J., Cleveland, L., Smith, L.M., Lebo, J.A., and Mayer, F.L., (1986) "Toxicity of Pure Pentachlorophenol and Chlorinated Phenoxyphenol Impurities to Fathead Minnows," *Environmental Toxicology and Chemistry*, 5(6), 543-552.

Hawthorne, S.B.; Lagadec, A.J.M.; Kalderis, D.; Lilke, A.V.; Miller, D.J. 2000. Pilot-scale destruction of TNT, RDX, and HMX on contaminated soils using subcritical water. Environ. Sci. Technol. 34(15), 3224-3228.

Hill, E. H., Moutier, M., Alfaro, J. Miller, C. T., 2001. Remediation of DNAPL pools using dense brine barrier strategies. Environ. Sci. Technol. 35(14), 3031-3039.

Hinchee, R.E., Anderson, D.B., Mitting, F.B., Jr., and Sayles, G.D., 1994. Applied Biotechnology for Site Remediation, Lewis Publishers, Boca Raton, FL.

Hirvonen, A., Trapido, M., Hentunen, J., and Tarhanen, J., (2000). "Formation of Hydroxylated and Dimeric Intermediates during Oxidation of Chlorinated Phenols in Aqueous Solution," *Chemosphere*, 41(8), 1211-1218.

Ho, C.L., M.A. Shebl, and R.J. Watts. 1995. Development of an injection system for *in situ* catalyzed peroxide remediation of contaminated soils. 1995. *Haz. Waste Haz. Mater.* 12: 15-25.

Hogg, R.V., and Ledolter, J. (1992). "Applied Statistics for Engineers and Physical Scientists." Macmillan Publishing Co., N. Y.

Hoigné, H, Bader, H., Haag, W., and Staehelin, J. (1985). "Rate constants of reactions of ozone with organic and inorganic compounds in water." *Water Res*., 19(8), 993-1004.

Hoigné, I and H. Bader. 1976. The role of hydroxyl radical reactions in ozonation processes in aqueous solutions. *Water Res.* 10:377-386.

Hoigné, J. and H. Bader. 1983. Rate constants of reactions of ozone with organic and inorganic compounds in water. II. Dissociating organic compounds. *Water Res.* 17:185-194.

Howsawkeng, J., Watts, R. J., Washington, D. L., Teel, A. L., Hess, T. F., and Crawford, R. L. 2001. Evidence for simultaneous abiotic-biotic oxidations in a microbial-Fenton's system. *Environ. Sci. Technol.*, 35(14):2845-2850.

Huang, H. H., Lu, M. C., and Chen, J. N. (2001). "Catalytic decomposition of hydrogen peroxide and 2-chlorophenol with iron oxides." *Water Res.,* 35(9), 2291-2299.

Huling, S. G., Arnold, R. G., Sierka, R. A., and Miller, M. R. (1998). "Measurement of hydroxyl radical activity in a soil slurry using the spin trap alpha-(4-pyridyl-1-oxide)-N-tert-butylnitrone." *Environ. Sci. Technol.,* 32(21), 3436-3441.

Huling, S.G., Arnold, R.G., Sierka, R.A., and Miller, M.R. (2001). "Influence of peat on Fenton oxidation." *Water Res*., 35(7), 1687-1694.

Hunt, J. R., Sitar, N., Udell, K. S. (1988). "Nonaqueous phase liquid transport and cleanup I.

Ingles, D.L. 1972. Studies of oxidations by Fenton's reagent using redox titration. I. Oxidation of some organic compounds. *Aust. Jour. Chem.* 25:87.

Ingles, D.L. 1972. Studies of oxidations by Fenton's reagent using redox titration. I. Oxidation of some organic compounds. *Aust. Jour. Chem.* 25:87-95.

Jackson, M.L., Lim, C.H., and Zelazny, L.W. (1986) In: A. Klute et al. (Eds), Methods of Soil Analysis, Part 1. ASA and SSSA, Madison, Wisconsin, 124.

Jerome, K., Rhia, B., and Looney, B. B. (1997). "Final report for demonstration of in situ oxidation of DNAPL using the Geo-Cleanse technology." Westinghouse Savannah River Company, September 19, 1997.

Johnson, R.L., Pankow, J.F., 1992. Dissolution of dense chlorinated solvents into groundwater. 2. Source functions for pools of solvent Environ. Sci. Technol. 26(5), 896-901.

Kakarla, P.K.C. and R.J. Watts. 1997. Depth of Fenton-like oxidation in remediation of surface soil. *J. Environ. Eng.*, 123:11-17.

Kao, C. M., and Wu, M. J. (2000). "Enhanced TCDD degradation by Fenton's reagent preoxidation." *J. Hazard. Mater.,* 74(3), 197-211.

Karickhoff, S.W., D.S. Brown, and T.A. Scott. 1979. Sorption of hydrophobic pollutants on natural sediments. Water Res. 13:241-248.

Karimi, A.A., J.A. Redman, W.H. Glaze, and G.F. Stolarik. 1997. Evaluating an AOP for TCE and PCE removal. *J. Am. Water Works Assoc.* 89:41-53.

Kaslusky, S. F., Udell, K. S., 2002. A theoretical model of air and steam co-injection to prevent the downward migration of DNAPLs during steam-enhanced extraction. J. Contam. Hydrol. 55(3-4), 213-232.

Kawahara, F. K., Davila, B., Alabed, S. R., Vesper, S. J., Ireland, J. C., and Rock, S. (1995). "Polynuclear aromatic hydrocarbon (PAH) release from soil during treatment with Fenton's reagent." *Chemosphere,* 31(9), 4131-4142.

Khan, M.A.J., and R.J. Watts. 1996. Mineral-catalyzed peroxidation of tetrachloroethylene. *Water Air Soil Pollut.* 88:247-260.

Kibbey, T.C.G., Ramsburg, C.A., Pennell, K.D., Hayes, K.F., 2002. Implications of alcohol partitioning behavior for in situ density modification of entrapped dense nonaqueous phase liquids. Environ. Sci. Technol. 36(1), 104-111.

Kitajima, N., Fukuzumi, S., and Ono, Y. (1978). "Formation of superoxide ion during the decomposition of hydrogen peroxide on supported metal oxides." *J. Phys. Chem.,* 82(13), 1505-1509.

Kitao, T., Y. Kiso, and R. Yahashi. 1982. Studies on the mechanism of decolorization with Fenton's reagent. *Mizu Shori Gijutsu.* 23:1019-1026.

Klausen, J., Haderlein, S.B., and Schwarzenbach, R.P., (1997). "Oxidation of Substituted Anilines by Aqueous MnO_2: Effect of Co-Solutes on Initial and Quasi-Steady-State Kinetics," *Environ. Sci. Technol.,* 31(9), 2642-2649.

Klute, A. 1986. *Methods of Soil Analysis.* American Society of Agronomy, Inc. Madison, WI.

Kong, S., Watts, R.J., and Choi, J.H. 1998. Treatment of Petroleum-Contaminated Soils Using Iron Mineral Catalyzed Hydrogen Peroxide. *Chemosphere.* 37: 1473-1482.

Kornblum, N., and S. Singaram. 1979. Conversion of nitriles and esters to acids by the action of sodium superoxide. *J. Org. Chem.* 44:4727–4733.

Kriegman-King, M.R. and M. Reinhard. 1992. Transformation of carbon tetrachloride in the presence of sulfide, biotite, and vermiculite. *Environ. Sci. Technol.* 26: 2198-2206.

Kriegman-King, M.R. and M. Reinhard. 1994. Transformation of carbon tetrachloride by pyrite in aqueous solution. *Environ. Sci. Technol.* 28: 692-700.

Kueper, B. H., Redman, D., Starr, R. C., Reitsma, S. and Mah, M. (1993). "A field experiment to study the behavior of tetrachloroethylene below the water-table—spatial distribution of residual and pooled DNAPL." *Ground Water,* 31(5), 756-766.

Kuhlman, M.I., 2002. Analysis of the steam injection at the Visalia Superfund Project with fully compositional nonisothermal finite difference simulations. J. Hazard. Mater. 92(1), 1-19.

Kwan, W. P., Voelker, B. M., 2003. Rates of hydroxyl radical generation and organic compound oxidation in mineral-catalyzed Fenton-like systems. Environ. Sci. Technol. 37(6), 1150-1158.

Laha, S., and Luthy, R.G., (1990). "Oxidation of Aniline and Other Primary Aromatic Amines by Manganese Dioxide," *Environ. Sci. Technol.,* 24(3), 363-373.

Larson, R. A., Weber, E.J. 1994. Reaction Mechanisms in Environmental Organic Chemistry. Lewis Publishers, Inc, Chelsea, MI.

Lee, B. D., and Hosomi, M. (2001). "Fenton oxidation of ethanol-washed distillation-concentrated benzo(A)pyrene: reaction product identification and biodegradability." *Water Res.,* 35(9), 2314-2319.

Lee, B. D., Hosomi, M., and Murakami, A. (1998). "Fenton oxidation with ethanol to degrade anthracene into biodegradable 9,10-anthraquinon: A pretreatment method for anthracene-contaminated soil." *Water Sci. Technol.,* 38(7), 91-97.

Lee, S.H. and J.B. Carberry. 1992. Biodegradation of PCP enhanced by chemical oxidation pretreatment. *Water Environ. Res*. 64:682-690.

Lee, S.Z., Chang, L., Chen, C.M., Liu, M.C.,Tsai, L.J. Development of soil metal criteria to preserve groundwater quality. Wat. Sci. Tech. 1998; 38:131-139.

Lemke, L. D., Abriola, L. M., Goovaerts, P. 2004. Dense nonaqueous phase liquid (DNAPL) source zone characterization: influence of hydraulic property correlation on predictions of DNAPL infiltration and entrapment. Water Resour. Res. 40, W01511.

Leung, S.W., R.J. Watts, G.C. Miller. 1992. Degradation of perchloroethylene by Fenton's reagent: Speciation and pathway. *J. Environ. Qual.* 21:377.

Lewis, R.J., Sr. *Sax's Dangerous Properties of Industrial Materials*, 10th Ed; Wiley: New York, 2000.

Li, Z.M., S.D. Comfort, and P.J. Shea. 1997a. Destruction of 2,4,6-Trinitrotoluene by Fenton Oxidation. *J. Environ. Qual*. 26:480-487.

Li, Z.M., Shea, P.J., and Comfort, S.D. (1997) Fenton oxidation of 2,4,6-trinitrotoluene in contaminated soil slurries. *Environ. Eng. Sci*. 14, 55-56.

Li, Z.M.; Peterson, M.M.; Comfort, S.D.; Horst, G.L.; Shea, P.J.; Oh, B.T. (1997) Remediating TNT-Contaminated Soil by Soil Washing and Fenton Oxidation Sci. Total Env., 204, 107.

Lin, S. S., and Gurol, M. D. (1996). "Heterogeneous catalytic oxidation of organic compounds by hydrogen peroxide." *Water Sci. Technol.,* 34(9), 57-64.

Lin, S.S. and Gurol, M.D. 1998. Catalytic decomposition of hydrogen peroxide on iron oxide: kinetics, mechanisms, and implications. *Environ. Sci. Technol.* 32:1417-1423.

Lindsey, M. E., and Tarr, M. A. (2000b). "Inhibited hydroxyl radical degradation of aromatic hydrocarbons in the presence of dissolved fulvic acid." *Water Res.,* 34(8), 2385-2389.

Lindsey, M. E., and Tarr, MA. (2000a). "Quantitation of hydroxyl radical during Fenton oxidation following a single addition of iron and peroxide." *Chemosphere,* 41(3), 409-417.

Lipczynska-Kochany, E. (1991) Degradation of Aqueous Nitrophenols and Nitrobenzene by Means of the Fenton Reaction. Chemosphere 22, 777-782.

Lipczynska-Kochany, E., Sprah, G., Harms, S. (1994) Determined Reaction Rate Constants for the Oxidation of 4-Chlorophenol using Fenton's Reagent. Chemosphere 30, 9-___.

Lipczynska-Kochany, G., Sprah, G., and Harms, S. (1995) Influence of some groundwater and surface waters constituents on the degradation of 4-chlorophenol by the Fenton reaction. *Chemosphere*. 30, 9-20.

Luzzatto, E., Cohen, H., Stockheim, C., Wieghardt, K., and Meyerstein, D. (1995). "Reactions of low-valent transition-metal complexes with hydrogen peroxide. Are they Fenton-like or not. 4. The case of Fe(II)L, L= EDTA, HEDTA and TCMA." *Free Radical Res.,* 23(5), 453-463.

Lynch, R.E., and Fridovich, I., 1978. Permeation of the erythrocyte stroma by superoxide radical. J. Biol. Chem. 253, 4697-4699.

Macdonald, T.L. Chemical mechanisms of halocarbon metabolism, Crit. Rev. Toxicol., 11 (1982) 85-120.

Maestri, B., Dorman, M.E., and Hartigan J. (1988). "Managing Pollution from Highway Storm Water Runoff." *Trans. Res. Rec.*, 1166, 15-21.

Marklund, S. 1976. Spectrophotometric study of spontaneous disproportionation of superoxide anion radical and sensitive direct assay for superoxide dismutase. *J. Biol. Chem.*

Martel, R., and Gélinas, P. J. (1996). "Surfactant solutions developed for NAPL recovery in contaminated aquifers." *Ground Water,* 34(1), 143-154.

Martens, D. A., and Frankenberger, W. T., Jr. (1994). "Feasibility of in situ chemical oxidation of refractile chlorinatic organics by hydrogen peroxide-generated oxygen radicals in soil." In *Emerging Technol. Biomed. Metal*, 2nd ed. 74-84.

Masschelein, W., M. Denis, R. Ledent, Spectrophotometric determination of residual hydrogen peroxide, *Wat. Sew. Works* 32 (1977) 69-72.

Masten, S. and Davies, S. (1997). "Efficacy of in-situ oxidation for the remediation of PAH contaminated soils." *J. Contam. Hydrol.*, 28, 327-335.

Masten, S.J., M.J. Galbraith, and S.H.R. Davies. 1997. Oxidation of 1,3,5-trichlorobenzene using advanced oxidation processes. *Ozone Sci. Eng.* 18:535-547.

Matheson, L.J. and Tratnyek, P.G. (1994). "Reductive Dehalogenation of Chlorinated Methanes by Iron Metal." *Environ. Sci. Technol.* 28, 2045-2053.

McBride, M.B. *Environmental Chemistry of Soils*; Oxford Press: New York, 1994.

Merenyi, G.; Lund, J.; Eriksen, T.E. 1984. The equilibrium reaction of luminol radical with oxygen and the one-electron reduction potential of 5-aminophthalazine-1,4-dione. *J. Phys. Chem.* 88:2320-2323

Merz, J.H. and W.A. Waters. 1949. The oxidation of aromatic compounds by means of the free hydroxyl radical. *J. Chem. Soc*. 120:2427-2433.

Michelcic, J.R., and Luthy, R.C. (1988) Degradation of polycyclic aromatic hydrocarbon compounds under various redox conditions in soil-water systems. Appl. Environ. Microbiol. 54, 1182-1187.

Miller, C. M., and Valentine, R. L. (1999). "Mechanistic studies of surface catalyzed H_2O_2 decomposition and contaminant degradation in the presence of sand." *Water Res.,* 33(12), 2805-2816.

Miller, C. M., and Valentine, R. L. 1995. Hydrogen peroxide decomposition and quinoline degradation in the presence of aquifer material. *Water Res*. 29:2353-2359.

Miller, C. M., Valentine, R. L., Roehl, M. E., and Alvarez, P. J. J. (1996). "Chemical and microbiological assessment of pendimethalin-contaminated soil after treatment with Fenton's reagent." *Water Res.,* 30(11), 2579-2586.

Miller, C.T., Hill, E.H., Moutier, M., 2000. Remediation of DNAPL-contaminated subsurface systems using density-motivated mobilization. Environ. Sci. Technol. 34(4), 719-724.

Monig, J.; Bahnemann, D.; Asmus, K.-D. (1983) One Electron Reduction of CCl_4 in Oxygenated Aqueous Solutions: A CCl_3O_2-Free Radical Mediated Formation of Cl- and CO_2. Chem. Biol. Interact., 47, 15.

Motekaitis, R.J. and A.E. Martell. 1994. The iron(III) and iron(II) complexes of nitrilotriacetic acid. *J. Coordin. Chem.* 31:67-73.

Mulligan, C.N., Yong, R.N., Gibbs, B.F. Remediation technologies for metal-contaminated soils and groundwater: an evaluation. Engineering Geology, 2001; 60:193-207.

Murakami, Y., K. Hagiwara, H. Kazuyoshi, S. Kunishige, O, Toshihide, and S. Honda. 1982. Treatment of wastewater containing refractory organic compounds by Fenton's and biological oxidations. *Mizu Shori Gijutsu.* 23:1031-1040.

Murphy, A.P., W.J. Boegli, M.K. Price and C.D. Moody. 1989. A Fenton-like reaction to neutralize formaldehyde waste solutions. *Environ. Sci. Technol.* 23:166-169.

Musso, H. *Oxidative Coupling of Phenols;* Taylor, W.I., Battersby, A.R., Eds.; Marcel Dekker: New York, 1967.

Nelson, C. and Brown, R. (1994). "Adapting ozonation for soil and groundwater cleanup." *Chemical Engineering*, Nov. Issue.

Nelson, D.W., and Sommers, L.E. In A.L. Page (Ed.), Methods of soil analysis, part 2. chemical and microbiological methods, American society of agronomy and soil science society of America, Madison, WI, 1982; p. 539-579.

Nelson, M.D., Parker, B.L., Al, T.A., Cherry, J.A., Loomer, D., 2001. Geochemical reactions resulting from in situ oxidation of PCE-DNAPL by $KMnO_4$ in a sandy aquifer. Environ. Sci. Technol. 35(6), 1266-1275.

Neta, P., Madhavan, V., Zemel, H., and Fessenden, R. W. (1976). "Rate constants and mechanism of reaction of SO_4^- with aromatic compounds." *J. Amer. Chem. Soc*, 99, 163-164.

NIOSH . 1985. Analytical Methodology for Sampling Industrial Environments. NIOSH 660/324-111.

NIOSH. 1985. Analytical Methodology for Sampling Industrial Environments. NIOSH 660/324-111.

Office of Technology Assessment. 1989. *Coming clean: Supedlind's problem can be solved.* Report OTA-ITE-433, U.S. Government Printing Office, Washington, D.C.

Ogram AN., R.E. Jessup, L.T. Ou, and P.D.C. Rao. 1985. Effects of sorption on biological degradation of 2,4-dechlorophenoxy acetic acid in soils. *Appl. Environ. Microbiol.* 49: 582-587.

Ong, S.K.; Lion, L.W. (1991) Mechanisms for Trichloroethylene Vapor Sorption onto Soil Minerals. J. Environ. Qual., 20, 180.

Onodera, S., Yamada, K., Ymaji, Yoko., and Ishikura, S., (1984). "Chemical Changes of Organic Compounds in Chlorinated Water: IX. Formation of Polychlorinated Phenoxyphenols during the Reaction of Phenol with Hypochlorite in Dilute Aqueous Solution," *J. Chromatography*, 288(1), 91-100.

Pardieck, D.L., Bouwer, E.J., and Stone, A.T., 1992. Hydrogen peroxide use to increase oxidant capacity for in situ bioremediation of contaminated soils and aquifers: A review. J. Contam. Hydrol. 9, 221-242.

Pardiek, D.L., E.J. Bouwer, and A.T. Stone. 1992. Hydrogen peroxide use to increase oxidant capacity for in situ bioremediation of contaminated soils and aquifers, *J. Contaminant Hydrology,* 9: 221-242.

Pavlostathis, S. G.; Jaglal, K. (1991) Desorptive Behavior of Trichloroethylene in Contaminated Soil. Environ. Sci. Technol., 25, 274.

Pennell, K.D., Abriola, L.M., Weber Jr., W.J. 1993. Surfactant-enhanced solubilization of residual dodecane in soil columns: 1. Experimental investigation. Environ. Sci. Technol. 27 (12), 2332– 2340.

Perret, J., S.O. Prasher, A. Kantzas, and C. Langford. 1999. Three-dimensional quantification of macropore networks in undisturbed soil cores. *Soil Sci. Soc. Am. J.* 63:1530–1543.

Peyton, G.R., LaFaivre, M.H., Smith, M.A.. (1990). "Treatability of Contaminated Groundwater and Aquifer Solids at Town Gas Sites Using Photocatalytic Oxidation and Chemical *In Situ* Oxidation." Illinois State Water Survey Division Report HWRIC-RR-048.

Peyton, G.R., O.J. Bell, E. Girin, and M.H. Lefaivre. 1995. Evidence of a reductive mechanism in the degradation of contaminants in water by advanced oxidation processes. Environ. Sci. Technol. 29:1710-1713.

Pignatello, J. J., and Day, M. (1996). "Mineralization of methyl parathion insecticide in soil by hydrogen peroxide activated with iron(III)-NTA or -HEIDA complexes." *Hazard. Waste Hazard. Mater.,* 13(2), 237-244.

Pignatello, J.J. and Baehr, K., 1994. Waste management: ferric complexes as catalysts for "Fenton" degradation of 2,4-D and metolachlor in soil. J. Environ. Qual. 23, 365-369.

Pillai, P., Helling, C.S., and Dragun, J. (1982). "Soil-Catalyzed Oxidation of Aniline." *Chemosphere*, 11, 299-317.

Poupko, R., and Rosenthal, I. (1973). "Electron transfer interactions between superoxide ion and organic compounds." *J. Phys. Chem.,* 77(13), 1722-1724.

Prados, M., H. Paillard, and P. Roche. 1995. Hydroxyl radical oxidation processes for the removal of triazine from natural water. *Ozone Sci. Eng.* 17:183-194.

Preis, S., S. Kamenev, J. Kallar, and R. Munter. 1995. Advanced oxidation processes against phenolic compounds in wastewater treatment. *Ozone Sci. Eng.* 17:399-418.

Prousek, J. 1995. Fenton reaction after a century. *Chemicke Listy.* 89:11-21.

Quan, H. N., Teel, A. L., and Watts, R. J. (2003). "Effect of contaminant hydrophobicity on H_2O_2 dosage requirements in the Fenton-like treatment of soils." *J. Hazard. Mater.,* 102(2-3), 277-289.

Ramsburg, C. A., and Pennell, K. D. (2002). "Density-modified displacement of dense nonaqueous-phase liquid source-zone remediation: Density conversion using a partitioning alcohol." *Environ. Sci. Technol.,* 36(9), 2082-2087.

Ravikumar, J. X., and Gurol, M. D. 1994. Chemical oxidation of chlorinated organics by hydrogen peroxide in the presence of sand. *Environ. Sci. Technol.* 28:394-400.

Ravikumar, J.X., and M. Gurol. 1991. Effectiveness of chemical oxidation to enhance the biodegradation of pentachlorophenol in soil: A laboratory study. In: R.D. Neufeld and L.W. Casson, Eds. *Proceedings of the 23rd Mid Atlantic Industrial Waste Conference.* Techmonic, Lancaster, PA. pp 211-221.

Reddi, L. N., and Wu, H. (1996). "Mechanisms involved in vibratory destabilization of NAPL ganglia in sands." *J. Environ. Eng.,* 122(12), 1115-1119.

Renaud, P., and Sibi, M. P. (2001). *Radicals in Organic Synthesis*. John Wiley and Sons. New York, N. Y.

Renn, T., T.F. Hess, and R.J. Watts. Oxidative-Reductive Degradation of 2,4,6-Trinitrotoluene in Fenton's Reactions. . First International Conference on Oxidation-Reduction Technologies for Soil and Groundwater Remediation. Niagara Falls, ON.

Rittman, B. E., and McCarty, P. L. (2002). *Environmental Biotechnology: Principles and Applications*. McGraw-Hill. New York, N. Y.

Rivett, M. O., Feenstra, S., Cherry, J. A., 2001. A controlled field experiment on groundwater contamination by a multicomponent DNAPL: creation of the emplaced-source and overview of dissolved plume development. J. Contam. Hydrol. 49(1-2), 111-149.

Rizkalla, E.N., El-Shafey, O.H., Guindy, N.M., 1982. The kinetics of decomposition of hydrogen peroxide in the presence of ethylenediaminetetraacetatoiron(III) complex. Inorg. Chim. Acta 57, 199-205.

Roberts, J. L., Jr., Calderwood, T. S., Sawyer, D. T., 1983. Oxygenation by superoxide ion of CCl_4, $FCCl_3$, $HCCl_3$, *p,p'*-DDT and related trichloromethyl substrates ($RCCl_3$) in aprotic solvents. J. Amer. Chem. Soc. 105(26), 7691-7696.

Roberts, J.L., Jr. and Sawyer, D.T. 1981. Facile degradation by superoxide ion of carbon tetrachloride, chloroform, methylene chloride, and p,p'-DDT in aprotic media. *J. Amer. Chem. Soc.* 103:712.

Rush, J.D. and W.H. Koppenol. 1986. Oxidizing intermediates in the reaction of ferrous EDTA with hydrogen peroxide. *J. Biog. Chem.* 15:6730-6733.

Rush, J.D., Bielski, B.H.J. Pulse radiolytic studies of the reaction of perhydroxyl/superoxide O_2^- with iron (II)/iron (III) ions: the reactivity of HO_2/O_2^- with ferric ions and its implication on the occurrence of the Haber-Weiss reaction. J. Phys. Chem.1985*;* 89:5062.

Sato, S., T. Kobayashi, and Y. Sumi. 1975. Removal of sodium dodecylbenzene sulfonate with Fenton's reagent. *Yukagaku.* 24:863-868.

Schmelling, D. C., Gray, K. A., and Kamat, P. V. (1998). "Radiation-induced reactions of 2,4,6-trinitrotoluene in aqueous solution." *Environ. Sci. Technol.,* 32(7), 971-974.

Schnarr, M., and Farquhar, G. (1992). "An in situ oxidation technique to destroy residual DNAPL from soil." *Subsurface Restoration Conference, Third International Conference of Ground Water Quality.* Dallas, Texas, Jun 21-24, 1992.

Schnoor, J.L. *Environmental Modeling: Fate and Transport of Pollutants in Water, Air, and Soil*; Wiley: New York, 1996.

Schroeder, D.; Schwartz, H. Unimolecular dissolution of ketone/iron complexes and evidence for successive carbon-hydrogen/C-C bond activation of different sets of flexible molecules. J. Amer. Chem. Soc. 1990, 112, 5947-53.

Schulte, P., A Bayer, F. Kuhn, T. Lug, and M. Volmer. 1995. H202/03, H202/UV and H202/Fe2+ processes for the oxidation of hazardous wastes. *Ozone Sci. Eng.* 17:119-134.

Schumb, W. C., C. N. Stratterfield, and R. L. Wentworth. 1955. Hydrogen Peroxide. American Chemical Society, Reinholt Publishing Co., New York.

Schwarzenbach, R. P.; Gschwend, P. M.; Imboden, D. M. *Environmental Organic Chemistry*; 2nd ed.; John Wiley & Sons: Hoboken, NJ, 2003.

Schwertzmann, U., and R.M. Cornell. 1991. *Iron oxides in the laboratory: preparationa and characterization.* Weinheim. New York.

Scott, J.P., and D.F. Ollis. 1995. Integration of chemical and biological oxidative processes in water treatment: review and recommendations. *Environ. Prog.* 14:88-103.

Scott, M.J., and Morgan, J.J., (1996). "Reactions at Oxide Surfaces. 2. Oxidation of Se (IV) by Synthetic Birnessite," *Environ. Sci. Technol.,* 30(6), 1990-1996.

Sedlak, D.L. and A.W. Andren. 1991. Aqueous-phase oxidation of polychlorinated biphenyls by hydroxyl radicals. *Environ. Sci. Technol.* 25:1419-1427.

Sedlak, D.L. and Andren, A.W., 1994. The effect of sorption on the oxidation of polychlorinated biphenyls (PCBs) by hydroxyl radical. Water Res. 28, 1207-1215.

Semprini, L., D. Grbic-Galic, P.L. McCarty, and P.V. Roberts. 1992. Methodologies for evaluating in-situ bioremediation of chlorinated solvents. U.S. EPA/600/R-92/042.

Seol, Y., Schwartz, F. W., and Lee, S. (2001). "Oxidation of binary DNAPL mixtures using potassium permanganate with a phase transfer agent." *Ground Water Monitor Remed.,* 21(2), 124-132.

Seol, Y., Schwartz, F.W., 2000. Phase-transfer catalysis applied to the oxidation of nonaqueous phase trichloroethylene by potassium permanganate. J. Contam. Hydrol. 44(2), 185-201.

Sheldon, R.A., Kochi., J.K., 1981. Metal-catalyzed reactions of organic compounds: Mechanistic principles and synthetic methodology including biochemical processes. Academic Press, New York, NY.

Siegrist, R. L., Urynowicz, M. A., West, O. R., Crimi, M. L., and Lowe, K. S. (2001). *Principles and Practices of In Situ Chemical Oxidation Using Permanganate.* Batelle Press. Columbus, OH.

Siegrist, R.L. 1999. In situ chemical oxidation: technology features and applications. *Abiotic In Situ Technologies for Groundwater Remediation Conference,* Dallas, Texas, Aug. 3 1 -Sept. 2, 1999.

Siegrist, R.L. and Watts, R.J., 2001. Chemical processes for the in situ oxidation of hazardous contaminants. First International Conference on Oxidation-Reduction Technologies for the Remediation of Soils and Groundwater, June 25-28, Niagara Falls, ON.

Skeen, R.S., K.M Amos and J.N. Petersen. 1994. Influence of nitrate concentration on carbon tetrachloride transformation by a denitrifying microbial consortium. *Wat. Res.* 28: 2433-2438.

Small, M. C. (1998). "Risk based corrective action, natural attenuation, and changing regulatory paradigms." *Bioremed. J.*, 2(3), 221-225.

Smith, B. A., A. L. Teel, and R. J. Watts. 2004a. Identification of the reactive oxygen species responsible for carbon tetrachloride degradation in modified Fenton's systems. *Environ. Sci. Technol.,* 38(20):5465–5469.

Smith, B. A., A. L. Teel, and R. J. Watts. 2006. Destruction of carbon tetrachloride and chloroform DNAPLs by modified Fenton's reagent. *J. Contam. Hydrol.* In Press.

Soil Conservation Service. Soil survey laboratory methods and procedures for collecting soil samples. Soil Survey Investigation: Report 1, US Government Printing Office, Washington, D.C. 1986.

Soloman, D.H., Loft, B.C., and Swift, J.D. (1968). "Reactions Catalyzed by Minerals. 4. The Mechanism of the Benzidine Blue Reaction." *Clay Miner.*, 7, 389-397.

Spain, J.C., J.D. Milligan, D.C. Downey, and J.K Slaughter. 1989. Excessive bacterial decomposition of H_2O_2 during enhanced biodegradation. *Ground Water.* 27:163-167.

Spencer, C.J., P.C. Stanton and R.J. Watts. 1994. On site treatment of contaminated soils and wastes from transportation maintenance activities using oxidative processes. *Trans. Res. Record* 144: 47-50.

Spencer, C.J., P.C. Stanton and R.J. Watts. 1996. A central composite rotatable design for the catalyzed hydrogen peroxide remediation of contaminated soils. *Jour. Air Waste Manage. Assoc.* 46:1067-1074.

Sposito, G. (1989). *Soil Chemistry.* Oxford University Press, New York.

Steinberg, S. M.; Swallow, C. E.; Ma, W.K. (1999) Vapor Phase Sorption of Benzene by Cationic Surfactant Modified Soil. Chemosphere, 38, 2143.

Steiner, M. G., and Babbs, C. F. (1990) Quantitation of the hydroxyl radical by reaction with dimethyl sulfoxide. *Arch. Biochem. Biophys.* 278, 478-481.

Stenkamp, V.S., and M.M. Benjamin. (1994). Effect of Iron Oxide Coating of Sand Filtration. *J. Amer. Water Works Assn.* 86(8) 37-50.

Stone, A.T. (1987). "Reductive Dissolution of Manganese (III/IV) Oxides by Substituted Phenols." *Environ. Sci. Technol.*, 21, 979-988.

Stone, A.T. and J.J. Morgan. 1984. Reduction and dissolution of manganese (III) and manganese (IV) oxides. *Environ. Sci. Technol.* 18:617-624.

Stone, A.T., (1987). "Reductive Dissolution of Manganese (III/IV) oxides by Substituted Phenols," *Environ. Sci. Technol.*, 21(10), 979-988.

Stroo, H.F., Unger, M., Ward, C.H., Kavanaugh, M.C., Vogel, C., Leeson, A., Marqusee, J.A., Smith, B.P., 2003. Remediating chlorinated solvent source zones. Environ. Sci. Technol. 37, 224A-230A.

Stucki. S., R. Kbtz, and B. Carcer. 1991. Electrochemical waste waster treatment using high overvoltage anodes. 11: Anode performance and applications. J. *App. Electrochem.,* 21:99-104.

Sudoh, M., T. Kodera, K. Sakai, J. Quan, and K. Koide. 1986. Oxidative degradation of aqueous phenol effluent with electrogenerated Fenton's reagent. *J. Chem. Eng. Japan,* 19, 513518.

Sudoh, M., T. Sasase, T. Yonebayachi, and K. Koide. 1985. Oxidative degradation of aqueous phenol effluent with Fenton's reagent. *Kagaku Kogaku Ronbunshu,* 11, 70-7 6.

Sullivan, J.B. Jr.; Krieger, G.R. *Hazardous Materials Toxicology: Clinical Principles of Environmental Health*; Williams & Wilkins: Baltimore, MD, 2001.

Sullivan, J.B., and Krieger, G.R. (1992) Hazardous Materials Toxicology, Williams and Wilkins, Baltimore, MD.

Sun, Y., and J.J. Pignatello. 1992. Chemical treatment of pesticide wastes. Evalutation of Fe(III) chelates for catalytic hydrogen peroxide oxidation of 2,4-D at circumneutral pH. *J. Agric. Food Chem.* 40:322-327.

Sun, Y., and Pignatello, J.J. (1995). "Evidence for a Surface Dual Hole-Radical Mechanism in the TiO_2 Photocatalytic Oxidation of 2,4-Dichlorophenoxyacetic Acid." *Environ. Sci. Technol.*, 29, 2065-2072.

Tchobanoglous, G. and F.L. Burton. 1991. *Wastewater Engineering: Treatment, Disposal, and Reuse*. Third edition. McGraw-Hill. New York. 1334 p.

Teel, A.L. C.R. Warberg, D.A. Atkinson, and R.J. Watts. 2001. Comparison of mineral and soluble iron Fenton's catalysts for the treatment of trichloroethylene. *Water Res.* 35(4): 977-984.

Teel, A.L., and R. J. Watts. 2002. Degradation of carbon tetrachloride by Fenton's reagent. *J. Hazard. Mater.* 94:179–189.

Thomas, J. M., and Ward, C. H. (1989). "In situ biorestoration of organic contaminants in the subsurface." *Environ. Sci. Technol.*, 23(7), 760-766

Torrents, A.; Stone, A.T. Catalysis of picolinate ester hydrolysis at the oxide/water interface: inhibition by coadsorbed species. *Environ. Sci. Technol.* 1993, *27*, 2381-2386

TRI 94. 1996. Toxic chemical release inventory for 1994. National Laboratory of Medicine, Bethesda, MD.

Tyre, B.W., R.J. Watts and G.C. Miller. 1991. Treatment of four biorefractory contaminants in soils using catalyzed hydrogen peroxide. *J. Environ. Qual.* 20:832.

U.S. DOE (1999). *Innovative Technology Summary Report: Fenton's Reagent (DOE/EM-0484).* Office of Science and Technology, Washington, D.C.

U.S. Environmental Protection Agency (US EPA), Integrated Risk Information System (IRIS) on Carbon Tetrachloride, Environmental Criteria and Assessment Office, Office of Health and Environmental Assessment, Office of Research and Development, Cincinnati, OH, 1993.

U.S. Environmental Protection Agency, 1993. Evaluation of the Likelihood of DNAPL Presence at NPL Sites: National Results. EPA 540-R-93-073, Washington D.C.

U.S. Environmental Protection Agency, 1998. Field Applications of In Situ Remediation Technologies: Chemical Oxidation. EPA 542-R-98-008, Washington D.C.

U.S. Environmental Protection Agency. 1988. Report to Congress: Solid waste disposal in the United States, Vol. II, EPA/530-SW-88-011B. U.S. EPA, U.S. Government Printing Office, Washington, DC.

U.S. EPA. Recent developments for in situ treatment of metal contaminated soils; Office of Solid Waste and Emergency Response: Washington, DC. 1997.

U.S. Geological Survey. 1998. Water Quality in the Columbia Plateau, 1992-95. Reston, VA.

U.S. Soil Conservation Service. (1972) Soil Survey Investigation: Report 1. U.S. Government Printing Office, Washington, D.C.

Ulrich, H.-J. and Stone, A.T. (1989). "Oxidation of Chlorophenols Absorbed to Manganese Oxide Surfaces." *Environ. Sci. Technol.*, 23, 421-428.

Unger, D.R.; Lam, T.T.; Schaefer, C.E.; Kosson, D.S. (1996) Predicting the Effect of Moisture on Vapor-Phase Sorption of Volatile Organic Compounds to Soils. Environ. Sci. Technol., 30, 1081.

Uri. N. 1952. Inorganic free radicals in solution. *Chem. Rev.* 50: 375-454.

Valentine, R. L., and Wang, D. C. A. 1998. Iron oxide surface catalyzed oxidation of quinoline by hydrogen peroxide. *J. Environ. Eng*. 124:31-38.

Vallyathan, V., 1994. Generation of oxygen radicals by minerals and its correlation to cytotoxicity. Oxygen Radicals and Lung Injury, Environmental Health Perspective. 102 (10), 111-115.

Valsaraj, K.T., and Thibodeaux, L.J. (1989) Relationships between micelle-water and octanol:water partition constants for hydrophobic organics of environmental interest. Water Res. 23, 183-187.

Vella, P.A., Veronda, B., 1992. First International Symposium for Chemical Oxidation: Technologies for the Nineties. Technomic Publishing, Lancaster, PA,.

Vella, P.A., Veronda, B., 1992. First International Symposium for Chemical Oxidation: Technologies for the Nineties. Technomic Publishing, Lancaster, PA,.

Venkatadri, R. and Peters, R.W. (1993). "Chemical Oxidation Technologies: Ultraviolet Light/Hydrogen Peroxide, Fenton's Reagent, and Titanium Dioxide-Assisted Photocatalysis." *Haz. Was. Haz. Mat.*, 10, 107-149.

Verschueren, K. (1983) Handbook of Environmental Data on Organic Compounds. Van Nostrand Reinhold: New York.

Vogel, T.M., and P.L. McCarty. 1985. Biotransformation of tetrachloroethylene to trichloroethylene, dichloroethylene, vinyl chloride, and carbon dioxide under methanogenic conditions. *Applied and Environmental Microbiology*. 49:1080-1083.

Vogel, T.M., C.S. Criddle, and P.L. McCarty. 1987. Transformation of halogenated aliphatic compounds. *Environmental Science and Technology*. 21:722-735.

Walling, C, and R.A. Johnson. 1975. Fenton's reagent. V. Hydroxylation and side-chain cleavage of aromatics. *J. Am. Chem.* Soc., 97, 363-367.

Walling, C. 1975. Fenton's reagent revisited. *Acc. Chem. Res.,* 8, 125-13 1.

Walling, C. and R.A. Johnson. 1975. Fenton's reagent. V. Hydroxylation and side-chain cleavage of aromatics. *J. Americ. Chem. Soc.* 97(2):363-367.

Walling, C. and T. Weil. 1974. The ferric ion catalyst decomposition of hydrogen peroxide in perchloric acid. *Int. J. Chem. Kinet.* 6:507-516.

Wang, X. J., and Brusseau, M. L. (1998). "Effect of pyrophosphate on the dechlorination of tetrachloroethene by the Fenton reaction." *Environ. Toxicol. and Chem.,* 17(9), 1689-1694.

Wang. Y.T. 1992. Effect of chemical oxidation on anaerobic biodegradation of model phenolic compounds. *Water Environ. Res.*64:268-273.

Warner, H. P., Cohen, J.M., and Ireland, J.C, Determination of Henry's Law Constants of Selected Priority Pollutants, EPA-600/D-87/229, U.S. Environmental Protection Agency, Washington, DC, 1987.

Waters, W.A., (1971). "Comments on the Mechanism of One-Electron Oxidation of Phenols: A Fresh Interpretation of Oxidative Coupling Reactions of Plant Phenols," *J. Chem. Soc. (B),* 2026-2029.

Watts R.J., S. Kong, M.P. Orr, and G.C. Miller. 1995. Photocatalytic inactivation of coliform bacteria and viruses in secondary wastewater effluent. *Water Res.* 29:95- 100.

Watts, R. J. (1992). "Hydrogen peroxide for physicochemically degrading petroleum-contaminated soils." *Remediation,* 2(4), 413-425.

Watts, R. J. 1998. *Hazardous Wastes: Sources, Pathways, Receptors.* John Wiley & Sons. New York. 764 p.

Watts, R. J., Haller, D. R., Jones, A. P., and Teel, A. L. (2000). "A foundation for the risk-based treatment of gasoline-contaminated soils using modified Fenton's reactions." *J. Hazard. Mater.,* B76(1), 73-89.

Watts, R. J., and Dilly, S. E. (1996). "Evaluation of iron catalysts for the Fenton-like remediation of diesel-contaminated soils." *J. Hazard. Mater.,* 51(2), 209-224.

Watts, R. J., and Greenberg, R. S. (1995) Laboratory and pilot development of hydrogen peroxide for abiotic in situ remediation of contaminated groundwater. Presented at the *ACS Symposium on Emerging Technologies in Hazardous Waste Treatment,* Atlanta, GA, September 1995.

Watts, R. J., and Stanton, P . C. (1999). "Mineralization of sorbed and NAPL-phase hexadecane by catalyzed hydrogen peroxide." *Water Res.,* 33(6), 1405-1414.

Watts, R. J., and Teel, A. L. (2005). "Chemistry of Modified Fenton's Reagent (Catalyzed H_2O_2 Propagations—CHP) for *In Situ* Soil and Groundwater Remediation." *J. Environ. Eng.,* In Press.

Watts, R. J., Bottenberg, B. C., Hess, T. F., Jensen, M. D., Teel, A. L., 1999. Mechanism of the enhanced treatment of chloroaliphatic compounds by Fenton-like reactions. Environ. Sci. Technol. 33, 3432-3437.

Watts, R. J., Foget, M. K., Kong, S. H., and Teel, A. L. 1999. Hydrogen peroxide decomposition in model subsurface systems. *J. Hazard. Mater.* B69:229-243.

Watts, R. J., Haller, D. R., Jones, A. P., and Teel, A. L. (2000). "A foundation for the risk-based treatment of gasoline-contaminated soils using modified Fenton's reactions." *J. Hazard. Mater.,* B76(1), 73-89.

Watts, R. J., Jones, A. P., Chen, P. H., and Kenny, A. (1997). "Mineral catalyzed Fenton-like oxidation of sorbed chlorobenzenes." *Water Environ. Res.,* 69(2), 269-275.

Watts, R. J., Kong, S., Dippre, M., and Barnes, W. T. (1994). "Oxidation of sorbed hexachlorobenzene in soils using catalyzed hydrogen peroxide." *J. Hazard Mater.,* 39(1), 33-47.

Watts, R. J., Sarasa, J., Loge, F. J., and Teel, A. L. (2004). "Oxidative and reductive pathways in manganese-catalyzed Fenton's reactions." *J. Environ. Eng.,* In Press.

Watts, R. J., Stanton, P. C., Spencer, C. J., Kong, S., and Haeri-McCarrol, T. M. (1993a) Process conditions for the treatment of contaminated soils using catalyzed hydrogen peroxide. In *Managing Contaminated Sites: A Water Environment Specialty Conference,* Miami, FL, March, paper 6d.

Watts, R. J., Udell, M. D., and Monsen, R. M. (1993). "Use of iron minerals in optimizing the peroxide treatment of contaminated soils." *Water Environ. Res.,* 65(7), 839-844.

Watts, R. J., Udell, M. D., Kong, S. H., Leung, S. W. (1999b). "Fenton-like remediation catalyzed by naturally occurring iron minerals." *Environ. Eng. Sci.,* 16(1), 93-103.

Watts, R. J., Udell, M. D., Rauch, P. A., and Leung, S. W. (1990). "Treatment of pentachlorophenol-contaminated soils using Fenton's reagent." *Hazard. Wastes Hazard. Mater.,* 7(4), 335-345.

Watts, R. J., Washington, D., Howsawkeng, J., Loge, F. J., and Teel, A. L. 2003. Comparative toxicity of hydrogen peroxide, hydroxyl radicals, and superoxide anion to *Escherichia coli. Adv. Environ. Res.* 7(4):961-968.

Watts, R. J., Washington, D., Howsawkeng, J., Loge, F. J., and Teel, A. L. (2003b). "Comparative toxicity of hydrogen peroxide, hydroxyl radicals, and superoxide anion to *Escherichia coli." Adv. Environ. Res.,* 7(4), 961-968.

Watts, R. J.; Howsawkeng, J.; Teel, A. L. (2005) Destruction of a Carbon Tetrachloride DNAPL by Modified Fenton's Reagent. J. Environ. Eng., 131(7), 1114-1119.

Watts, R. J.; Jones, A.P.; Chen, P.H.; Kenny, A. (1997) Mineral Catalyzed Fenton-Like Oxidation of Sorbed Chlorobenzenes. Water Environ. Res., 69, 269.

Watts, R. J.; Stanton, P. C. (1999) Mineralization of Sorbed and NAPL-Phase Hexadecane by Catalyzed Hydrogen Peroxide. Water Res., 33, 1405.

Watts, R.J. Hazardous wastes: sources, pathways, receptors. John Wiley and Sons, New York. 1998.

Watts, R.J. Recent Advances in the Use of Fenton's Reagent for In Situ Chemical Oxidation. First International Conference on Oxidation-Reduction Technologies for Soil and Groundwater Remediation. Niagara Falls, ON.

Watts, R.J. 1992. Hydrogen peroxide for physicochemically degrading petroleum-contaminated soils. *Remediation* 2:413-425.

Watts, R.J., A.P. Jones, P.H. Chen, and A. Kenny. 1997. Mineral catalyzed Fenton-like oxidation of sorbed chlorobenzenes. *Water Environ. Res.* 69:269-275.

Watts, R.J., and S.E. Dilly. 1996. Evaluation of iron catalysts for the Fenton-like remediation of diesel-contaminated soils. *J. Hazard. Mater.,* 51:209-224.

Watts, R.J., and V.D. Adams. 1993. Elimination of sulfur (IV) interference in five day biochemical oxygen demand deten-ninations. *Analyst., Royal Soc. Chem.* 118: 1515-1518.

Watts, R.J., B.R. Smith and G.C. Miller. 1991. Treatment of octachlorodibenzo-*p*-dioxin (OCDD) in surface soils using catalyzed hydrogen peroxide. *Chemosphere.* 23:949-955.

Watts, R.J., D.A. Atkinson, and A.L. Teel. Chemical Processes for the In Situ Oxidation of Contaminants in Soils and Groundwater. Inland Northwest Research Alliance Annual Conference. Idaho Falls, ID

Watts, R.J., Kong, S., Dippre, M., and Barnes, W.T. (1994). Oxidation of sorbed hexachlorobenzene in soils using catalyzed hydrogen peroxide. *J. Haz. Mater.*, 39, 33-47.

Watts, R.J., M.D. Udell and R.M. Monsen. 1993. Use of iron minerals in optimizing the peroxide treatment of contaminated soils. *Water Environ. Res.* 65:839-845.

Watts, R.J., M.D. Udell and S.W. Leung. 1991. Treatment of contaminated soils using catalyzed hydrogen peroxide. In: W.W. Eckenfelder et al. (Eds), Chemical Oxidation: Technology for the 90's.

Watts, R.J., M.D. Udell, P.A. Rauch, S.W. Leung. 1990. Treatment of pentachlorophenol-contaminated soils using Fenton's reagent. *Hazard. Waste Hazard. Mater.* 7:335.

Watts, R.J., M.E. Nubbe, and T.F. Hess. 1995. Hazardous wastes: assessment, management, minimization. Water Environ. Res. 67:553-559.

Watts, R.J., P.C. Stanton, C.J. Spencer, S. Kong, and T.M. Haeri-McCarroll. 1993. Process conditions for the treatment of contaminated soils using catalyzed hydrogen peroxide. Contaminated Sites Specialty Conference of the Water Environ. Fed., Miami, FL.

Watts, R.J., Sarasa, J., Howsawkeng, J., and Teel, A. 2006. Reaction-Specific Probes for the Detection of Hydroxyl Radicals, Superoxide, and Hydroperoxide in Modified Fenton's Reactions. *Environ. Sci. Technol*. In Preparation.

Watts, R.J., Stanton, P.C., Howsawkeng, J., and Teel, A.L. (2002). "Mineralization of a sorbed polycyclic aromatic hydrocarbon in two soils using catalyzed hydrogen peroxide." *Water Res.*, 36(12), 4283-4292.

Watts, R.J., Stanton, P.C., Howsawkeng, J., and Teel, A.L. 2002. Mineralization of a sorbed polycyclic aromatic hydrocarbon in two soils using catalyzed hydrogen peroxide. *Water Res.*, 36:4283-4292

Watts, R.J., U.R. Hui, T.F. Hess, and A.L Teel. Reaction-Specific Probe Compounds for the Detection of Hydroxyl Radicals, Superoxide Anion, and Hydroperoxide Anion in Modified Fenton's Reactions. . First International Conference on Oxidation-Reduction Technologies for Soil and Groundwater Remediation. Niagara Falls, ON.

Watts, R.J., Udell, M.D. and Leung, S.W. (1991). "Treatment of Contaminated Soils Using Catalyzed Hydrogen Peroxide." *In* J.A. Roth, Ed. *Chemical Oxidation: Technology for the 90's.* Techmonic Press, pp. 46-55.

Wayman, M.J.V. 1983. Treatment of phenols: a case history. *Chem. Ind. (London),* 14, 549551.

Wayt, HJ, and Wilson, D.J. (1989) Soil cleanup by in situ surfactant flushing. II. Theory of micellular solubilization. Sep. Sci. Technol. 24, 905-909.

Weissenfels, W.D., H.-J. Klewer, and J. Langhoff. 1992. Adsorption of polycyclic aromatic hydrocarbons (PAHs) by soil particles-- Influence on biodegradability and biotoxicity. Appl. Microbial. Biotechnol., 36,689-696.

Wells, P.R. (1968). "Linear Free Energy Relationships." Academic Press, New York.

Westrick, J.J., J.W. Mills, and R.F. Thomas. 1983. *The Ground Water Supply Survey: Summary of Volatile Organic Contaminant Occurrence Data.* U.S. EPA Office of Drinking Water, Cincinnati, OH.

Whittig, L.D.; Allardice, W.R. *Methods of Soil Analysis: Part 1-Physical and Mineralogical Methods*; Klute, A. Ed.; Soil Science Society of America: Madison, WI, 1986.

Wiedemeier, T. H., Rifai, H. S., Wilson, J. T., and Newell, C. (1999). *Natural Attenuation of Fuels and Chlorinated Solvents in the Subsurface*. John Wiley and Sons. New York, N. Y.

Wilson, R.L. 1971. Pulse radiolysis studies on reaction of triacetoneamine-N-oxyl with radiation-induced free radicals. *Trans. Faraday Soc.* 67:3020-_____.

Wolff, S.P., Gamer, A., and Dean, R.T., 1986. Free radicals, lipids, and protein degradation. Trends Biochem. Sci. 11, 27-31.

Wong, J., Nolan, G.L, and Lim, C.H. (1997). "Design of Remediation Systems." Lewis Publishers, Boca Raton, FL.

Yan, Y. E., and Schwartz, F. W. (1998). "Oxidation of chlorinated solvents by permanganate." *Proc. Intern. Conf. on Remediation of Chlorinated and Recalcitrant Compounds*. Batelle Press. Columbus, OH.

Yang, Y. R., McCarty, P. L., 2002. Comparison between donor substrates for biologically enhanced tetrachloroethene DNAPL dissolution. Environ. Sci. Technol 36(15), 3400-3404.

Yasuyoshi, M.; Yokoi, H. Studies on the interaction between iron (III) and glycerol or related polyols over a wide pH range. Bull. Chem. Soc. Japan. 1994, 67(10), 2724-2730.

Yeh, C. K.-J., Wu, H.-M., and Chen, T.-C., 2003. Chemical oxidation of chlorinated non-aqueous phase liquid by hydrogen peroxide in natural sand systems. J. Hazard. Mater. 96(1), 29-51.

Yeh, C.K., and J.T. Novak. 1995. The effect of hydrogen peroxide on the degradation of methy and ethyl tert-butyl ether in soils. *Water Environ. Res.* 67:828-834.

Yeh, C.K.-J., H.-M. Wu, and T.-C. Chen. 2003. Chemical oxidation of chlorinated non-aqueous phase liquid by hydrogen peroxide in natural sand systems. *J. Hazard. Mater.* 96(1):29–51.

Zafiriou, O.C., Voelker, B.M., Sedlak, D.L. Chemistry of the superoxide radical ($O_2\bullet^-$) in seawater: reactions with inorganic copper complexes. J. Phys. Chem. A.1998; 102(28):5693-5700.

Zepp, R. G., B. C. Faust, and J. Hoigne. 1992. Hydroxyl Radical Formation in Aqueous Reactions (pH 3-8) of Iron (II) with Hydrogen Peroxide: The Photo-Fenton Reaction. *Environ. Sci. Technol.*, 26: 313-319.

Zhang, H.; Huang, C.-H. Oxidative Transformation of Triclosan and Chlorophene by Manganese Oxides. *Environ. Sci. Technol.* 2003, 37, 2421-2430

Zhang, Y., Crittenden, J.C., Hand, D.W., and Perram, D.L. (1994). "Fixed-Bed Photocatalysis for Solar Decontamination of Water." *Environ. Sci. Technol.*, 28, 435-442.